STEREOSELECTIVE EPOXIDE POLYMERIZATION: EXPLORING ISOSELECTIVE BIMETALLIC CATALYSTS, IONIC COCATALYSTS, AND THE USE OF ALCOHOLS AS CHAIN TRANSFER AGENTS

A Dissertation

Presented to the Faculty of the Graduate School

of Cornell University

In Partial Fulfillment of the Requirements for the Degree of

Doctor of Philosophy

by

Peter Carsten Bailey Widger

August 2011

STEREOSELECTIVE EPOXIDE POLYMERIZATION: EXPLORING ISOSELECTIVE BIMETALLIC CATALYSTS, IONIC COCATALYSTS, AND THE USE OF ALCOHOLS AS CHAIN TRANSFER AGENTS

Peter Carsten Bailey Widger, Ph.D.

Cornell University 2011

For over 50 years, researchers have attempted to create catalysts for stereoselectively polymerizing epoxides. Until very recently, catalysts for the polymerization of racemic epoxides gave mixtures of atactic and isotactic material or moderate tacticity polyethers. In 2008, the Coates Research Group reported a bimetallic catalyst system for enantioselectively polymerizing racemic epoxides to highly isotactic enantiopure polyethers. Catalyst simplification led to a highly active, isoselective catalyst. This catalyst is capable of quantitatively polymerizing racemic terminal epoxides to yield isotactic polyethers. Organic ionic compounds were synthesized and investigated as cocatalyts. The identities of both the cation and anion were systematically varied and subsequent polymerization reactivity was studied. The nature of the ionic cocatalyst dramatically impacted the rate and enantioselectivity of the catalyst system. The ionic cocatalyst $[P(N{=}P(N(CH_2)_4)_3)_4^+][^tBuCO_2^-]$ produced a catalyst system that exhibited the greatest activity and selectivity for a variety of mono-substituted epoxides. The addition of alcohols to these bimetallic polymerization systems leads a lowering of molecular weight due to chain transfer. Polymer end-groups can be determined by choice of alcohol, addition of diols allows for the synthesis of isotactic telechelic poly(propylene oxide) diols.

BIOGRAPHICAL SKETCH

Peter was born August 5th, 1984 in Manchester, NH to Edward Bailey Jr. and Barbara Widger. During high school at Manchester Central, he was active in science, engineering, and music. As an undergraduate at the University of New Hampshire, he researched the synthesis of polycyclic tetraamines under the guidance of Professor Gary Weisman. He received his B.S. in chemistry from UNH in 2006. He then began graduate studies at Cornell University and joined the research lab of Geoff Coates; exploring catalytic systems for polymer synthesis. In 2010, he married his wife Kenyon. Upon graduating, he is looking forward to moving to Boston, MA and beginning work at E Ink.

Dedicated to my wife, Kenyon, for all her love and support.

ACKNOWLEDGMENTS

I would like to thank Professor Coates for all of his support and guidance during my time at Cornell. The Coates Group has wonderful people, ideas and resources to work with. I would also like to thank my committee members Professor Collum and Professor Sogah for their insights before and after my A Exam.

Several groups deserve acknowledgement for their generous funding. Many thanks to the Cornell University Department of Chemistry and Chemical Biology for supporting me as a teaching assistant for my first two years of graduate school. I would also like to thank the following organizations for generously supporting me: The National Science Foundation, the Cornell Center for Materials Research, and the King Abdullah University of Science and Technology.

My sincere gratitude goes to the senior group members who taught me the majority of new lab techniques and research strategies when I joined. Dr. Ryan Jeske and Dr. Tim Clark were truly extraordinary students and researchers who always made Room 565 a great place to be. Thanks to Dr. Greg Domski, and Dr. Jeff Rose for helping me during my short time working with poly-olefins. Thanks to Dr. Kevin Noonan for helping me with the synthesis of phosphazeniums and phosphoniums – good luck professor! Thanks also to Dr. Jeung Kim for helping prepare me for the professional world and helping my find my first job. Dr. Anne LaPointe deserves many thanks for all of her helpful advice and hard work proof reading manuscripts.

Major thanks to Renee Thomas for introducing me to the stereoselective epoxide

polymerization project and helping me get through many difficult columns. Thanks to Syud Ahmed (Taz) for helping me with my scientific writing and getting our papers published. Best of luck to Ian Childers and Rachna Khurana our newest sub-group members.

Thanks to Henry Kostalik and Bryan Whiting for their friendship and support during the past five years. Thanks also to Angie Diccio and Christina “C” Cowman for their support and encouragement and for keeping the lab extremely cheerful. I would also like to thank Dr. Ivan Keresztes for all of his help with running NMR experiments and characterization.

Finally I would like to thank my family for all of their support.

TABLE OF CONTENTS

BIOGRAPHICAL SKETCH iii

DEDICATION iv

ACKNOWLEDGEMENTS v

LIST OF FIGURES xi

LIST OF SCHEMES xv

LIST OF TABLES xvii

Chapter 1: Stereoselective Catalysts For the Ring-Opening Polymerization of Epoxides 1

1.1. Introduction **2**

1.1.2. Scope of Chapter **2**

1.2. Basic Concepts in Stereoselective Epoxide Polymerization **3**

1.2.1. Regiochemistry

1.2.2. Analysis of Polymer Stereochemistry **4**

1.2.3. Chain-End Control and Enantiomorphic-Site Control of Stereochemistry **4**

1.3. Stereoselective Epoxide Polymerization **6**

1.3.1. Aluminum-Based Catalysts **6**

1.3.1.1. Aluminum-acetylacetonate complexes **7**

1.3.1.2. Aluminum systems featuring chiral alkoxides **11**

1.3.1.3. Aluminum-porphyrin complexes **12**

1.3.1.4. Aluminum-schiff-base complexes **13**

1.3.1.5. Aluminum-calixerene complexes **14**

1.3.1.6. Other well-defined aluminum systems **14**

1.3.2. Zinc-Based Catalysts **15**

1.3.2.1. Zinc alkoxide catalysts **15**

1.3.2.2. Chiral zinc alkoxide catalysts **16**

1.3.2.3. Zinc alkoxide clusters **17**

1.3.2.4. Zinc porphyrin-based catalysts **20**

1.3.2.5. Zinc catalysts for asymmetric cyclohexene oxide/CO_2 copolymerizations **21**

1.3.3. Cobalt-Based Catalysts **24**

1.3.3.1. Epoxide-carbon dioxide copolymerization systems **25**

1.3.3.2. Recent stereoselective epoxide homopolymerization systems **28**

1.3.4. Tin-Based Catalysts **34**

1.3.5. Chromium-Based Catalysts **35**

1.4. Outlook and Conclusions **36**

1.5. References **37**

Chapter 2: Isoselective Polymerization of Racemic Epoxides: A Catalyst System for the Synthesis of Highly Isotactic Polyethers **43**

2.1. Introduction **44**

2.2. Results and Discussion **45**

2.2.1. Characterization of Co(III) Complexes **52**

2.3. Conclusions **57**

2.4. Experimental **57**

2.4.1. General Considerations **57**

2.4.2. Determination of Epoxide Enantiomeric Excess **58**

2.4.3. Polymer Characterization **58**

2.4.4. NMR Quantification of Polymer Tacticity **59**

2.4.5. Calculation of Polymer Tacticity **60**

2.4.6. Materials **61**

2.4.7. Synthetic Procedures and Characterization **63**

2.4.8. Polymerization of Epoxides **76**

2.4.8.1. Representative isoselective polymerization of racemic epoxides **79**

2.4.9. Crystal Data and Refinement for compounds **2.15**, **2.16**, and **2.17** **88**

2.5. Notes and References **91**

Chapter 3: Exploration of Cocatalyst Effects on a Bimetallic Cobalt Catalyst System: Enhanced Activity and Enantioselectivity in Epoxide Polymerization **94**

3.1. Introduction **95**

3.2. Results and Discussion **98**

3.3. Conclusions **103**

3.4. Experimental **103**

3.4.1. General Considerations **103**

3.4.2. Materials **104**

3.4.3. Polymer Characterization and NMR Quantification of Polymer Tacticity, Enantiomeric Excess and *s*-factor **105**

3.4.4. Synthesis of Cocatalysts **106**

3.4.5. Enantioselective Polymerization of Epoxides **118**

3.5. References and Notes **130**

Chapter 4: Synthesis of Telechelic Poly(Propylene Oxide) Diols from Racemic Propylene Oxide **133**

4.1. Introduction **134**

4.2. Results and Discussion **137**

4.2.1. Initial Polymerization Studies with **4.1**/**4.2** and Alcohols as Chain Transfer Agents **137**

4.2.2. Screening of Chain Transfer Agents **141**

4.2.3. Diols as Chain Transfer Agents **144**

4.3. Conclusions **146**

4.4. Experimental **147**

4.4.1. General Considerations **147**

4.4.2. Materials **147**

4.4.3. Polymer Characterization and NMR Quantification of Polymer Tacticity, Enantiomeric Excess and *s*-factor **148**

4.4.4. MALDI-TOF-MS Analysis **149**

4.4.5. Polymerization Procedures and Additional Tables **149**

4.5. Notes and References **165**

LIST OF FIGURES

Figure 1.1. Well-defined complexes for the polymerization of epoxides (tpp = 5, 10, 15, 20-tetraphenylporphyrin; salcy = *N,N′*-bis-(2-hydroxybenzylidene)-(1*R*,2*R*)-1,2-cyclohexanediamine); dmca = dimethylcalixarene. **13**

Figure 1.2. Structures of zinc cluster catalysts **1.7**, **1.8**, and **1.9**. **18**

Figure 1.3. Chiral zinc catalyst **1.14** for the enantioselective, alternating copolymerization of cycloalkene oxides and CO_2. **24**

Figure 1.4. Preparation of organotin phosphate condensate catalysts. **35**

Figure 1.5. Structure of SalanCr(III) complex. **36**

Figure 2.1. Methine regions of the ^{13}C NMR spectra of PPO produced using a) Catalyst **2.3** and Cocatalyst **2.4**; b) Catalyst **2.3** and cocatalyst **2.6**. **48**

Figure 2.2. Molecular structure of *rac*-**2.15** (hydrogen atoms omitted and pyridine ligands truncated for clarity; carbon atoms are unlabelled). Thermal ellipsoids are at the 30% probability level. **54**

Figure 2.3. Molecular structure of **2.16** crystallized from pyridine and toluene (hydrogen atoms omitted and pyridine ligands truncated for clarity; carbon atoms are unlabelled). Thermal ellipsoids are at the 30% probability level. **55**

Figure 2.4. Molecular structure of **2.17** crystallized from pyridine and toluene (hydrogen atoms omitted and pyridine ligands truncated for clarity; carbon atoms are unlabelled). Thermal ellipsoids are at the 30% probability level. **56**

Figure 2.5. Calculation of $ee_{(P)}$ for PPO by ^{13}C NMR spectroscopy using *rr* triad resonance. **61**

Figure 2.6. ^{1}H NMR spectrum of **2.18** in $CDCl_3$. **64**

Figure 2.7. ^{1}H NMR spectrum of **2.8** in $CDCl_3$. **67**

Figure 2.8. ^{1}H NMR spectrum of **2.2** in pyridine-d_5. **68**

Figure 2.9. ^{1}H NMR spectrum of **2.10** in $CDCl_3$. **70**

Figure 2.10. ^{1}H NMR spectrum of **2.3** in pyridine-d_5. **71**

Figure 2.11. NMR spectra of **2.5** in $CDCl_3$. A) ^{1}H NMR spectrum. B) ^{13}C NMR spectrum. **73**

Figure 2.12. NMR spectra of **2.6** in $CDCl_3$. A) ^1H NMR spectrum. B) ^{13}C NMR spectrum. **74**

Figure 2.13. NMR spectra of **2.7** in $CDCl_3$. a) ^1H NMR spectrum. b) ^{13}C NMR spectrum. **75**

Figure 2.14. ^{13}C NMR spectra of poly(propylene oxide) in $CDCl_3$. A) Full spectrum. B) Methine region. **78**

Figure 2.15. ^{13}C NMR spectra of poly(propylene oxide) in $CDCl_3$. A) Full spectrum. B) Methine region. **80**

Figure 2.16. ^{13}C NMR spectra of poly(butene oxide). a) Full spectrum. b) Methine region. **81**

Figure 2.17. ^{13}C NMR spectra of poly(phenyl glycidyl ether). A) Full spectrum. B) Methine region. **82**

Figure 2.18. ^{13}C NMR spectra of poly(3,4-epoxy-1-butene). A) Full spectrum. B) Methylene region. C) Hydrogenated polymer methine region. **83**

Figure 2.19. ^{13}C NMR spectra of poly(styrene oxide). A) Full spectrum. B) Methine region. **84**

Figure 2.20. ^{13}C NMR spectra of poly(1,1,1-trifluoro-2,3-epoxypropane). A) Full spectrum. B) Methylene region. **85**

Figure 2.21. ^{13}C NMR spectra of poly(propylene oxide). A) Full spectrum. b) Methine region. **87**

Figure 3.1. Isoselective Polymerization of PO Using System **3.1b**/**3.3e** **103**

Figure 3.2. 3.3a in CD_3OD. Top: ^1H NMR spectrum. Bottom: ^{13}C NMR spectrum. **107**

Figure 3.3. 3.3b in CD_3OD. Top: ^1H NMR spectrum. Bottom: ^{13}C NMR spectrum. **108**

Figure 3.4. 3.3c in CD_3OD. Top: ^1H NMR spectrum. Bottom: ^{13}C NMR spectrum. **109**

Figure 3.5. 3.3d in CD_3OD. Top: ^1H NMR spectrum. Bottom: ^{13}C NMR spectrum. **110**

Figure 3.6. 3.3e in CD_3OD. Top: ^1H NMR spectrum. Bottom: ^{13}C NMR spectrum. **111**

Figure 3.7. 3.3f in CD_3OD. Top: ^1H NMR spectrum. Bottom: ^{13}C NMR spectrum. **112**

Figure 3.8. 3.3g in CD_3OD. Top: ^1H NMR spectrum. Bottom: ^{13}C NMR spectrum. **113**

Figure 3.9. 3.3h in CD_3OD. Top: ^1H NMR spectrum. Center: $^{13}C\{^{19}F\}$NMR spectrum. Bottom: ^{19}F NMR spectrum. **115**

Figure 3.10. 3.3i in $CDCl_3$. Top: ^1H NMR spectrum. Bottom: ^{13}C NMR spectrum. **116**

Figure 3.11. 3.4 in $CDCl_3$. Top: ^1H NMR spectrum. Bottom: ^{13}C NMR spectrum. **117**

Figure 3.12. ^{13}C NMR spectra of poly(propylene oxide). Top: Full spectrum. Bottom: Methine region. **119**

Figure 3.13. ^{13}C NMR spectra of poly(butene oxide). Top: Full spectrum. Bottom: Methine region. **121**

Figure 3.14. ^{13}C NMR spectra of poly(phenyl glycidyl ether). Top: Full spectrum. Bottom: Methine region. **123**

Figure 3.15. ^{13}C NMR spectra of poly(3,4-epoxy-1-butene). Top: Full spectrum. Center: Methylene region. Bottom: Hydrogenated polymer methine region. **125**

Figure 3.16. ^{13}C NMR spectra of poly(styrene oxide). Top: Full spectrum. Bottom: Methylene region. **127**

Figure 3.17. ^{13}C NMR spectra of poly(1,1,1-trifluoro-2,3-epoxypropane). Top: Full spectrum. Bottom: Methylene region. **129**

Figure 4.1. Enantioselective polymerization of epoxides using **4.1**/**4.2**. **135**

Figure 4.2. GPC chromatographs of poly(1-butene) diolate initiated PPO (Table 4.5). **145**

Figure 4.3. Isopropoxide initiated PPO (Table 4.1, entry 5) Top: ^1H NMR spectrum in $CDCl_3$. Center: ^{13}C NMR spectrum in $CDCl_3$. Bottom: Expansion of methine region showing predominantly site-control errors. **150**

Figure 4.4. MALDI-MS of isopropoxide initiated PPO (Table 4.1, entry 5). **151**

Figure 4.5. NMR spectra of isopropoxide initiated PPO in $CDCl_3$. A: Expansion of methine region showing predominantly site-control errors (Table 4.1, entry 5). B: Expansion of methine region showing predominantly chain-end errors (Table 4.3, entry 4). **152**

Figure 4.6. NMR spectra of (*S*)-1-methoxy-2-propoxide initiated PPO (Table 4.2, entry 1) in CDCl3. Top: ^1H NMR spectrum. Bottom: ^{13}C NMR spectrum. **153**

Figure 4.7. ^{13}C NMR spectra of 1-methoxy-2-propoxide initiated PPO in $CDCl_3$ Top: Expansion of methine region (Table 4.2, entry 1). Bottom: Expansion of methine region (Table 4.2, entry 2). **154**

Figure 4.8. MALDI-MS of (*S*)-1-methoxy-2-propoxide initiated PPO (Table 4.2, entry 1). **155**

Figure 4.9. NMR spectra of PMB initiated PPO (Table 4.4, entry 4 before deprotection) in $CDCl_3$. Top: ^{1}H NMR spectrum. Center: ^{13}C NMR spectrum. Bottom: Expansion of methine region. **156**

Figure 4.10. MALDI-MS of PMB initiated PPO (Table 4.4, entry 4). **157**

Figure 4.11. Poly(1-butene) diolate initiated PPO. (Table 4.5, entry 4) in $CDCl_3$. Top: ^{1}H NMR spectrum. Center: ^{13}C NMR spectrum. Bottom: Expansion of methine region. **158**

Figure 4.12. NMR spectra of 1,8-octanediolate initiated PPO (Table 4.7, entry 5) in $CDCl_3$. Top: ^{1}H NMR spectrum. Center: ^{13}C NMR spectrum. Bottom: Expansion of methine region. **160**

Figure 4.13. MALDI-MS of 1,8-octanediolate initiated PPO (Table 4.7, entry 5). **161**

Figure 4.14. NMR spectra of 1,6-hexanediolate initiated PPO (Table 4.6, entry 5) in $CDCl_3$. Top: ^{1}H NMR spectrum. Center: ^{13}C NMR spectrum. Bottom: Expansion of methine region. **162**

Figure 4.15. MALDI-MS of 1,6-hexanediolate initiated PPO (Table 4.6, entry 5). **163**

Figure 4.16. NMR spectra of PPO diol (Table 4.4, entry 4 after deprotection) in $CDCl_3$. Top: ^{1}H NMR spectrum. Center: ^{13}C NMR spectrum. Bottom: Expansion of methine region. **164**

Figure 4.17. MALDI-MS of PPO diol (Table 4.4, entry 4 after deprotection). **165**

LIST OF SCHEMES

Scheme 1.1. Methine Region of the ^{13}C NMR Spectrum of Partially Isotactic Poly(propylene oxide) Showing Triad Stereoerrors **3**

Scheme 1.2. a) Chain-End b) Enantiomorphic-Site Mechanisms of Stereocontrol in Epoxide Polymerization c) Scenarios for the Construction of Tactic Polymers (L^{R}_{n}M-OR is an enantiomerically pure catalyst that prefers *R*-Monomer) **5**

Scheme 1.3. Synthesis of AlR_3/H_2O/acac Epoxide Polymerization Catalysts (R = alkyl) **7**

Scheme 1.4. Stereoselectivity of Polymerization of *cis*- and *trans*-2,3-Epoxybutane Using AlR_3/H_2O catalysts (R = alkyl) **9**

Scheme 1.5. Proposed Bimetallic Enchainment of Epoxides Using (acac)Al Complexes (acac = acetylacetonate, P = polymeryl) **11**

Scheme 1.6. Polymerization of Propylene Oxide with $[(R\text{-dmbd})_{1.5}Al]n/ZnCl_2$ Catalysts (dmbd = 3,3-dimethyl-1,2-butanediolate) **12**

Scheme 1.7. Attempted Enantioselective Polymerization of Racemic Propylene Oxide Using **1.4** **14**

Scheme 1.8. Polymerization of Epoxides with $ZnEt_2$/1-Phenoxy-2-propanol or 4-*tert*-Butylcatechol **16**

Scheme 1.9. Preparation of a Mixture of Isotactic and Syndiotactic Poly(cyclohexene oxide) Using Chiral Zinc Alkoxide Catalysts **17**

Scheme 1.10. Polymerization of Racemic Propylene Oxide with Zinc Alkoxide Cluster Catalysts **1.7**-**1.9** **19**

Scheme 1.11. Syndioselective Polymerization of Cyclohexene Oxide with **1.9** and Subsequent Degradation **20**

Scheme 1.12. Syndioselective Polymerization of Propylene Oxide with **1.10** **21**

Scheme 1.13. Chiral Zinc Catalysts for the Stereoselective, Alternating Copolymerization of Cyclohexene Oxide and CO_2 **22**

Scheme 1.14. Enantioselective Polymerization of Racemic *tert*-Butyl Ethylene Oxide and Epichlorohydrin Using **1.15**/$AlEt_3$ **25**

Scheme 1.15. Enantioselective Polymerization of Racemic Propylene Oxide Using

1.16 and **1.17**/[Ph_3PNPPh_3]Cl **26**

Scheme 1.16. Syndioselective Copolymerization of Cyclohexene Oxide and CO_2 with **1.18** **27**

Scheme 1.17. Synthesis of Stereogradient Iso-enriched Poly(propylene carbonate) **28**

Scheme 1.18. a) Isoselective Polymerization of Propylene Oxide Using **1.19**; b) Molecular Structure of Methoxide Analogue **1.20** **30**

Scheme 1.19. Enantioselective Polymerization of Epoxides with **1.21** **32**

Scheme 1.20. Isoselective Polymerization of Epoxides with **1.22** **33**

Scheme 1.21. Proposed Mechanism of Polymerization for **1.21** and **1.22** **34**

Scheme 2.1. Enantioselective and Isoselective Polymerization of Racemic Epoxides Using Bimetallic Cobalt Catalysts **45**

Scheme 2.2. Synthesis of Bimetallic Complex **2.2** **46**

Scheme 2.3. Synthesis of Bimetallic Complex **2.3** **47**

Scheme 2.4. Synthesis of Silver Carboxylates: **2.12**, **2.13**, **2.14** and PPN Carboxylates: **2.5**, **2.6**, **2.7** **49**

Scheme 2.5. Proposed Mechanism of Polymerization (P = polymer chain; X = Cl or carboxylate) **50**

Scheme 2.6. Synthesis of Ligand **2.18** **63**

Scheme 3.1. Bimetallic Complexes for the Synthesis of Isotactic Polyethers **96**

Scheme 3.2. Proposed Mechanism of Polymerization for **3.1a** and **3.1b** (P = polymer chain; X = chloride or carboxylate; C = cocatalyst cation) **97**

Scheme 3.3. Phosphazenium (**3.3**) and Phosphonium (**3.4**) Ionic Organic Cocatalysts for Bimetallic Cobalt Enantioselective Epoxide Polymerization Catalysts **98**

Scheme 4.1. Enantioselective Epoxide Polymerization Using Catalyst System **4.1**/**4.2**. A) Without Added Alcohols B) With Added Alcohols as Chain Transfer Agents **137**

Scheme 4.2. Stereochemical Possibilities During Polymerization of *rac*-PO with *rac*-**4.1**/**4.2** in the Presence of CTAs **139**

LIST OF TABLES

Table 2.1. Polymerization of Racemic Propylene Oxide with **2.3** and Cocatalysts **2.4**-**2.7** **49**

Table 2.2. Screening of Racemic Epoxides for Isoselective Polymerization Catalyzed by System **2.3**/**2.6** **51**

Table 2.3. Quantitative Conversion of Racemic Epoxides to Isotactic Polyethers Catalyzed by System **2.3**/**2.6** **52**

Table 2.4. Assignments of ^{1}H and ^{13}C NMR Chemical Shifts of Pyridine Adduct of **2.1** (**2.15**) **65**

Table 2.5. Crystal Data and Structure Refinement for **2.15** **88**

Table 2.6. Crystal Data and Structure Refinement for **2.16** **89**

Table 2.7. Crystal Data and Structure Refinement for **2.17** **90**

Table 3.1. Screening of Acetate–Based Cocatalysts for the Polymerization of PO with **3.1a**: Effect of Cation **99**

Table 3.2. Screening of Phosphazenium-Based Cocatalysts for the Polymerization of PO with **3.1a**: Effect of Anion **101**

Table 3.3. Enantioselective Polymerization of Epoxides with (**3.1a**/**3.3e**) **102**

Table 4.1. Polymerization of *rac*-PO Using ^{i}PrOH as CTA and Catalyst System **4.1**/**4.2** **138**

Table 4.2. Polymerization of *rac*-PO Using 1-Methoxy-2-propanol and Catalyst System **4.1**/**4.2** **140**

Table 4.3. Polymerization of *rac*-PO Using ***i***PrOH and Catalyst System *rac*-**4.1**/**4.2** **141**

Table 4.5. Polymerization of *rac*-PO Using Catalyst System **4.1**/**4.2** and Poly(1-butene) Diol **144**

Table 4.6. Polymerization of *rac*-PO Using Catalyst System **4.1**/**4.2** and 1,6-Hexanediol **146**

Table 4.7. Polymerization of *rac*-PO Using Catalyst System **4.1**/**4.2** and 1,8-Octanediol **159**

Chapter 1

Stereoselective Catalysts for the Ring-Opening Polymerization of Epoxides

Reproduced in part with permission from:

H. Ajiro, P. C. B. Widger, S. M. Ahmed, S. D. Allen, G. W. Coates

Comprehensive Polymer Science II

1.1. Introduction

1.1.1. Background

In the 1950s Baggett and Pruitt reported that iron (III) chloride was capable of polymerizing racemic propylene oxide to give a polymeric material that could be separated into amorphous as well as crystalline materials using solvent fractionation.[1-4] Shortly thereafter, Natta[5] and Price[6,7] provided evidence that the crystalline material was isotactic poly(propylene oxide), in which the main-chain stereogenic centers of each macromolecule were of the same relative configuration. This finding marked the first discovery of a stereoselective catalyst for epoxide polymerization. This chapter highlights the significant advances made in the field of stereoselective epoxide polymerization, including copolymerizations since the initial findings of Baggett, Pruitt, Natta and Price.

1.1.2. Scope of Chapter

Many of the important contributors to the field of stereoselective epoxide polymerization have written accounts of their research,[8-20] but there are few collective contemporary reviews of the work done in this area.[21] This chapter focuses on discrete catalysts for the stereoselective polymerization of racemic epoxides. Due to space limitations, only catalysts bearing at least one ancillary ligand that is not likely to react with epoxides are discussed; catalysts only bearing ligands that are well-known to react with epoxides are not covered. A discussion of strategies for controlling the relative configuration of main-chain stereogenic centers of epoxide polymers is included. The polymerization of enantiopure epoxides[6] is not covered as the emphasis of this chapter is on stereochemical control of polymerization by the catalyst or initiator.

1.2. Basic Concepts in Stereoselective Epoxide Polymerization

1.2.1. Regiochemistry

Both the ancillary ligands (L_n) surrounding the active metal center (M) and the growing polymer chain (OR) influence the regiochemistry and stereochemistry of epoxide polymerization.[22] When the epoxide is unsymmetrically substituted (i.e. propylene oxide), enchainment commonly occurs in two ways: (1) S_N2 attack by the polymer's alkoxide chain-end at the less substituted methylene with retention of the stereochemistry of the substituted carbon to give a secondary metal alkoxide; or (2) S_N2 attack at the substituted methine with inversion of stereochemistry to give a primary metal alkoxide. The polymer is regioregular when only one process dominates; the polymer is regioirregular when both processes occur. The regiochemistry of a polyether (such as poly(propylene oxide)) can be readily determined by ^{13}C NMR spectroscopy.[23-25]

Scheme 1.1. Methine Region of the ^{13}C NMR Spectrum of Partially Isotactic Poly(propylene oxide) Showing Triad Stereoerrors

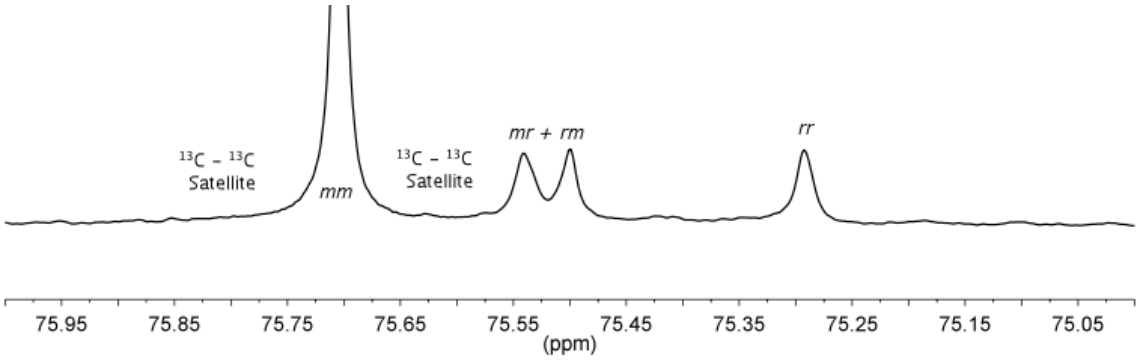

1.2.2. Analysis of Polymer Stereochemistry

NMR spectroscopy is the most useful method for determining polymer tacticity.[26,27] In many cases, the chemical shifts for the various polymer nuclei are sensitive to adjacent stereogenic centers, resulting in fine structure that can provide quantitative information about the polymer microstructure once the shift identities are assigned. For example, the methyl, methylene, and methine regions of a high-resolution ^{13}C NMR spectrum of regioregular atactic poly(propylene oxide) display several resonances, each of which represents a different set of consecutive stereocenters. As each resonance in the spectrum has been assigned (Scheme 1.1),[23,24,28] a routine ^{13}C NMR experiment can reveal both the tacticity and the degree of stereoregularity of a sample of poly(propylene oxide).

1.2.3. Chain-End Control and Enantiomorphic-Site Control of Stereochemistry

In a chain-growth polymerization reaction, one end of the polymer chain remains at the active metal center during monomer enchainment. Thus, the stereogenic center in the polymer chain from the last enchained monomer unit will have an influence on the stereochemistry of monomer enchainment. If this influence is significant, the mode of stereochemical regulation is referred to as "polymer chain-end control" (Scheme 1.2a). If the active site is chiral and overrides the influence of the polymer chain end, the mechanism of stereochemical direction is termed "enantiomorphic-site control" (Scheme 1.2b).[9-11] The Bovey formalism is a convenient way to describe polymer tacticity, where an "*m*" for *meso* (same stereo-configuration), or an "*r*" for *racemic* (opposite stereo-configuration) describes relationships between adjacent stereogenic centers (dyads). These dyads are seen as unique signals in ^{13}C NMR. The monomer enchainment

mechanism can be easily identified by observing the stereochemical errors propagated in a polymer chain. The ratio of the signals in a ^{13}C NMR spectrum can be used to determine the mechanism of stereocontrol. In the case of an isotactic polymer, a "chain-end control" mechanism produces polymers in which stereoerrors are propagated (i.e. would display primarily *mm*, *mr*, and *rm* triads, Scheme 1.2a). In the "enantiomorphic-site control" mechanism, correction of stereoerrors occurs because the ligands direct the stereochemical events, leading to an isolated error (i.e. produces a polymer which would display primarily *mm*, *mr*, *rm*, and *rr* triads, Scheme 1.2b).

Scheme 1.2. a) Chain-End b) Enantiomorphic-Site Mechanisms of Stereocontrol in Epoxide Polymerization c) Scenarios for the Construction of Tactic Polymers (L^R_nM-OR is an enantiomerically pure catalyst that prefers *R*-Monomer)

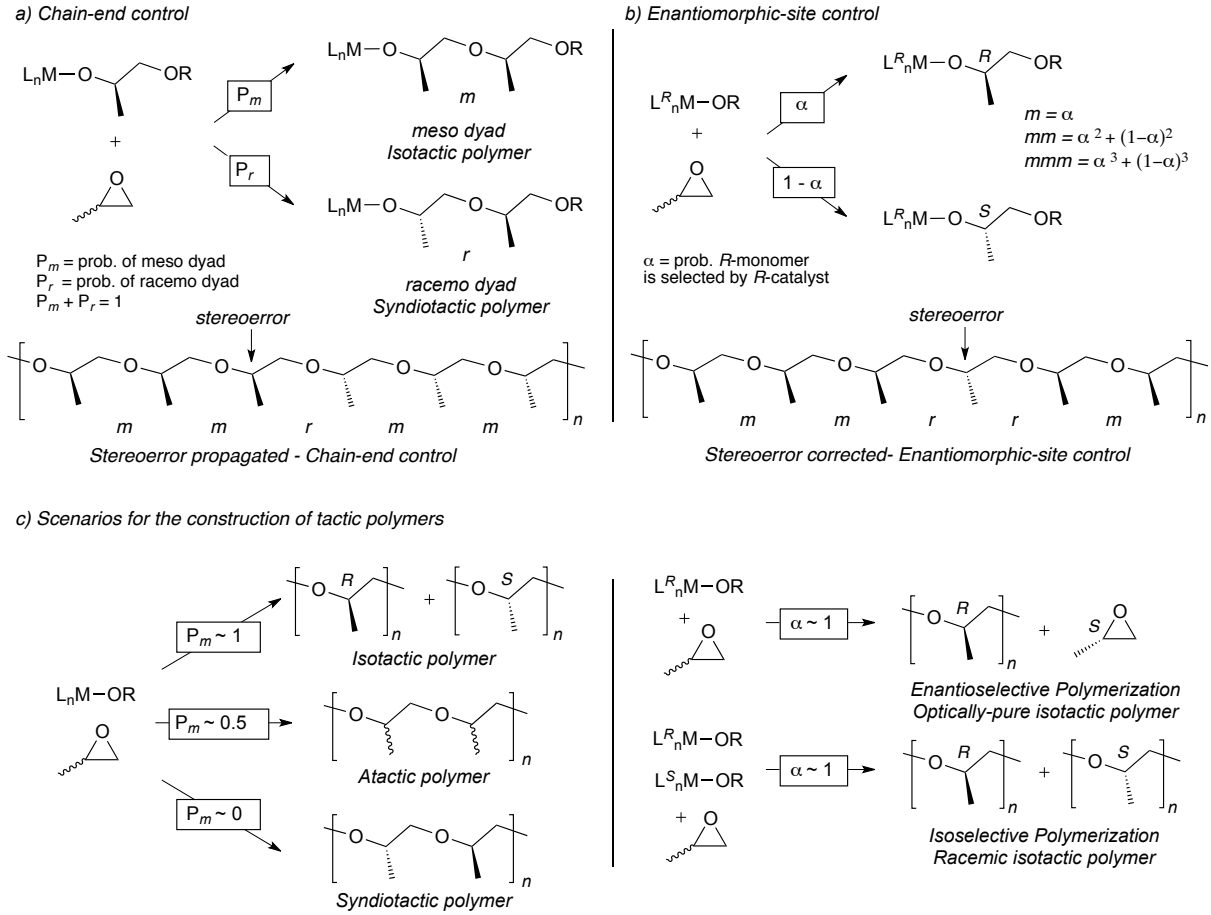

Optically active catalysts can kinetically resolve racemic monomers (Scheme 1.2c) via enantioselective polymerization producing optically active polymers as well as enantiomerically enriched monomers. The nonpreferred enantiomer remains unreacted in the reaction mixture after the preferred enantiomer of monomer has been enchained as a polymer. The quantitative measure of stereocontrol in such a system is given by the selectivity factor (s = s-factor), which is the ratio of the rate constants for the polymerization of the fast enantiomer converted to polymer with respect to the slow enantiomer enchained [$s = k_{fast}/k_{slow} = \alpha/(1 - \alpha)$].[29] A racemic enantioselective catalyst can polymerize both enantiomers of racemic monomer via isoselective polymerization to give racemic isotactic polymer.

1.3. Stereoselective Epoxide Polymerization

The vast majority of papers reporting stereoselective epoxide polymerization focus on the polymerization of propylene oxide using different metal-based catalysts. Thus, this chapter is organized based on the metal of the active center of the catalyst. Aluminum, zinc, cobalt, tin and chromium are the most commonly used metals for discrete stereoselective epoxide polymerization catalysts and their use in this field of research forms the foundation of this review.

1.3.1. Aluminum-Based Catalysts

Although aluminum alkoxide- and aluminoxane-based catalysts have shown promise for the isoselective polymerization of epoxides, the poorly defined nature of these species has significantly hampered their use in such polymerizations due to the formation of large amounts

of atactic polyether.[30] Some examples of discrete aluminum complexes have been reported herein.

1.3.1.1. Aluminum–acetylacetonate complexes

The prevailing theory for the mechanism of epoxide polymerization has been that epoxide coordination to the metal center precedes insertion. To support this mechanism, Vandenberg proposed that the addition of chelating agents such as acetylacetone (acac) to an R_3Al/H_2O (R = alkyl) polymerization system would block potential coordination sites on the metal center, thus hindering the reaction. Instead, these additives enhanced the polymerization rate and ushered in a new class of versatile and highly active catalysts.[12,31-33] The presumed structure of the active aluminum-acac catalyst is shown in Scheme 1.3. Although the precise structure of the active catalyst is unknown, a few structural features have been determined: (1) an oxygen atom bridges two aluminum centers (although the presence of multiple linkages, such as those in oligomeric aluminoxanes, cannot be ruled out); (2) alkyl groups are present on the aluminum atoms; and (3) the acac ligand is chelated to the aluminum center.[20]

Scheme 1.3. Synthesis of AlR_3/H_2O/acac Epoxide Polymerization Catalysts (R = alkyl)

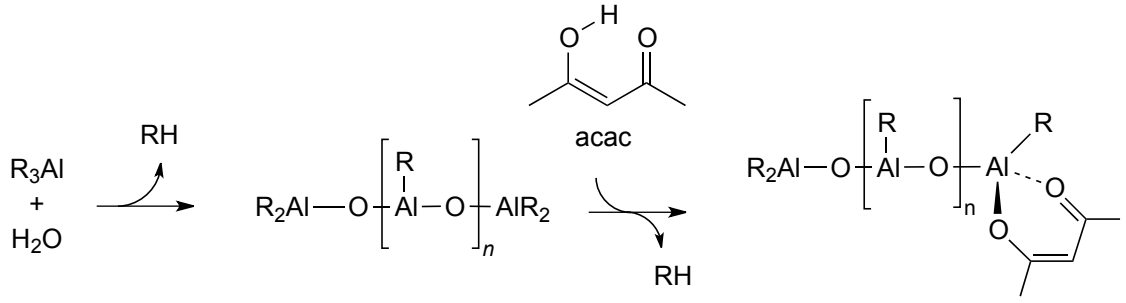

Tuning the AlR_3/H_2O/acac catalyst (R = alkyl) composition by varying the R groups and the ratio of components creates systems that conduct epoxide polymerizations to give high conversions, in many instances achieving >90% conversion to give high-molecular-weight, acetone-insoluble polyethers. The fraction of acetone-insoluble, isotactic polymer produced varies according to the exact composition of the catalyst system used, and is approximately 30% of the total mass of the ether-insoluble material, while the remaining 70% is acetone-soluble atactic polymer.[32,33]

In work investigating the mechanism of this system, Vandenberg used AlR_3/H_2O catalysts to polymerize *cis*- and *trans*-2,3-epoxybutane. Mechanistic information for the polymerization was obtained from the properties of the resultant polymers and the examination of the diol decomposition products. These results are summarized in Scheme 1.4.[12,20,34-36]

Scheme 1.4. Stereoselectivity of Polymerization of *cis*- and *trans*-2,3-Epoxybutane Using AlR_3/H_2O catalysts (R = alkyl)

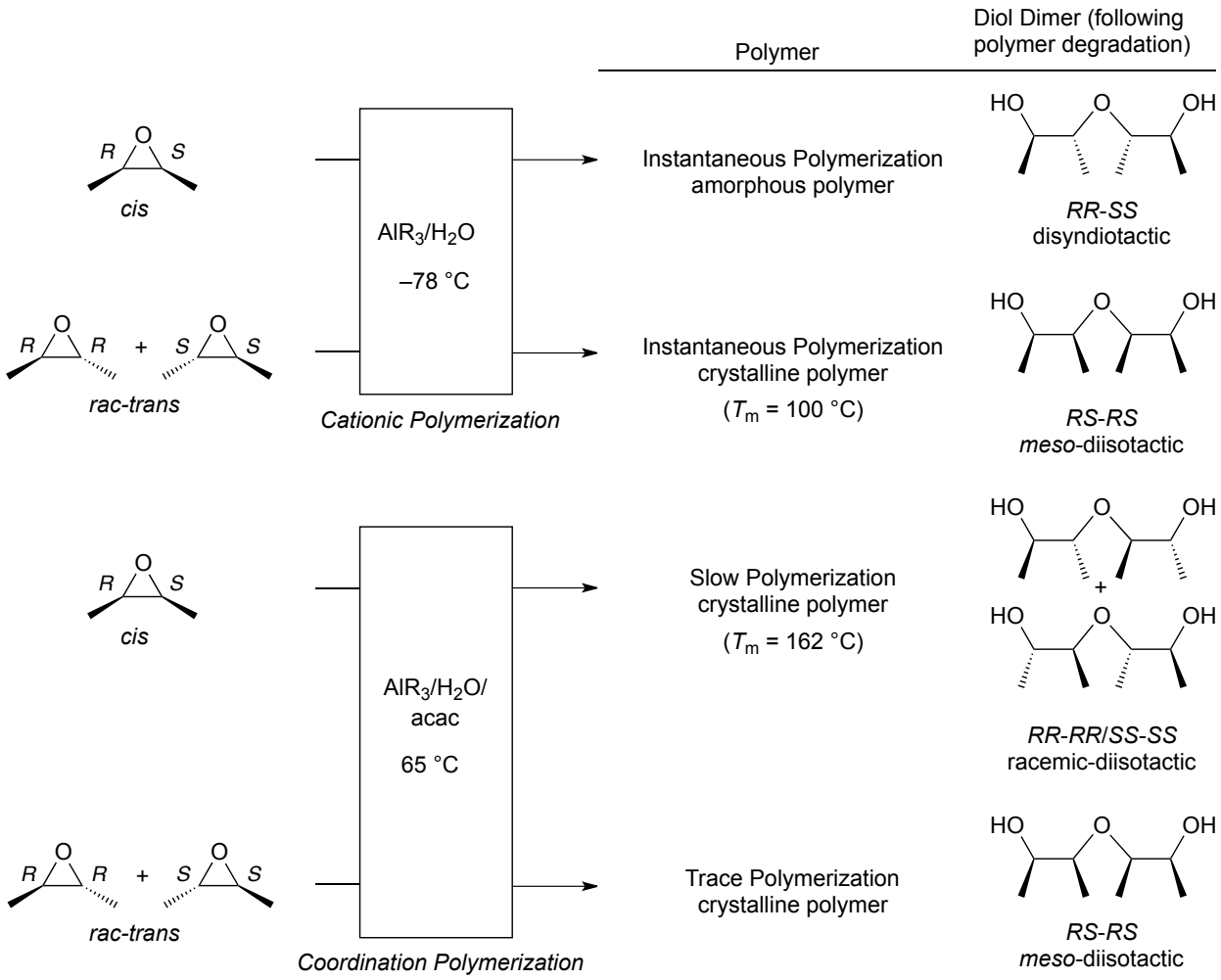

The AlR_3/H_2O catalysts polymerize both *cis*- and *trans*-2,3-epoxy butane instantaneously at –78 °C, consistent with a cationic process for monomer enchainment. The polymer isolated from the *cis* isomer is an amorphous rubber, whereas the polymer isolated from the *trans* isomer is crystalline with a T_m of 100 °C. This finding is in contrast to the AlR_3/H_2O/acac system, which only slowly polymerizes the same monomers at 65 °C, presumably through a much slower coordination–insertion mechanism. The coordination polymerization of the *cis* isomer yields a crystalline polymer with a T_m of 162 °C, whereas the *trans* isomer polymerizes extremely

slowly, producing only trace amounts of a crystalline polymer with a T_m similar to that obtained with the cationic polymerization. Vandenberg attributes the extremely slow polymerization of the *trans* isomer to its increased steric bulk compared to the *cis* isomer at the metal coordination site. The steric bulk hinders the required pre-coordination to the metal center for monomer insertion.

Through the controlled degradation of the polyethers to diol dimers using *n*-butyl lithium, the stereochemistry of the monomer units in the polymer chain was determined.[34] The decomposition of all four polymers showed that inversion of stereochemistry at the site of attack on the epoxide ring occurred in both cationic and coordination-insertion polymerization mechanisms. The *cis* epoxides (*RS* stereocenters) produce monomeric units in the polymer chain with *RR* and *SS* stereocenters, and the *trans* epoxides (either *RR* or *SS*) produce monomeric units in the polymer chain with only *RS* units. This observation shows that both polymerizations are stereospecific, with inversion of configuration occurring at the site of attack, regardless of the polymerization mechanism.

To obtain the geometry required for a S_N2 attack in a coordination–insertion mechanism, Vandenberg proposed the transition structure shown in Scheme 1.5. In this scheme, an epoxide is activated by coordination to an aluminum center, while the adjacent aluminum center delivers the growing polymer chain. During this process, coordination bonds are exchanged to keep the charges balanced. Despite the evidence for bimetallic epoxide ring-opening events in other systems,[37-39] there is little evidence beyond the epoxide inversion, to show that it occurs in these heterogeneous aluminum-based systems.

Scheme 1.5. Proposed Bimetallic Enchainment of Epoxides Using (acac)Al Complexes (acac = acetylacetonate, P = polymeryl)

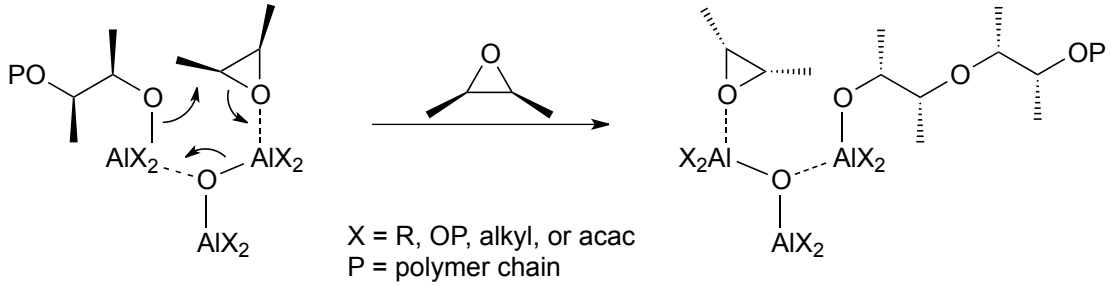

1.3.1.2. Aluminum systems featuring chiral alkoxides

Haubenstock and coworkers synthesized chiral aluminum alkoxides for the stereoselective polymerization of propylene oxide.[40] Addition of 1.5 equiv. of (*R*)-(–)-3,3-dimethyl-1,2-butanediol ((*R*-dmbd)H_2) to AlH_3 generated the active complex $[(R\text{-dmbd})_{1.5}/Al]_n$. Alone, $[(R\text{-dmbd})_{1.5}/Al]_n$ displayed very low activity for the polymerization of propylene oxide, achieving 85% conversion in 3 weeks with negligible optical activity in the unreacted monomer. The addition of $ZnCl_2$ (Al:Zn = 1:1) to the $[(R\text{-dmbd})_{1.5}/Al]_n$ initiator generated a much more active catalyst, as shown in Scheme 1.6. Furthermore, the optical activity of the unreacted propylene oxide was observed to increase with increasing conversion to polymer, and based on the optical rotation of the unreacted monomer, Haubenstock and coworkers determined that the catalyst system preferentially reacted with (*R*)-propylene oxide because the reaction solution became enriched in the (*S*) enantiomer, although with modest selectivity (s = 1.05).[40] On fractionation, 10% of the total mass of the isolated polymer was acetone-insoluble and highly isotactic (>99% *m*-dyads), whereas the remainder of the polymer was acetone-soluble and atactic. Although a slight enantiomeric enrichment of monomer was achieved, this system did not significantly improve the yield of isotactic poly(propylene oxide) compared to similar systems,[41-43] and it is unclear whether the selective enchainment of the *R*-enantiomer was

contributing to the formation of the 10% of crystalline polymer as opposed to it arising from a different mechanism.

Scheme 1.6. Polymerization of Propylene Oxide with $[(R\text{-dmbd})_{1.5}Al]_n/ZnCl_2$ Catalysts (dmbd = 3,3-dimethyl-1,2-butanediolate)

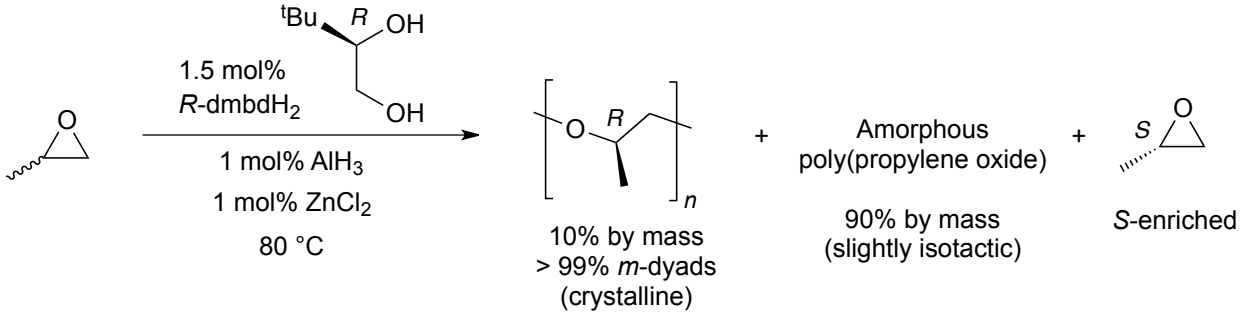

1.3.1.3. Aluminum–porphyrin complexes

Inoue first reported that 5, 10, 15, 20-tetraphenylporphyrin (tpp) aluminum chloride (Figure 1.1, **1.1**) was active for the living polymerization of propylene oxide.[44-46] Although the polymer microstructure was not studied in great detail, ^{13}C NMR spectra showed the polymers to be highly regioregular and slightly isotactic.[44,45] The activity of (tpp)AlCl was relatively low, requiring 6 days to achieve completely polymerize 200 equiv. of propylene oxide. The addition of Cl or OMe substituents on the porphyrin ligand, as in (*p*-Cl-tpp)AlCl (**1.2**) and (*p*-OMe-tpp)AlCl (**1.3**), increased the activity by a factor of two, but the tacticity of the resulting polymers was not discussed.[45] More detailed ^{13}C NMR analyses by Le Borgne and coworkers showed that the poly(propylene oxide) derived from **1.1** was slightly isotactic, with an *m*-dyad content of 69% and an *mm*-triad content of 45%, confirming the initial results reported by Inoue.[24]

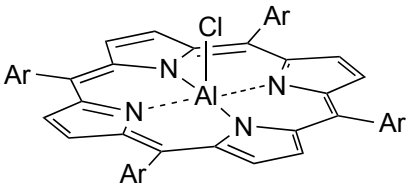

Ar = C_6H_5 (tpp); **1.1**
Ar = *p*-C_6H_4Cl (*p*-Cl-tpp); **1.2**
Ar = *p*-C_6H_4OMe (*p*-OMe-tpp); **1.3**

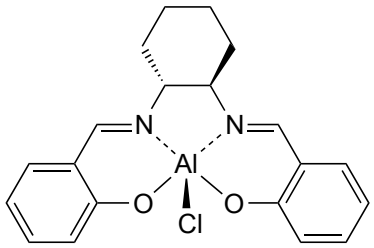

(*R,R*-salcy)AlCl; **1.4**

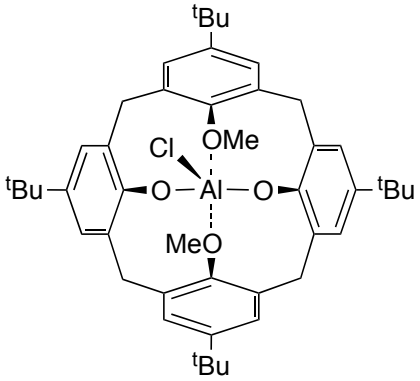

(dmca)AlCl; **1.5**

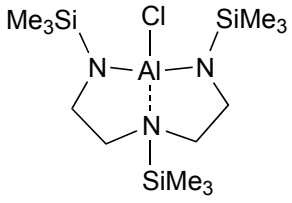

1.6

Figure 1.1. Well-defined complexes for the polymerization of epoxides (tpp = 5, 10, 15, 20-tetraphenylporphyrin; salcy = *N,N′*-bis-(2-hydroxybenzylidene)-(1*R*,2*R*)-1,2-cyclohexanediamine); dmca = dimethylcalixarene.

1.3.1.4. Aluminum–schiff-base complexes

Well-defined [*N,N*'-bis-(2-hydroxybenzylidene)-(1*R*,2*R*)-1,2-cyclohexane-diamine] (*R,R*-salcy) aluminum complexes (Figure 1.1, **1.4**) have been used as enantioselective epoxide polymerization catalysts.[47-49] Polymerization of racemic propylene oxide in the presence of 5 mol% **1.4** yields approximately 70% conversion to poly(propylene oxide) after 62 hours. The remaining unreacted monomer exhibits an optical rotation of +1.85°, which corresponds to an *ee*

of 15% (Scheme 1.7). The modest *s*-factor of 1.3 obtained in this system is slightly higher than that observed for the previously discussed heterogeneous aluminum systems.[50] Examination of the isolated polymer reveals both chloro and hydroxyl end-groups, suggesting that each metal center produces a single polymer chain since each chain bears a Cl atom from initiation and a hydroxyl group from termination.[48]

Scheme 1.7. Attempted Enantioselective Polymerization of Racemic Propylene Oxide Using **1.4**

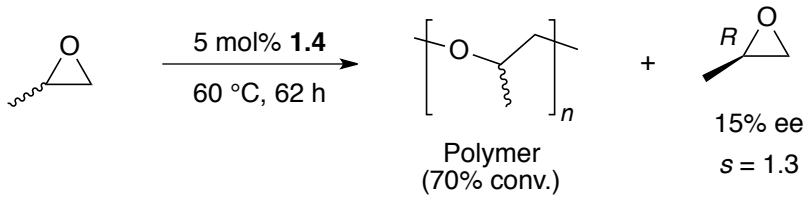

1.3.1.5. Aluminum–calixarene complexes

Kuran and coworkers synthesized a dimethylcalixarene-based system (Figure 1.1, **1.5**) that exhibited low activity for propylene oxide polymerization TOF = 0.06 h^{-1}.[51] The polymerization of propylene oxide produced predominantly isotactic poly(propylene oxide) with an *m*-dyad content of approximately 74%.

1.3.1.6. Other well-defined aluminum systems

N,*N*′,*N*″-Tris(trimethylsilyl)diethylenetriamine complexes of aluminum have been shown to be active oligomerization catalysts for propylene oxide.[52] Over the course of 2 days, catalyst **1.6** (Figure 1.1) produces low-molecular-weight poly(propylene oxide) (M_n < 500 g mol^{-1}) with predominantly head-to-tail linkages and an *m*-dyad content of 60%.

1.3.2. Zinc-Based Catalysts

During research on aluminum catalysts for the stereoselective polymerization of epoxides, it was discovered that the addition of zinc cocatalysts to these systems greatly enhanced catalyst activity.[41] These enhancements prompted a number of studies focusing on the design of zinc-based catalyst systems.

1.3.2.1. Zinc alkoxide catalysts

Furukawa and coworkers explored catalysts derived from the addition of methanol or ethanol to diethylzinc as epoxide polymerization systems,[53] and found that both the yield and crystallinity of the resulting polymers were inferior to those for polymers synthesized with the $ZnEt_2/H_2O$ system. The use of achiral alcohols as co-catalysts was revisited in 1994 when Kuran and coworkers reported the polymerization of propylene oxide and cyclohexene oxide (a *meso* substrate) with $ZnEt_2$/polyhydric phenol (such as 4-*tert*-butyl-catechol), phenol, or 1-phenoxy-2-propanol.[54] The poly(propylene oxide) formed from these systems contained mostly isotactic dyads (72% *m*), while the poly(cyclohexene oxide) contained mostly syndiotactic dyads (80% *r*) (Scheme 1.8).

Scheme 1.8. Polymerization of Epoxides with $ZnEt_2$/1-Phenoxy-2-propanol or 4-*tert*-Butylcatechol

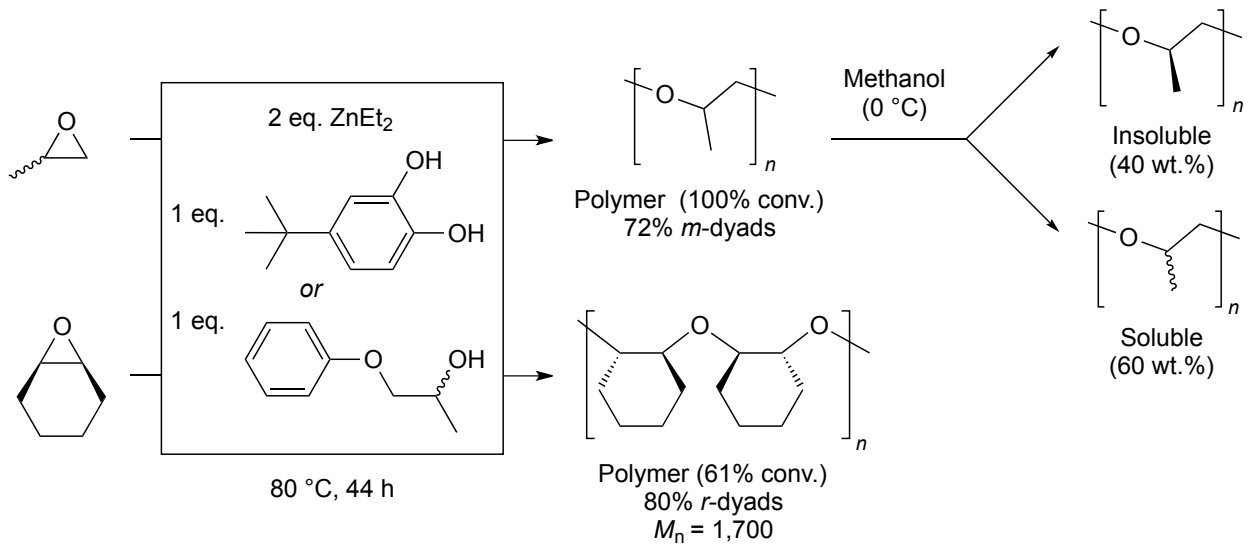

1.3.2.2. Chiral zinc alkoxide catalysts

Sigwalt and coworkers noted higher stereoselectivity during the polymerization of propylene sulfide using a (*R*)-3,3-dimethyl-1,2-butanediol/$ZnEt_2$ system when compared to a similar chiral alcohol/$ZnEt_2$ system. Based on these results, they applied this system to propylene oxide polymerization, but noticed that stereoselectivity was actually lower than that for the polymerization of propylene sulfide.[16,55,56] This lower stereoselectivity was attributed to the weaker coordination of the "harder" epoxide oxygen atom to zinc, as compared to the "softer" coordination of the episulfide sulfur atom.

Sepulchre and coworkers investigated the polymerization of cyclohexene oxide using $ZnEt_2$ activated with water, alcohols, and chiral alcohols. In their study, a mixture of $ZnEt_2$ and 1-methoxy-2-propanol or (1*S*,2*R*)-ephedrine simultaneously afforded a mixture of isotactic and syndiotactic poly(cyclohexene oxide) that was characterized using ^{1}H and ^{13}C NMR spectroscopy (Scheme 1.9).[57,58] They proposed a "flip-flop" mechanism (similar to that proposed

by Vandenberg as shown in Scheme 1.5) involving neighboring zinc centers to explain this observation.[20]

Scheme 1.9. Preparation of a Mixture of Isotactic and Syndiotactic Poly(cyclohexene oxide) Using Chiral Zinc Alkoxide Catalysts

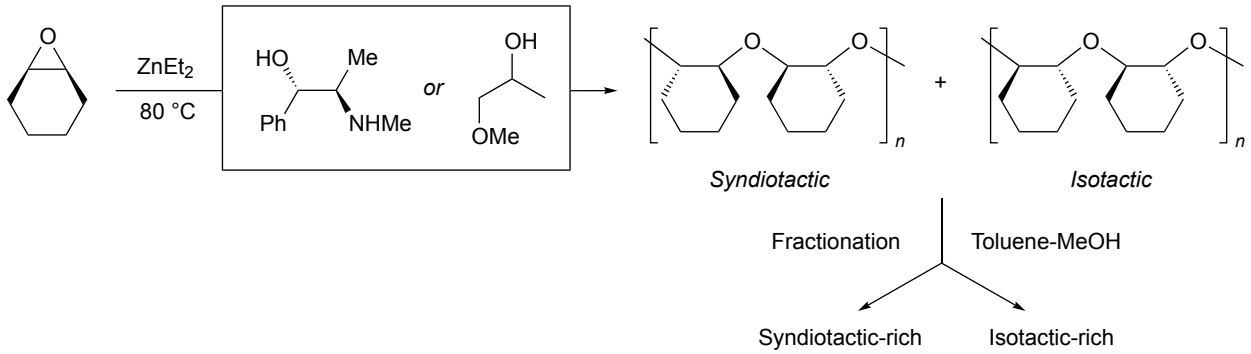

1.3.2.3. Zinc alkoxide clusters

Tsuruta and coworkers synthesized and investigated the epoxide polymerization activity of several well-defined zinc clusters (Figure 1.2).[59-68] Complexes $[Zn(OMe)_2 \bullet (EtZnOMe)_6]$ (**7**), $[Zn(OCH_2CH_2OMe)_2 \bullet (EtZnOCH_2CH_2OMe)_6]$ (**1.8**), and $[\{CH_3OCH_2CH(Me)OZnOCH(Me)CH_2OCH_3\}_2 \bullet \{EtZnOCH(Me)CH_2OCH_3\}_2]$ ($[Zn\text{-}MP]_{2,2}$) (**1.9**), were synthesized by the dropwise addition of 1.1 equiv. of the corresponding alkoxyalcohols to $ZnEt_2$ in heptanes at 5 °C. Each complex was crystalline, and its molecular structure was determined using X-ray crystallography (Figure 1.2).[59,62,68]

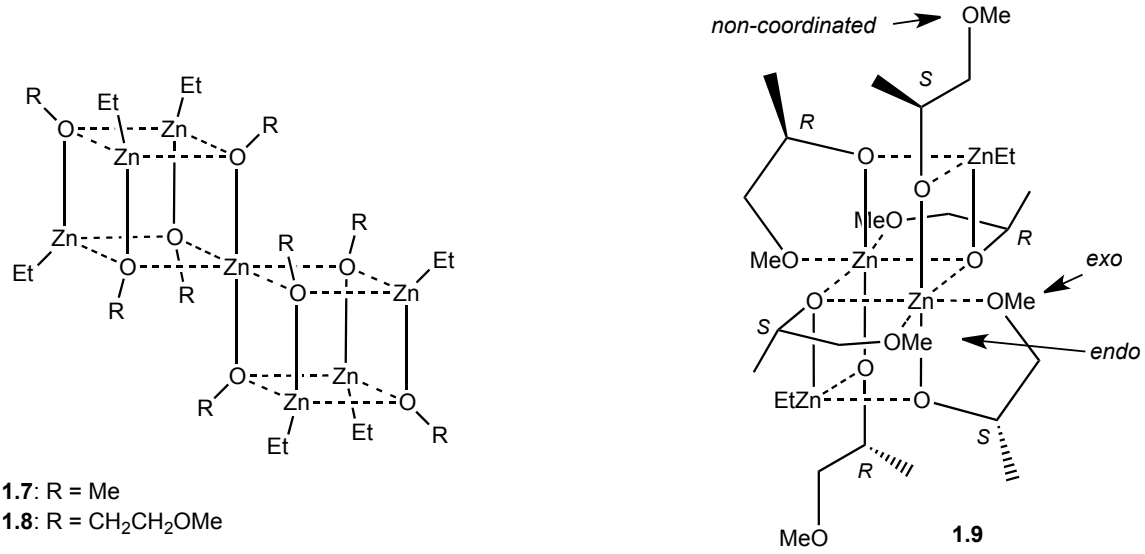

Figure 1.2. Structures of zinc cluster catalysts **1.7**, **1.8**, and **1.9**.

The propylene oxide polymerization activity for each complex is shown in Scheme 1.10. Surprisingly, isostructural complexes **1.7** and **1.8** had significantly different polymerization activities; **1.7** achieved 91% conversion in 216 hours, while **1.8** only attained 22% conversion in 240 hours. Catalyst **1.9**, however, was twice as active as complex **1.7**. This catalyst has a different molecular structure, as shown in Figure 1.2. Complex **1.9** bears six methoxy isopropyl groups in a chair-like structure in three different coordination environments; the methoxy groups are either *endo*- and *exo*-coordinated to the central zinc atoms through dative bonds, or non-coordinated.

Scheme 1.10. Polymerization of Racemic Propylene Oxide with Zinc Alkoxide Cluster Catalysts **1.7**-**1.9**

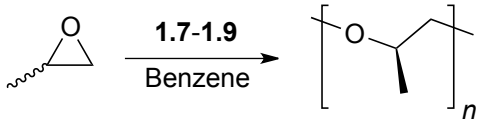

Catalyst	Temp. (°C)	Time (h)	Yield (%)	*m*-Dyads (%)
1.7	80	216	91	63
1.8	80	240	22	59
1.9	80	100	93	79
1.9	35	240	9	81

Studies using a deuterated version of **1.9** revealed that the non-coordinating methoxyisopropoxide groups initiated the polymerization by attack on the propylene oxide monomer, whereas the coordinated methoxyisopropoxide groups provided the chiral structure which remained unchanged during the polymerization.[63] When these complexes were screened for cyclohexene oxide polymerization, only **1.9** was found to be active.[69,70] Through ^{1}H NMR spectroscopic analysis of polymer decomposition products (using Vandenberg's method[34]), Tsuruta and coworkers determined that the poly(cyclohexene oxide) obtained was predominantly syndiotactic (Scheme 1.11).

Scheme 1.11. Syndioselective Polymerization of Cyclohexene Oxide with **1.9** and Subsequent Degradation

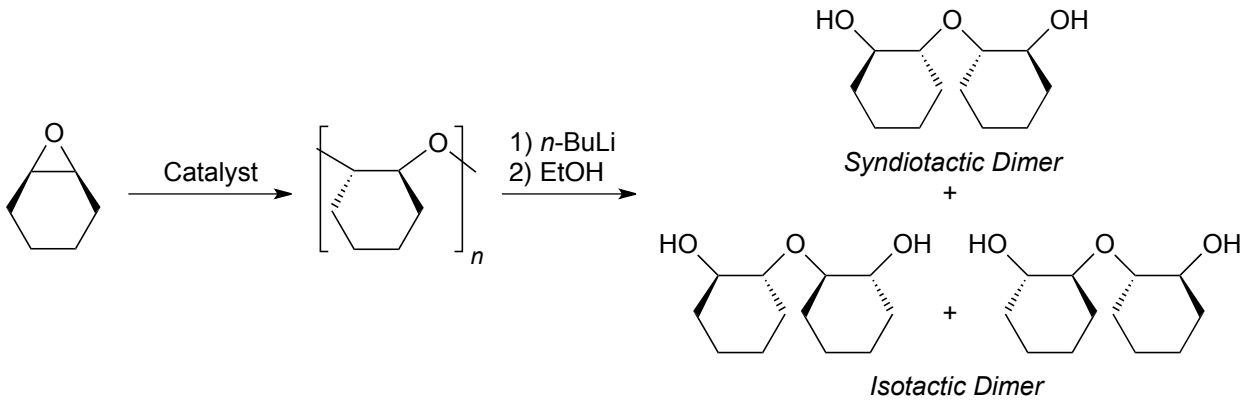

Catalyst	Syndiotactic Dimer (%)	Isotactic Dimer (%)
$ZnEt_2$	66	34
$(EtZnOMe)_4$	66	34
1.9	81	19

1.3.2.4. Zinc porphyrin–based catalysts

Inoue and coworkers reported that the polymerization of propylene oxide at 20 °C with the zinc porphyrin catalyst (Et_2Zn/*N*-methyl-5, 10, 15, 20-tetraphenylporphyrin, **1.10**) produced syndiotactic poly(propylene oxide) (M_w = 31,000, 60% *r*) (Scheme 1.12). This result was in contrast to those seen for all other zinc-based systems, which afford isotactic poly(propylene oxide). The authors attributed the unexpected syndiotactic microstructure of the polymer to the planar ligand and the isolated nature of the zinc center, which is different than that present in most other zinc aggregate systems.[44]

Scheme 1.12. Syndioselective Polymerization of Propylene Oxide with **1.10**

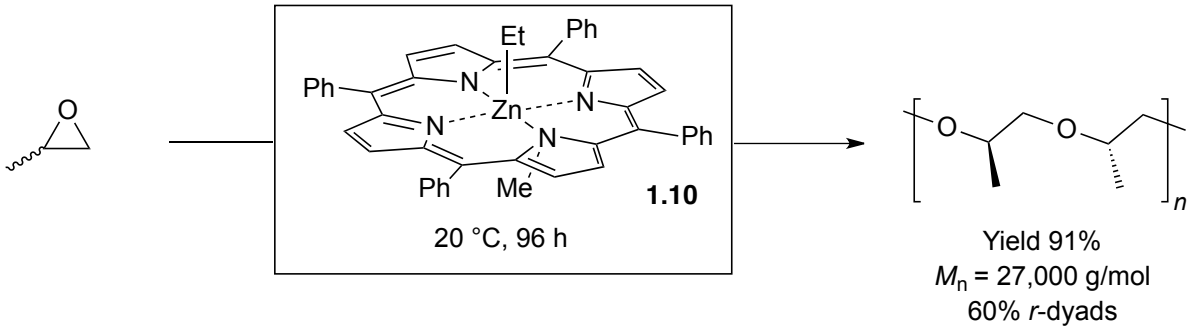

1.3.2.5. Zinc catalysts for asymmetric cyclohexene oxide/CO_2 copolymerization

There is significant interest in controlling the absolute stereochemistry of ring-opening in epoxide/CO_2 copolymerization. Cyclohexene oxide, a *meso* molecule, is an ideal substrate for desymmetrization using chiral catalysts. In 1999, Nozaki reported that a 1:1 mixture of $ZnEt_2$ and (*S*)-α,α-diphenylpyrrolidine-2-yl-methanol (**1.11**) (Scheme 1.13) was active for stereoselective cyclohexene oxide/CO_2 copolymerization at 40 °C and 30 atm CO_2.[71] The resultant polycarbonate contained 100% carbonate linkages, had an M_n of 8,400 g mol^{-1}, and had a M_w/M_n of 2.2. Hydrolysis of this poly(cyclohexene carbonate) with base produced the corresponding *trans*-cyclohexane-1,2-diol with 73% *ee*. ^{13}C NMR spectroscopy studies of model polycarbonate oligomers afforded spectral assignments for the isotactic (153.7 ppm) and syndiotactic dyads (153.3–153.1 ppm) of poly(cyclohene oxide),[72] which agreed with those proposed by Coates *et. al*.[73] Finally, the ring-opening polymerization proceeded stereospecifically via complete inversion of configuration (S_N2 mechanism) of one carbon of each repeat unit; hence, no *cis*-cyclohexane-1,2-diol was observed after base-catalyzed degradation of the polycarbonate.

Scheme 1.13. Chiral Zinc Catalysts for the Stereoselective, Alternating Copolymerization of Cyclohexene Oxide and CO_2

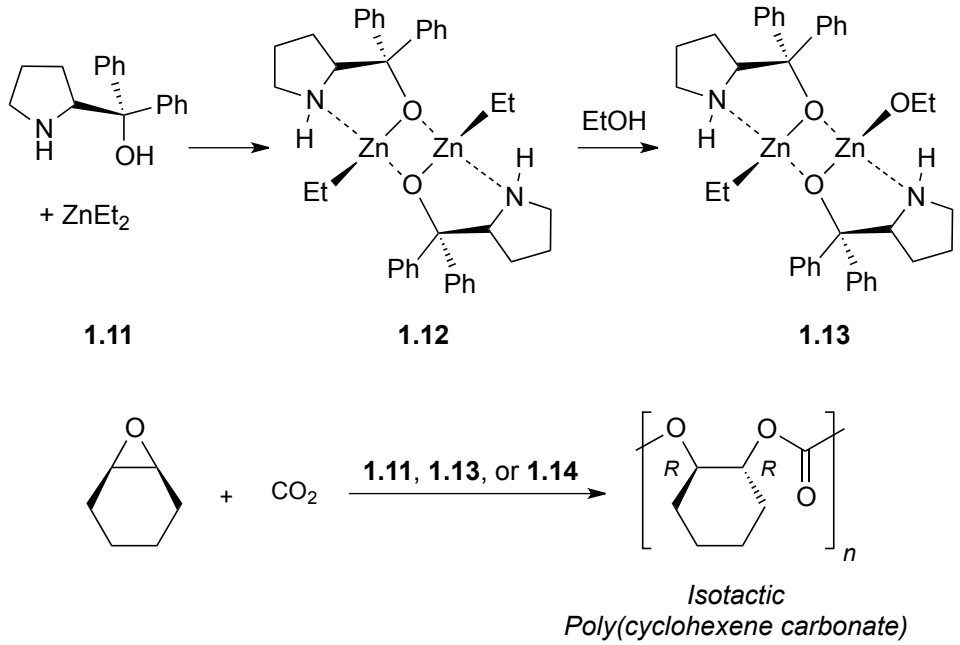

In a 2003 report, Nozaki and coworkers isolated presumed intermediates in the asymmetric alternating copolymerization of cyclohexene oxide with CO_2.[74] Reaction of a 1:1 mixture of $ZnEt_2$ and (*S*)-α,α-diphenylpyrrolidine-2-yl-methanol (**1.11**, Scheme 1.13) yielded dimeric **1.12**, which was structurally characterized by X-ray diffraction studies. At 40 °C and 30 atm CO_2, **1.12** catalyzed the formation of isotactic poly(cyclohexene carbonate) (M_n = 11,800 g mol^{-1}, M_w/M_n = 15.7) with a turnover frequency of 0.6 h^{-1}. Hydrolysis of the resulting poly(cyclohexene carbonate) yielded the *trans*-cyclohexane-1,2-diol of 49% *ee*, which was lower than that seen with catalyst **1.11**. When copolymerization was attempted using a catalyst system consisting of **1.12** and 0.2–1.0 equiv. EtOH (**1.12**/EtOH), the *ee* of the hydrolyzed cyclohexane diol increased up to 80%. The catalyst and EtOH combination resulted in better control of polymer molecular weights and molecular weight distributions in comparison to polymerization

using only **1.12**. Compound **1.13** (Scheme 1.13) was proposed to be the active initiating species in this polymerization. End-group analysis of the poly(cyclohexene carbonate)s prepared with **1.12** and **1.12**/0.2 EtOH by matrix-assisted laser desorption/ionization time-of-flight (MALDI-TOF) mass spectrometry revealed that in the absence of ethanol or in the presence of 0.2 eq. ethanol, end group signals assignable to an aminoalcohol-initiated polymerization were identified. However, as EtOH addition was increased from 0.2 to 1.0 equiv., signals corresponding to the aminoalcohol-initiated polycarbonate disappeared as signals corresponding to end-group structures for EtOH-initiated poly(cyclohexene carbonate) emerged. This result was further confirmed by end-group analysis using ^{1}H NMR spectroscopy. Finally, mechanistic studies suggested that the dimeric form of the catalyst, **1.13**, was in fact the active species.

In 2000, Coates and coworkers developed C_1-symmetric imine-oxazoline ligated zinc bis(trimethylsilyl)amido compounds (Figure 1.3, **1.14**) for the isoselective, alternating copolymerization of cyclohexene oxide and CO_2.[73] Through multiple electronic and steric manipulations of the imine-oxazoline ligand framework, compound **1.14** was found to exhibit the highest enantioselectivity for polymerization (*RR*:*SS* ratio in polymer = 86:14; 72% *ee*). Poly(cyclohexene carbonate) prepared with this catalyst possessed 100% carbonate linkages, an M_n of 14,700 g mol^{-1}, and an M_w/M_n of 1.35. This poly(cyclohexene carbonate) was crystalline with a glass transition temperature (T_g) of 120 °C, and a melting temperature (T_m) of 220 °C. Furthermore, stereocontrol was also achieved in the alternating copolymerization of cyclopentene oxide and CO_2, producing poly(cyclopentene carbonate) with an *RR*:*SS* ratio of 88:12 (76% *ee*). As revealed by ^{13}C NMR spectroscopy, the experimental carbonyl tetrad concentrations of this material matched the predicted tetrad concentrations for an enantiomorphic-site control mechanism.[73]

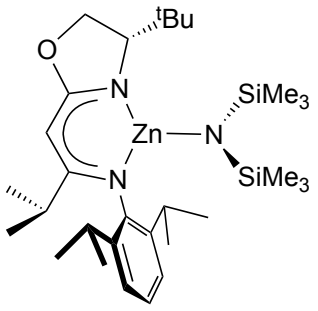

1.14

Figure 1.3. Chiral zinc catalyst **1.14** for the enantioselective, alternating copolymerization of cycloalkene oxides and CO_2.

1.3.3. Cobalt–Based Catalysts

Tsuruta found that the optically pure complex [(*R,R*-salcy)Co] (**1.15**) was active for epoxide polymerization (Scheme 1.14) when activated with $AlEt_3$. Although the system exhibited no enantioselectivity for the polymerization of propylene oxide, it was moderately selective ($s \sim 1.5$) for the enantioselective polymerization of *tert*-butyl ethylene oxide and epichlorohydrin (Scheme 1.14).[75]

Scheme 1.14. Enantioselective Polymerization of Racemic *tert*-Butyl Ethylene Oxide and Epichlorohydrin Using **1.15**/$AlEt_3$

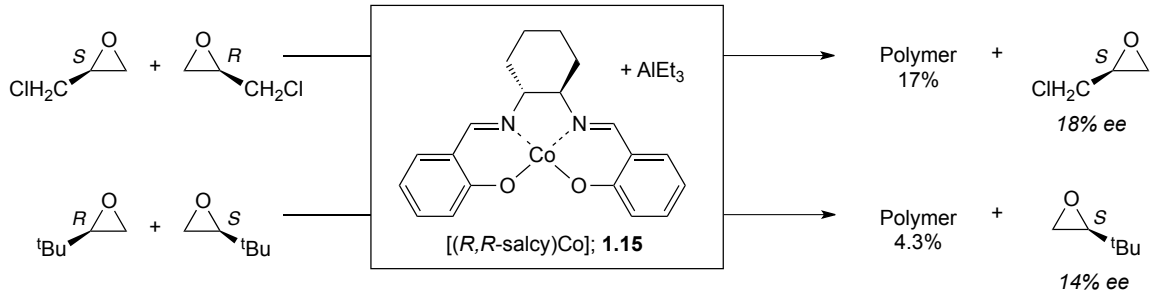

1.3.3.1. Epoxide-carbon dioxide copolymerization systems

Coates and coworkers reported that [(*R,R*-salcy-^{t}Bu)CoOAc] (**1.16**) copolymerizes propylene oxide and CO_2 (Scheme 1.15).[76] Novel features of the catalyst are high regioregularity and alternation, coupled with high selectivity for polycarbonate formation (cyclic propylene carbonate is not formed). (*S*)-Propylene oxide is consumed faster than (*R*)-propylene oxide with a modest *s*-factor of 2.8. Given the same absolute monomer configuration and similar *s*-factor observed by Jacobsen for the cobalt-catalyzed ring-opening of aliphatic epoxides with benzoic acid,[39] a related mechanism was proposed to occur for polymerization with [(*R,R*-salcy-^{t}Bu)CoOAc], giving a cobalt-alkoxide catalyst resting state to produce the regioregular structure shown in Scheme 1.15.

Lu and coworkers found that the addition of quaternary ammonium salts increased the *s*-factor to 3.5.[77] The use of cobalt salen complexes, [SalenCo^{III}X] in conjunction with an ionic organic ammonium salt or a sterically hindered strong organic base allowed for the stereoselective alternating copolymerization of CO_2 and racemic aliphatic epoxides. By using a 7-methyl-1,5,7-triazabicyclo[4.4.0]dec-5-ene (MTBD) cocatalyst with the cobalt catalyst, it was

possible to produce poly(propylene carbonates) with a *s*-factor of 5.6, >95% head-to-tail connectivity and >99% carbonate linkages. The same catalytic system was also used for the copolymerization of cyclohexene oxide and CO_2 to produce polycarbonates with an *ee* of 36.6% and greater than 99% carbonate linkages.[78] More recently, Coates and Cohen have reported that a combination of complex **1.17** and bis(triphenylphosphine)iminium chloride (PPNCl) exhibits an *s*-factor of 9.7 for the copolymerization of propylene oxide and CO_2 at –20 °C (Scheme 1.15).[79]

Scheme 1.15. Enantioselective Polymerization of Racemic Propylene Oxide Using **1.16** and **1.17**/[Ph_3PNPPh_3]Cl

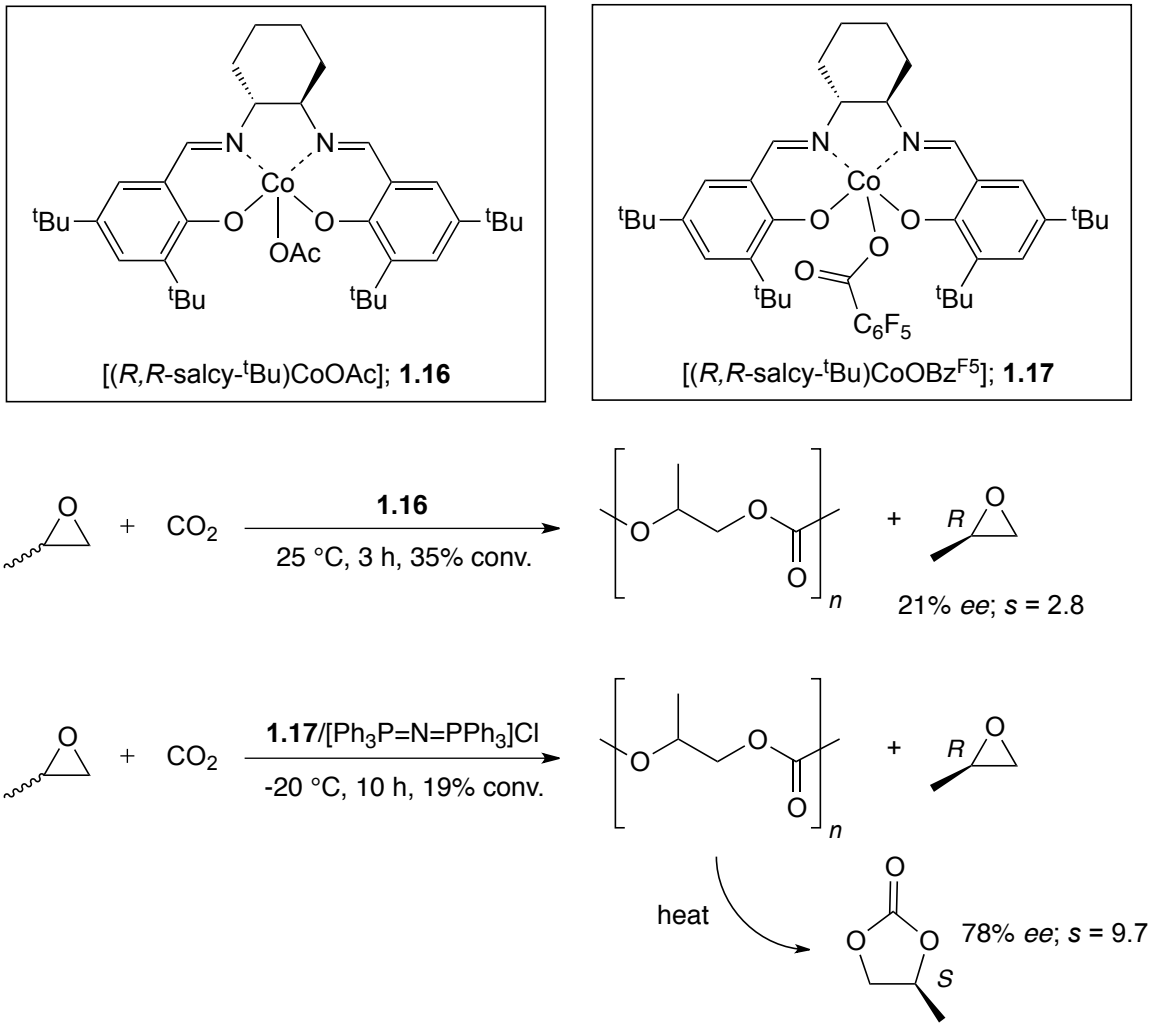

Coates and coworkers also reported the first syndioselective copolymerization of cyclohexene oxide and CO_2 (Scheme 1.16).[80] Using complex [*rac*-(salpr-^{t}Bu)CoBr] (**1.18**), poly(cyclohexene carbonate) was formed with 80% *r*-dyads, as determined by ^{13}C NMR spectroscopy. The carbonyl and methylene regions were best simulated using Bernoullian statistical methods, supporting a chain-end stereochemical control mechanism.

Scheme 1.16. Syndioselective Copolymerization of Cyclohexene Oxide and CO_2 with **1.18**

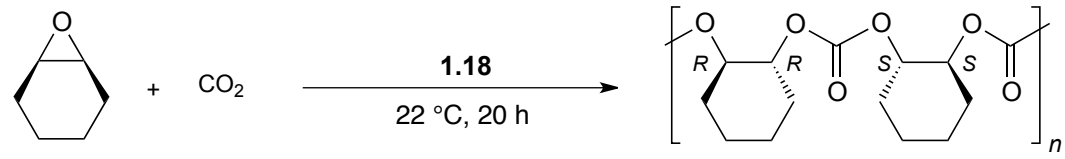

Syndiotactic
Poly(cyclohexene carbonate)
80% *r*-dyads
87% conv.

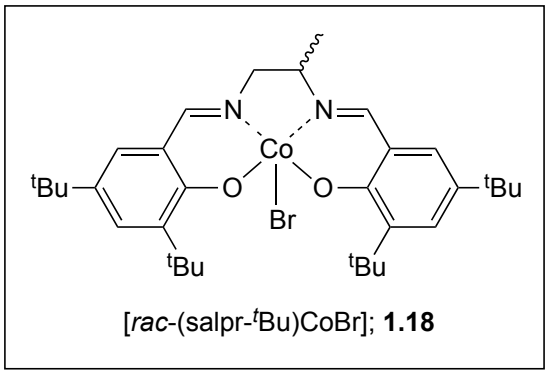

[*rac*-(salpr-^{t}Bu)CoBr]; **1.18**

The Nozaki group reported cobalt salcy complexes with pendant ammoniums for the synthesis of stereogradient iso-enriched poly(propylene carbonate) from racemic propylene oxide and CO_2 (Scheme 1.17).[81] The *s*-factors measured were between 1.1 and 3.5 but complete conversion of monomer was possible with minimal formation of cyclic propylene carbonate by-product. The stereo gradient poly(propylene carbonate) was found to have a higher decomposition temperature (T_d = 281 °C) than its isotactic analogue (T_d = 233 °C) which was attributed to intramolecular stereocomplex formation.

Scheme 1.17. Synthesis of Stereogradient Iso-enriched Poly(propylene carbonate)

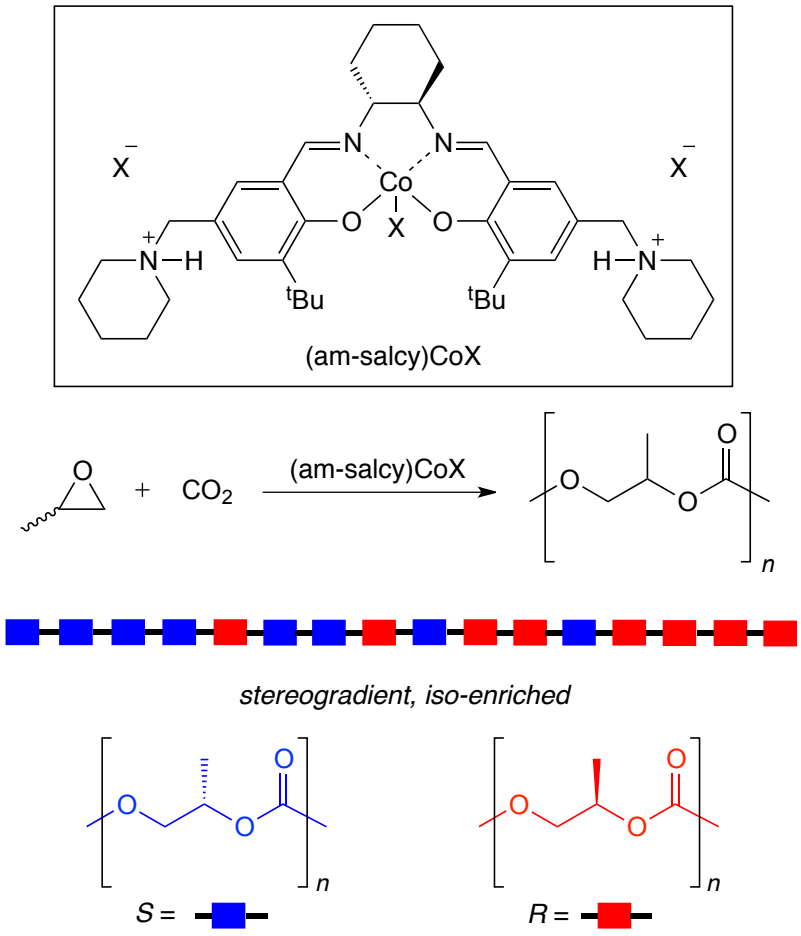

1.3.3.2. Recent stereoselective epoxide homopolymerization systems

In 2005, Coates and coworkers reported a highly active and isoselective (TOF = 220 h^{-1}, *mm* > 99%) cobalt complex, [(salph-^{t}Bu)CoOAc] **1.19** (Scheme 1.18a) for the polymerization of racemic propylene oxide.[82] This is the first example of highly isotactic poly(propylene oxide) generation from racemic propylene oxide without concomitant atactic byproduct. 1-Butene oxide and 1-hexene oxide, though structurally similar to propylene oxide, displayed only trace activity with **1.19**, while all other substituted epoxides screened showed no activity. Though suitable

crystals of **1.19** were not obtained, the crystal structure of the methoxide analogue **1.20**, revealed the formation of chiral clefts that are proposed to facilitate its isoselective nature. Adjacent cobalts were separated by 7.13 Å with the salen planes oriented 52° to each other, as shown in Scheme 1.18b.[83] Studies found that samples of crystalline **1.20** that had been ground mechanically displayed significantly higher activity than unground **1.20**. This large increase in polymerization activity of **1.20** with increased surface area supports that polymerization occurs on the surface of crystalline **1.19** and **1.20**. The supramolecular structure of **1.19** and **1.20** limits any attempts at catalyst optimization through substituent modification due to the inability to accurately predict structural packing, leading to desire for a soluble modular system to synthesize isotactic polyethers.

Scheme 1.18. a) Isoselective Polymerization of Propylene Oxide Using **1.19**; b) Molecular Structure of Methoxide Analogue **1.20**

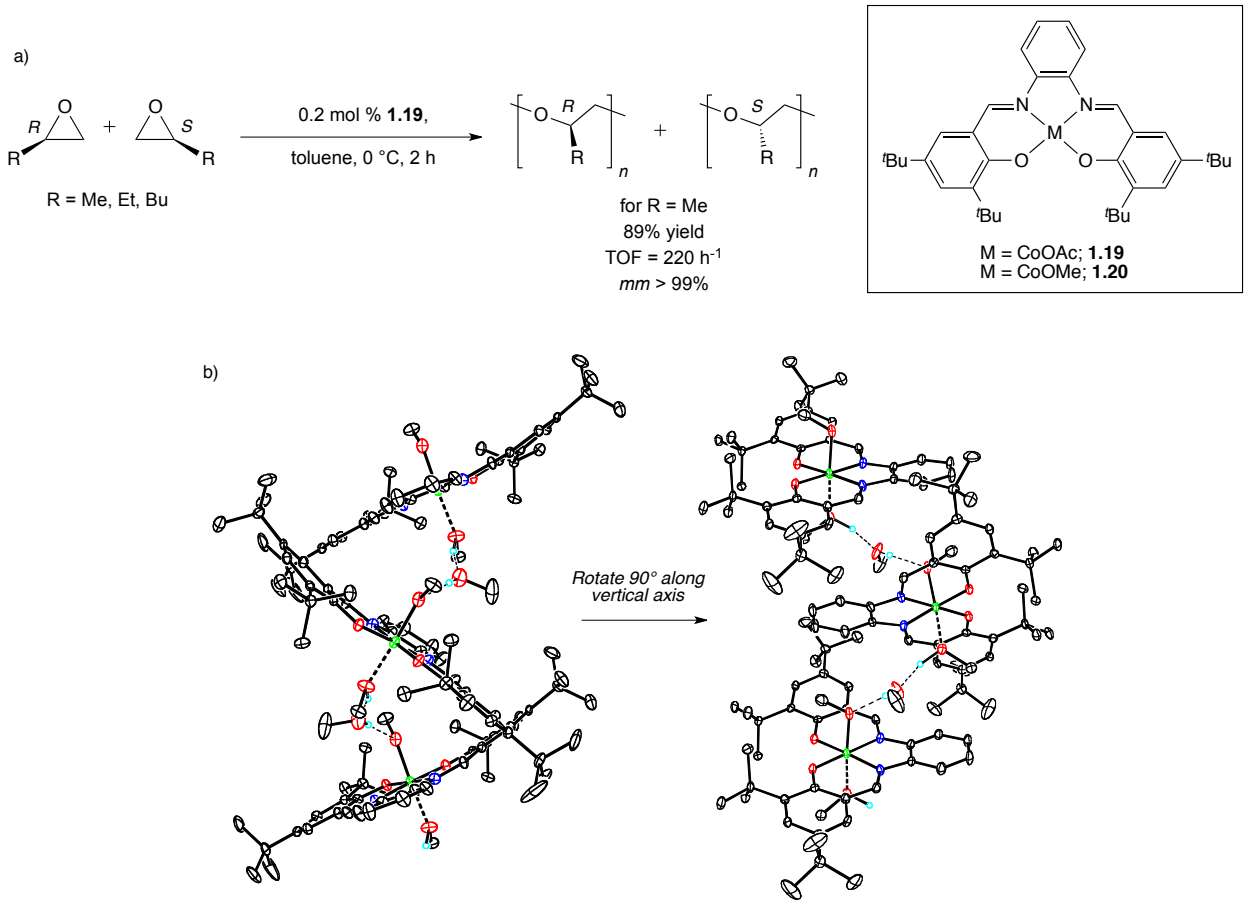

Mechanistic studies of **1.19** and **1.20** lead to the design of the complex **1.21**, which was reported by Coates and coworkers in 2008.[84,85] An axially chiral binaphthol linker covalently oriented the cobalt centers in the appropriate geometry and maintained the ideal distance between metal centers for epoxide polymerization (Scheme 1.19). The catalytic system consisting of **1.21** and co-catalyst, [PPN]OAc, can enantioselectively polymerize propylene oxide with *s*-factor greater than 300 and TOF of 5400 h^{-1}. The system displayed enantiomorphic site control as determined by ^{13}C NMR spectroscopy. A variety of monosubstituted racemic

monomers including alkyl, glycidyl, vinyl, styrenic, and fluorinated epoxides were shown to be enantioselectively polymerized to form highly isotactic enantiopure polyethers. This left valuable enantiopure epoxides in the starting material with *s*-factors ranging from 20-300. Racemic catalyst was shown to isoselectively polymerize epoxides in quantitative yield at low (0.1 mol%) catalyst loading. Many of the isotactic polyethers synthesized were crystalline unlike their atactic analogs and nearly all had high M_n values.

Scheme 1.19. Enantioselective Polymerization of Epoxides with **1.21**

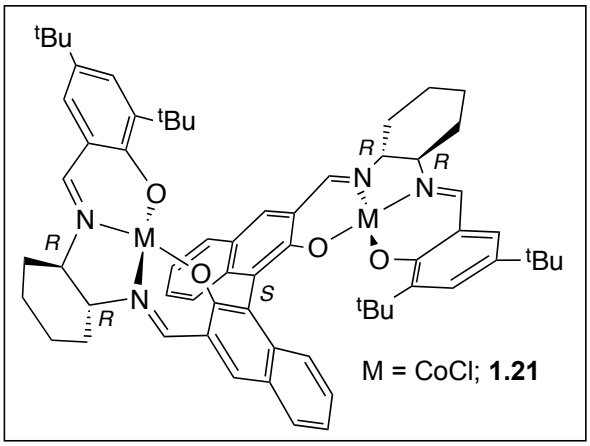

[PPN]OAc = $\left[Ph_3P{=}N{=}PPh_3 \right]^{+}\ ^{-}OAc$

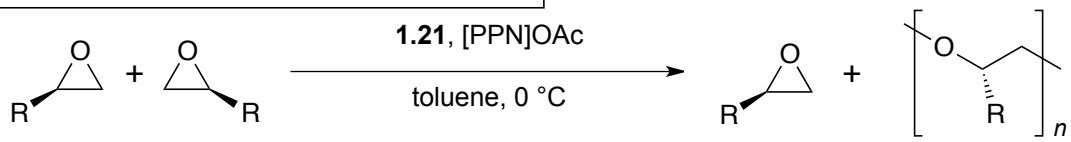

epoxide	TOF (min^{-1})	M_n (kg mol^{-1})	*s*-factor	epoxide	TOF (min^{-1})	M_n (kg mol^{-1})	*s*-factor
	91	26	>300	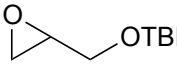	760	140	>70
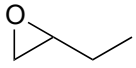	16	61	>300	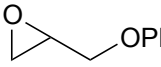	960	130	>70
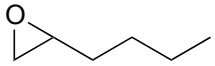	6	77	>100	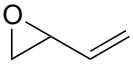	14	79	>20
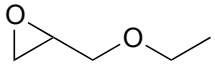	10	8	>50	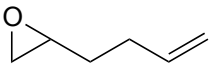	21	46	>300
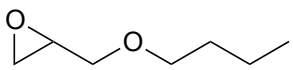	14	33	>50	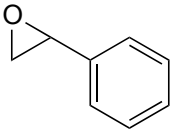	11	50	>70
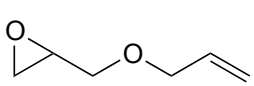	130	110	>100	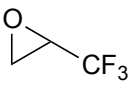	190	20	>300
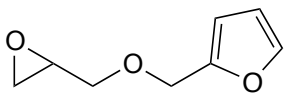	230	69	>80				

Subsequent work developed a simplified isoselective variant of the catalyst (**1.22**) by substituting the cyclohexanediamine bridge for ethylenediamine and using a racemic binaphthol

linker (Scheme 1.20).[86] This complex displayed low activity and selectivity for propylene oxide polymerization when combined with [PPN]OAc. The identity of the cocatalyst was found to dramatically affect reactivity, the bulkier [PPN]OPiv cocatalyst gave the highest rates and isoselectivities for a broad range of epoxides. This system displays the highest rate reported for highly isoselective propylene oxide polymerization (TOF = 1000 h^{-1}) and high tacticity, (*mm* = 97%).

Scheme 1.20. Isoselective Polymerization of Epoxides with **1.22**

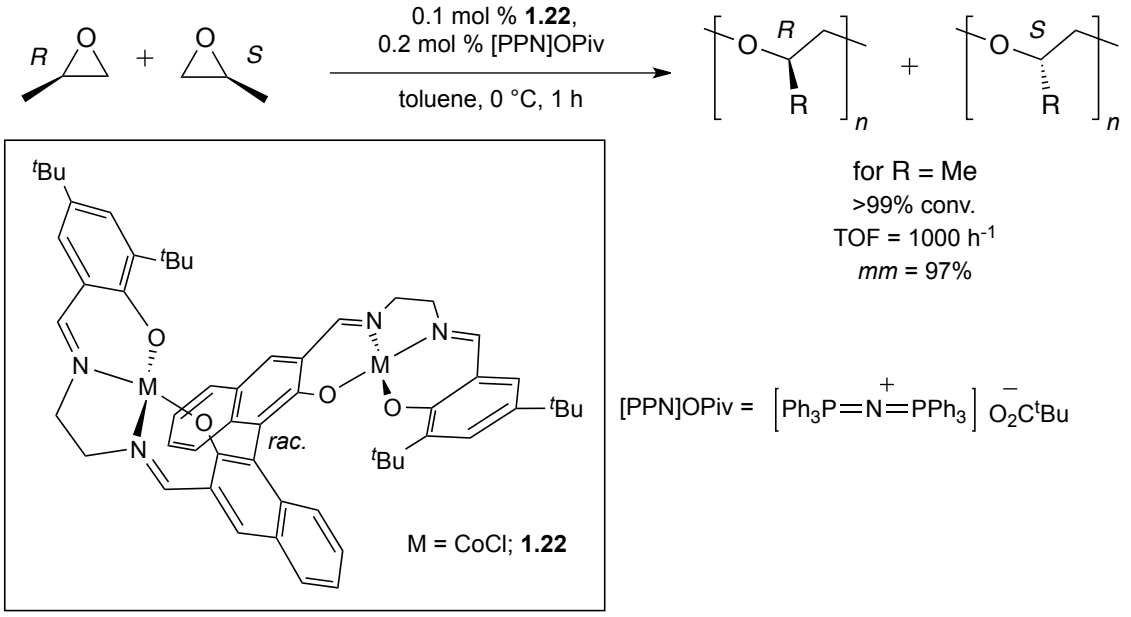

Studies of these bimetallic systems have shown that the axial chirality of the binaphthol linker determines the enantiopreference for epoxide enchainment,[86] rather than the stereochemistry of the diamine, unlike related cobalt salen systems.[39,87] Complexes **1.21** and **1.22** are currently believed to exist as mixtures of exo/endo chloride diastereomers. Addition of cocatalyst leads to an active anionic complex as shown in Scheme 1.21 where X can be either a

chloride or carboxylate. These bimetallic cobalt catalysts display induction periods and poor agreement between theoretical and experimental M_n values likely due to slow initiation relative to propagation. Molecular weight distributions were approximately two, consistent with a single site mechanism.[85]

Scheme 1.21. Proposed Mechanism of Polymerization for **1.21** and **1.22**

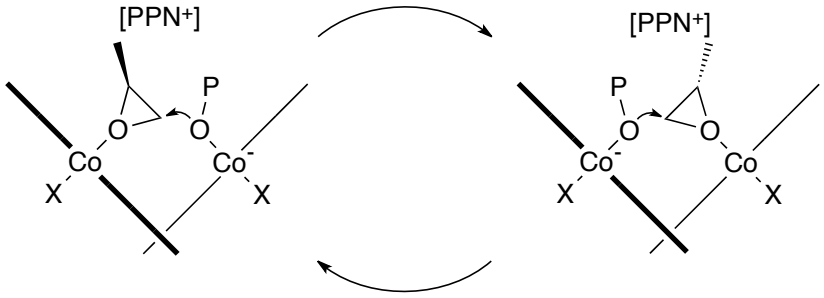

1.3.4. Tin-Based Catalysts

In 1993, Nakata and coworkers studied the use of organotin-alkyl phosphate condensates derived from dibutyltin oxide and tributyl phosphate to catalyze the polymerization of propylene oxide.[88] They observed that the polymeric product could be fractionated into benzene-hexane soluble and insoluble fractions. On studying the stereoerrors of the product by ^{13}C NMR spectroscopy, they determined that the insoluble fraction was isotactic poly(propylene oxide) with 94% *m*-dyads (91% *mm*-triads). A direct correlation was found between increasing the molecular weights of the tin condensate initiators with increasing molecular weight and stereoregularity of the polyethers synthesized. Kragl and coworkers later demonstrated the further use of organotin phosphate coordination polymers to synthesize isotactic poly(propylene oxide).[89] The tin phospate polymers were made by the condensation of tributyl phosphate and butyl tin trichloride (Figure 1.4). Propylene oxide was polymerized with high activity (TOF =

100 h^{-1}). After fractionation of the polymeric product, 10% was found to be insoluble in acetone and highly isotactic with 88% *m*-dyads. No allyl end groups were detected; these polymerizations have been proposed to undergo a bimetallic mechanism for enchainment.

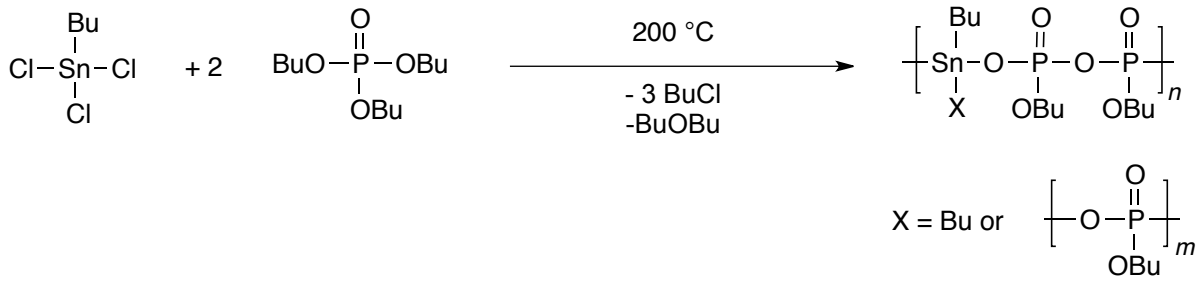

Figure 1.4. Preparation of organotin phosphate condensate catalysts.

1.3.5. Chromium-Based Catalysts

A significant contribution towards developing regioregular polycarbonates has been made by the Lu research group, including developing a saturated salicylaldamine chromium(III) catalyst ([SalanCr(III)], Figure 1.5), which in conjunction with quaternary ammonium salts can produce high molecular weight poly(propylene carbonate) with regiochemical control (>95% head-to-tail linkages) while also displaying moderate enantioselectivity ($2 < s < 8$) depending on the quaternary ammonium cocatalyst used.[90]

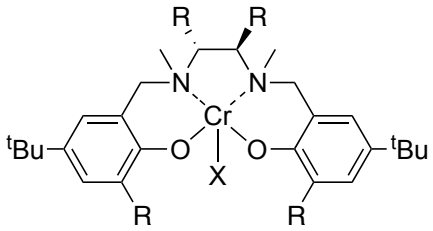

SalanCr(III)

Figure 1.5. Structure of SalanCr(III) complex.

1.4. Outlook and Conclusions

Although significant advances in stereoselective epoxide polymerization have been achieved over the last half-century, only recently have catalysts been developed that are capable of high levels of stereocontrol. Historically, most catalysts for stereoselective epoxide polymerization have been heterogeneous and have exhibited poor selectivity. The current work in the development of well-defined, homogeneous, multimetallic catalysts with controlled spatial orientation of the active catalyst centers could lead to new generations of improved stereoselective epoxide polymerization catalysts. Major frontiers in stereoselective epoxide polymerization have yet to be explored, these include the development of new systems that are: highly stereoselective for epoxide/CO_2 copolymerization, highly selective for polysubstituted epoxide polymerization, stereoselective as well as living allowing for the formation of block copolymers. New catalysts are still needed to accomplish the challenge of synthesizing precisely defined highly tactic polyethers and polycarbonates.

1.5. References

(1) Pruitt, M. E.; Baggett, J. M. US Patent 2706181, 1955.

(2) Pruitt, M. E.; Baggett, J. M.; Bloomfield, R. J.; Templeton, J. H. US Patent 2706182, 1955.

(3) Pruitt, M. E.; Baggett, J. M. US Patent 2706189, 1955.

(4) Booth, C.; Jones, M. N.; Powell, E. *Nature* **1962**, *196*, 772-773.

(5) Natta, G.; Corradini, P.; Dall'Asta, G. *Atti Accad. Naz. Lincei Cl. Sci. Fis. Mat. Nat.* **1956**, *20*, 408-413.

(6) Price, C. C.; Osgan, M. *J. Am. Chem. Soc.* **1956**, *78*, 4787-4792.

(7) Price, C. C.; Osgan, M.; Hughes, R. E.; Shambelan, C. *J. Am. Chem. Soc.* **1956**, *78*, 690-691.

(8) Vandenberg, E. J. *Polymer* **1994**, *35*, 4933-4939.

(9) Spassky, N.; Dumas, P.; Le Borgne, A.; Momtaz, A.; Sepulchre, M. *Bull. Soc. Chim. Fr.* **1994**, *131*, 504-514.

(10) Spassky, N.; Momtaz, A.; Kassamaly, A.; Sepulchre, M. *Chirality* **1992**, *4*, 295-299.

(11) Spassky, N. *Makromol. Chem., Macromol. Symp.* **1991**, *42/43*, 15-49.

(12) Vandenberg, E. J. In *Coordination Polymerization*; Vandenberg, E. J., Price, C. C., Eds.; Plenum Publishing Corp.: New York, 1983, p 11-44.

(13) Tsuruta, T. *Pure Appl. Chem.* **1981**, *53*, 1745-1751.

(14) Spassky, N.; Leborgne, A.; Sepulchre, M. *Pure Appl. Chem.* **1981**, *53*, 1735-1744.

(15) Spassky, N. *ACS Symp. Ser.* **1977**, *59*, 191-209.

(16) Sigwalt, P. *Pure Appl. Chem.* **1976**, *48*, 257-266.

(17) Price, C. C. *Acc. Chem. Res.* **1974**, *7*, 294-301.

(18) Tsuruta, T. *J. Polym. Sci., Part D: Macromol. Rev.* **1972**, *6*, 179-250.

(19) Duda, A. *Polimery* **2004**, *49*, 469-478.

(20) Vandenberg, E. J. *J. Polym. Sci., Polym. Chem. Ed.* **1969**, *7*, 525-567.

(21) Coates, G.; Allen, S.; Ajiro, H. In *Stereoselective Polymerization with Single-Site Catalysts*; CRC Press: Boca Raton, FL, 2007, p 627-644.

(22) Farina, M. *Top. Stereochem.* **1987**, *17*, 1-111.

(23) Schilling, F. C.; Tonelli, A. E. *Macromolecules* **1986**, *19*, 1337-1343.

(24) Le Borgne, A.; Spassky, N.; Jun, C. L.; Momtaz, A. *Makromol. Chem.* **1988**, *189*, 637-650.

(25) Ugur, N.; Alyuruk, K. *J. Polym. Sci., Part A: Polym. Chem.* **1989**, *27*, 1749-1761.

(26) Cheng, H. N. In *Modern Methods of Polymer Characterization*; Barth, H. G., Mays, J. W., Eds.; John Wiley & Sons: New York, 1991, p 409-493.

(27) Bovey, F. A.; Mirau, P. A. *NMR of Polymers*; Academic Press: San Diego, 1996.

(28) Chisholm, M. H.; Navarro-Llobet, D. *Macromolecules* **2002**, *35*, 2389-2392.

(29) Gawley, R. E. *J. Org. Chem.* **2006**, *71*, 2411-2416.

(30) Wu, B.; Harlan, C. J.; Lenz, R. W.; Barron, A. R. *Macromolecules* **1997**, *30*, 316-318.

(31) Vandenberg, E. J. *J. Polym. Sci.* **1960**, *47*, 486-489.

(32) Vandenberg, E. J. US Patent 3135705, 1964.

(33) Vandenberg, E. J. US Patent 3219591, 1965.

(34) Vandenberg, E. J. *J. Polym. Sci., Part B: Polym. Lett.* **1964**, *2*, 1085-1088.

(35) Vandenberg, E. J. *J. Am. Chem. Soc.* **1961**, *83*, 3538-3539.

(36) Vandenberg, E. J. *J. Polym. Sci.* **1960**, *47*, 489-491.

(37) Braune, W.; Okuda, J. *Angew. Chem., Int. Ed.* **2003**, *42*, 64-68.

(38) Moore, D. R.; Cheng, M.; Lobkovsky, E. B.; Coates, G. W. *J. Am. Chem. Soc.* **2003**, *125*, 11911-11924.

(39) Tokunaga, M.; Larrow, J. F.; Kakiuchi, F.; Jacobsen, E. N. *Science* **1997**, *277*, 936-938.

(40) Haubenstock, H.; Panchalingam, V.; Odian, G. *Makromol. Chem.* **1987**, *188*, 2789-2799.

(41) Osgan, M.; Price, C. C. *J. Polym. Sci.* **1959**, *34*, 153-156.

(42) Kasperczyk, J.; Dworak, A.; Jedlinski, Z. *Makromol. Chem., Rapid Commun.* **1981**, *2*, 663-666.

(43) Dworak, A.; Jedlinski, Z. *Polymer* **1980**, *21*, 93-96.

(44) Takeda, N.; Inoue, S. *Makromol. Chem.* **1978**, *179*, 1377-1381.

(45) Aida, T.; Inoue, S. *Macromolecules* **1981**, *14*, 1166-1169.

(46) Aida, T.; Inoue, S. *Macromolecules* **1981**, *14*, 1162-1166.

(47) Vincens, V.; Le Borgne, A.; Spassky, N. *Makromol. Chem., Rapid Commun.* **1989**, *10*, 623-628.

(48) Vincens, V.; Le Borgne, A.; Spassky, N. *Makromol. Chem., Macromol. Symp.* **1991**, *47*, 285-291.

(49) Le Borgne, A.; Vincens, V.; Jouglard, M.; Spassky, N. *Makromol. Chem., Macromol. Symp.* **1993**, *73*, 37-46.

(50) Matsuura, K.; Inoue, S.; Tsuruta, T. *Makromol. Chem.* **1965**, *86*, 316-319.

(51) Kuran, W.; Listos, T.; Abramczyk, M.; Dawidek, A. *J. Macromol. Sci., Pure Appl. Chem.* **1998**, *A35*, 427-437.

(52) Emig, N.; Nguyen, H.; Krautscheid, H.; Reau, R.; Cazaux, J.-B.; Bertrand, G. *Organometallics* **1998**, *17*, 3599-3608.

(53) Furukawa, J.; Tsuruta, T.; Sakata, R.; Saigusa, T.; Kawasaki, A. *Makromol. Chem.* **1959**, *32*, 90-94.

(54) Kuran, W.; Listos, T. *Macromol. Chem. Phys.* **1994**, *195*, 401-411.

(55) Coulon, C.; Spassky, N.; Sigwalt, P. *Polymer* **1976**, *17*, 821-827.

(56) Kassamaly, A.; Sepulchre, M.; Spassky, N. *Polym. Bull. (Berlin)* **1988**, *19*, 119-122.

(57) Sepulchre, M.; Kassamaly, A.; Spassky, N. *Polym. Prepr. (Am. Chem. Soc., Div. Polym. Chem.)* **1990**, *31*, 91-92.

(58) Sepulchre, M.; Kassamaly, A.; Spassky, N. *Makromol. Chem., Macromol. Symp.* **1991**, *42/43*, 489-500.

(59) Ishimori, M.; Hagiwara, T.; Tsuruta, T.; Kai, Y.; Yasuoka, N.; Kasai, N. *Bull. Chem. Soc. Jpn.* **1976**, *49*, 1165-1166.

(60) Tsuruta, T. *J. Polym. Sci., Polym. Symp.* **1980**, *67*, 73-82.

(61) Tsuruta, T. *Macrmol. Chem. Phys., Supp.* **1981**, *5*, 230-233.

(62) Kageyama, H.; Miki, K.; Tanaka, N.; Kasai, N.; Ishimori, M.; Heki, T.; Tsuruta, T. *Makromol. Chem., Rapid Commun.* **1982**, *3*, 947-951.

(63) Hasebe, Y.; Tsuruta, T. *Makromol. Chem.* **1988**, *189*, 1915-1926.

(64) Yoshino, N.; Suzuki, C.; Kobayashi, H.; Tsuruta, T. *Makromol. Chem.* **1988**, *189*, 1903-1913.

(65) Tsuruta, T. *Makromol. Chem., Macromol. Symp.* **1991**, *47*, 277-283.

(66) Tsuruta, T.; Hasebe, Y. *Macromol. Chem. Phys.* **1994**, *195*, 427-438.

(67) Tsuruta, T. *Makromol. Chem., Macromol. Symp.* **1986**, *6*, 23-31.

(68) Kageyama, H.; Kai, Y.; Kasai, N.; Suzuki, C.; Yoshino, N.; Tsuruta, T. *Makromol. Chem., Rapid Commun.* **1984**, *5*, 89-93.

(69) Hasebe, Y.; Tsuruta, T. *Makromol. Chem.* **1987**, *188*, 1403-1414.

(70) Hasebe, Y.; Izumitani, K.; Torii, M.; Tsuruta, T. *Makromol. Chem.* **1990**, *191*, 107-119.

(71) Nozaki, K.; Nakano, K.; Hiyama, T. *J. Am. Chem. Soc.* **1999**, *121*, 11008-11009.

(72) Nakano, K.; Nozaki, K.; Hiyama, T. *Macromolecules* **2001**, *34*, 6325-6332.

(73) Cheng, M.; Darling, N. A.; Lobkovsky, E. B.; Coates, G. W. *Chem. Commun.* **2000**, 2007-2008.

(74) Nakano, K.; Nozaki, K.; Hiyama, T. *J. Am. Chem. Soc.* **2003**, *125*, 5501-5510.

(75) Tezuka, Y.; Ishimori, M.; Tsuruta, T. *Makromol. Chem.* **1983**, *184*, 895-906.

(76) Qin, Z. Q.; Thomas, C. M.; Lee, S.; Coates, G. W. *Angew. Chem., Int. Ed.* **2003**, *42*, 5484-5487.

(77) Lu, X. B.; Wang, Y. *Angew. Chem., Int. Ed.* **2004**, *43*, 3574-3577.

(78) Lu, X.-B.; Shi, L.; Wang, Y.-M.; Zhang, R.; Zhang, Y.-J.; Peng, X.-J.; Zhang, Z.-C.; Li, B. *J. Am. Chem. Soc.* **2006**, *128*, 1664-1674.

(79) Cohen, C.; Coates, G. W. *J. Poly. Sci. Part A* **2006**, *44*, 5182-5191.

(80) Cohen, C.; Thomas, C.; Peretti, K.; Lobkovsky, E.; Coates, G. *Dalton Trans.* **2006**, 237-249.

(81) Nakano, K.; Hashimoto, S.; Nakamura, M.; Kamada, T.; Nozaki, K. *Angew. Chem., Int. Ed.* **2011**, *50*, 4868-4871.

(82) Peretti, K.; Ajiro, H.; Cohen, C.; Lobkovsky, E.; Coates, G. *J. Am. Chem. Soc.* **2005**, *127*, 11566-11567.

(83) Ajiro, H.; Peretti, K. L.; Lobkovsky, E. B.; Coates, G. W. *Dalton Trans.* **2009**, 8828-8830.

(84) Hirahata, W.; Thomas, R. M.; Lobkovsky, E. B.; Coates, G. W. *J. Am. Chem. Soc.* **2008**, *130*, 17658-17659.

(85) Thomas, R. M.; Widger, P. C. B.; Ahmed, S. M.; Jeske, R. C.; Hirahata, W.; Lobkovsky, E. B.; Coates, G. W. *J. Am. Chem. Soc.* **2010**, *132*, 16520-16525.

(86) Widger, P. C. B.; Ahmed, S. M.; Hirahata, W.; Thomas, R. M.; Lobkovsky, E. B.; Coates, G. W. *Chem. Commun.* **2010**, *46*, 2935-2937.

(87) Cohen, C. T.; Coates, G. W. *J. Polym. Sci., Part A: Polym. Chem.* **2006**, *44*, 5182-5191.

(88) Miura, K.; Kitayama, T.; Hatada, K.; Nakata, T. *Polym. J.* **1993**, *25*, 685-696.

(89) Schütz, C.; Dwars, T.; Schnorpfeil, C.; Radnik, J.; Menzel, M.; Kragl, U. *J. Polym. Sci., Part A: Polym. Chem.* **2007**, *45*, 3032-3041.

(90) Li, B.; Wu, G.-P.; Ren, W.-M.; Wang, Y.-M.; Rao, D.-Y.; Lu, X.-B. *J. Polym. Sci., Part A: Polym. Chem.* **2008**, *46*, 6102-6113.

Chapter 2

Isoselective Polymerization of Racemic Epoxides: A Catalyst System for the Synthesis of Highly Isotactic Polyethers

Reproduced in part with permission from:

P. C. B. Widger, S. M. Ahmed, W. Hirahata, R. M. Thomas, E. B. Lobkovsky, G. W. Coates

Chemical Communications, **2010**, *46*, 2935-2937

R. M. Thomas, P. C. B. Widger, S. M. Ahmed, R. C. Jeske, W. Hirahata, E. B. Lobkovsky, G. W. Coates

Journal of the American Chemical Society, **2010**, *132*, 16520-16525

2.1. Introduction

Stereoregular polymers often display superior mechanical and thermal properties compared to their atactic analogues.[1] Polyethers are an important class of polymers with industrial and biological applications.[2] Much progress has been made in controlling the regiochemistry and molecular weight of polyethers,[3] but controlling the stereochemistry of polyethers synthesized from racemic epoxides remains a challenge.[4] Previous isoselective polymerization systems for racemic epoxides produced mixtures of atactic and isotactic materials or generated only moderately isotactic polymers.[5]

We previously reported a highly active and isoselective cobalt catalyst for the polymerization of racemic propylene oxide (*rac*-PO).[6] Using the information gained by studying the mechanism of this catalyst,[7] we have recently designed a highly active and enantioselective polymerization catalyst system that exhibits a broader scope of terminal epoxides. The catalytic system consists of a bimetallic cobalt complex (**2.1**) and a bis(triphenylphosphine)iminium (PPN) acetate cocatalyst (**2.4**, Scheme 2.1). This system selectively polymerizes one enantiomer of racemic terminal epoxides to produce highly isotactic polyethers and enantiopure epoxides.[8] Unfortunately, this limits the theoretical maximum yield of polymer at ca. 50% unless the racemic form of **2.1** is used.[8] Attempts to synthesize *rac*-**2.1** (equimolar mixture of (*R,R,S,R,R*)- **2.1** and (*S,S,R,S,S*)- **2.1**) from racemic starting materials produced inseparable diastereomers, which lead us to develop a new catalyst that is active and isoselective while being derived from inexpensive racemic and/or achiral starting materials.

Scheme 2.1. Enantioselective and Isoselective Polymerization of Racemic Epoxides Using Bimetallic Cobalt Catalysts

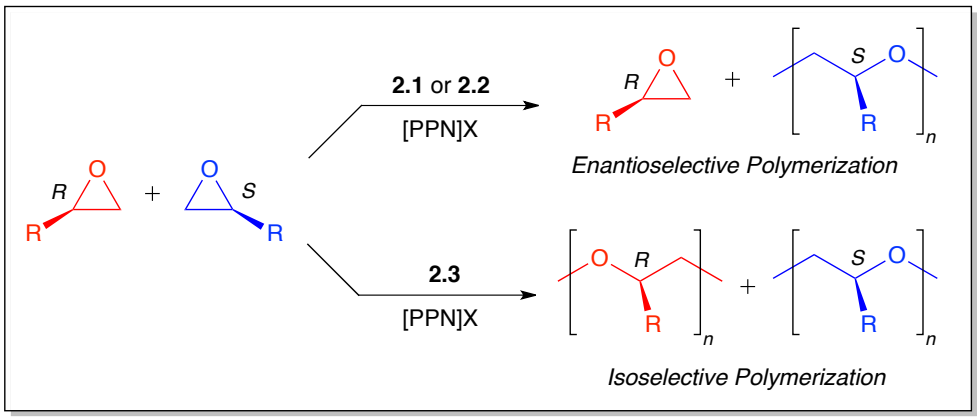

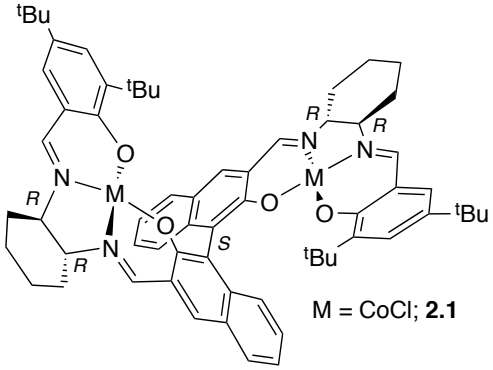

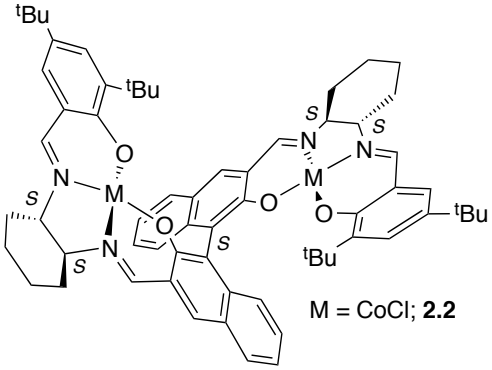

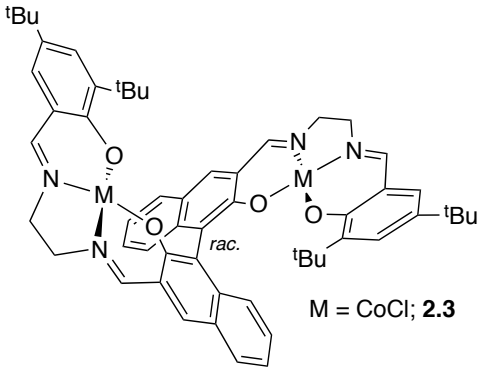

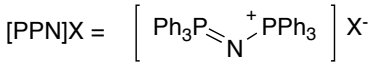

X = $MeCO_2$; **2.4**
X = $Me(CH_2)_3CHEtCO_2$; **2.5**
X = $^tBuCO_2$; **2.6**
X = $^tBuCH_2CO_2$; **2.7**

2.2. Results and Discussion

Insight into the origin of enantioselectivity of **2.1** was gained through the reactivity

of the diastereomeric cobalt complex **2.2**, which posesses all *S* stereochemistry. The complex was synthesized from (1*S*,2*S*)-diaminocyclohexane and (*S*)-1,1'-bi-2-naphthol as shown in Scheme 2.2.

Scheme 2.2. Synthesis of Bimetallic Complex **2.2**

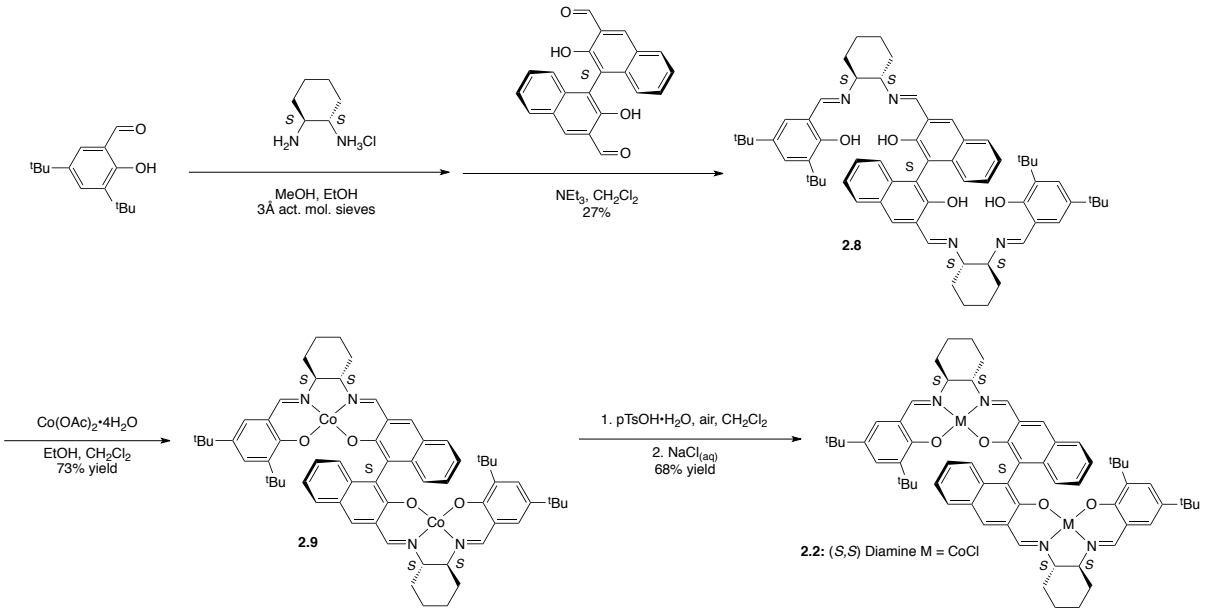

When activated with PPNOAc (**2.4**), complex **2.2** displayed lower activity than **2.1** for the polymerization of neat *rac*-PO (T_{rxn} = 0 °C), but it preferred the same enantiomer (*S*-PO) with a k_S/k_R selectivity factor of 210. This is in contrast to previous catalytic systems using (*S*,*S*)-(salcy)CoOAc which have shown selectivity for the hydrolysis of *R*-PO.[9] This result confirmed that the stereochemistry of the binaphthol linker determines which enantiomer of monomer is enchained, possibly allowing simplification of **2.1** and **2.2** by using an achiral diamine linker.

Having determined that the axial chirality of the binaphthol linker is responsible for the stereoselectivity of the polymerization, we synthesized complex **2.3**, which

incorporated ethylene diamine and a *rac*-binaphthol linker (Scheme 2.3).

Scheme 2.3. Synthesis of Bimetallic Complex **2.3**

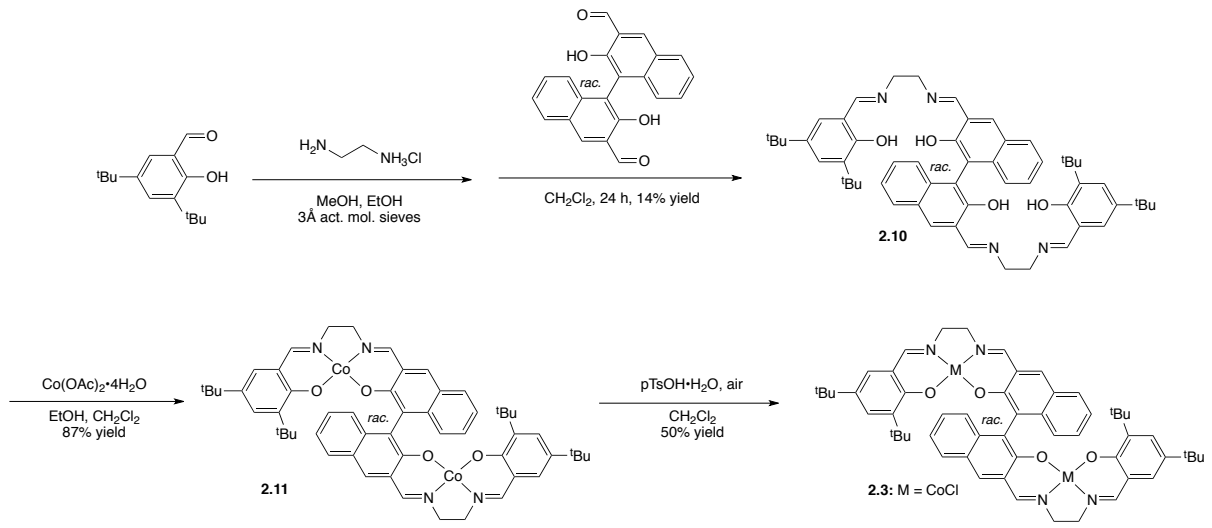

Initial polymerizations of neat *rac*-PO using catalyst system **2.3** and **2.4** (**2.3**/**2.4**) (Table 2. 1, entry 1) were less active in comparison with system **2.1**/**2.4**, yielding regioregular poly(propylene oxide) (PPO) with moderate isotacticity (67% [*mm*] triad content, Figure 2.1a). Analysis of the polymer tacticity using ^{13}C NMR spectroscopy showed stereoerrors[10] (*mr* = *rm* = *rr*) indicative of enantiomorphic site control.[11]

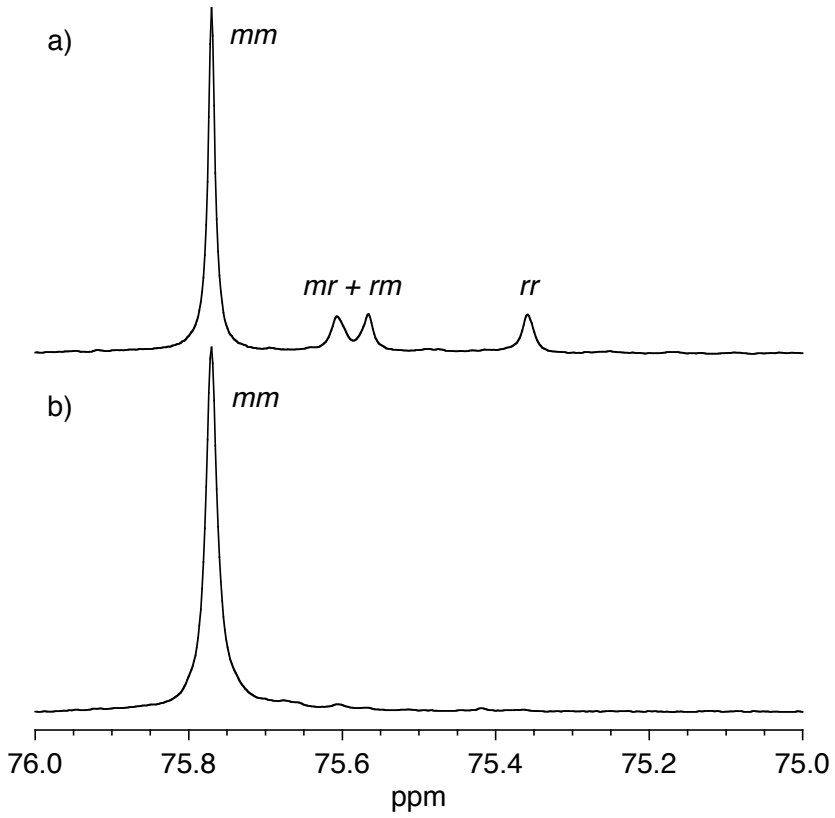

Figure 2.1. Methine regions of the ^{13}C NMR spectra of PPO produced using a) Catalyst **2.3** and Cocatalyst **2.4**; b) Catalyst **2.3** and cocatalyst **2.6**.

In an effort to increase the activity of **2.3**, we modified the anions of PPN salts, which have been found to have dramatic effects on the activity and selectivity of PO/CO_2 copolymerizations.[12] We synthesized cocatalyst **2.5** via salt metathesis of silver 2-ethyl hexanoate with [PPN]Cl (Scheme 2.4), and found that when combined with **2.3** the rate of polymerization dramatically increased. When run neat, the reaction exothermed vigorously; thus, further polymerizations were conducted in toluene at 0 °C for 5 min. Cocatalyst **2.5** also dramatically increased the selectivity, producing highly isotactic PPO with 96% [*mm*] triad content (Table 2.1, entry 2).

Scheme 2.4. Synthesis of Silver Carboxylates: **2.12**, **2.13**, **2.14** and PPN Carboxylates: **2.5**, **2.6**, **2.7**

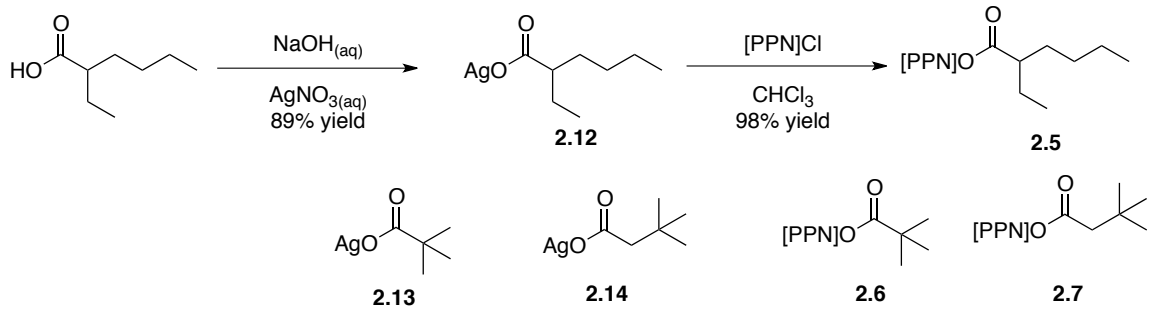

Two bulky achiral cocatalysts **2.6** and **2.7** were synthesized to determine if the enhanced selectivity resulting from **2.5** originated from its chirality or increased sterics. Both **2.6** and **2.7** were very active for the polymerization of PO in the presence of **2.3** and produced highly isotactic polymer (Table 2.1, entries 3 and 4).[13] Cocatalyst **2.6** produced the highest rates and isoselectivity (Figure 2.1b) when combined with **2.3**. Thus **2.6** was used in all subsequent polymerizations.

Table 2.1. Polymerization of Racemic Propylene Oxide with **2.3** and Cocatalysts **2.4**-**2.7**[a]

entry	[PPN]X	t_{rxn} (min)	T_{rxn} (°C)	conv. (%)[b]	M_n (kg/mol)[c]	M_w/M_n[c]	[*mm*] (%)[d]
1[e]	**2.4**	1440	20	29	57	2.2	67
2	**2.5**	5	0	43	153	1.7	96
3	**2.6**	5	0	55	134	1.8	97
4	**2.7**	5	0	7	47	3.6	96

[a] General conditions: [**2.3**]:[PPN]X:[PO] = 1:2:4000, and [PO] = 2 M in toluene. [b] Determined by ^{1}H NMR spectroscopy. [c] Determined by gel-permeation chromatography calibrated with polystyrene standards in 1,2,4-$Cl_3C_6H_3$ at 140 °C. [d] [*mm*] triad content determined by ^{13}C NMR spectroscopy. [e] Reaction run in neat PO, [**2.3**]:[PO] = 1:2000.

The role of the cocatalyst anion in the polymerization is currently unclear. We propose that the cocatalyst anion coordinates to one cobalt center. An epoxide molecule

then coordinates to the adjacent cobalt center inside the catalyst cleft, and is ring opened by a nucleophile (chloride or carboxylate, depending on initial position of chloride ligands) to initiate polymerization (Scheme 2.5). Subsequent ring-opening events occur alternatively at the adjacent cobalt centers to create the polymer chain. Our working hypothesis is that the increased bulk of **2.6** compared to **2.4** prevents its carboxylate from entering the catalyst cleft, favoring its position *anti* to the epoxide/polymer alkoxide.[14]

Scheme 2.5. Proposed Mechanism of Polymerization (P = polymer chain; X = Cl or carboxylate)

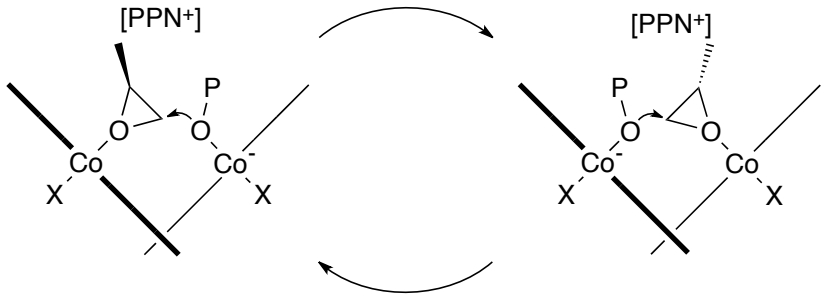

The new catalyst system (**2.3**/**2.6**) was screened for the polymerization of a number of terminal epoxides possessing aliphatic, ether, vinyl, aromatic and fluorinated side chains (Table 2.2). Catalyst system **2.3**/**2.6** produced racemic, highly isotactic polyethers at rapid rates. Nearly all polymers had molecular weights significantly higher than the theoretical molecular weights calculated from one polymer chain per metal complex. This is consistent with **2.3** being a mixture of chloride diastereomers, of which only a fraction are catalytically active.[8] The molecular weight distributions (M_w/M_n) are ca. 2 consistent with a single site catalyst.

PO and 1-butene oxide were both polymerized at rapid rates with high

isoselectivities to polymer with high molecular weight (Table 2.2, entries 1 and 2). Phenyl glycidyl ether was polymerized very rapidly and displayed very high isotacticity (entry 3). Isotactic poly(phenyl glycidyl ether) is a toughening agent in epoxy resins.[15] It has previously been synthesized using coordination polymerization[16] and anionic polymerization of enantiopure monomer.[17] Butadiene monoepoxide was polymerized rapidly, but had moderate isotacticity (entry 4). Poly(butadiene monoepoxide) possesses a pendant olefin potentially allowing for functionalization. Styrene oxide[18,19] was polymerized at a reasonable rate with high tacticity (entry 5). There are limited reports on the polymerization of 1,1,1-trifluoro-2,3-epoxypropane.[20] Fluorinated polyethers have unique properties and often require fluorinated solvents for good reactivity.[20c] Trifluoropropylene oxide was polymerized slowly but the resulting polymer was highly isotactic (entry 6). The polymer was insoluble in traditional GPC solvents and had to be chromatographed using DMF, making molecular weight comparisons difficult.

Table 2.2. Screening of Racemic Epoxides for Isoselective Polymerization Catalyzed by System **2.3**/**2.6**[a]

entry	epoxide subs. (R)	t_{rxn} (min)	conv. (%)[b]	M_n (kg/mol)[c]	M_w/M_n[c]	[*mm*] (%)[d]
1	Me	5	55	134	1.8	97
2	Et	5	60	239	1.5	97
3	CH_2OPh	1	89	328	1.4	≥97
4	$CH{=}CH_2$	10	46	212	1.5	92
5	Ph	45	23	77	1.9	≥97
6	CF_3	90	32	20[e]	13[e]	≥97

[a] General conditions: [**2.3**]:[**2.6**]:[epoxide] = 1:2:4000, T_{rxn} = 0 °C and [epoxide] = 2 M in toluene. [b] Determined by ^{1}H NMR spectroscopy. [c] Determined by gel-permeation chromatography calibrated with polystyrene standards in 1,2,4-$Cl_3C_6H_3$ at 140 °C. [d] [*mm*] triad content determined by ^{13}C NMR spectroscopy. [e] Determined by gel-permeation chromatography calibrated with poly(methyl methacrylate) in *N*,*N*-dimethylformamide containing 0.01 M lithium nitrate and 1% formic acid at 35 °C.

Racemic epoxides were quantitatively polymerized to racemic isotactic polyether at slightly higher loading of catalyst and higher dilution as shown in Table 2.3. The rates of polymerization were quite rapid, and all polymers displayed high isotacticity.

Table 2.3. Quantitative Conversion of Racemic Epoxides to Isotactic Polyethers Catalyzed by System **2.3**/**2.6**[a]

entry	epoxide subs. (R)	t_{rxn} (h)	conv. (%)[b]	M_n (kg/mol)[c]	M_w/M_n[c]	[*mm*] (%)[d]
1	Me	1	>99	107	1.8	97
2	Et	1	>99	163	1.6	97
3	CH_2OPh	0.08	>99[e]	278	1.3	≥97
4	$CH{=}CH_2$	1	>99	135	2.1	92
5	Ph	15	>99	59	2.0	≥97
6	CF_3	6	>99	85[f]	6.9[f]	≥97

[a] General conditions: [**2.3**]:[**2.6**]:[epoxide] = 1:2:1000, T_{rxn} = 0 °C and [epoxide] = 0.6 M in toluene. [b] Determined by ^{1}H NMR spectroscopy. [c] Determined by gel-permeation chromatography calibrated with polystyrene standards in 1,2,4-$Cl_3C_6H_3$ at 140 °C. [d] [*mm*] triad content determined by ^{13}C NMR spectroscopy. [e] Determined gravimetrically. [f] Determined by gel-permeation chromatography calibrated with poly(methyl methacrylate) in *N*,*N*-dimethylformamide containing 0.01 M lithium nitrate and 1% formic acid at 35 °C.

2.2.1. Characterization of Co(III) Complexes

The bimetallic complexes **2.1**, **2.2**, and **2.3** were all isolated as black solids. All attempts at crystallization of these complexes from non-donating solvents have been unsuccessful thus far. We propose that this is due to these complexes being a mixture of diastereomers in the form of exo-exo, exo-endo, and endo-endo chlorides. Crystals of the tetrapyridine adduct of *rac*-**2.1**, (*rac*-**2.15**) were obtained from pyridine and toluene as shown in Figure 2.2. The presence of two chlorides confirms that the complex is Co(III)-Co(III). Two pyridines are bound to each cobalt atom, and the complex has a pseudo-C_2 symmetry. The complex displays a Co-Co distance of 6.45 Å and an endo naphthol-naphthol dihedral

angle of 79°. In comparison to the reduced Co(II) complex (**2.19**),[8a] *rac*-**2.15** has a wider Co-Co separation, consistent with the flexible nature of the binaphthol linker. Complex **2.15** was also studied by NMR spectroscopy. In the strongly donating solvent pyridine-d_5, **2.1**, (**2.15**) displays sharper resonances than our previous report using DMSO-d_6,[8a,21] allowing for characterization by a combination of ^{1}H, ^{13}C, COSY, and HMBC spectroscopy.[11] The spectra were consistent with **2.15** forming a single C_2 symmetric tetrapyridine adduct in solution.

Complex **2.2** was also crystalized from pyridine to give the tetrapyridine adduct **2.16** as shown in Figure 2.3. The pseudo C_2 symmetric complex displayed a Co-Co distance of 6.94 Å and an endo naphthol-naphthol dihedral angle of 88.4 °.

Figure 2.4 shows the tetrapyridine adduct of **2.3** (**2.17**) with hydrogens omitted and pyridine ligands truncated for clarity. Two pyridines are bound to each cobalt center displacing the chlorides giving a pseudo C_2 symmetric complex. The Co-Co distance is 6.77 Å and the endo naphthol-naphthol dihedral angle is 84.3º.

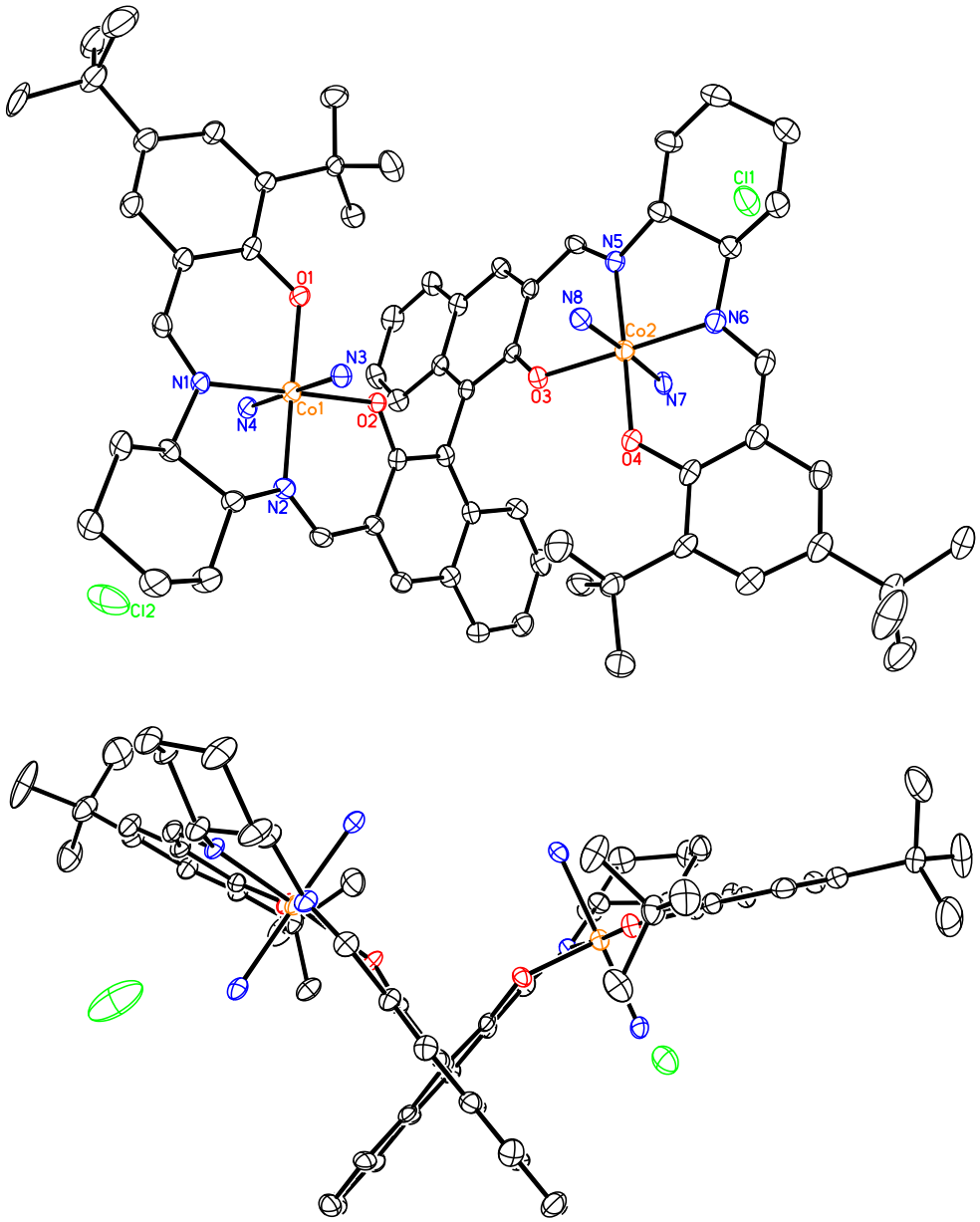

Figure 2.2. Molecular structure of *rac*-**2.15** (hydrogen atoms omitted and pyridine ligands truncated for clarity; carbon atoms are unlabelled). Thermal ellipsoids are at the 30% probability level.

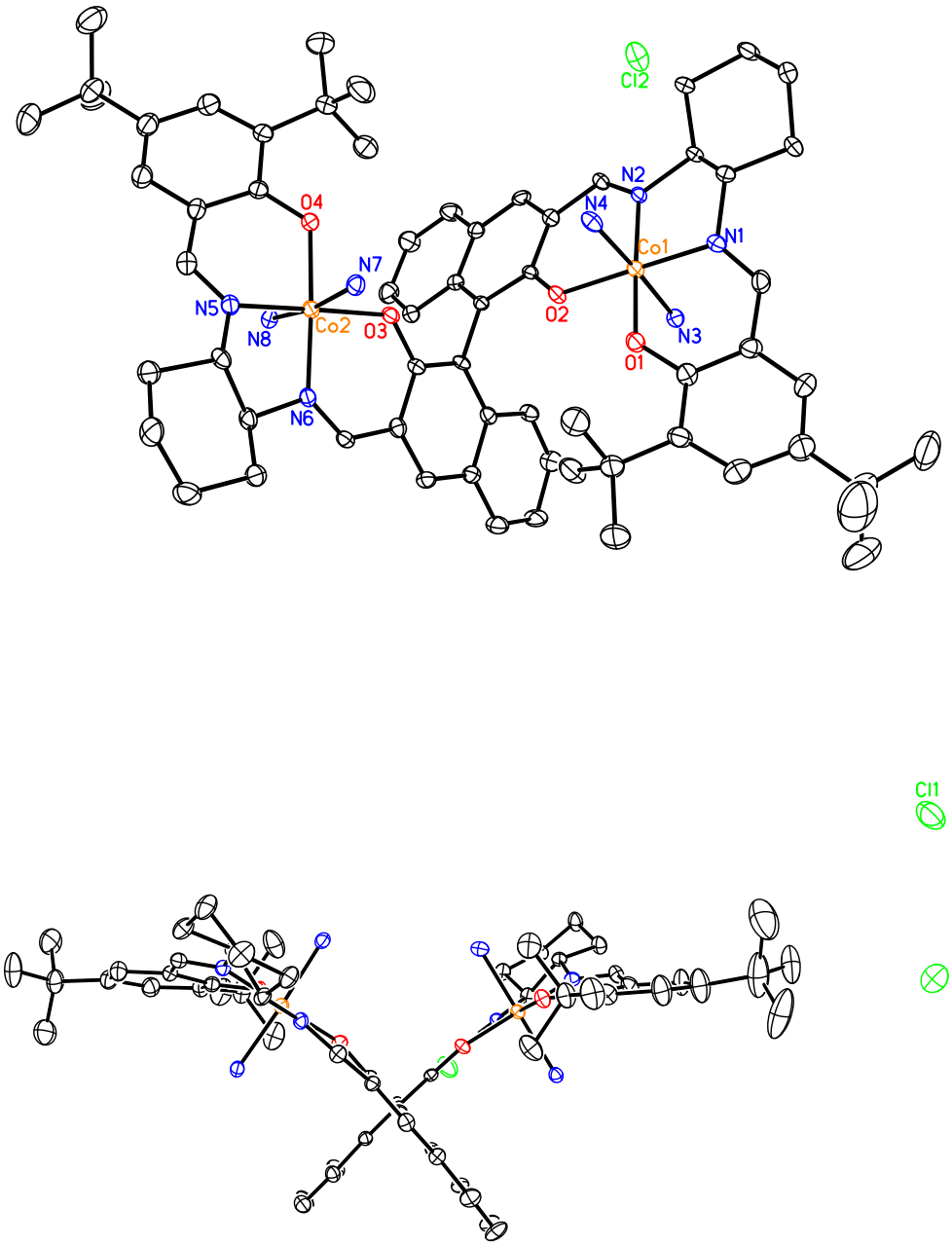

Figure 2.3. Molecular structure of **2.16** crystallized from pyridine and toluene (hydrogen atoms omitted and pyridine ligands truncated for clarity; carbon atoms are unlabelled). Thermal ellipsoids are at the 30% probability level.

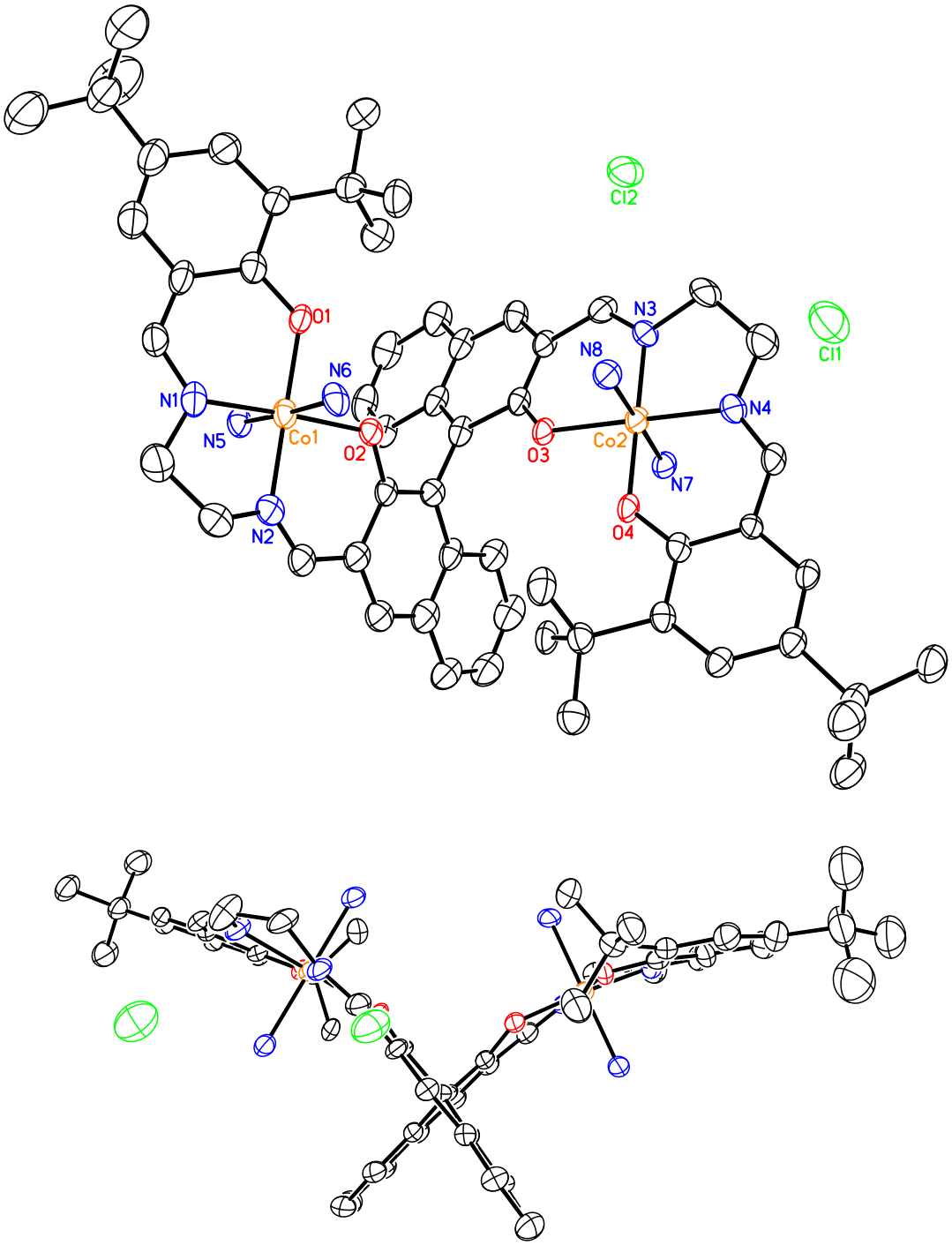

Figure 2.4. Molecular structure of **2.17** crystallized from pyridine and toluene (hydrogen atoms omitted and pyridine ligands truncated for clarity; carbon atoms are unlabelled). Thermal ellipsoids are at the 30% probability level.

2.3. Conclusions

In conclusion, we have shown that the axial chirality of the binaphthol linker in our bimetallic cobalt catalysts is responsible for enantioselectivity of monomer enchainment in epoxide polymerization. We synthesized a new racemic bimetallic cobalt complex (**2.3**) that can quantitatively polymerize racemic terminal epoxides to highly isotactic polyethers. We have also synthesized a new cocatalyst (**2.6**) that increased the rate and selectivity of **2.3**. This catalyst system (**2.3**/**2.6**) displays high activity, surpassing that of system **2.1**/**2.4**. Future work will focus on understanding the mechanism of this polymerization system and the origin of the effect of the cocatalyst on activity and selectivity.

2.4. Experimental

2.4.1. General Considerations

All air or water sensitive reactions were carried out under nitrogen in a Braun Labmaster drybox or using standard Schlenk techniques. NMR spectroscopy was performed using Varian Unity spectrometers INOVA 400 MHz, INOVA 500 MHz or INOVA 600 MHz. ^{1}H NMR spectra were referenced to residual non- or partially-deuterated solvent signals ($CHCl_3$ = 7.24 ppm, acetone-d_5 = 2.05 ppm, 1,1,2,2-tetrachloroethane-d_1 = 6.0 ppm, pyridine-d_4 = 8.74 ppm). ^{13}C NMR spectra were referenced to solvent signals ($CDCl_3$ = 77.23 ppm, acetone-d_6 = 29.92 ppm, 1,1,2,2-tetrachloroethane-d_2 = 73.78 ppm, pyridine-d_5 = 150.35 ppm). Mass spectrometry analyses were conducted at the School of Chemical Sciences Mass Spectrometry

Laboratory at the University of Illinois at Urbana-Champaign or they were acquired using a JEOL GCMate II mass spectrometer operating at 3000 resolving power for high resolution measurements in positive ion mode and an electron ionization potential of 70 eV.

2.4.2. Determination of Epoxide Enantiomeric Excess

The enantiomeric excess (*ee*) of recovered propylene oxide was determined by chiral gas chromatography (GC). Gas chromatograms were obtained on a Hewlett-Packard 6890 series gas chromatograph using a flame ionization detector, He carrier gas, and an Alltech CHIRALDEX A-TA chiral capillary column (50 m x 0.25 mm). The absolute stereochemistry of the PO remaining after the polymerization was determined by comparison to a commercially available enantiopure sample.

2.4.3. Polymer Characterization

Number average molecular weights (M_n) and molecular weight distributions (M_w/M_n) were measured using high temperature gel-permeation chromatography (GPC) using a Waters Alliance GPCV 2000 size exclusion chromatograph equipped with a Waters differential refractometer detector and viscometer. The set of five sequential columns (four Waters HT 6E and one Waters HT 2) was eluted with 1,2,4-trichlorobenzene containing approximately 0.01 wt % 2,6-di-*tert*-butylhydroxytoluene at 1.0 mL/min at 140 ºC. The Waters refractometer processing method was used for data

analysis. The chromatograms generated from the Waters refractometer were calibrated using polystyrene standards. Poly(1,1,1-trifluoro-2,3-epoxypropane) was examined using GPC at 35.0 °C in *N*,*N*-dimethylformamide containing 0.01 M lithium nitrate and 1% formic acid. The column set consisted of three 8 mm x 300 mm GRAM Linear M columns from Polymer Standards Services, calibrated with narrow-molecular-weight distribution poly(methyl methacrylate) standards. Polymer optical rotation was determined using a Perkin Elmer 241 Polarimeter. Polymer melting points were measured by differential scanning calorimetry (DSC) using a TA instruments Q1000 calorimeter equipped with an automated sampler. Analyses were performed in crimped aluminum pans under nitrogen and data were collected from the second heating run at a heating rate of 10 °C/min from -100 to 200 °C, and processed with the TA Q series software.

2.4.4. NMR Quantification of Polymer Tacticity

The signals in the ^{13}C NMR spectra of the polyethers synthesized in this paper exhibit distinct resonances that result from stereochemical defects in the polymer chain. Many of the polyethers synthesized in this paper exhibit triad resolution of the methine carbon (assignments from literature). However, some have significant overlap between the *mm*, *mr*, *rm*, and *rr* signals of the methine resonance. In these cases, the methylene resonance was used to quantify the triad resolution and calculate [*mm*]. Since the *mr* and *rm* triads occur in the same region as the ^{13}C-^{13}C satellite peaks of the *mm* triad, the distinct *rr* triad signal is instrumental in accurately calculating [*mm*] for highly isotactic samples, especially when the *mr* and *rm* triads are smaller than the satellite signal. The

value of the integration of the [*rr*] triad is multiplied by two (to equal the value of the *mr* and *rm* triads), and this value is subtracted from the integration of the *mm*, *mr*, and *rm* triads to give the value of the *mm* triad. In some instances, the *rr* was not apparent, and the largest stereoerror signal was taken to be the *rr* signal (Table 2.2, entry 3 and Table 2.3, entry 3). In these cases, the eventual calculation of the [*mm*] gives a lower limit for that value. For example, the [*mm*] of PPO can be calculated by integration of the [*rr*] triad, from which the value of [*mr*] and [*rm*] triads can be calculated and subtracted from the total integration of [*mm*], [*mr*], and [*rm*]. This method is used due to the ^{13}C NMR baseline separation of the [*rr*] triad signal from the other triad signals and was used to calculate the [*mm*] for all polyethers in this paper.

2.4.5. Calculation of Polymer Tacticity: (From ^{13}C NMR integrations of the methine resonances, Figure 2.5)

[*rr*] = 120/1120 = 0.107

[*mr* + *rm*] = [2(120)]/1120 = 0.215

[*mm*] = [1000-2(120)]/1120 = 0.678

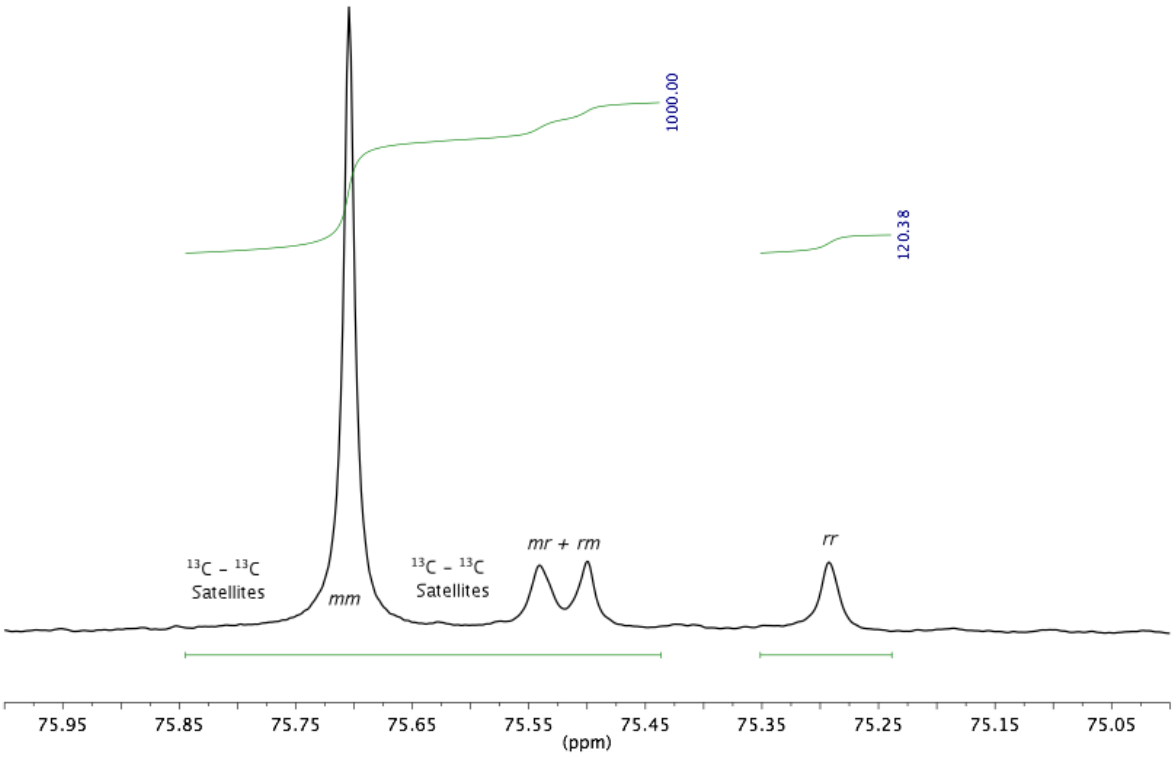

Figure 2.5. Calculation of $ee_{(P)}$ for PPO by ^{13}C NMR spectroscopy using *rr* triad resonance.

2.4.6. Materials

HPLC grade tetrahydrofuran, methylene chloride, and toluene were purchased from Fisher Scientific and purified over solvent columns. Reagent grade acetone, *n*-pentane, and chloroform, were purchased from Fisher Scientific and were used as received. Absolute ethanol and methanol were degassed by sparging with dry nitrogen, and stored over activated 3 Å molecular sieves. Styrene oxide was synthesized according to the procedure of Fringuelli and Pizzo,[22] dried over calcium hydride, degassed through several freeze-pump-thaw cycles, fractionally distilled under N_2 and stored in the glovebox. All other epoxides were purchased from commercial sources and were dried over calcium

hydride, degassed through several freeze-pump-thaw cycles, then vacuum transferred and stored under nitrogen in a glovebox. (1*S*,2*S*)-Diaminocyclohexane (99% *ee*) was purchased from Aldrich, 3,5-di-*tert*-butylsalicylaldehyde was purchased from Advanced Asymmetrics Inc. and (*S*)- and (*rac*)-1,1'-bi-2-naphthol was purchased from TCI. (1*S*,2*S*)-2-(3,5-di-*tert*-butyl-2-hydroxybenzylideneamino)cyclohexanammonium chloride,[23] and bis(triphenylphosphine)iminium acetate ([PPN]OAc), **2.4**[27] were prepared according to literature procedures. All other reagents were purchased from commercial sources and used as received.

2.4.7. Synthetic Procedures and Characterization

Scheme 2.6. Synthesis of Ligand **2.18**

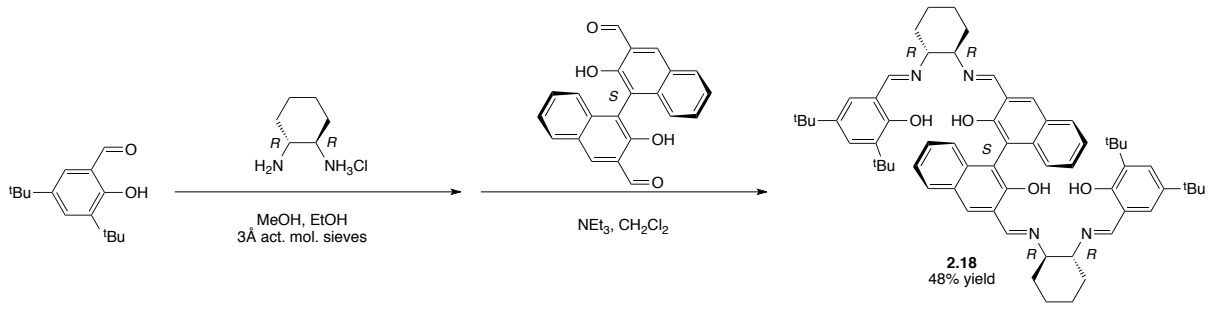

Synthesis of 2.18.[24] In a dry side arm adapted round bottom flask, (700 mg, 4.66 mmol) (1*R*,2*R*)-diaminocyclohexane and (1.04 g, 4.43 mmol) 3,5-di-*tert*-butyl salicylaldehyde were combined with 3 Å activated molecular sieves (5 g). The flask was then evacuated and purged with anhydrous nitrogen. A 50:50 mixture of anhydrous methanol and ethanol (20 mL) was then added and the suspension was stirred for 1 hour after which a solution of (*S*)-3,3'-diformyl-1,1'-bi-2-naphthol (759 mg, 2.21 mmol) and (1.3 mL, 9.3 mmol) anhydrous triethylamine in 50 mL anhydrous methylene chloride was added quickly. The resulting solution was allowed to stir over night, then filtered through celite, rinsed with 2x50 mL aqueous ammonium chloride, dried over sodium sulfate and concentrated under reduced pressure. The orange solid was purified by column chromatography on silica using 2% NEt_3, 10-15% ethyl acetate/hexanes leaving a bright yellow solid. Yield, 1.04 g, 48%. R_f = 0.44 (20%, EtOAc/hexanes, 1% Et_3N) ^1H NMR ($CDCl_3$, 500 MHz) δ 13.81 (s, 2H), 12.95 (s, 2H), 8.59 (s, 2H), 8.23 (s, 2H), 7.82 (s, 2H), 7.73 (m, 2H), 7.32 (d, J = 2.5 Hz, 2H), 7.21 (m, 4H), 7.08 (m, 2H), 6.98 (d, J = 2.4 Hz, 2H), 3.44 (m, 2H), 3.17 (m, 2H), 2.04-1.98 (m, 4H), 1.92-1.78 (m, 4H), 1.74-1.60 (m, 4H), 1.49 (s, 18H), 1.47-1.36 (m, 4H), 1.25 (s, 18 H). ^{13}C NMR ($CDCl_3$, 125 MHz) δ 166.13, 165.33, 157.92, 154.50,

139.89, 136.22, 135.01, 133.65, 128.77, 128.07, 127.48, 126.85, 126.20, 124.64, 123.11, 120.82, 117.66, 116.14, 72.94, 71.35, 34.98, 34.05, 33.46, 32.44, 31.46, 29.46, 24.19, 24.01. Elemental Analysis: Anal. Calcd. for $C_{64}H_{78}N_4O_4$: C, 79.46; H, 8.13; N, 5.79. Found: C, 79.05; H, 8.37; N, 5.55.

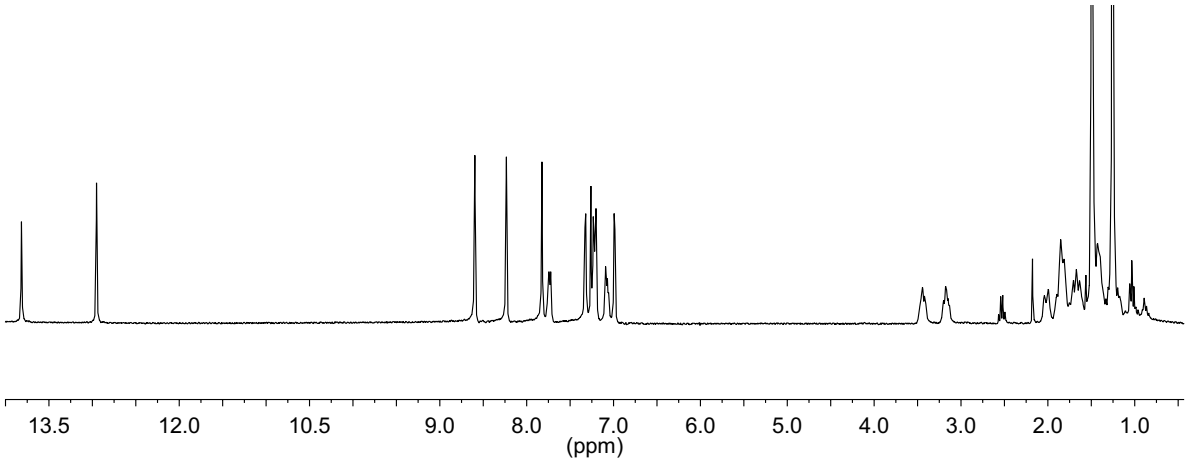

Figure 2.6. ^{1}H NMR spectrum of **2.18** in $CDCl_3$.

Table 2.4. Assignments of ^{1}H and ^{13}C NMR Chemical Shifts of Pyridine Adduct of **2.1** (**2.15**)

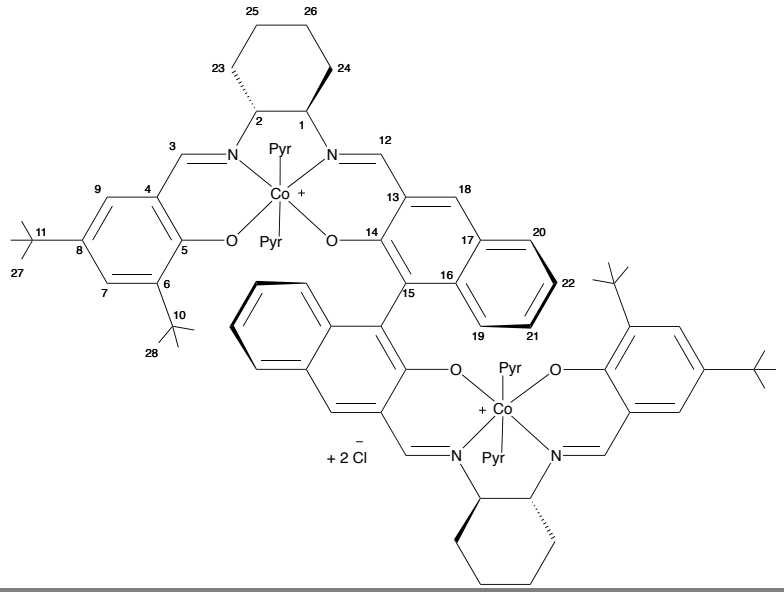

Nucleus	δ (ppm)	Nucleus	δ (ppm)	Nucleus	δ (ppm)
H1	2.41 (t, *J* = 11Hz, 1H)	H18	8.67 (s, 1H)	$H24_{(eq + ax)}$	3.04 (m, 1H) 3.20 (m, 1H)
H2	5.39 (t, *J* = 11 Hz, 1H)	H19	6.38 (d, *J* = 8 Hz, 1H)	$H25_{(eq + ax)}$	1.66 (m, 1H) 2.12 (m, 1H)
H3	8.55 (s, 1H)	H20	7.79 (d, *J* = 8 Hz, 1H)	$H26_{(eq + ax)}$	1.67 (m, 1H) 1.79 (m, 1H)
H7	7.63 (s, 1H)	H21	6.81 (t, *J* = 8 Hz, 1H)	H27	1.23 (s, 9H)
H9	7.45 (s, 1H)	H22	7.05 (t, *J* = 8 Hz, 1H)	H28	1.38 (s, 9H)
H12	9.42 (s, 1H)	$H23_{(eq + ax)}$	1.17 (m, 1H) 3.12 (m, 1H)		

Nucleus	δ (ppm)	Nucleus	δ (ppm)	Nucleus	δ (ppm)
C1	74.85	C10	35.27	C19	126.23
C2	67.58	C11	34.53	C20	130.61
C3	169.07	C12	168.72	C21	129.46
C5	161.20	C14	162.59	C22	122.02
C6	143.79	C15	125.70	C27	31.86
C7	131.87	C16	139.01	C28	30.82
C8	137.15	C17	127.27		
C9	130.63	C18	139.86		

Unassigned carbons: C4, C13, C23, C24, C25, C26 δ: 132.36, 129.28, 31.82, 29.95, 29.39, 25.25. Assignments were made using a combination of ^{1}H, ^{13}C, COSY and HMBC spectroscopy in pyridine-d_5 using a Varian 600 MHz spectrometer

Ligand 2.8. A procedure analogous to the synthesis of the (*R,R,S,R,R*) ligand was used for the synthesis of the (*S,S,S,S,S*) ligand **2.8**.[8] Under nitrogen, molecular sieves (3 Å, 5.0 g), methylene chloride (50 ml), (*S*)-3,3'-diformyl-1,1'-bi-2-naphthol (1.11 g, 3.22 mmol), triethylamine (1.85 mL, 13.3 mmol) and (1*S*, 2*S*)-2-(3,5-di-*tert*-butyl-2-hydroxybenzylideneamino)cyclohexanammonium chloride (2.43 g, 6.62 mmol) were added sequentially into a 200 mL Schlenk tube. After stirring for 24 hr, the reaction mixture was filtered through a pad of celite on a medium glass fritted funnel. The filtrate was washed with ammonium chloride aqueous solution, dried over $MgSO_4$, concentrated under reduced pressure and purified by chromatography on silica gel (12% EtOAc, 86% hexanes, 2% Et_3N) to provide pure product as a yellow solid in 26.6% yield. ^{1}H NMR ($CDCl_3$, 600 MHz): δ 13.79 (s, 1H), 13.09 (s, 1H), 8.54 (s, 1H), 8.19 (s, 1H), 7.80 (s, 1H), 7.72 (d, *J* = 8.8 Hz, 1H), 7.31 (d, *J* = 2.5 Hz, 1H), 7.20 (m, 1H), 7.15 (m, 1H), 7.04 (d, *J* = 8.8 Hz, 1H), 6.89 (d, *J* = 2.5 Hz, 1H), 3.47-3.35 (m, 1H), 3.21 (m, 1H), 2.58-2.25 (m, 1H), 2.16 (s, MeCN), 2.04-1.92 (m, 1H), 1.92-1.82 (m, 2H), 1.79 (m, 1H), 1.76-1.52 (m, 2H), 1.52-1.41 (m, 1H), 1.45 (s, 9H), 1.18 (s, 9H). (Figure 2.7) ^{13}C ($CDCl_3$, 151 MHz): δ 166.09, 165.42, 158.18, 154.70, 140.14, 136.57, 135.29, 133.79, 128.95, 128.39, 127.70, 127.07, 126.05, 124.90, 123.34, 120.96, 117.94, 116.47, 73.48, 71.91, 35.21, 34.21, 33.48, 33.02, 31.59, 29.63, 24.48, 24.37. HRMS-EI (m/z): calcd for $C_{64}H_{78}N_4O_4$, 966.6023; found, 966.6055.

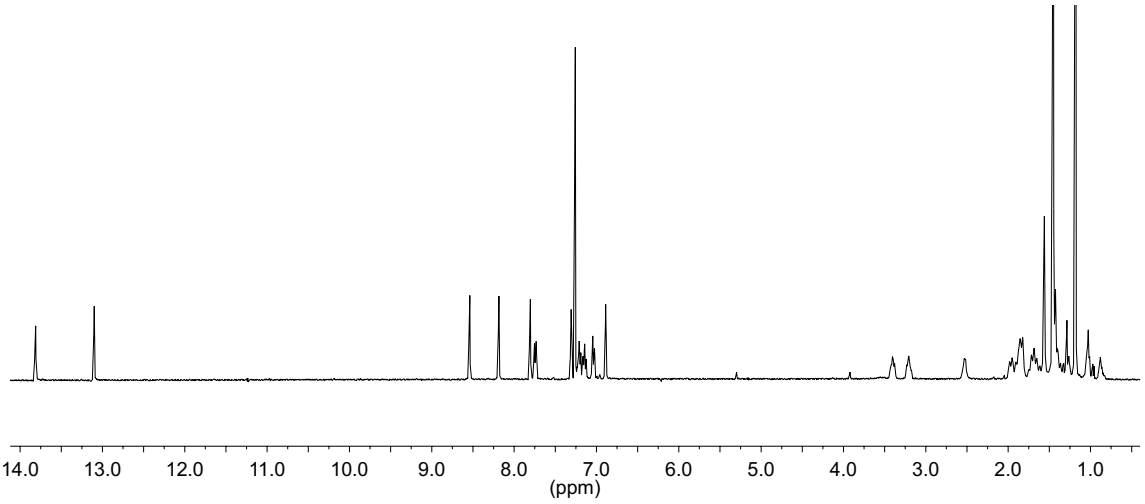

Figure 2.7. ^{1}H NMR spectrum of **2.8** in $CDCl_3$.

Complex 2.9. Under nitrogen, $Co(OAc)_2$ (110 mg, 0.620 mmol) was added to a 50 mL Schlenk tube with a stir-bar. **2.8** (290 mg, 0.299 mmol) was dissolved in methlylene chloride (3 mL) under nitrogen, and the ligand solution was cannulated into an anhydrous ethanol solution (8 mL) of $Co(OAc)_2$. The mixture was heated at 60 °C for 135 min, and then cooled slowly to room temperature. The solvent was removed in vacuo leaving a brick-red precipitate, which was collected by filtration using a fine glass-fritted funnel. The obtained solid was washed with pentane (20 mL) yielding a dark red powder, yield 262 mg, 73%. HRMS-EI (*m/z*): calcd for $C_{64}H_{74}Co_2N_4O_4$ 1080.4374; found, 1080.4392.

Complex 2.2. A procedure analogous to that reported by Jacobsen and co-workers for the synthesis of (*R*,*R*)-(salcy)CoCl[25] was applied for the synthesis of complex **2.2**. Complex **2.9** (262 mg, 0.242 mmol) was dissolved in 20 mL of methylene chloride in a beaker, and *para*-toluenesulfonic acid monohydrate (99 mg, 0.52 mmol) was added. The dark brown

solution was stirred open to air for 24 h, during which all the methylene chloride evaporated. The dark shiny solids were redissolved in methylene chloride and washed three times with concentrated aqueous sodium chloride, then dried over $MgSO_4$ and filtered. Solvent was removed in vacuo, and the dark brown solids were washed with pentane to yield 189 mg of **2.2** as a dark brown powder (68% yield). ^{1}H NMR (pyridine-d_5, 600 MHz): δ 9.21 (s, 1H), 8.71 (s, d_4 pyridine), 8.59 (s, 1H), 8.51 (s, 1H), 7.99-1.97 (m, 1H), 7.54 (s, d_4 pyridine), 7.49-7.48 (m, 2H), 7.19-7.03 (m, 2H), 7.18 (s, d_4 pyridine), 7.18-7.15 (m, 2H), 7.03-7.01 (m, 1H), 5.39-5.36 (m, 1H), 3.27 (m, 1H), 2.48 (m, 1H), 2.13-2.07 (m, 1H), 1.84-1.82 (m. 2H), 1.70-1.67 (m, 2H), 1.29 (s, 9H), 1.19 (s, 9H), 1.07-1.01 (m, 2H). (Figure 2.8)The complex was reduced to **2.9** during mass spectrometry analysis.

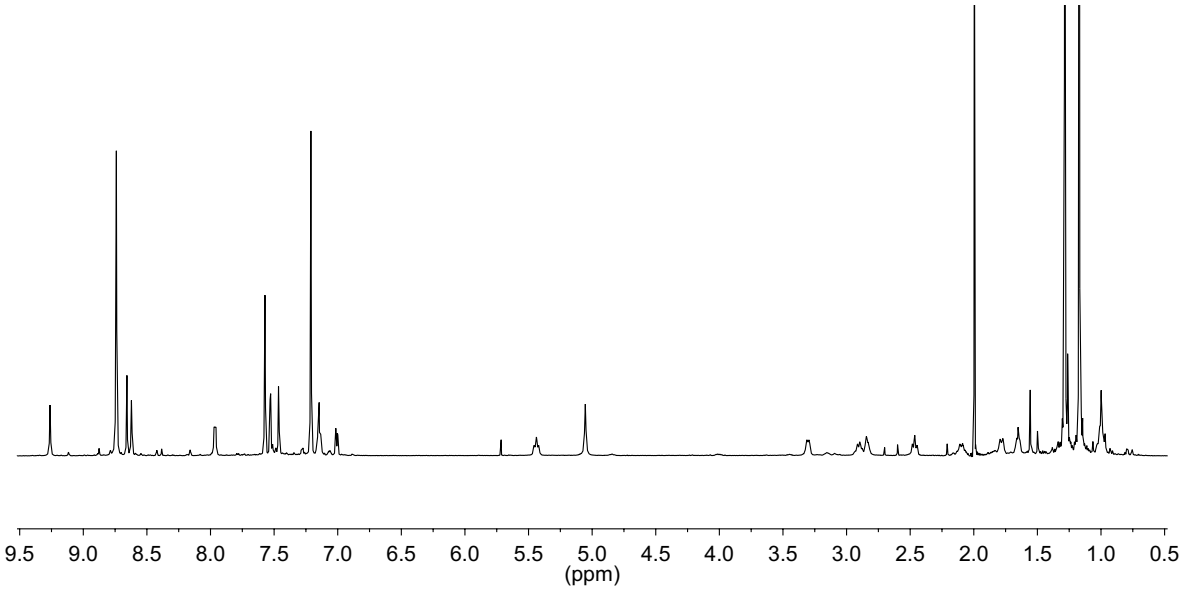

Figure 2.8. ^{1}H NMR spectrum of **2.2** in pyridine-d_5.

Ligand 2.10. 3,5-Di-*tert*-butyl salicylaldehyde (0.50 g, 2.2 mmol) was combined with ethylene diamine hydrochloride (0.21 g, 2.2 mmol) in a flask with activated 3Å molecular

sieves (5.0 g). The flask was purged with N_2 and 25 mL of dry methanol and 25 mL of dry ethanol was added via cannula and stirred under N_2 at room temperature. The reaction was monitored by TLC until complete disappearance of salicylaldehyde was observed (2 h). At this point a solution of (*rac*)-3,3'-diformyl-1,1'-bi-2-naphthol 0.40 g (1.1 mmol) and triethylamine 0.25 mL were dissolved in 100 mL of anhydrous methylene chloride then cannulated into the reaction mixture and stirred overnight. The reaction was filtered through celite and rinsed with dichloromethane. The solution was concentrated, and purified by chromatography on silica gel (15%, EtOAc 84% hexanes, 1% Et_3N increased to 40%, EtOAc 59% hexanes, 1% Et_3N) The obtained yellow solid was rinsed with 4 x 5 mL of acetonitrile leaving pure ligand as a pale yellow solid. 0.1287 g 14% yield. R_f = 0.73 (40%, EtOAc / hexanes, 1% Et_3N). ^1H NMR ($CDCl_3$, 300 MHz): δ 13.59 (s, 1H), 13.07 (s, 1H), 8.62 (s, 1H), 8.32 (s, 1H), 7.92 (s, 1H), 7.83-7.81 (m, 2H), 7.33 (s, 1H), 2.25 (m, 1H) 7.24 (s, $CHCl_3$), 7.13 (s, 1H), 6.99 (s, 1H), 5.28 (s, CH_2Cl_2), 3.92-3.97 (m, 4H), 3.86-3.88 (m, 4H), 1.42 (s, 9H), 1.23 (s, 9H). (Figure 2.9) ^{13}C NMR ($CDCl_3$, 125 MHz): δ 196.92, 167.81, 167.75, 166.93, 158.14, 154.89, 154.77, 140.22, 136.74, 135.45, 134.18, 133.82, 130.07, 129.22, 129.08, 128.69, 128.54, 127.85, 127.71, 127.22, 126.25, 125.36, 124.92, 124.54, 124.47, 123.65, 123.49, 120.96, 117.89, 116.72, 77.48, 77.23, 76.98, 60.26, 59.44, 35.20, 35.05, 34.26, 31.65, 31.50, 29.63. HRMS-EI (m/z): calc for $C_{56}H_{66}N_4O_4$, 858.5084; found, 858.5084.

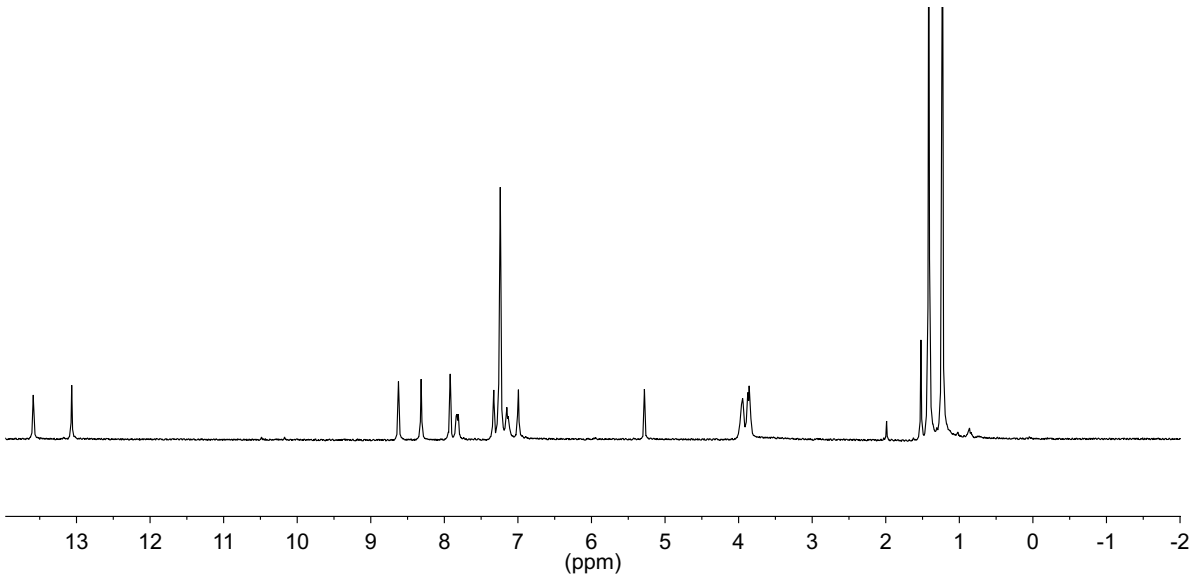

Figure 2.9. ^{1}H NMR spectrum of **2.10** in $CDCl_3$.

Complex 2.11. Ligand **2.10** (227 mg, 0.264 mmol) was dissolved in 10 mL anhydrous degassed methylene chloride. In a separate flask $Co(OAc)_2 \cdot 4H_2O$ (145 mg, 0.581 mmol) was evacuated and dehydrated with a heat gun until solid changed color from pink to purple. The solid $Co(OAc)_2$ was then dissolved in 20 mL of anhydrous degassed EtOH via cannula. The ligand solution was transferred to the ethanol solution via cannula and a brown, red solid precipitate formed. The suspension was heated to 60 °C for 2 h after which it was allowed to cool. The solvent was removed in vacuo to yield a brown precipitate. Product was collected by filtration using a fine frit, and rinsed with 3 x 100 mL pentanes yielding **2.11** as a brown powder. Yield: 225 mg (87 %). Compound is paramagnetic. HRMS-EI (m/z): calc for $C_{56}H_{62}N_4O_4,Co_2$ 972.3435; found, 972.3446.

Complex 2.3. The cobalt complex **2.11** (142 mg, 0.146 mmol) was dissolved in 50 mL of methylene chloride. $TsOH \cdot H_2O$ (62 mg, 0.32 mmol) was added and the reaction mixture

was stirred open to air in a beaker for 17 h over which time most of the solvent evaporated. Methylene chloride, 50 mL, was added and the solution was rinsed with 3 x 50 mL brine, dried over Na_2SO_4, and filtered. Solvent was removed in vacuo providing a shiny black solid which was rinsed with 4 x 100 mL pentanes. Yield: 76 mg 50%. ^{1}H NMR (pyridine-d_5, 300 MHz): δ 9.42 (s, 1H), 8.61 (s, d_4 pyridine), 8.40 (m, 2H), 7.83 (d, J = 8.3 Hz, 1H), 7.56 (s, d_4 pyridine) 7.55 (m, 1H), 7.29 (s, d_4 pyridine), 7.26-7.04 (m, 2H), 7.02-6.74 (m, 1H), 6.65 (d, J = 8.3 Hz, 1H), 4.97 (s, H_2O), 4.09-4.06 (m, 2H), 3.57-3.50 (m, 2H), 1.25 (s, 9H), 1.18 (s, 9H). (Figure 2.10) The complex was reduced to **2.11** during mass spectrometric analysis.

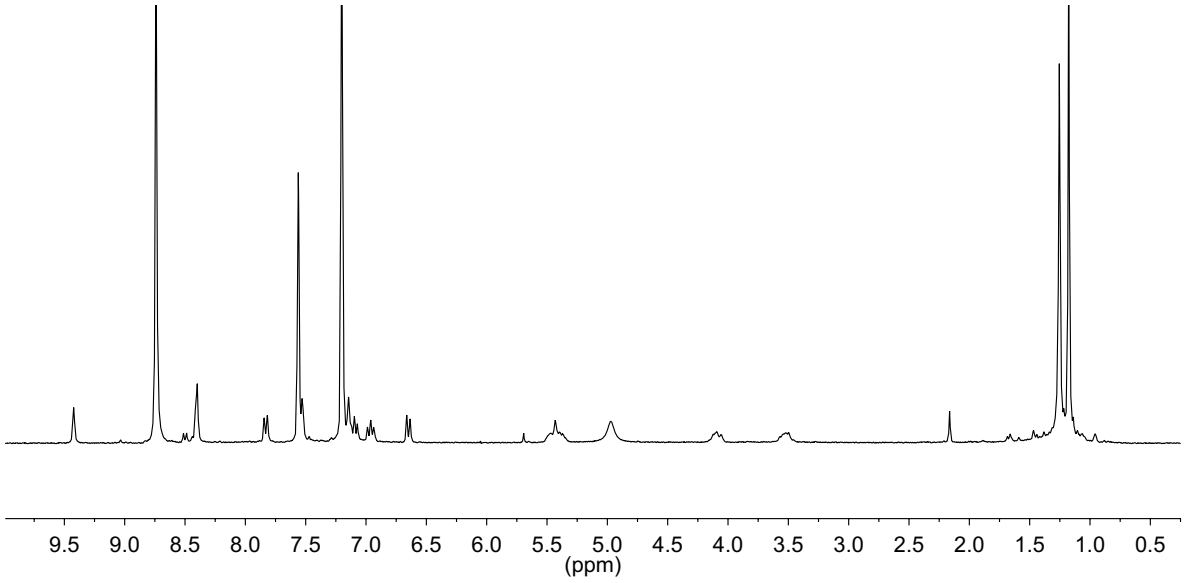

Figure 2.10. ^{1}H NMR spectrum of **2.3** in pyridine-d_5.

Representative synthesis of silver carboxylates 2.12, 2.13, 2.14.[26]

Silver 2-ethylhexanoate 2.12. An aqueous solution of silver nitrate (50 mL, 1 M) was added to an aqueous sodium 2-ethylhexanoate solution (50 mL, 1.2 M). The resulting mixture was stirred in the absence of light for 15 min. The precipitate was filtered and

rinsed with 50 mL water, 50 mL methanol, and 50 mL diethyl ether yielding a white solid which was dried in vacuo. Yield 1.3 g, 89% Elemental analysis: Calcd for $C_8H_{15}AgO_2$: C, 38.3%; H, 6.0%.Found: C, 38.2%; H, 5.9%.

Silver 2,2-dimethylpropionate 2.13. Yield 0.48 g, 39% Elemental analysis: Calcd for $C_5H_9AgO_2$: C, 28.7%; H, 4.3%. Found: C, 29.0%; H, 4.2%.

Silver 3,3-dimethylbutyrate 2.14. Yield 1.1 g, 83% Elemental analysis: Calcd for $C_6H_{11}AgO_2$: C, 32.3%; H, 5.0%. Found: C, 32.4%; H, 4.8%.

Representative synthesis of PPN carboxylates 2.5, 2.6, 2.7.[27]

Bis(triphenylphosphine)iminium chloride ([PPN]Cl) (561 mg, 0.976 mmol) and silver carboxylate **2.12** (250 mg, 0.996 mmol) were combined in 10 mL $CHCl_3$ and stirred at room temperature in the absence of light. After 3 days, stirring was stopped and the gray solid was allowed to settle and the liquid was decanted. Any remaining solid was removed by centrifugation, yielding a clear colorless liquid. Solvent was removed under vacuum yielding a clear viscous oil which solidified upon standing to give a white solid. Typical yields were 85-99%.

Bis(triphenylphosphine)iminium 2-ethylhexanoate 2.5. Isolated as a viscous clear oil in 98% yield. ^{1}H NMR ($CDCl_3$, 400 MHz): δ 7.64 (m, 6H), 7.52-7.36 (m, 24H), 7.24 (s, $CHCl_3$), 2.31-2.21 (m, 1H), 1.71-1.57 (m, 2H), 1.46-1.17 (m, 6H), 0.90 (t, J = 7.4 3H), 0.79 (t, J = 7.2, 3H,). ^{13}C NMR ($CDCl_3$, 151 MHz): δ 134.05, 132.31-131.99 (m), 129.90-129.57 (m), 127.01 (dd, J = 1.9, 110 Hz), 77.25 ($CDCl_3$), 49.25, 32.83, 30.17, 26.22,

23.24, 14.30, 12.48. Figure 2.11.

A)

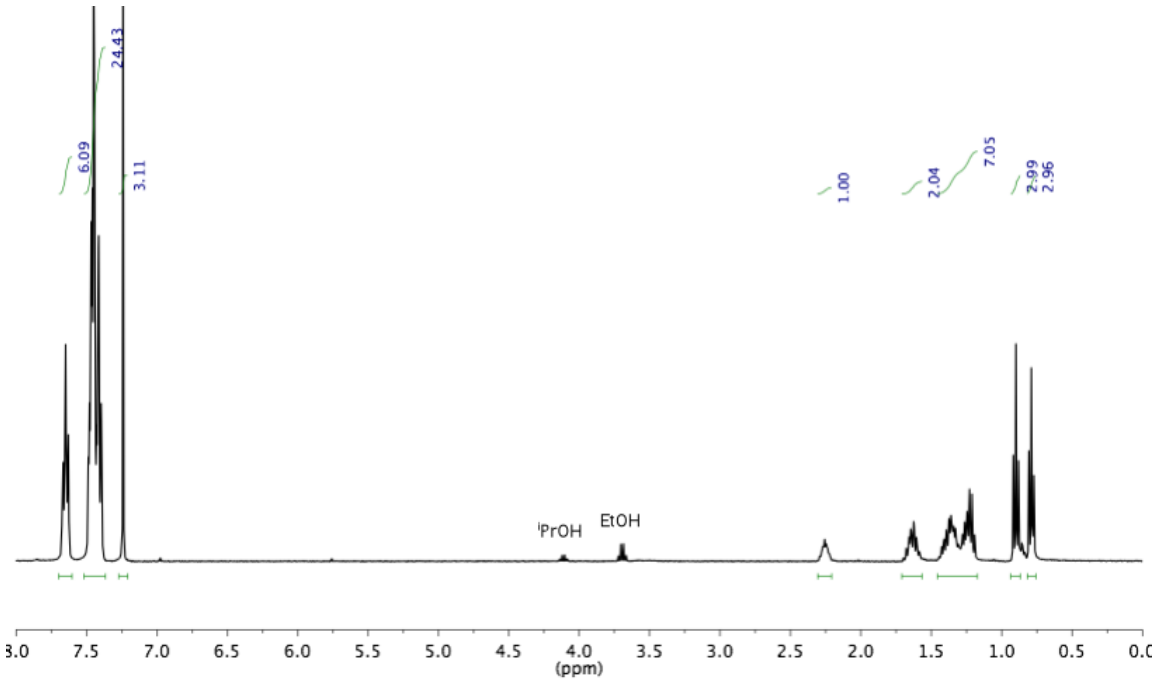

B)

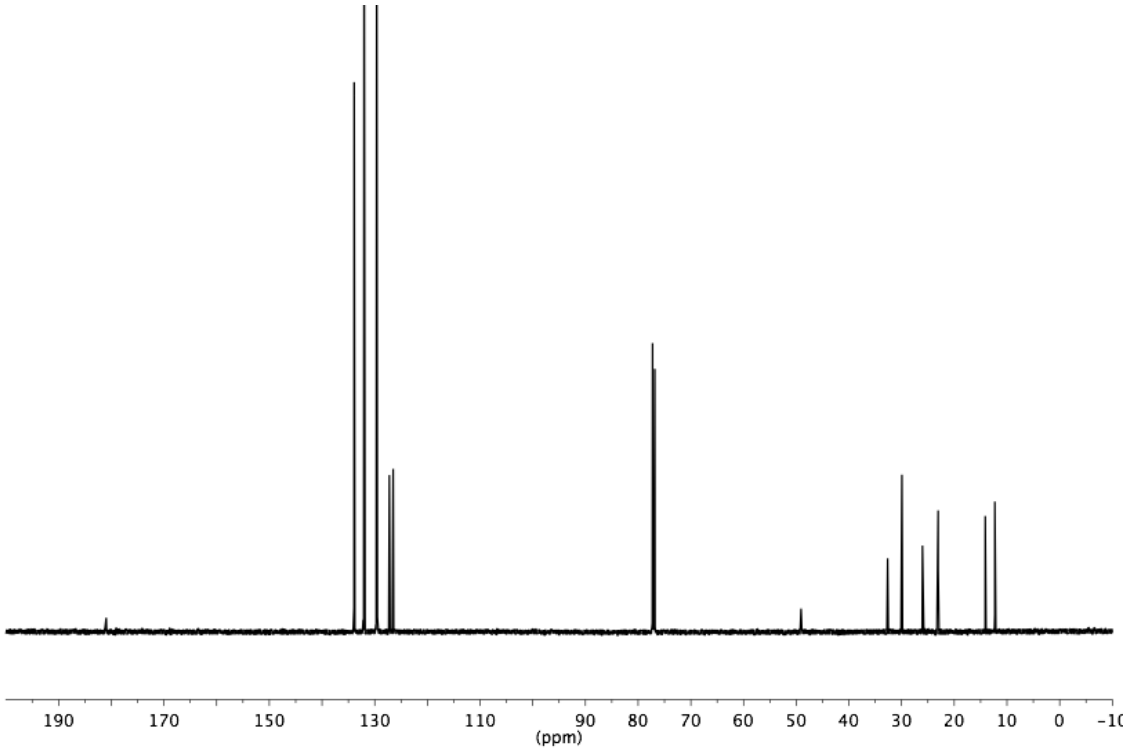

Figure 2.11. NMR spectra of **2.5** in $CDCl_3$. A) ^{1}H NMR spectrum. B) ^{13}C NMR spectrum.

Bis(triphenylphosphine)iminium 2,2-dimethylpropionate 2.6. Isolated as a white solid in 87% yield. ^{1}H NMR ($CDCl_3$, 300 MHz): δ 7.70-7.59 (m, 6H), 7.53-7.35 (m, 24H), 7.24 (s, $CHCl_3$), 1.19 (s, 9H). ^{13}C NMR (151 MHz, $CDCl_3$) δ 181.13, 134.05, 132.31-131.99 (m), 129.90-129.57 (m), 127.01 (dd, J = 1.9, 110 Hz), 77.25 ($CDCl_3$), 28.98. Figure 2.12.

A)

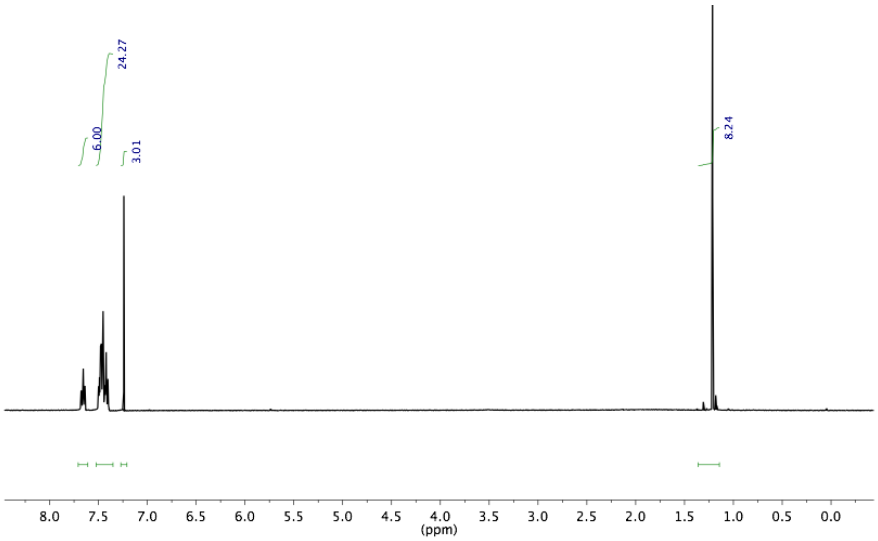

B)

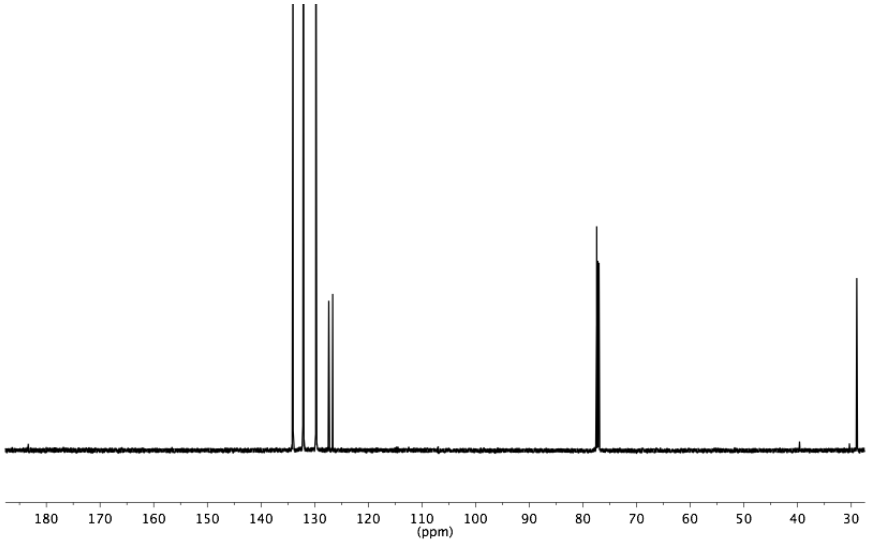

Figure 2.12. NMR spectra of **2.6** in $CDCl_3$. A) ^{1}H NMR spectrum. B) ^{13}C NMR spectrum.

Bis(triphenylphosphine)iminium 3,3-dimethylbutyrate 2.7. Isolated as a white solid in 98% yield. ^{1}H NMR ($CDCl_3$, 300 MHz): δ 7.70-7.58 (m, 6H), 7.53-7.33 (m, 24H), 7.24 (s, $CHCl_3$), 2.20 (s, 2H), 1.01 (s, 9H). ^{13}C NMR ($CDCl_3$, 151 MHz): δ 177.57, 134.05, 132.31-131.99 (m), 129.90-129.57 (m), 127.01 (dd, J = 1.9, 110 Hz), 77.25 ($CDCl_3$), 51.79, 30.34. Figure 2.13.

A)

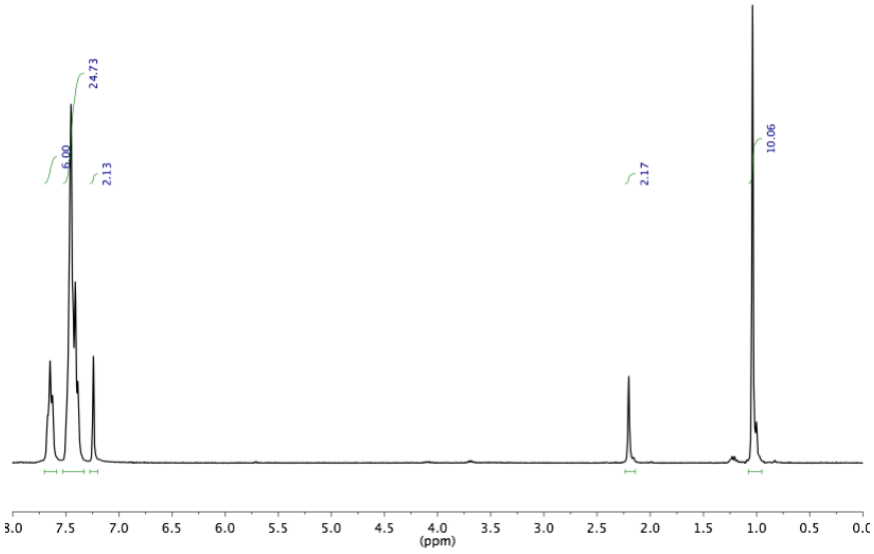

B)

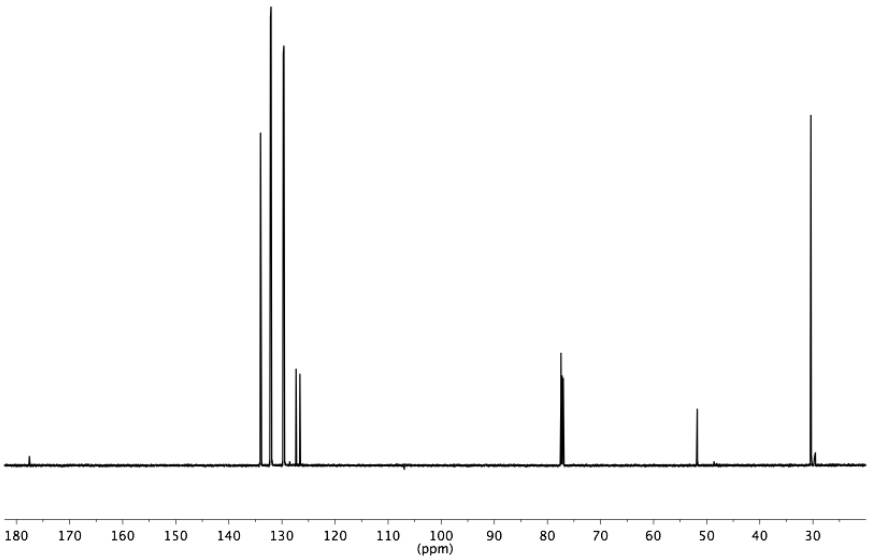

Figure 2.13. NMR spectra of **2.7** in $CDCl_3$. a) ^{1}H NMR spectrum. b) ^{13}C NMR spectrum.

2.4.8. Polymerization of Epoxides

Determination of *S*-factor of 2.2, Enantioselective Polymerization of Propylene Oxide.

In a nitrogen drybox, **2.2** (4.2 mg, 0.0035 mmol) and **2.4** (4.4 mg, 0.0074 mmol) were added to a Schlenk tube containing a stir bar. A vacuum adapter was attached to the Schlenk tube, and was sealed under nitrogen before removing from the drybox. The Schlenk tube was placed under dry nitrogen on the Schlenk line, and subsequently cooled in an ice bath. Anhydrous toluene (6 mL) was added to the Schlenk tube via syringe, and the resulting solution was stirred for 15 min at 0 °C. Propylene oxide (0.831 g, 14.3 mmol) was added via syringe and the polymerization reaction was kept at 0 °C. After 90 min, the unreacted propylene oxide was vacuum transferred to another Schlenk tube cooled in liquid nitrogen. The remaining polymer solution was transferred to a pre-weighed round bottom flask and dried overnight under vacuum. Conversion was determined by polymer mass to be 21.7%. The *ee* of recovered propylene oxide was measured by chiral GC to be 18% (*R*)-propylene oxide, with t_R (major, *R*) = 14.2 min and t_R (minor, *S*) = 14.7 min. The absolute stereoconfiguration was confirmed by chiral GC using commercially available (*R*)-propylene oxide. The conditions for separation were: flow, 1.4 mL/min; velocity, 34 cm/sec; pressure, 7 psi; isothermal at 40 ºC. The optical rotation of the polymer was measured ($[\alpha]_D^{23}$ = -24.7 °, c = 1.5 g / 100 mL, $CHCl_3$) and matched closely that reported by Price et al.[28] The negative rotation shows that the polymer synthesized with **2.2** is (*S*)-poly(propylene oxide), giving evidence for epoxide ring-opening at the methylene carbon with retention of the configuration at the methine carbon. A concentrated sample of polymer in $CDCl_3$ was made for analysis by ^{13}C NMR

spectroscopy to determine polymer tacticity. 50 mg of polymer was dissolved in 0.5 mL of $CDCl_3$. An INOVA 500 Varian spectrometer was used to obtain the ^{13}C NMR spectrum (taken over 2 h, with more than 2000 scans), as well as a ^{1}H NMR spectrum of the dried polymer. Polymer tacticity (Figure 2.14): [*mm*]:[*mr* + *rm*]:[*rr*] = [0.982]:[0.012]:[0.006]. [*m*] = 0.991, and $ee_{(p)}$ = 98.8%. *s*-factor calculated using equation: s = *s*-factor = k_s/k_r = $ln[1\text{-}c(1+ee_{(P)})]/ln[1\text{-}c(1\text{-}ee_{(P)})]$ where c is the conversion of epoxide *s*-factor = 210. ^{13}C NMR ($CDCl_3$, 125 MHz): δ 75.70, 73.61, 17.64. ^{1}H NMR ($CDCl_3$, 500 MHz): δ 3.56-3.49 (m, 2H), 3.39 (m, 1H), 1.11 (m, 3H). M_n = 36,800 g/mol, M_w/M_n = 7.8.

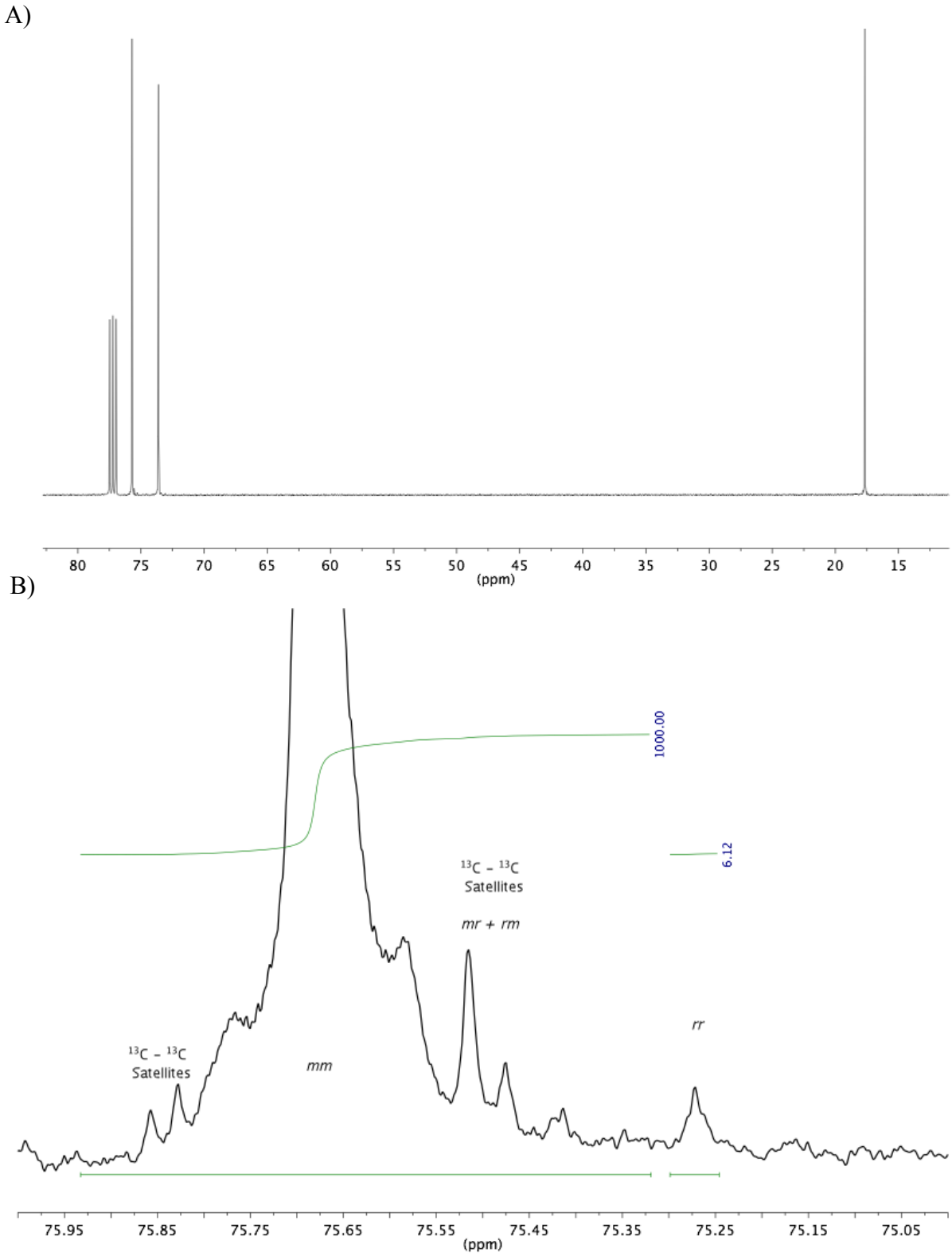

Figure 2.14. ^{13}C NMR spectra of poly(propylene oxide) in $CDCl_3$. A) Full spectrum. B) Methine region.

Representative Isoselective Polymerization of Racemic Epoxides

Polymerization of Racemic Propylene Oxide with 2.3/2.6 (Table 2.2, entry 1).

In a drybox under nitrogen atmosphere, **2.3** (4.0 mg, 0.0038 mmol) and **2.6** (4.9 mg, 0.0076 mmol) were added to 6 mL of anhydrous toluene in a Schlenk tube containing a stir bar. The Schlenk tube was sealed under nitrogen and removed from the drybox. The Schlenk tube was placed under nitrogen on the Schlenk line and subsequently cooled in an ice bath and stirred for 15 min at 0 °C. Propylene oxide (0.831 g, 14.3 mmol) was added via syringe. The polymerization was kept at in an ice bath during the course of the reaction. After 5 min an aliquot was taken for NMR analysis then 1 mL of methanol containing a trace amount of HCl was added to the mixture to quench the catalyst. Volatiles were then removed under vacuum. The remaining polymer solution was transferred to a pre-weighed round bottom flask and dried overnight under vacuum. Conversion was determined by ^{1}H NMR of the aliquot taken and determined to be 55%. An INOVA 500 Varian spectrometer was used to obtain the ^{13}C NMR spectrum (taken over 2 hrs, with more than 2000 scans), as well as a ^{1}H NMR spectrum of the dried polymer. Polymer tacticity (Figure 2.15) [*mm*] = 0.97. ^{1}H NMR ($CDCl_3$, 500 MHz): δ 3.52 (m, 2H), 3.39 (m, 1H), 1.11 (m, 3H). ^{13}C NMR ($CDCl_3$, 125 MHz): δ 75.70, 73.61, 17.64. M_n = 134,000 g/mol, M_w/M_n = 1.84.[29]

A)

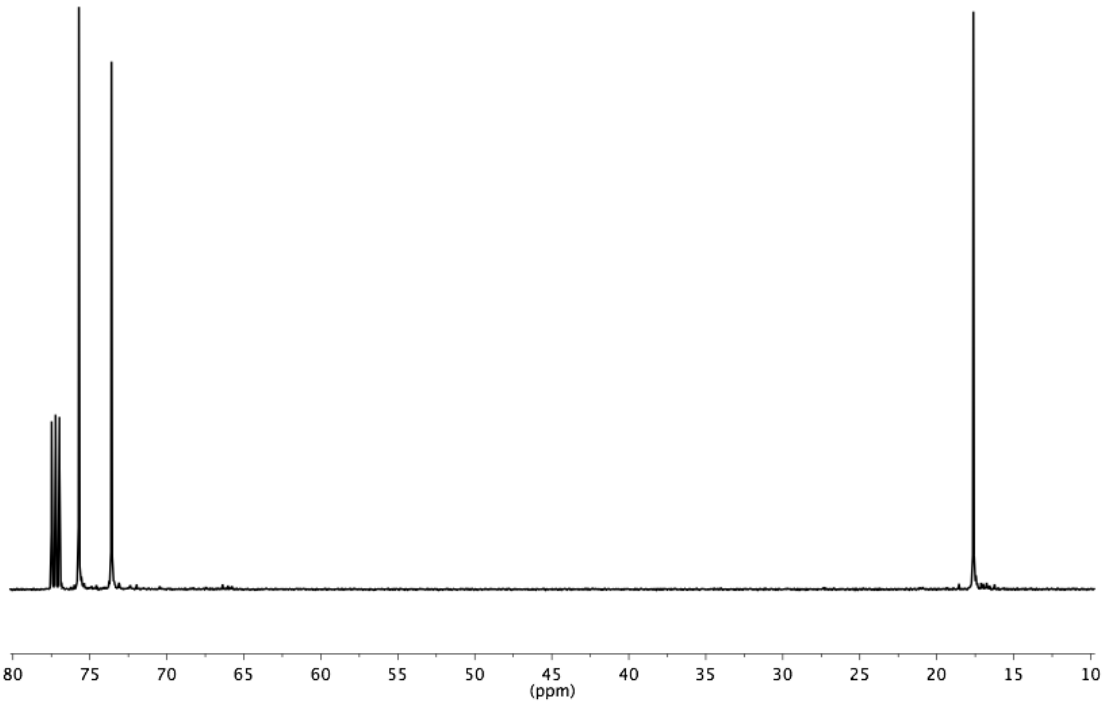

B)

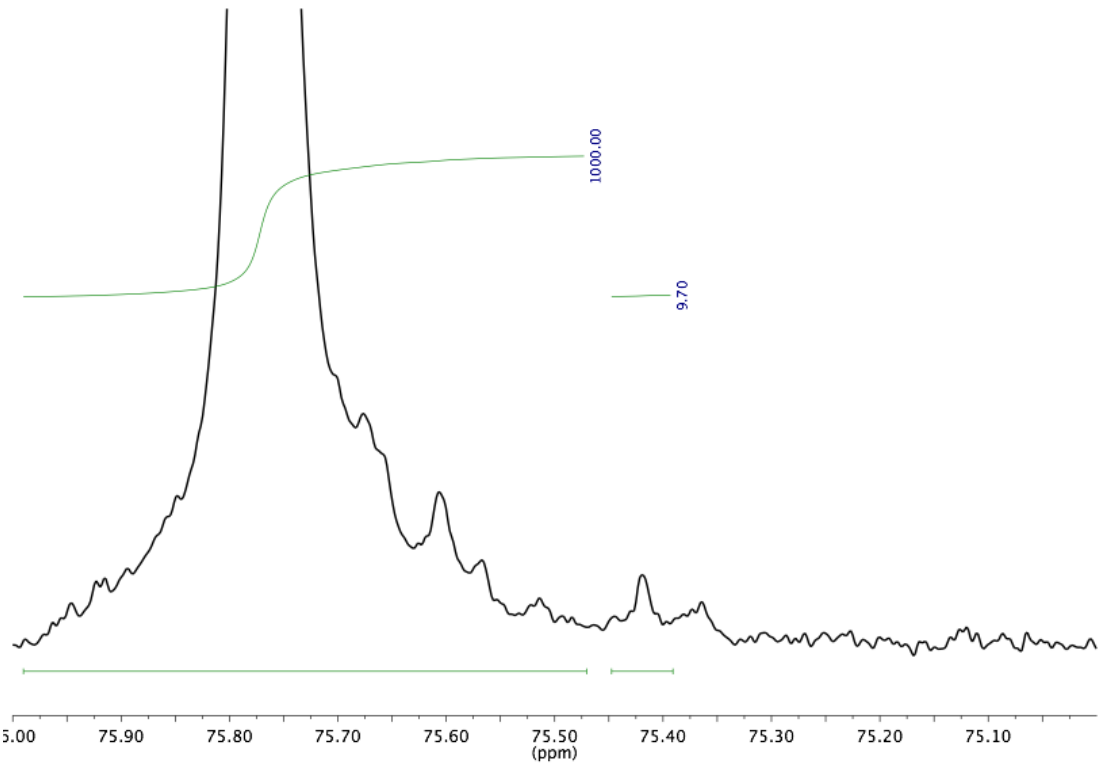

Figure 2.15. ^{13}C NMR spectra of poly(propylene oxide) in $CDCl_3$. A) Full spectrum. B) Methine region.

Polymerization of Racemic 1-Butene Oxide (Table 2.2, entry 2).

The polymerization procedure was the same as that for propylene oxide except that 1.27 mL of butene oxide was used. Conversion was determined after 5 min by ^{1}H NMR to be 60%. Polymer tacticity (Figure 2.16) [*mm*] = 0.97. ^{1}H NMR ($CDCl_3$, 400 MHz): δ 3.63 (m, 1H), 3.56 – 3.49 (m, 1H), 3.40 – 3.30 (m, 1H), 1.62 – 1.48 (m, 2H), 0.95 (t, J = 7.4 Hz, 3H). ^{13}C NMR ($CDCl_3$, 126 MHz): δ 81.07, 72.62, 25.04, 10.06. M_n = 239,000 g/mol, M_w/M_n = 1.47.

A)

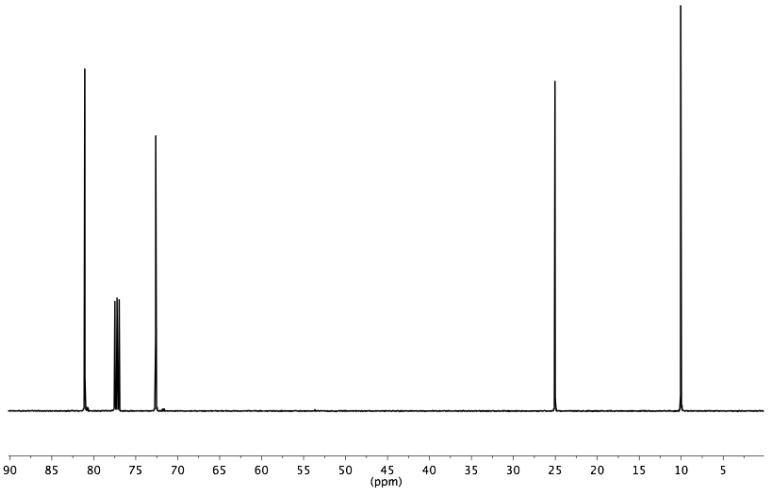

B)

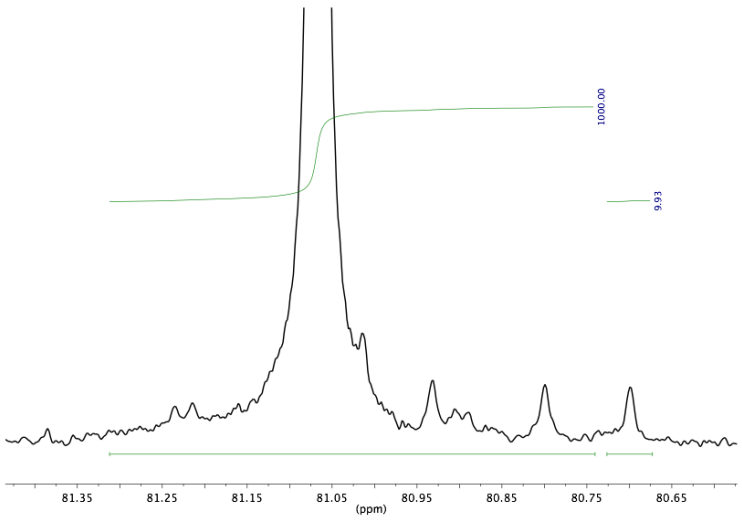

Figure 2.16. ^{13}C NMR spectra of poly(butene oxide). a) Full spectrum. b) Methine region.

Polymerization of Racemic Phenyl Glycidyl Ether (Table 2.2, entry 3).

The polymerization procedure was the same as that for propylene oxide except that 1.98 mL of phenyl glycidyl ether was used. Conversion was determined after 1 min by ^{1}H NMR to be 89 %. Polymer tacticity (Figure 2.17) [*mm*] = 0.97. ^{1}H NMR (1,1,2,2,-tetrachloroethane-d_2, 500 MHz, 135 °C): δ 7.30 (m, 2H), 6.94 (m, 3H), 4.13 (m, 1H), 4.08 (m, 1H), 3.85 (m, 3H). ^{13}C NMR (1,1,2,2-tetrachloroethane-d_2, 126 MHz, 135°C) δ 158.91, 129.13, 120.76, 115.01, 78.47, 70.06, 68.64. M_n = 328,000 g/mol, M_w/M_n = 1.39.[30]

A)

B)

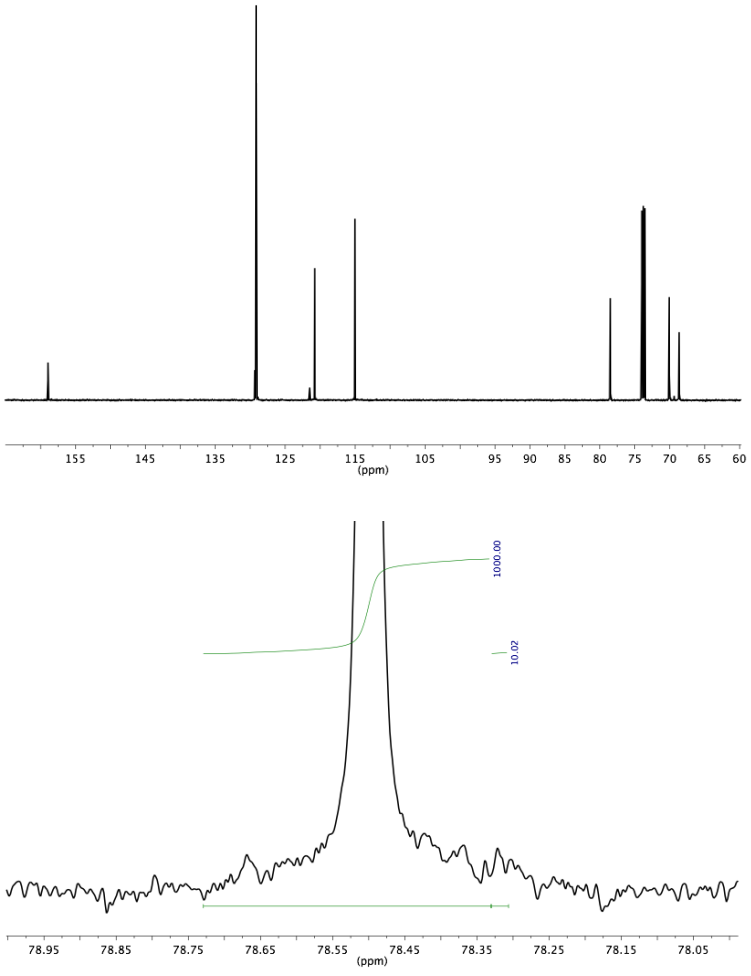

Figure 2.17. ^{13}C NMR spectra of poly(phenyl glycidyl ether). A) Full spectrum. B) Methine region.

Polymerization of Racemic 3,4-Epoxy-1-Butene (Table 2.2, entry 4).

The polymerization procedure was the same as that for propylene oxide except that 1.18 mL of 3,4-epoxy-1-butene was used. Conversion was determined after 10 min by ^{1}H NMR to be 46%. Polymer tacticity (Figure 2.18) [*mm*] = [0.92]. ^{1}H NMR ($CDCl_3$, 400 MHz): δ 5.75 (m, 1H), 5.32 (m, 1H), 5.19 (m, 1H), 4.08 – 3.80 (m, 1H), 3.68 – 3.52 (m, 1H), 3.45 (m, 1H). ^{13}C NMR ($CDCl_3$, 126 MHz): δ 136.27, 117.64, 80.79, 72.31. M_n = 212,000 g/mol, M_w/M_n = 1.52.

(Note: The polymer displays tetrad resolution of the methylene carbon. The tacticity was confirmed by complete hydrogenation to poly(1-butene oxide), which had [*mm*] = 0.92)

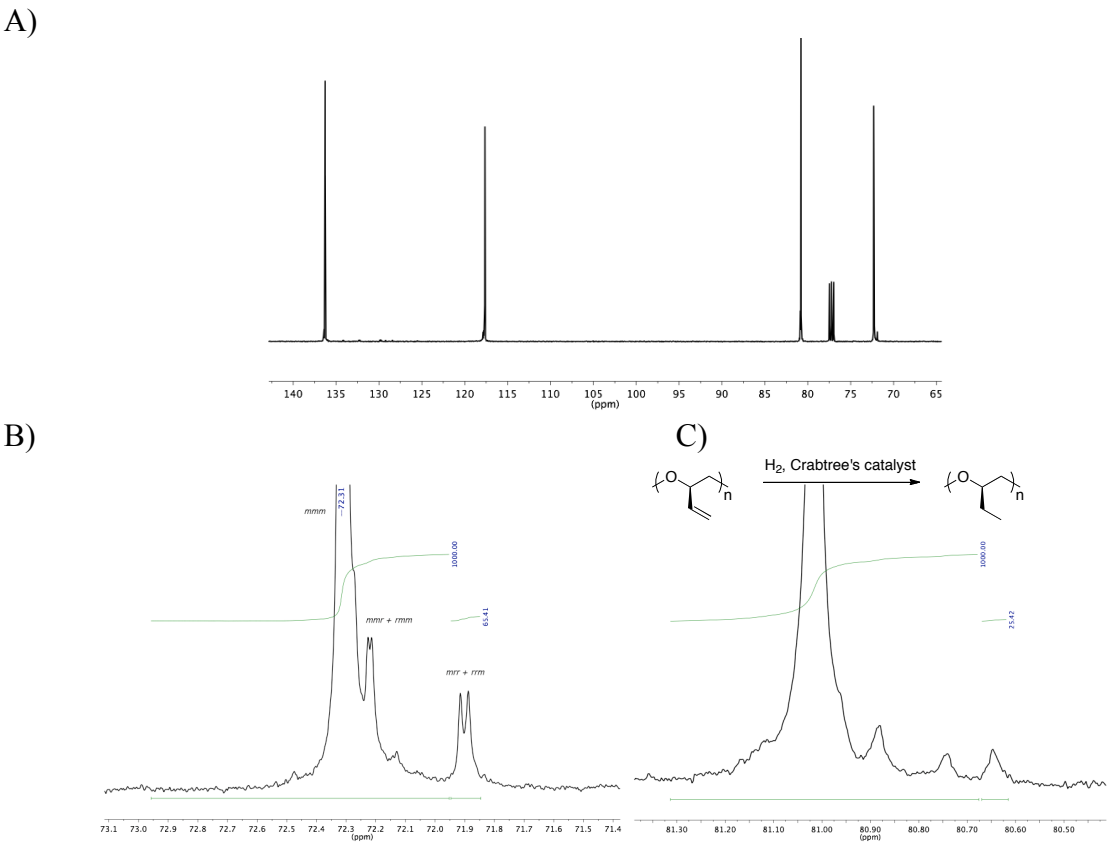

Figure 2.18. ^{13}C NMR spectra of poly(3,4-epoxy-1-butene). A) Full spectrum. B) Methylene region. C) Hydrogenated polymer methine region.

Polymerization of Racemic Styrene Oxide (Table 2.2, entry 5).

The polymerization procedure was the same as that for propylene oxide except that 1.66 mL of styrene oxide was used. Conversion was determined after 45 min by ^{1}H NMR to be 23%. Polymer tacticity (Figure 2.19) [*mm*] = 0.93. ^{1}H NMR ($CDCl_3$, 600 MHz): δ 7.37 (s, 5H), 4.57 (m, 1H), 3.69 (m, 1H), 3.55 (m, 1H). ^{13}C NMR ($CDCl_3$, 126 MHz): δ 81.07, 72.62, 25.04, 10.06. M_n = 77,000 g/mol, M_w/M_n = 1.92.

A)

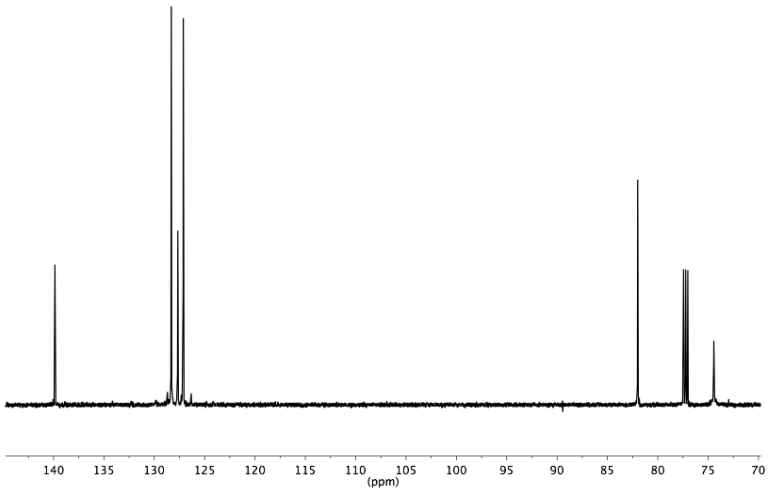

B)

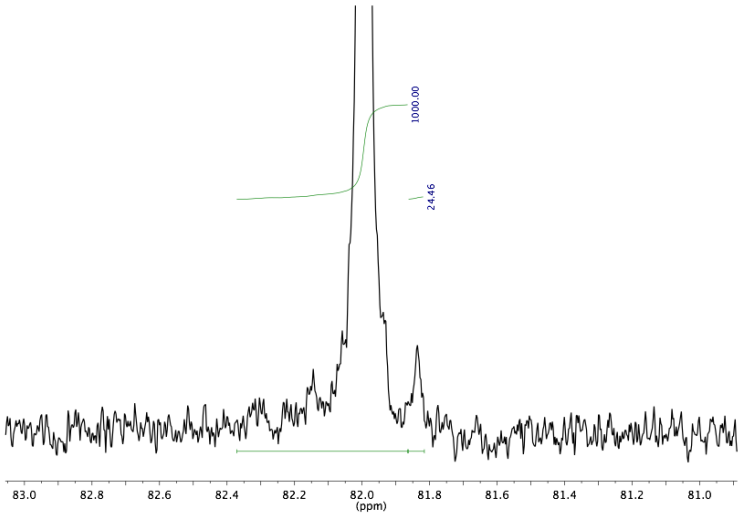

Figure 2.19. ^{13}C NMR spectra of poly(styrene oxide). A) Full spectrum. B) Methine region.

Polymerization of Racemic 1,1,1-trifluoro-2,3-epoxypropane (Table 2.2, entry 6).

The polymerization procedure was the same as that for propylene oxide except that 1.25 mL of 1,1,1-trifluoro-2,3-epoxypropane was used. Conversion was determined after 90 min by ^{1}H NMR to be 32%. Polymer tacticity (Figure 2.20) [*mm*] = 0.94. ^{1}H NMR (Acetone-d_6, 500 MHz): δ 4.35 (m, 1H), 4.21 (dd, J = 10.5, 3 Hz, 1H), 4.05 (dd, J = 10.5, 7.5 Hz, 1H). ^{13}C NMR (Acetone-d_6, 126 MHz): δ 125.00 (q, $^{1}J_{CF}$ = 282.2 Hz), 78.84 (q, $^{2}J_{CF}$ = 29.8 Hz), 71.45. M_n = 20,000 g/mol, M_w/M_n = 13.[31]

A)

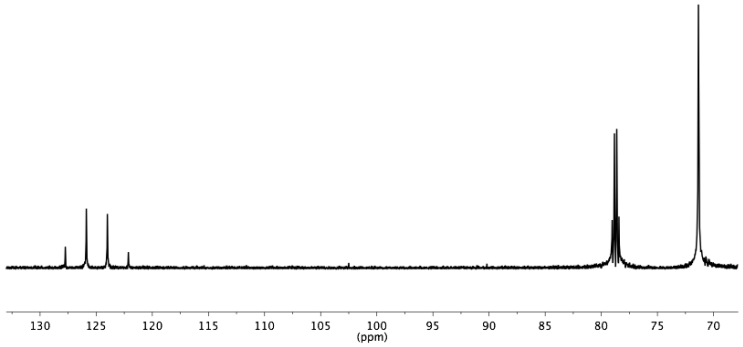

B)

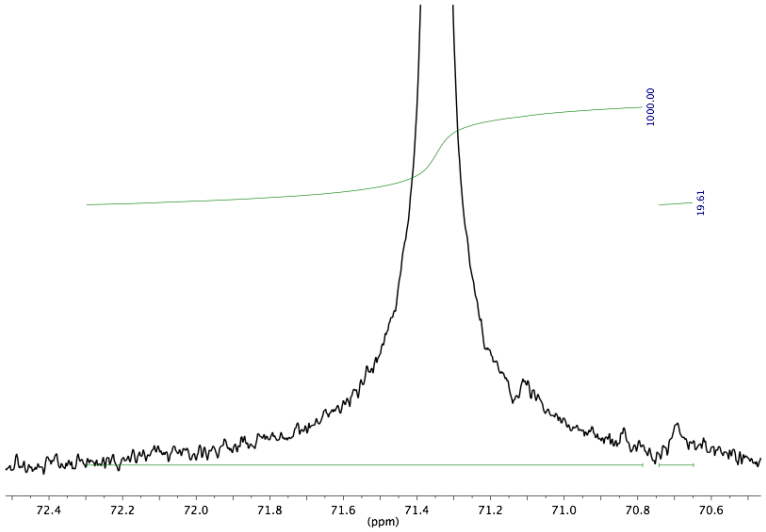

Figure 2.20. ^{13}C NMR spectra of poly(1,1,1-trifluoro-2,3-epoxypropane). A) Full spectrum. B) Methylene region.

Representative Quantitative Isoselective Polymerization of Racemic Epoxides.

Polymerization of Racemic Propylene Oxide with 2.3/2.6 (Table 2.3, entry 1).

In a drybox under nitrogen atmosphere, **2.3** (4.0 mg, 0.0038 mmol) and **2.6** (4.9 mg, 0.0076 mmol) were added to a Schlenk tube containing a stir bar. The Schlenk tube was sealed under nitrogen and removed from the drybox. The Schlenk tube was placed under dry nitrogen on the Schlenk line, and subsequently cooled in an ice bath. Anhydrous toluene (6 mL) was added to the Schlenk tube via syringe, and the resulting solution was stirred for 15 min at 0 °C. Propylene oxide (0.21 g, 3.7 mmol) was added via syringe. The polymerization was kept at 0 °C during the course of the reaction. After 60 min an aliquot was taken for NMR analysis, 1 mL of methanol containing a trace amount of HCl was added to the mixture to quench the catalyst, and volatiles were removed under vacuum. The remaining polymer solution was transferred to a pre-weighed round bottom flask and dried overnight under vacuum. Conversion was determined by ^{1}H NMR of the aliquot taken and determined to be over 99%. An INOVA 500 Varian spectrometer was used to obtain the ^{13}C NMR spectrum (taken over 2 h, with more than 2000 scans), as well as a ^{1}H NMR spectrum of the dried polymer. Polymer tacticity (Figure 2.21) [*mm*] = 0.97. ^{1}H NMR ($CDCl_3$, 500 MHz): δ 3.52 (m, 2H), 3.39 (m, 1H), 1.11 (m, 3H). ^{13}C NMR ($CDCl_3$, 125 MHz): δ 75.70, 73.61, 17.64. M_n = 107,000 g/mol, M_w/M_n = 1.80.

A)

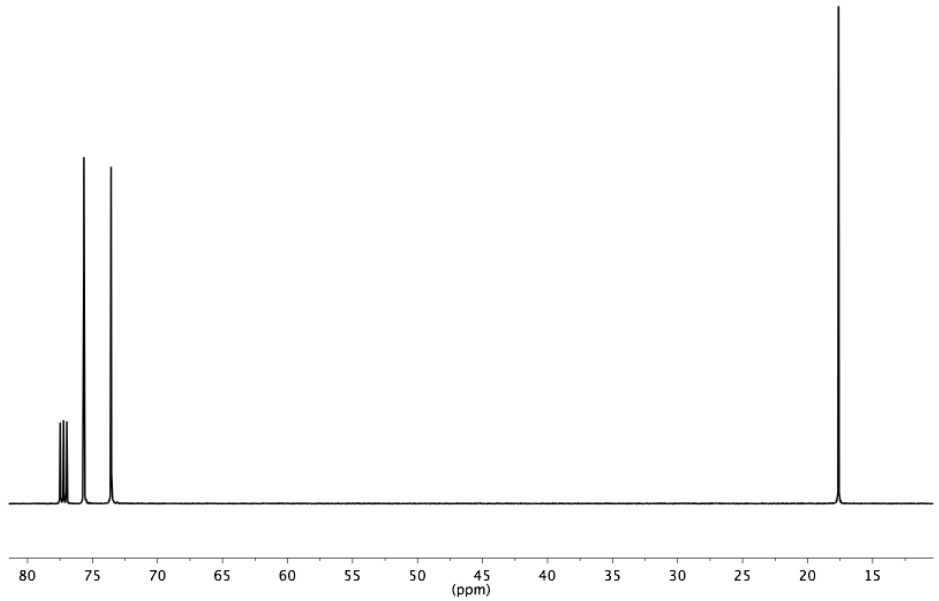

B)

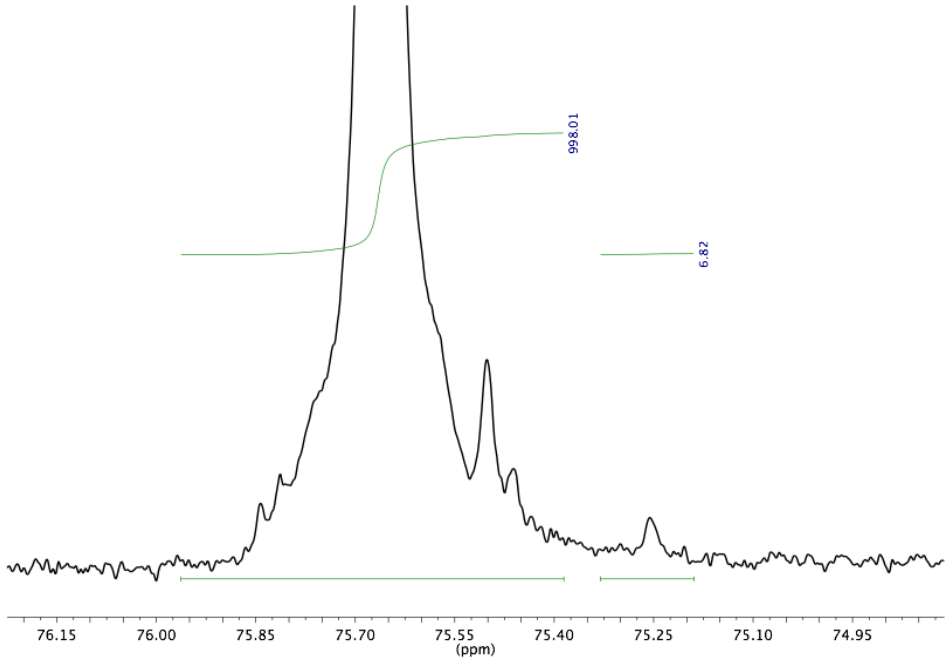

Figure 2.21. ^{13}C NMR spectra of poly(propylene oxide). A) Full spectrum. b) Methine region.

2.4.9. Crystal Data and Refinement for compounds 2.15, 2.16, and 2.17

Table 2.5. Crystal Data and Structure Refinement for **2.15**

Identification code	pw4	
Empirical formula	$C_{119}\ H_{129}\ Cl_2\ Co_2\ N_{15}\ O_5$	
Formula weight	2038.13	
Temperature	173(2) K	
Wavelength	0.71073 Å	
Crystal system	Triclinic	
Space group	P-1	
Unit cell dimensions	a = 15.3654(8) Å	α= 100.623(3)°.
	b = 17.7225(9) Å	β= 93.620(2)°.
	c = 21.0786(10) Å	γ = 94.919(3)°.
Volume	5602.5(5) $Å^3$	
Z	2	
Density (calculated)	1.208 Mg/m^3	
Absorption coefficient	0.403 mm^{-1}	
F(000)	2152	
Crystal size	0.40 x 0.15 x 0.03 mm^3	
Theta range for data collection	1.67 to 22.23°.	
Index ranges	-16<=h<=16, -18<=k<=18, -22<=l<=22	
Reflections collected	62501	
Independent reflections	13877 [R(int) = 0.0690]	
Completeness to theta = 22.23°	98.0 %	
Absorption correction	Semi-empirical from equivalents	
Max. and min. transmission	0.9900 and 0.8555	
Refinement method	Full-matrix least-squares on F^2	
Data / restraints / parameters	13877 / 708 / 1322	
Goodness-of-fit on F^2	1.028	
Final R indices [I>2sigma(I)]	R1 = 0.0574, wR2 = 0.1471	
R indices (all data)	R1 = 0.0974, wR2 = 0.1641	
Largest diff. peak and hole	0.815 and -0.458 $e.Å^{-3}$	

Table 2.6. Crystal Data and Structure Refinement for **2.16**

Identification code	pw8	
Empirical formula	$C_{104}\ H_{118}\ Cl_2\ Co_2\ N_{12}\ O_4$	
Formula weight	1788.86	
Temperature	173(2) K	
Wavelength	0.71073 Å	
Crystal system	Orthorhombic	
Space group	P2(1)2(1)2(1)	
Unit cell dimensions	a = 11.2391(5) Å	α= 90°.
	b = 26.7837(14) Å	β= 90°.
	c = 35.8843(17) Å	γ = 90°.
Volume	10802.1(9) $Å^3$	
Z	4	
Density (calculated)	1.100 Mg/m^3	
Absorption coefficient	0.408 mm^{-1}	
F(000)	3784	
Crystal size	0.60 x 0.15 x 0.05 mm^3	
Theta range for data collection	1.52 to 24.71°.	
Index ranges	-13<=h<=11, -31<=k<=24, -41<=l<=42	
Reflections collected	46749	
Independent reflections	18418 [R(int) = 0.0579]	
Completeness to theta = 24.71°	100.0 %	
Absorption correction	Semi-empirical from equivalents	
Max. and min. transmission	0.9799 and 0.7920	
Refinement method	Full-matrix least-squares on F^2	
Data / restraints / parameters	18418 / 78 / 1117	
Goodness-of-fit on F^2	0.974	
Final R indices [I>2sigma(I)]	R1 = 0.0560, wR2 = 0.1280	
R indices (all data)	R1 = 0.0856, wR2 = 0.1399	
Absolute structure parameter	0.026(13)	
Largest diff. peak and hole	0.466 and -0.359 e.$Å^{-3}$	

Table 2.7. Crystal Data and Structure Refinement for **2.17**

Identification code	pw2	
Empirical formula	$C_{86}\ H_{92}\ Cl_2\ Co_2\ N_{10}\ O_4$	
Formula weight	1518.46	
Temperature	173(2) K	
Wavelength	0.71073 Å	
Crystal system	Monoclinic	
Space group	Cc	
Unit cell dimensions	a = 23.7527(10) Å	α= 90°.
	b = 37.5983(15) Å	β= 95.983(2)°.
	c = 11.4249(4) Å	γ = 90°.
Volume	10147.6(7) $Å^3$	
Z	4	
Density (calculated)	0.994 Mg/m^3	
Absorption coefficient	0.424 mm^{-1}	
F(000)	3192	
Crystal size	0.50 x 0.30 x 0.15 mm^3	
Theta range for data collection	1.02 to 24.11°.	
Index ranges	-27<=h<=27, -31<=k<=43, -13<=l<=13	
Reflections collected	31936	
Independent reflections	15586 [R(int) = 0.0368]	
Completeness to theta = 24.11°	100.0 %	
Absorption correction	Semi-empirical from equivalents	
Max. and min. transmission	0.9392 and 0.8161	
Refinement method	Full-matrix least-squares on F^2	
Data / restraints / parameters	15586 / 41 / 937	
Goodness-of-fit on F^2	1.008	
Final R indices [I>2sigma(I)]	R1 = 0.0602, wR2 = 0.1522	
R indices (all data)	R1 = 0.0781, wR2 = 0.1625	
Absolute structure parameter	0.026(14)	
Largest diff. peak and hole	0.435 and -0.294 $e.Å^{-3}$	

2.5. Notes and References

(1) *Stereoselective Polymerization with Single Site Catalysts*; Baugh, L. S. and Canich, J. M. Eds.; CRC Press: Boca Raton, FL, 2007.

(2) (*a*) *Encyclopedia of Chemical Technology*; Kroschwitz, J. I.; Howe-Grant, M. Eds.; Wiley: Chichester, UK, 1993; Vol. 8, pp 1079-1093. (*b*) Wilms, D.; Stiriba, S.; Frey, H. *Acc. Chem. Res.* **2010**, *43*, 129-141.

(3) For some recent examples of discrete catalysts for epoxide polymerization, see: (*a*) Gervais, M.; Labé, A.; Carlotti, S.; Deffieux, A. *Macromolecules* **2009**, *42*, 2395-2400; (*b*) Raynaud, J.; Absalon, C.; Gnanou, Y.; Taton, D. *J. Am. Chem. Soc*, **2009**, *131*, 3201-3209; (*c*) Tang, L.; Wasserman, E. P.; Neithamer, D. R.; Krystosek, R. D.; Cheng, Y.; Price, P. C.; He, Y.; Emge, T. J. *Macromolecules* **2008**, *41*, 7306-7315; (*d*) Labbé, A.; Carlotti, S.; Billouard, C.; Desbois, P.; Deffieux, A., *Macromolecules* **2007**, *40*, 7842-7847; (*e*) Allgaier, J.; Willbold, S.; Chang, T. *Macromolecules* **2007**, *40*, 518-525; (*f*) Kim, I.; Ahn, J-T; Ha, C. S.; Yang, C. S.; Park, I. *Polymer* **2003**, *44*, 3417-3428; (*g*) Braune, W.; Okuda, J. *Angew. Chem. Int. Ed.*, **2003**, *42*, 64-68; (*h*) Chakraborty, D.; Rodriguez, A.; Chen, E. Y.-X. *Macromolecules* **2003**, *36*, 5470–5481. (*i*) Rexin, O.; Mülhaupt, R. *Macromol. Chem. Phys.* **2003**, *204*, 1102-1109; (*j*) Eβwein, B.; Steidl, N. M.; Möller, M. *Macromol. Rapid Commun.* **1996**, *17*, 143-148.

(4) Kuran, W. *Prog. Poly. Sci.* **1998**, *23,* 919-992.

(5) For a review, see: Ajiro, H.; Allen, S. D.; Coates, G. W. "Discrete Catalysts for Stereoselective Epoxide Polymerization" in ref. 1, Chapter 24, 627-644.

(6) Peretti, K. L.; Ajiro, H.; Cohen, C. T.; Lobkovsky, E. B.; Coates, G. W. *J. Am. Chem. Soc.* **2005**, *127*, 11566-11567.

(7) Ajiro, H.; Peretti, K. L.; Lobkovsky, E. B.; Coates, G. W. *Dalton Trans.* **2009**, 8828–8830

(8) (*a*) Hirahata, W.; Thomas, R. M.; Lobkovsky, E.; Coates, G. W. *J. Am. Chem. Soc.* **2008**, *130*, 17658-17659. (*b*) Thomas, R. M.; Widger, P. C. B.; Ahmed, S. M.; Jeske, R. C.; Hirahata, W.; Lobkovsky, E. B.; Coates, G. W. *J. Am. Chem. Soc.* **2010**, *132*, 16520-16525.

(9) Tokunaga, M.; Larrow, J. F.; Kakiuchi, F.; Jacobsen, E. N. *Science* **1997**, *277*, 936-938.

(10) Schilling, F. C.; Tonelli, A. E. *Macromolecules* **1986**, *19*, 1337-1343.

(11) See experimental section.

(12) Cohen, C. T.; Chu, T.; Coates, G. W. *J. Am. Chem. Soc.* **2005**, *127*, 10869-10878.

(13) A sample of enantiopure **2.3** synthesized from *S*-binaphthol enchained *S*-PO with a k_S/k_R selectivity factor of 160 when combined with **2.6** at 0 °C.

(14) Nielsen, L. P. C.; Stevenson, C. P.; Blackmond, D. G.; Jacobsen, E. N. *J. Am. Chem. Soc.* **2004**, *126*, 1360-1362.

(15) Zhang, Z.; Xu, J.; Yu, Y. *J. Appl. Polym. Sci.* **2002**, *84*, 1223-1232.

(16) Ronda, J. C.; Serra, A.; Mantecón, A.; Cádiz, V. *Acta Polym*. **1996**, *47*, 269–275.

(17) Sakakibara, K.; Nakano, K.; Nozaki, K. *Macromolecules* **2007**, *40*, 6136–6142.

(18) (a) Blanchette, J. A. U. S. Patent 2,916,463, 1959. (b) Kasperczyk, J.; Jedlinski, Z. J.; *Makromol. Chem*. **1986**, *187*, 2215–2221. (c) Huang, Y.; Gao, L.; Ding, M. *J. Polym. Sci., Part A: Polym. Chem*. **1999**, *37*, 4640–4645. (d) Ge, L.; Huang, Q.; Zhang, Y.;

Shen, Z. *Eur. Polym. J.* **2000**, *36*, 2699–2705. (e) Yahiaoui, A.; Belgachir, M. *J. Appl. Polym. Sci.* **2006**, *100*, 1681–1687.

(19) Harris, A. F.; Rodrigues, F. U.S. Patent 3,222,430, 1965.

(20) (a) Umezawa, J.; Hagiwara, T; Hamana, H.; Narita, T.; Furuhashi, K.; Nohira, H. *Polym. J.* **1994**, *26*, 715-721. (b) Umezawa, J.; Hagiwara, T.; Hamana, H.; Narita, T.; Furuhashi, K.; Nohira, H. *Macromolecules* **1995**, *28*, 833–837. (c) Sakakibara, K.; Nakano, K.; Nozaki, K. *Chem. Commun.* **2006**, *31*, 3334–3336.

(21) Kemper, S.; Hrobárik, P.; Kaupp, M.; Schlörer, N. E. *J. Am. Chem. Soc.* **2009**, *31*, 6641.

(22) Fringuelli, F.; Pizzo, F. *Organic Prep. Proced. Int.* **1989**, *21*, 757-761.

(23) Campbell, E. J.; Nguyen, S. T. *Tet. Lett.* **2001**, *42*, 1221–1225.

(24) Holbach, M.; Zheng, X.; Burd, C.; Jones, C. W.; Weck, M. *J. Org. Chem.* **2006**, *71*, 2903-2906.

(25) Nielsen, L. P. C.; Stevenson, C. P.; Blackmond, D. G.; Jacobsen, E. N. *J. Am. Chem. Soc.* **2004**, *126*, 1360-1362.

(26) Lazareva, A.; Daugulis, O. *Org Lett.* **2006**, *8*, 5211-5213.

(27) Kozitsyna, N. yu.; Bukharkina, A. A.; Martens, M. V.; Vargaftik, M. N.; Moiseev, I. I. *J. Organomet. Chem.* **2001**, *636*, 69-75.

(28) Price, C. C.; Osgan, M. *J. Am. Chem. Soc.* **1956**, *78*, 4787-4792.

(29) Schilling, F. C.; Tonelli, A. E. *Macromolecules* **1986**, *19*, 1337-1343.

(30) Sakakibara, K.; Nakano, K.; Nozaki, K. *Macromolecules* **2007**, *40*, 6136-6142.

(31) Umezawa, J.; Hagiwara, T.; Hamana, H.; Narita, T.; Furuhashi, K.; Nohira, H. *Polym. J.* **1994**, *26*, 715-721.

Chapter 3

Exploration of Cocatalyst Effects on a Bimetallic Cobalt Catalyst System: Enhanced Activity and Enantioselectivity in Epoxide Polymerization

Reproduced in part with permission from:

P. C. B. Widger, S. M. Ahmed, G. W. Coates

Accepted for publication in: *Macromolecules*, **2011** DOI:10.1021/ma201078m

3.1 Introduction

Isotactic polyethers are a potentially important class of materials that are difficult to synthesize from racemic epoxides.[1] Previous catalysts used to synthesize isotactic polyethers suffer from poor activity, low stereoselectivity, or limited substrate scope.[1b,2] In 2008, we reported a bimetallic cobalt complex (**3.1a**) (Scheme 3.1) that is active for the enantioselective polymerization of a broad range of racemic mono-substituted epoxides in the presence of the ionic cocatalyst bis(triphenylphosphine)iminium (PPN) acetate ($[Ph_3P\text{-}N{=}PPh_3^+][MeCO_2^-]$; **3.2a**), Scheme 3.1).[3] This system displays very high enantioselectivities (*s*-factor = $s = k_{fast}/k_{slow}$) for the synthesis of isotactic polyethers from racemic epoxides. A related isoselective cobalt complex **(3.1b)** displays moderate activity and selectivity in combination with **3.2a**, both of which are improved by using PPN pivalate ($[Ph_3P\text{-}N{=}PPh_3^+][^tBuCO_2^-]$; **3.2b**) as the cocatalyst.[4]

Scheme 3.1. Bimetallic Complexes for the Synthesis of Isotactic Polyethers

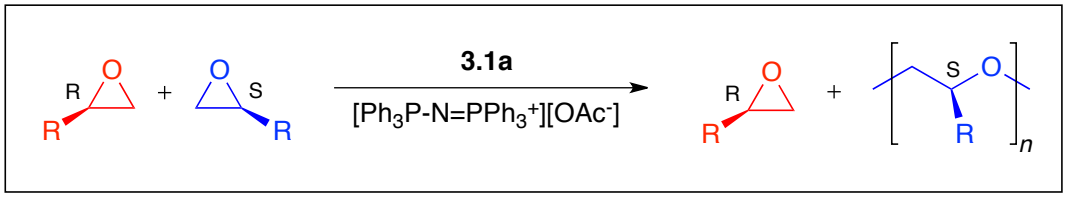

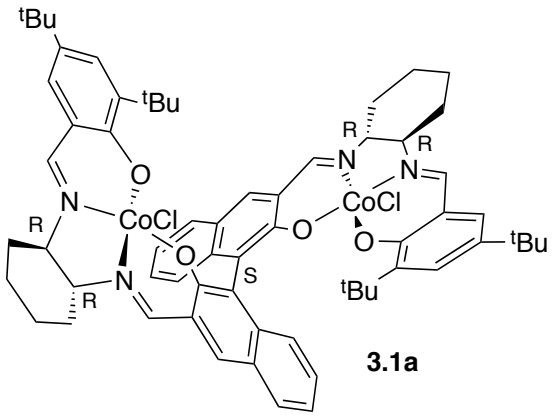

3.1a

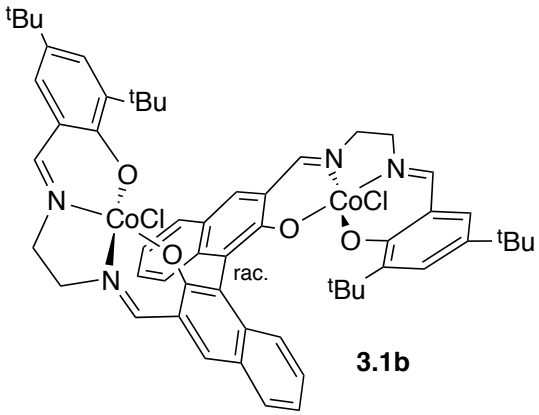

3.1b

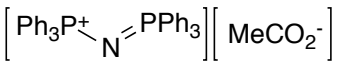

3.2a

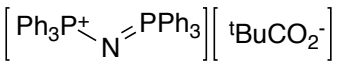

3.2b

Complexes **3.1a** and **3.1b** showed no appreciable polymerization activity in the absence of a cocatalyst. The addition of an ionic cocatalyst results in the formation of a catalytically active system. The exact identity of the catalytically active complex is currently unclear, but we propose that the anion of the cocatalyst binds to cobalt outside of the catalyst cleft, activating an interior *trans* ligand for nucleophilic ring opening of an epoxide bound to the adjacent cobalt center. We further propose that the bulky pivalate group of **3.2b** is less likely to enter the bimetallic cleft, consistent with its role as an axial donor and not an initiator (Scheme 3.2).[4] This postulate is supported by previous reports that cobalt(III) salen complexes for epoxide hydrolysis display dramatic rate differences with various axial donors. [5]

Scheme 3.2. Proposed Mechanism of Polymerization for **3.1a** and **3.1b** (P = polymer chain; X = chloride or carboxylate; C = cocatalyst cation)

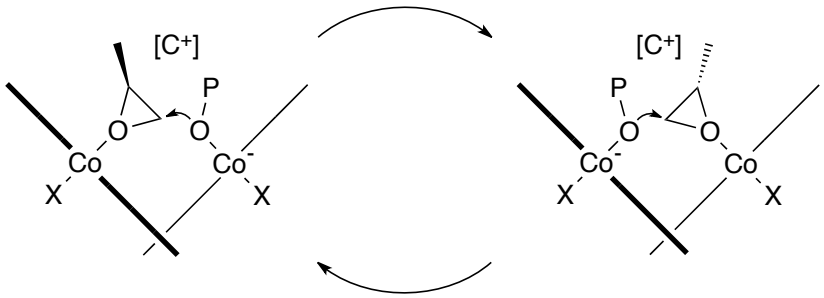

We propose that a suitable cocatalyst should contain an anion that is a good axial donor, and it must also contain a stable cation. PPN is believed to be a non-coordinating and unreactive cation; however, it decomposes in the presence of strong bases such as alkoxides that may be generated during the course of polymerization.[6] Additionally, PPN salts suffer from limited solubility under preferred epoxide polymerization conditions.

The large activity and selectivity differences between systems **3.1b**/**3.2a** and **3.1b**/**3.2b** demonstrate the importance of the cocatalyst for isoselective epoxide polymerization. Cobalt(III) salen epoxide/CO_2 copolymerization systems also show dramatic cocatalyst dependency.[7] On the basis of these prior results, the development of a more soluble and base-stable cocatalyst could improve this bimetallic polymerization system and other related systems.[7] In this paper, we report new polyatomic ionic cocatalysts (Scheme 3.3) for the enantioselective polymerization of epoxides with **3.1a**.

Scheme 3.3. Phosphazenium (**3.3**) and Phosphonium (**3.4**) Ionic Organic Cocatalysts for Bimetallic Cobalt Enantioselective Epoxide Polymerization Catalysts

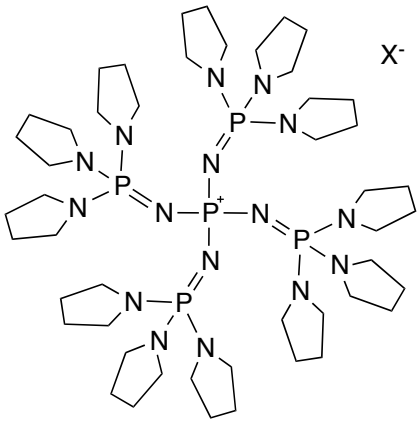

X = O_2CMe; **3.3a**
X = Cl; **3.3b**
X = Br; **3.3c**
X = I; **3.3d**
X = O_2C^tBu; **3.3e**
X = O_2CCPh_3; **3.3f**
X = O_2CPh; **3.3g**
X = O_2CPh^{F5}; **3.3h**
X = BPh_4; **3.3i**

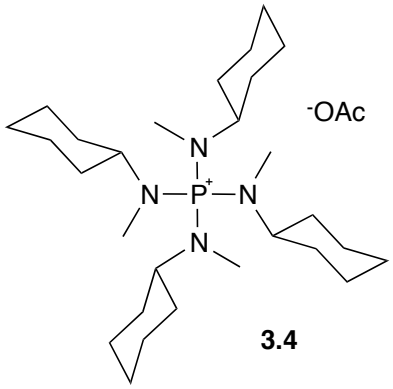

3.4

3.2 Results and Discussion

We first explored the effects of various cocatalyst cations on the polymerization of PO with **3.1a** while maintaining acetate as the anion (Table 3.1). After a solvent screen, the polar aprotic solvent dimethoxyethane (DME) was chosen to increase the solubility of these ionic cocatalysts while maintaining high activity. Given our mechanistic proposal of an anionic active species, we used one equivalent of cocatalyst relative to **3.1a**.[4] The enantiomeric purity of polymer repeat units (ee_P) was calculated from [*mm*] determined by ^{13}C NMR spectroscopy using equation 1.[3a]

$$ee_{(P)} = (2[mm] + [mr] + [rm] - 1)^{1/2} \qquad (1)$$

The *s*-factors for the polymerizations were calculated using equation 2, which is applicable only when monomer conversions are less than 50%.[3a]

$$s = s\text{-factor} = ln[1\text{-}c(1+ee_{(P)})]/ln[1\text{-}c(1\text{-}ee_{(P)})] \qquad (2)$$

Alkali metal salts (lithium, sodium, and potassium acetate) showed essentially no activity in 24 hours (entries 1-3), while tetrabutylammonium acetate gave moderate activity and polymer with low tacticity (entry 4). We hypothesize that the base instability of tetrabutylammonium acetate

accounted for its poor performance.[8] Thus, we decided to explore cations that have been reported to be base stable such as phosphoniums and phosphazeniums (Scheme 3.3).[8] Phosphonium ($(R_2N_4)P^+$), and phosphazenium ($((R_2N)_3P{=}N)_4P^+$) salts, as well as phosphazenes ($(R_2N)_3P{=}NR$), are used as initiators for anionic epoxide polymerizations.[9] Phosphazenium salts have applications as cocatalysts for controlled radical polymerizations[10] and catalysts for epoxide ring-opening reactions.[11]

Table 3.1. Screening of Acetate–Based Cocatalysts for the Polymerization of PO with **3.1a**: Effect of Cation[a]

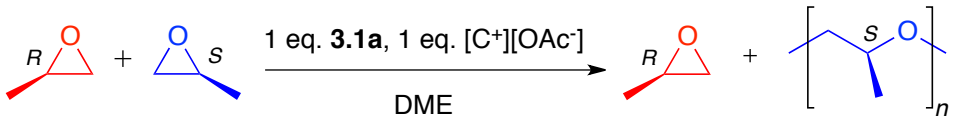

entry	cocatalyst	time (min)	T_{rxn} (°C)	[PO] (M)	conv. (%)[b]	M_n (kg/mol)[c]	M_w/M_n[c]	[*mm*] (%)[d]
1	Li[OAc]	1440	20	2	<1	-	-	-
2	Na[OAc]	1440	20	2	<1	-	-	-
3	K[OAc]	1440	20	2	<1	-	-	-
4	$[(Bu)_4N][OAc]$	1440	20	2	10.2	22	2.2	82.0
5	**3.2a**	30	0	1	43.5	126	2.6	89.7
6	**3.3a**	0.5	0	1	45.9	157	1.9	97.1
7	**3.4**	180	0	2	37.3	25	2.0	88.6

[a] General conditions: [**3.1a**]:[cocatalyst]:[PO]=1:1:4000 in DME. [b] Determined by gravimetric analysis of the polymer. [c] Determined by gel-permeation chromatography calibrated with polystyrene standards in 1,2,4-$Cl_3C_6H_3$ at 140 °C. [d] Isotactic *mm* triad content determined by ^{13}C NMR spectroscopy.

Phosphonium salt **3.4** showed good activity and moderate stereoselectivity but was less active than **3.2a** (entries 5 and 7).[12] Phosphazenium cocatalyst **3.3a** displayed the highest rate and a selectivity that is above the maximum measurable by ^{13}C NMR (s >300)[3] for polymerization of PO (entry 6). In summary, acetate cocatalysts with large charge-delocalized cations such as **3.3a** show the highest rates and selectivities. We propose that this is due to a

combination of increased stability of the solvent-separated ion pair and inability of the large cation to enter and block the catalyst cleft.

A variety of phosphazenium salts with different anions were synthesized by salt metathesis of tetrakis[(tri-1-pyrrolidinylphosphoranyliden)amino]phosphonium tetrafluoroborate with the appropriate potassium salt in aqueous methanol. These compounds were easily dried and not hygroscopic. These phosphazeniums were then screened as cocatalysts with **3.1a** (Table 3.2). Cocatalyst **3.3b** showed good activity and selectivity, while PPNCl displayed no activity, demonstrating the utility of phosphazenium cocatalysts (entry 2). Other halides such as bromide (**3.3c**), and iodide (**3.3d**) showed no activity (entries 3 and 4). The bulky pivalate cocatalyst (**3.3e**) displayed the highest rate (TOF ~ 8000/min) and selectivity (*s* >300, entry 5). Further increasing the steric bulk of the anion to the triphenylacetate (**3.3f**) led to a decrease in activity and selectivity (entry 6).[13] Benzoate cocatalyst (**3.3g**) showed good activity and high selectivity (entry 7), however the more electron deficient pentafluorobenzoate (**3.3h**) showed dramatically decreased performance (entry 8).[13] The noncoordinating anion tetraphenyl borate (**3.3i**) showed no activity (entry 9). These results suggest that the most active and selective cocatalysts contain anions that are strong donors with moderate steric bulk.

Table 3.2. Screening of Phosphazenium-Based Cocatalysts for the Polymerization of PO with **3.1a**: Effect of Anion[a]

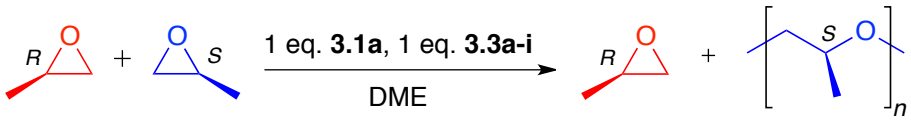

entry	cocatalyst	X	time (min)	conv. (%)[b]	M_n (kg/mol)[c]	M_w/M_n[c]	[*mm*] (%)[d]	*s*-*factor*
1	**3.3a**	O_2CMe	0.50	45.9	157	1.9	97.1	>300
2	**3.3b**	Cl[e]	10	48.6	36	2.4	94.7	>200
3	**3.3c**	Br	1440	<1	-	-	-	-
4	**3.3d**	I	1440	<1	-	-	-	-
5	**3.3e**	O_2C^tBu	0.25	49.3	157	1.9	95.8	>300
6	**3.3f**	O_2CCPh_3[f]	1440	25.2	42	1.8	91.7	50[g]
7	**3.3g**	O_2CPh	4	49.9	94	2.1	96.5	>300
8	**3.3h**	$O_2CPh\text{-}F_5$[f]	1440	34.3	114	3.1	88.2	40[g]
9	**3.3i**	BPh_4	1440	<1	-	-	-	-

[a] General conditions: [**3.1a**]:[cocatalyst]:[PO]=1:1:4000, T_{rxn} = 0 °C, [PO] = 1 M in DME. [b] Determined by gravimetric analysis of the polymer. [c] Determined by gel-permeation chromatography calibrated with polystyrene standards in 1,2,4-$Cl_3C_6H_3$ at 140 °C. [d] Isotactic *mm* triad content determined by ^{13}C NMR spectroscopy. [e] [**3.1a**]:[PO]=1:1000. [f] T_{rxn} = 20 °C. [g] The *s*-factor was calculated from *mm* content of crude polymer, which contains trace atactic PPO.[13]

We applied our optimized catalytic system **3.1a**/**3.3e**, to the polymerization of several other mono-substituted epoxides. This system (**3.1a**/**3.3e**) displayed significantly higher reactivity with epoxides than our previously reported system (**3.1a**/**3.2a**),[3] as shown in Table 3.3.[14] It is notable that the selectivities calculated for all polymerizations other than butadiene mono-epoxide were greater than we can accurately measure by ^{13}C NMR spectroscopy (*s* >300). Butadiene mono-epoxide was previously polymerized with system **3.1a**/**3.2a** and displayed an *s*-factor of 20,[3] while system **3.1a**/**3.3e** polymerized butadiene mono-epoxide with a TOF of 8000 min^{-1} and a more synthetically useful *s*-factor of 70.

Table 3.3. Enantioselective Polymerization of Epoxides with (**3.1a**/**3.3e**)[a]

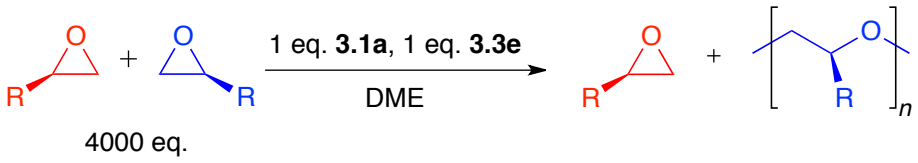

entry	epoxide subs. (R)	epoxide (M)	time (min)	conv. (%)[b]	M_n (kg/mol)[c]	M_w/M_n[c]	[*mm*] (%)[d]	*s-factor*	*s*-factor (**3.1a**/**3.2a**)[3]
1	-Bu	2	1	49.1	140	2.1	98.9	>300	>300
2	-CH_2OPh	0.5	0.25	49.2	100	2.2	96.9	>300	70
3	-CH_2=CH_2	2	0.25	49.8	97[f]	2.9[f]	87.6	70	20
4	-Ph	2	4	47.8[e]	77	5.3	98.5	>300	70
5	-CF_3	2	30	49.3	140[g]	1.8[g]	99.3	>300	>300

[a] General conditions: [**3.1a**]:[**3.3e**]:[epoxide]=1:1:4000, T_{rxn} = 0 °C in DME. [b] Determined by gravimetric analysis of the polymer. [c] Determined by gel-permeation chromatography calibrated with polystyrene standards in 1,2,4-$Cl_3C_6H_3$ at 140 °C. [d] Isotactic *mm* triad content determined by ^{13}C NMR spectroscopy. [e] Conversion determined by ^1H NMR. [f] Determined by gel-permeation chromatography at 40 °C in chloroform, calibrated with polystyrene standards. [g] Determined by gel-permeation chromatography at 33 °C in *N*,*N*-dimethylformamide, calibrated with polystyrene standards.

Cocatalyst **3.3e** also showed improved reactivity compared to **3.2b** in isoselective polymerizations of PO with racemic complex **3.1b**. System **3.1b**/**3.2b** had an initial TOF of 440 min^{-1} and *mm* = 97%[4] while **3.1b**/**3.3e** showed improved activity and high isoselectivity (initial TOF = 2600 min^{-1}, *mm* = 98.9%) for PO polymerization **(**Figure 3.1). Despite the base stability of **3.3e**, these systems did not show living polymerization behavior ($M_w/M_n \sim 2$). We are actively investigating the mechanism of these systems to determine the origin of the large rate and selectivity increases from **3.3e**.

Figure 3.1. Isoselective Polymerization of PO Using System **3.1b**/**3.3e**

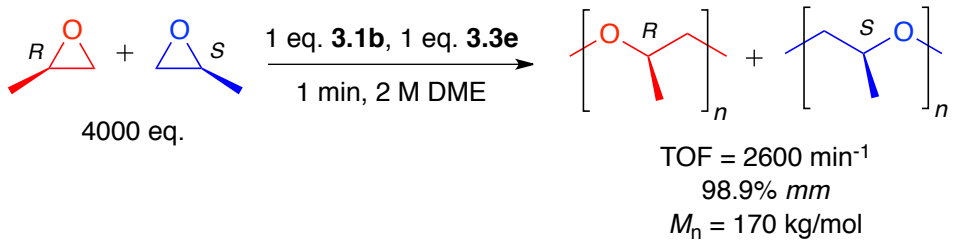

3.3 Conclusions

A wide range of cocatalysts were screened with **3.1a** for the enantioselective polymerization of PO. Variation of both the cation and the anion of the cocatalyst dramatically affected the activity and stereoselectivity of the catalyst system, and the bulky, base stable phosphazenium pivalate cocatalyst (**3.3e**) was found to give the highest activities and selectivities. This system showed improved polymerization performance for a number of epoxides, allowing for facile access to enantiopure as well as racemic isotactic polyethers.

3.4 Experimental

3.4.1 General Considerations

All manipulations of air or water sensitive compounds were carried out under dry nitrogen using a Braun Labmaster drybox or standard Schlenk line techniques. NMR spectra were recorded on Varian INOVA 400 (^{1}H, 400 MHz), or Varian INOVA 600 (^{1}H, 600 MHz) spectrometers. ^{1}H NMR spectra were referenced with residual solvent shifts ($CHCl_3$ = 7.26 ppm, CD_2HOD = 3.31 ppm, acetone-d_5 = 2.05 ppm, 1,1,2,2-tetrachloroethane-d_1 = 6.0 ppm). ^{13}C NMR spectra were referenced by solvent shifts ($CDCl_3$ = 77.16 ppm, CD_3OD = 49.00 ppm,

acetone-d_6 = 29.92 ppm, 1,1,2,2-tetrachloroethane-d_2 = 73.78 ppm). ^{19}F NMR spectra were referenced with an external standard (trifluoroacetic acid = -76.55 ppm).

3.4.2 Materials

HPLC grade methylene chloride and toluene were purchased from Fisher Scientific and purified over solvent columns. Styrene oxide was synthesized according to a literature procedure[15] and fractionally distilled at reduced pressure. All other epoxides were purchased from commercial sources and dried over calcium hydride, degassed through several freeze-pump-thaw cycles, vacuum transferred, and stored under nitrogen in a glovebox. Dimethoxyethane (DME) was distilled off of sodium metal after freeze-pump-thawing. Catalysts **3.1a**[3] and **3.1b**[4] were synthesized as previously reported. (1*R*,2*R*)-Diaminocyclohexane (99% *ee*) was purchased from Aldrich and (*S*)- and (*rac*)-1,1'-bi-2-naphthol was purchased from TCI. (*S*)- and (*rac*)- 3,3'-diformyl-1,1'-bi-2-naphthol,[16] tetrakis[cyclohexyl(methyl)amino]phosphonium tetrafluoroborate,[8] tetrakis[(tri-1-pyrrolidinylphosphoranyliden)amino]phosphonium tetrafluoroborate,[8] bis(triphenylphosphine)iminium acetate ([PPN]OAc, **3.2a**),[17] [PPN]OPiv[4] (**3.2b**), and potassium pentafluorobenzoate[18] were prepared according to literature procedures. Potassium carboxylates were synthesized by titration of commercial carboxylic acids with aqueous potassium hydroxide. All other reagents were purchased from commercial sources and used as received.

3.4.3 Polymer Characterization and NMR Quantification of Polymer Tacticity, Enantiomeric Excess and *s*-factor

Number average molecular weights (M_n) and molecular weight distributions (M_w/M_n) were measured by high temperature gel-permeation chromatography (GPC) using a Waters Alliance GPCV 2000 size exclusion chromatograph equipped with a Waters DRI detector and viscometer. The set of five sequential columns (four Waters HT 6E and one Waters HT 2) was eluted with 1,2,4-trichlorobenzene containing approximately 0.01 wt% 2,6-di-*tert*-butylhydroxytoluene at 1.0 mL/min at 140 °C. The Waters refractive index processing method was used for data analysis. The GPC chromatographs generated from the Waters DRI detector were calibrated using polystyrene standards. Poly(3,4-epoxy-1-butene) was examined using size-exclusion chromatography at analyses 40 °C in chloroform using a Waters instrument, (M515 pump, 717+ Autosampler) equipped with a Waters UV486 and Waters 2410 differential refractive index detectors, and three 5 μm PSS SDV columns (Polymer Standards Service; 50 Å, 500 Å, and Linear M porosities) in series. The GPC columns were eluted with chloroform at 1 mL/min and were calibrated with monodisperse polystyrene standards. Poly(1,1,1-trifluoro- 2,3-epoxypropane) was examined using size-exclusion chromatography at 33 °C in *N*,*N*-dimethylformamide. The column set consisted of three consecutive Polymer Standards Services columns (PSS gram 100, PSS gram 1000, PSS gram 3000), calibrated with narrow-molecular-weight distribution polystyrene standards. Polymer tacticity was characterized by ^{13}C NMR spectroscopy as previously reported.[3] Polymer enantiomeric excess was calculated using: $ee_{(p)} = (2[mm]+[mr]+[rm]-1)^{1/2}$, and selectivity (*s*-factor) was calculated using: s = *s*-factor = $ln[1-c(1+ee_{(P)})]/ln[1-c(1-ee_{(P)})]$ where c is conversion.[3] The enantiomeric excess (*ee*) of recovered PO was determined by chiral gas chromatography (GC). Gas chromatograms were obtained on a

Hewlett-Packard 6890 series gas chromatograph using a flame ionization detector, He carrier gas, and an Alltech CHIRALDEX A-TA chiral capillary column (50 m x 0.25 mm) was used for PO separation. Racemic PO was run first on the GC to confirm separation of enantiomers and retention times.

3.4.4 Synthesis of Cocatalysts

Tetrakis[(tri-1-pyrrolidinylphosphoranyliden)amino]phosphonium Acetate (3.3a). To a solution of tetrakis[(tri-1-pyrrolidinylphosphoranyliden)amino]phosphonium tetrafluoroborate (570 mg, 0.500 mmol) in 8 mL methanol was added potassium acetate (59 mg, 0.60 mmol) in 150 μL water. The resulting suspension was stirred at 20 °C for 5 min and subsequently filtered. The solution was concentrated under vacuum leaving a white solid, which was rinsed with 2x20 mL water then dried over night under vacuum leaving a pale blue powder (420 mg, 77.6%). ^{1}H NMR (CD_3OD, 600 MHz): δ 3.26 - 3.18 (m, 48H), 1.89 (s, 3H), 1.84 - 1.75 (m, 48H). $^{13}C\{^{1}H\}$ NMR (CD_3OD, 150 MHz): δ 180.08, 47.61 (d, J = 5.5 Hz), 27.43 (d, J = 9.0 Hz), 24.24. (Figure 3.2) Elemental analysis: Calcd for $C_{50}H_{99}N_{16}O_2P_5$: C, 54.04%; H, 8.98%; N, 20.17%. Found: C, 53.81%; H, 9.18%; N, 20.02%.

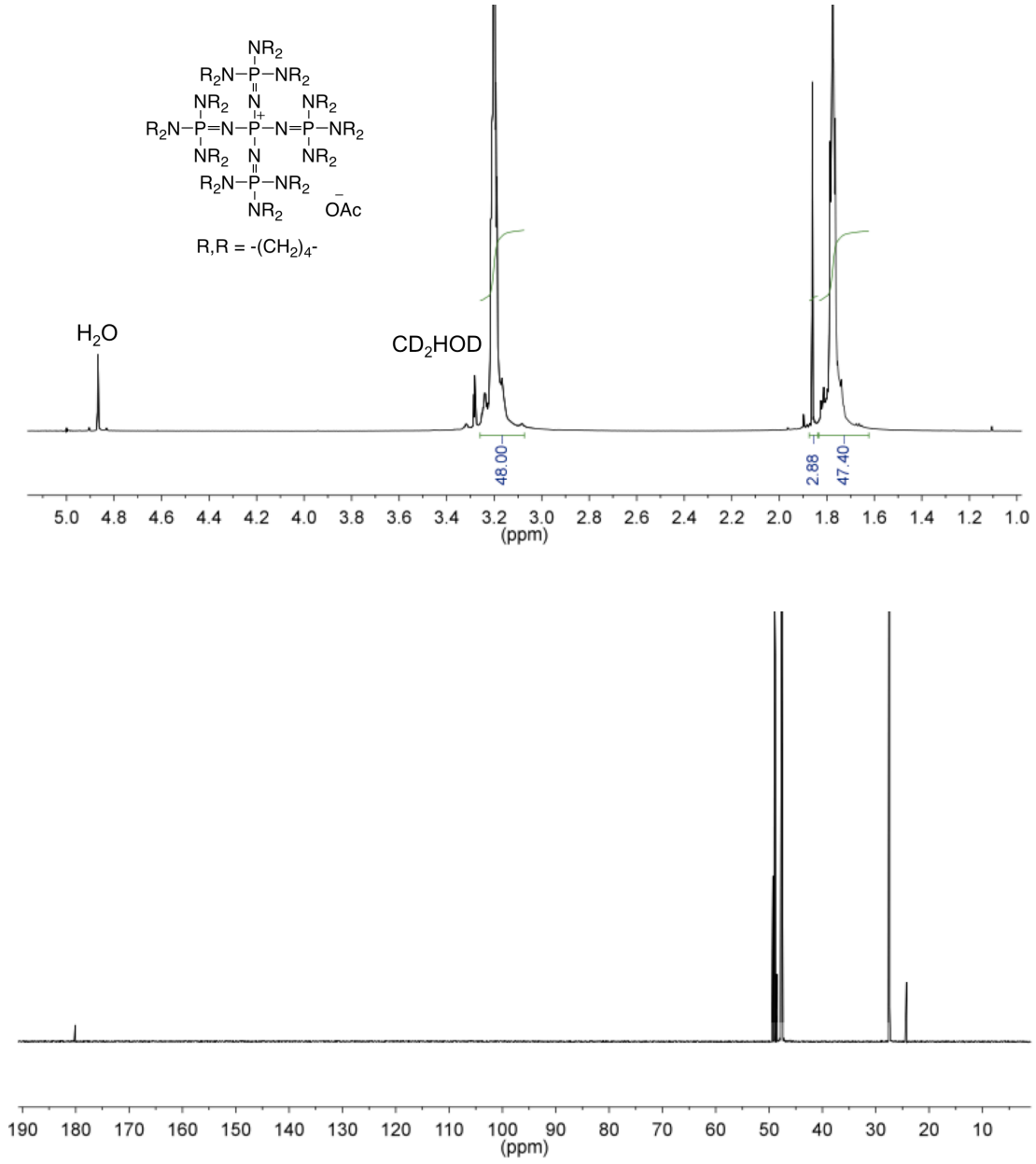

Figure 3.2. 3.3a in CD_3OD. Top: ^{1}H NMR spectrum. Bottom: ^{13}C NMR spectrum.

Tetrakis[(tri-1-pyrrolidinylphosphoranyliden)amino]phosphonium Chloride (**3.3b**). The procedure described for **3.3a** was followed using (570 mg, 0.500 mmol) tetrakis[(tri-1-pyrrolidinylphosphoranyliden)amino]phosphonium tetrafluoroborate, and (45 mg, 0.60 mmol) potassium chloride. Yield 424 mg, 78.0% white powder. ^{1}H NMR (CD_3OD, 600 MHz): δ 3.26 - 3.18 (m, 48H), 1.84 - 1.75 (m, 48H). $^{13}C\{^{1}H\}$ NMR (CD_3OD, 150 MHz): δ 47.61 (d, J = 5.5 Hz), 27.43 (d, J = 9.0 Hz). (Figure 3.3) Elemental analysis: Calcd for $C_{48}H_{96}N_{16}ClP_5$: C, 53.00%; H, 8.90%; N, 20.60%. Found: C, 52.99%; H, 9.18%; N, 20.47%.

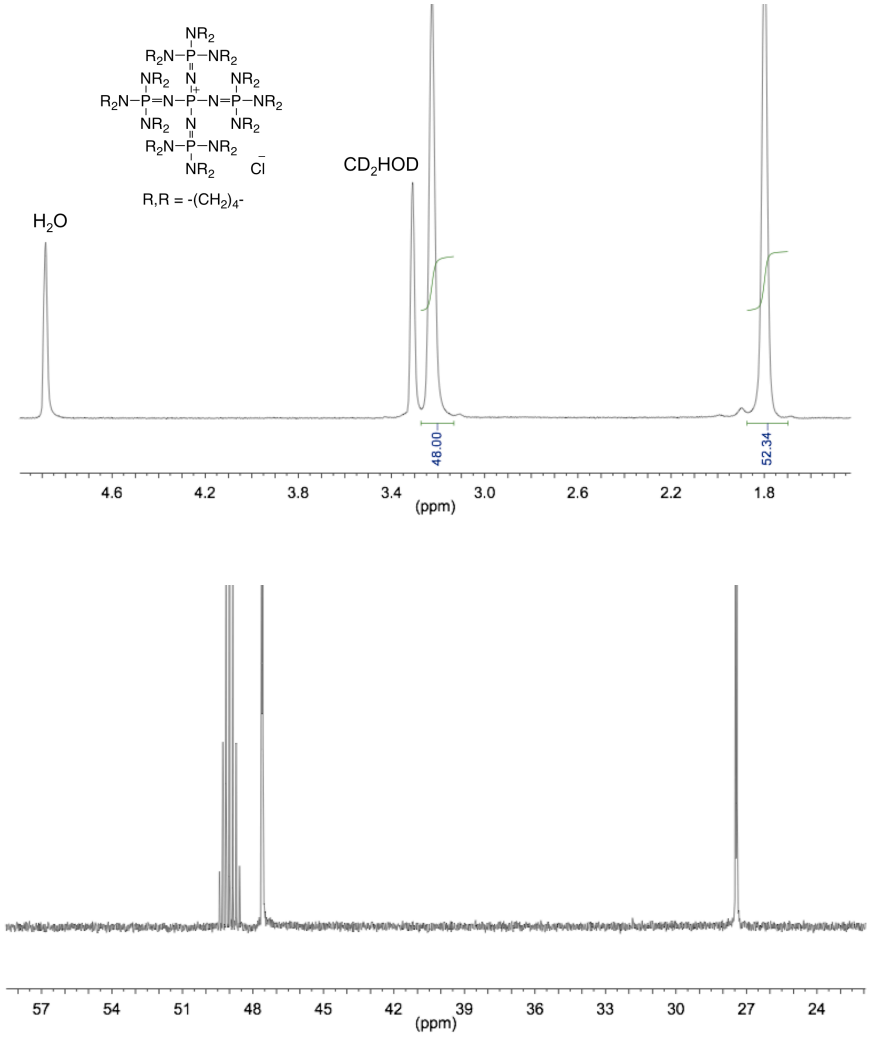

Figure 3.3. 3.3b in CD_3OD. Top: ^{1}H NMR spectrum. Bottom: ^{13}C NMR spectrum.

Tetrakis[(tri-1-pyrrolidinylphosphoranyliden)amino]phosphonium Bromide (**3.3c**). The procedure described for **3.3a** was followed using (300 mg, 0.263 mmol) tetrakis[(tri-1-pyrrolidinylphosphoranyliden)amino]phosphonium tetrafluoroborate, and (38 mg, 0.32 mmol) potassium bromide. Yield 261 mg, 87.7% white powder. ^{1}H NMR (CD_3OD, 600 MHz): δ 3.26 - 3.18 (m, 48H), 1.84 - 1.75 (m, 48H). $^{13}C\{^{1}H\}$ NMR (CD_3OD, 150 MHz): δ 47.61 (d, J = 5.5 Hz), 27.43 (d, J = 9.0 Hz). (Figure 3.4) Elemental analysis: Calcd for $C_{48}H_{96}N_{16}BrP_5$: C, 50.92%; H, 8.55%; N, 19.79%. Found: C, 50.88%; H, 8.83%; N, 19.57%.

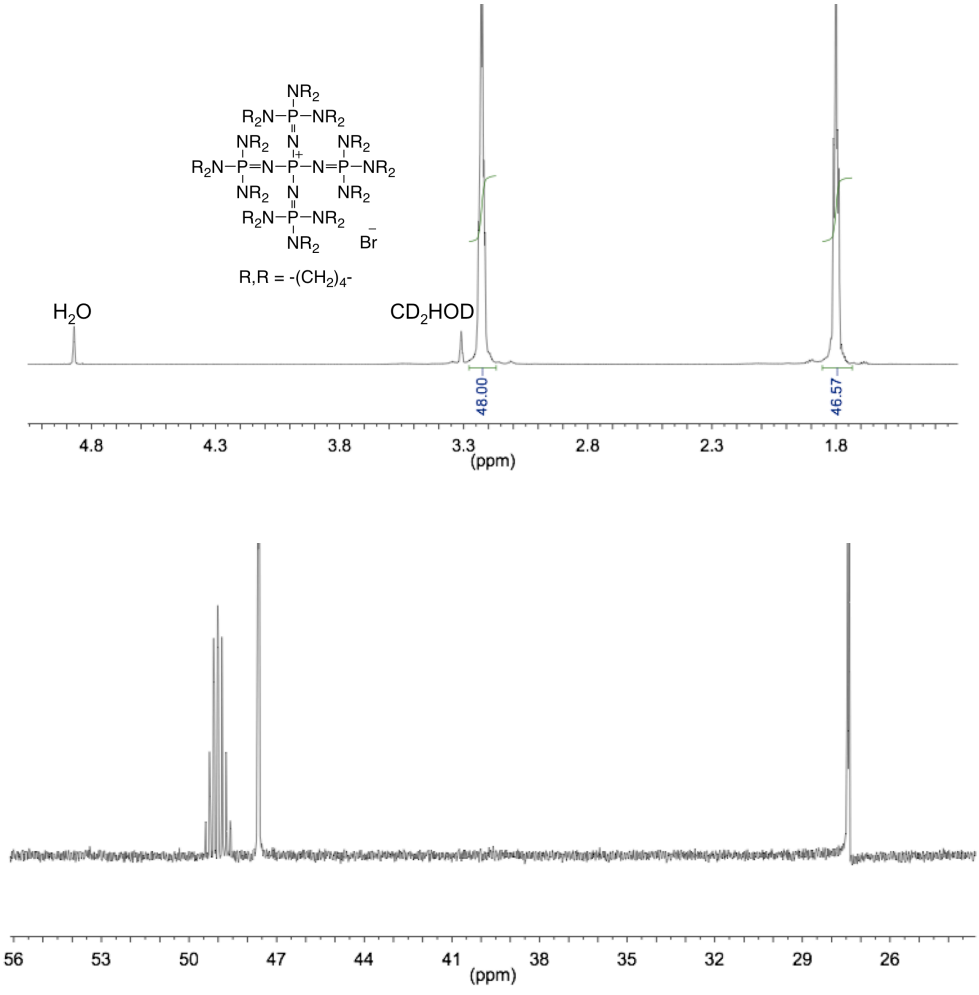

Figure 3.4. 3.3c in CD_3OD. Top: ^{1}H NMR spectrum. Bottom: ^{13}C NMR spectrum.

Tetrakis[(tri-1-pyrrolidinylphosphoranyliden)amino]phosphonium Iodide (**3.3d**). The procedure described for **3.3a** was followed using (300 mg, 0.263 mmol) tetrakis[(tri-1-pyrrolidinylphosphoranyliden)amino]phosphonium tetrafluoroborate, and (52 mg, 0.32 mmol) potassium iodide. Yield 278 mg, 89.6% white powder. ^{1}H NMR (CD_3OD, 600 MHz): δ 3.26 - 3.18 (m, 48H), 1.84 - 1.75 (m, 48H). $^{13}C\{^{1}H\}$ NMR (CD_3OD, 150 MHz): δ 47.61 (d, J = 5.5 Hz), 27.43 (d, J = 9.0 Hz). (Figure 3.5) Elemental analysis: Calcd for $C_{48}H_{96}N_{16}IP_5$: C, 48.89%; H, 8.21%; N, 19.01%. Found: C, 48.72%; H, 8.43%; N, 18.76%.

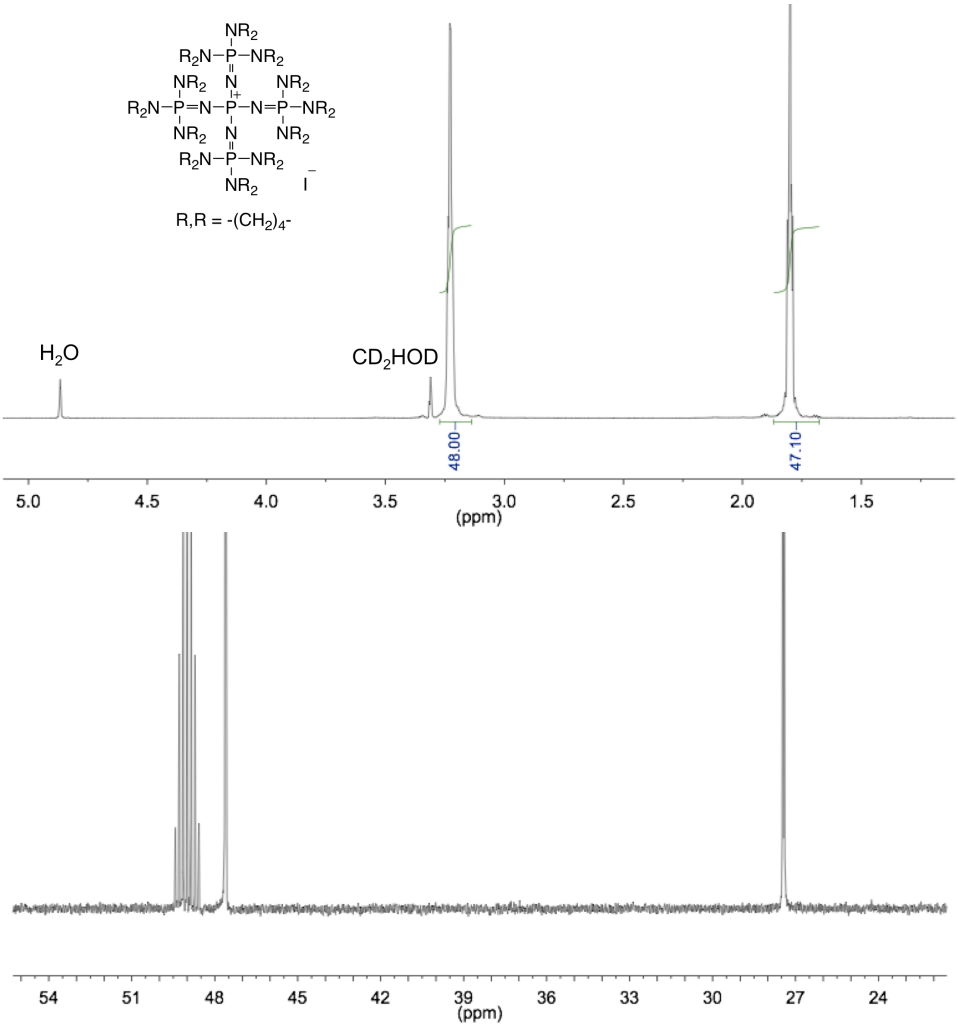

Figure 3.5. 3.3d in CD_3OD. Top: ^{1}H NMR spectrum. Bottom: ^{13}C NMR spectrum.

Tetrakis[(tri-1-pyrrolidinylphosphoranyliden)amino]phosphonium Pivalate (**3.3e**). The procedure described for **3.3a** was followed using (569 mg, 0.500 mmol) tetrakis[(tri-1-pyrrolidinylphosphoranyliden)amino]phosphonium tetrafluoroborate, and (84 mg, 0.60 mmol) potassium pivalate. Yield 470 mg, 81.5% blue powder. ^{1}H NMR (CD_3OD, 600 MHz): δ 3.26 - 3.18 (m, 48H), 1.84 - 1.75 (m, 48H) 1.13 (s, 9H). $^{13}C\{^{1}H\}$ NMR (CD_3OD, 150 MHz): δ 187.31, 47.61 (d, J = 5.5 Hz), 40.80, 28.93, 27.43 (d, J = 9.0 Hz). (Figure 3.6) Elemental analysis: Calcd for $C_{53}H_{105}N_{16}O_2P_5$: C, 55.19%; H, 9.18%; N, 19.43%. Found: C, 54.95%; H, 8.96%; N, 19.28%.

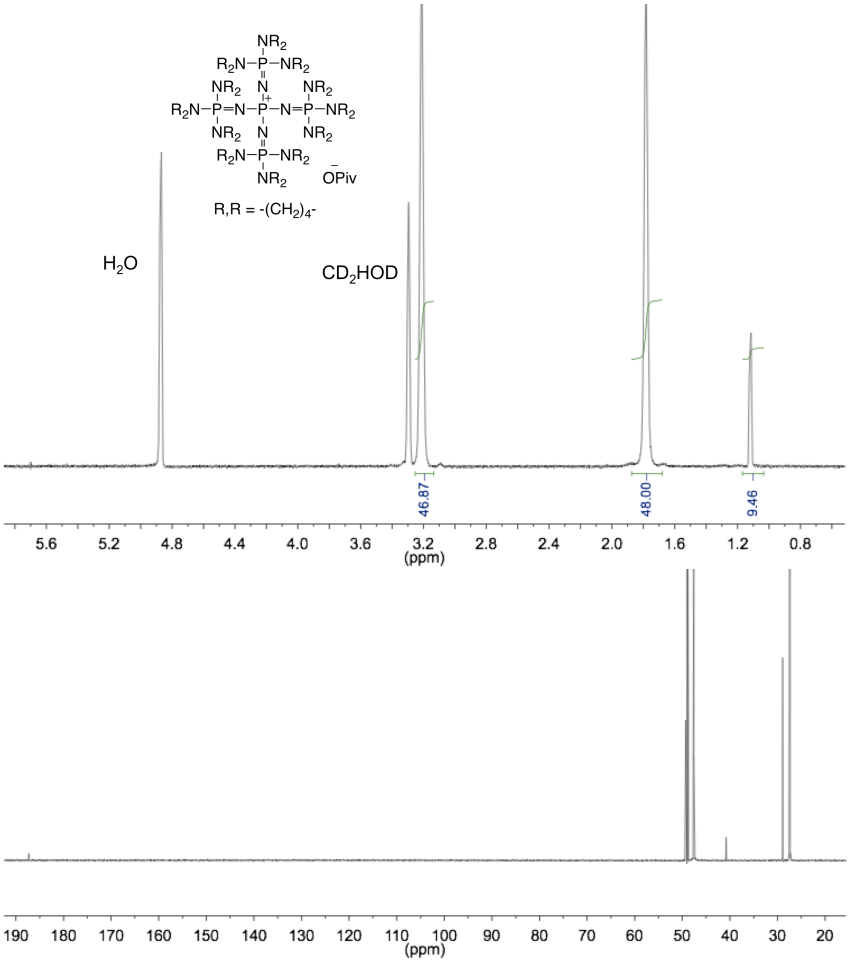

Figure 3.6. 3.3e in CD_3OD. Top: ^{1}H NMR spectrum. Bottom: ^{13}C NMR spectrum.

Tetrakis[(tri-1-pyrrolidinylphosphoranyliden)amino]phosphonium Triphenylacetate (**3.3f**). The procedure described for **3.3a** was followed using (285 mg, 0.250 mmol) tetrakis[(tri-1-pyrrolidinylphosphoranyliden)amino]phosphonium tetrafluoroborate, and (86 mg, 0.26 mmol) potassium triphenylacetate. Yield 295 mg, 88.1% white powder. ^{1}H NMR (CD_3OD, 600 MHz): δ 7.26 (t, J = 7.5 Hz, 6 H), 7.19 (t, J = 7.5 Hz, 3 Hz), 7.09 (d, J = 7.5 Hz, 6H) 3.26 - 3.18 (m, 48H), 1.84 - 1.75 (m, 48H). ^{13}C{^{1}H} NMR (CD_3OD, 150 MHz): δ 145.40, 130.46, 129.24, 127.28, 58.08, 47.61 (d, J = 5.5 Hz), 27.43 (d, J = 9.0 Hz). (Figure 3.7) Elemental analysis: Calcd for $C_{53}H_{105}N_{16}O_2P_5$: C, 60.97%; H, 8.35%; N, 16.73%. Found: C, 60.11%; H, 8.51%; N, 16.40%.

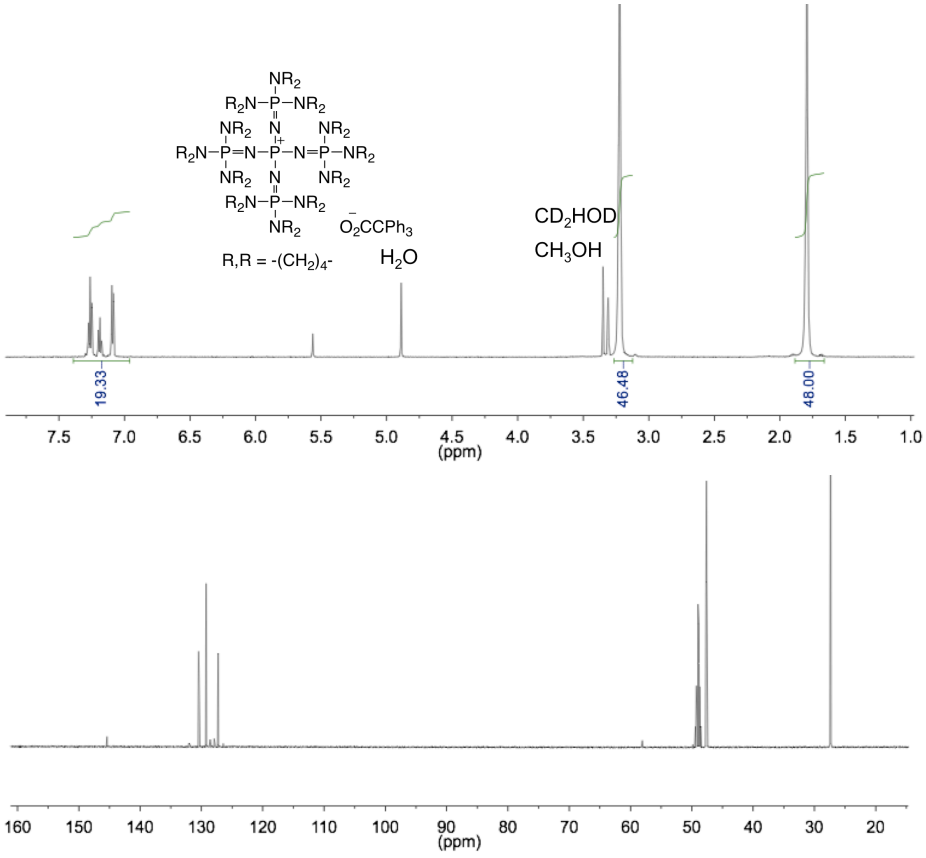

Figure 3.7. 3.3f in CD_3OD. Top: ^{1}H NMR spectrum. Bottom: ^{13}C NMR spectrum.

Tetrakis[(tri-1-pyrrolidinylphosphoranyliden)amino]phosphonium Benzoate (**3.3g**). The procedure described for **3.3a** was followed using (285 mg, 0.250 mmol) tetrakis[(tri-1-pyrrolidinylphosphoranyliden)amino]phosphonium tetrafluoroborate, and (42 mg, 0.26 mmol) potassium benzoate. Yield 290 mg, 98.9% blue powder. ^{1}H NMR (CD_3OD, 600 MHz): δ 7.94 (d *J* = 7.2 Hz, 2H), 7.38 (t, *J* = 7.2 Hz, 1H), 7.33 (t, *J* = 7.2 Hz, 2H), 3.26 - 3.18 (m, 48H), 1.84 - 1.75 (m, 48H). ^{13}C{^{1}H} NMR (CD_3OD, 150 MHz): δ 175.3, 139.30, 131.07, 130.27, 128.61, 47.61 (d, *J* = 5.5 Hz), 27.43 (d, *J* = 9.0 Hz). (Figure 3.8) Elemental analysis: Calcd for $C_{53}H_{105}N_{16}O_2P_5$: C, 56.30%; H, 8.68%; N, 19.10%. Found: C, 55.24%; H, 8.81%; N, 18.68%.

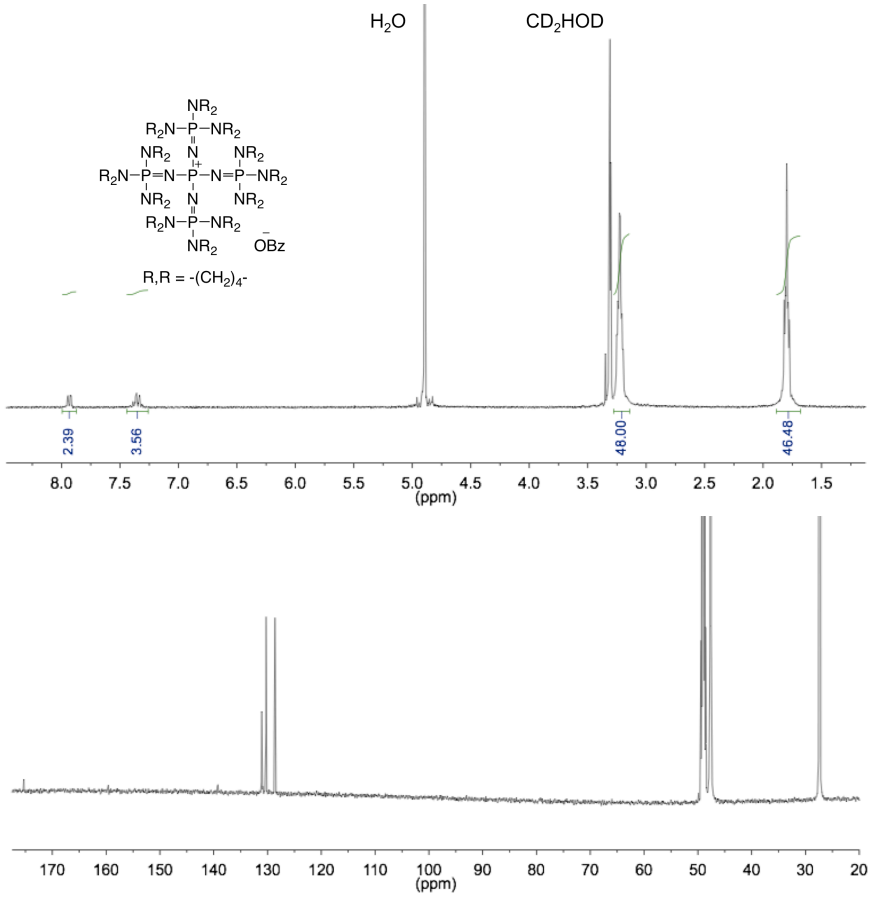

Figure 3.8. 3.3g in CD_3OD. Top: ^{1}H NMR spectrum. Bottom: ^{13}C NMR spectrum.

Tetrakis[(tri-1-pyrrolidinylphosphoranyliden)amino]phosphonium Pentafluorobenzoate (3.3h). The procedure described for **3.3a** was followed using (285 mg, 0.250 mmol) tetrakis[(tri-1-pyrrolidinylphosphoranyliden)amino]phosphonium tetrafluoroborate, and (65 mg, 0.26 mmol) potassium pentafluorobenzoate. Yield 297 mg, 94.0% white powder. ^{1}H NMR (CD_3OD, 600 MHz): δ 3.26 - 3.18 (m, 48H), 1.84 - 1.75 (m, 48H). $^{13}C\{^{19}F\}$ NMR (CD_3OD, 150 MHz): δ 162.4, 144.0, 141.4, 138.6, 118.4, 47.59 (td, J = 141 Hz, J = 5.5 Hz), 27.43 (td, J = 132 Hz, J = 9.0 Hz). ^{19}F NMR (CD_3OD, 564 MHz): -145.51 – 145.58 (m, 2F), -161.35 (t, J = 20Hz, 1F) -165.51 – -165.64 (m, 2F). (Figure 3.9) Elemental analysis: Calcd for $C_{55}H_{96}F_5N_{16}O_2P_5$: C, 52.29%; H, 7.66%; N, 17.74%. Found: C, 52.04%; H, 7.94%; N, 17.66%.

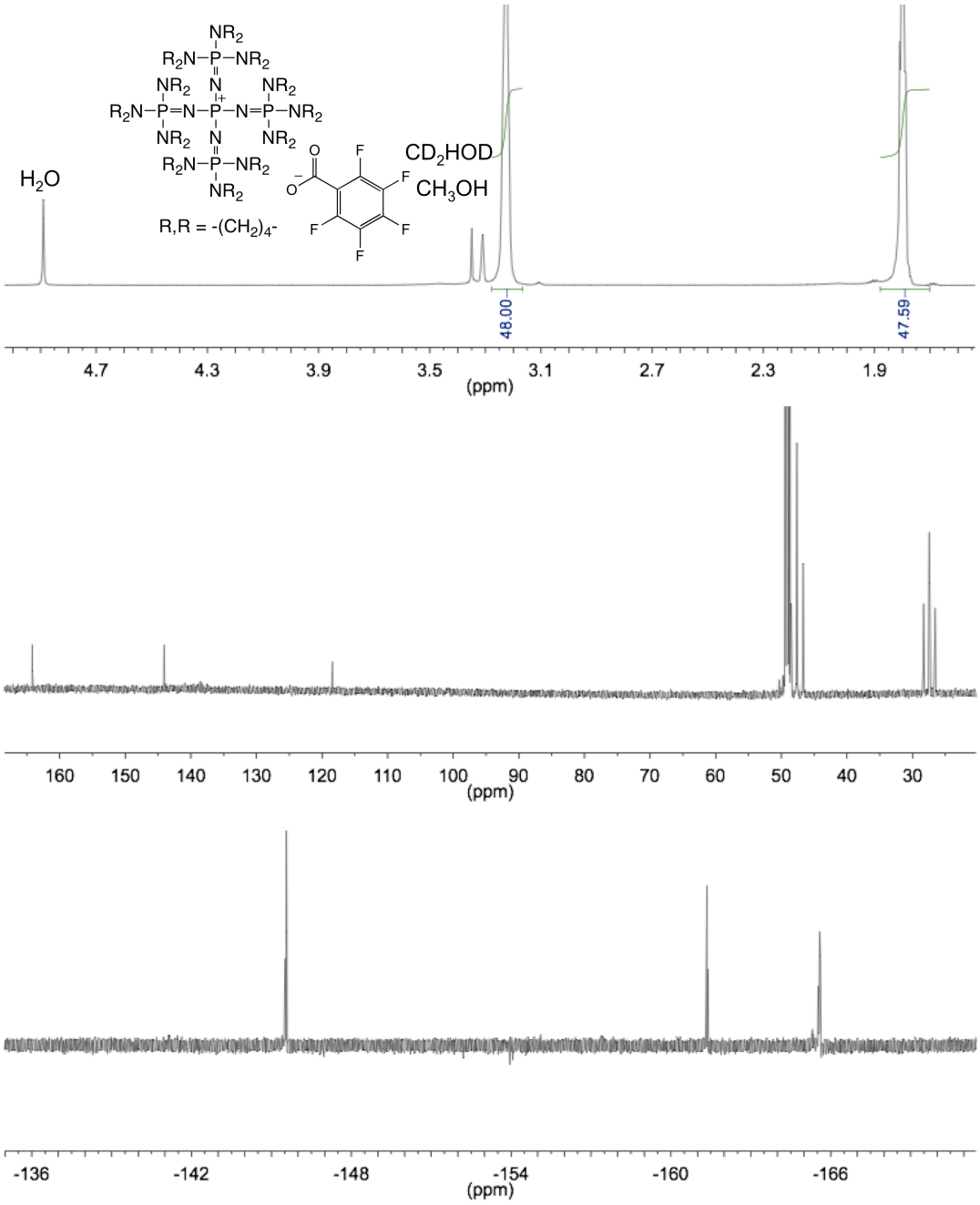

Figure 3.9. 3.3h in CD_3OD. Top: ^{1}H NMR spectrum. Center: $^{13}C\{^{19}F\}$ NMR spectrum. Bottom: ^{19}F NMR spectrum.

Tetrakis[(tri-1-pyrrolidinylphosphoranyliden)amino]phosphonium Tetraphenylborate (3.3i). To a solution of tetrakis[(tri-1-pyrrolidinylphosphoranyliden)amino]phosphonium tetrafluoroborate (285 mg, 0.250 mmol) in 2 mL methylene chloride was added potassium tetraphenylborate (93 mg, 0.26 mmol). The resulting suspension was then stirred at room temp for 30 min then filtered. The solution was then stripped down leaving a white solid. Yield 263 mg, 76.7%. ^{1}H NMR ($CDCl_3$, 600 MHz): δ 7.46-7.42 (m, 8H), 7.08 (t, J = 7.3 Hz, 8 H), 6.91 (t, J = 7.3 Hz, 4 H), 3.16 - 3.10 (m, 48 H), 2.62 - 2.34 (m, 48 H). ^{13}C{^{1}H} NMR ($CDCl_3$, 150 MHz): δ 164.39 (q, J = 197 Hz), 136.35, 125.35, 121.29, 46.32, 26.38. (Figure 3.10) Elemental analysis: Calcd for $C_{72}H_{116}BN_{16}P_5$: C, 63.05%; H, 8.53%; N, 16.34%. Found: C, 63.32%; H, 8.78%; N, 16.56%.

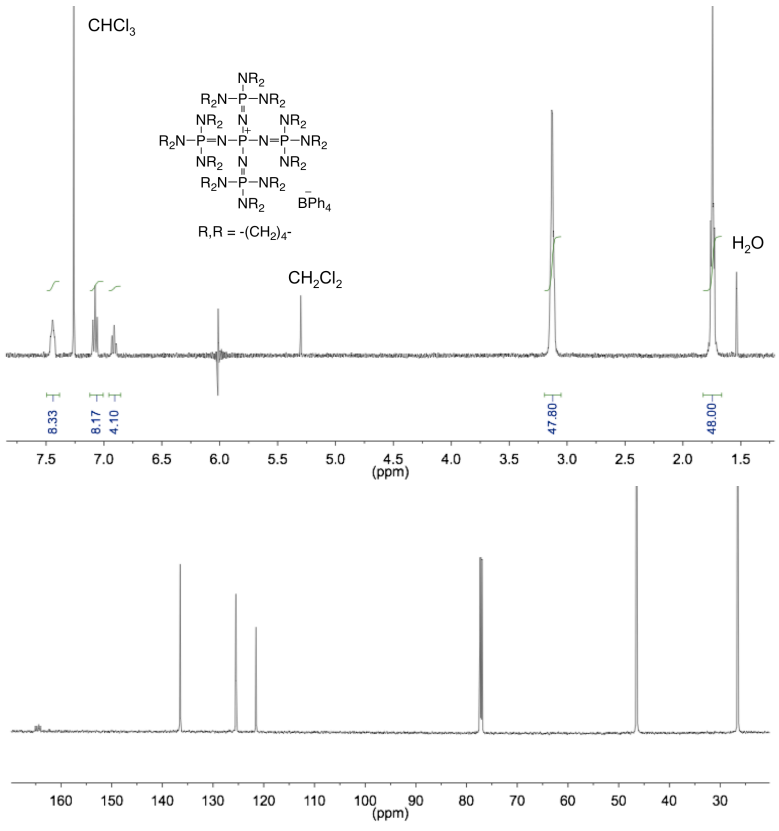

Figure 3.10. 3.3i in $CDCl_3$. Top: ^{1}H NMR spectrum. Bottom: ^{13}C NMR spectrum.

Tetrakis[cyclohexyl(methyl)amino]phosphonium Acetate (**3.4**). To a solution of tetrakis[cyclohexyl(methyl)amino]phosphonium tetrafluoroborate[8] (200 mg, 0.360 mmol) in 4 mL methanol was added potassium acetate (37 mg, 0.37 mmol) in 75 μL water. The resulting suspension was stirred at room temp for 5 min then filtered. The solution was then stripped down leaving a white solid, and dried over night under vacuum leaving a white powder (167 mg, 86.1%). ^{1}H NMR ($CDCl_3$, 600 MHz): δ 2.98 - 2.88 (m, 4H), 2.61 (d, J = 10 Hz, 12H), 1.94 (s, 3H), 1.9 - 1.84 (m, 8H), 1.69 - 1.44 (m, 20H), 1.26 - 1.17 (m, 8H), 1.12 - 1.03 (m, 4H). ^{13}C{^{1}H} NMR ($CDCl_3$, 150 MHz): δ 176.9, 55.85, 30.52, 30.05, 26.06, 25.11, 24.98. (Figure 3.11) Elemental analysis: Calcd for $C_{30}H_{59}N_4O_2P$: C, 66.88%; H, 11.04%; N, 10.40%. Found: C, 65.13%; H, 10.82%; N, 10.07%.

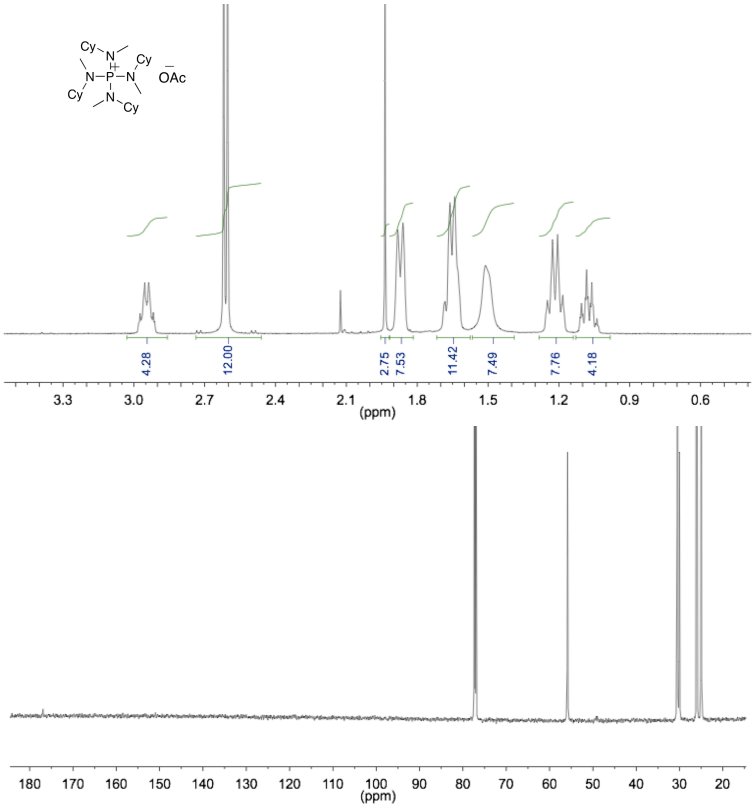

Figure 3.11. 3.4 in $CDCl_3$. Top: ^{1}H NMR spectrum. Bottom: ^{13}C NMR spectrum.

3.4.5 Enantioselective Polymerization of Epoxides

General Procedure for Propylene Oxide (PO) Polymerization (Table 3.1, entry 6).

In a drybox under nitrogen atmosphere, **3.1a** (4.0 mg, 3.5 μmol) and cocatalyst **3.3a** (3.9 mg, 3.5 μmol) were added to a reactor vial containing a stir bar and 12 mL dimethoxyethane (DME). The vial was sealed and removed from the drybox. The vial was cooled in an ice bath and PO (0.828 g, 14.3 mmol) was added via syringe. The polymerization was kept at 0 °C during the course of the reaction. After 30 seconds all volatiles were quickly removed under vacuum. The product was dried overnight. Conversion was determined by polymer mass (0.380 g, 45.9%). A concentrated sample of polymer (50 mg in 0.7 mL of $CDCl_3$) was analyzed using ^{13}C NMR spectroscopy to determine polymer tacticity (Figure 3.12). The recovered substrate was determined by chiral gas chromatography to be (*R*)-propylene oxide. The conditions for separation were: flow, 1.4 mL/min; velocity, 34 cm/sec; pressure, 7 psi; isothermal at 40 ºC.

$^{13}C\{^1H\}$ NMR ($CDCl_3$, 150 MHz): δ 75.70, 73.61, 17.64.

^1H NMR ($CDCl_3$, 600 MHz): δ 3.56 – 3.49 (m, 2H), 3.39 (m, 1H), 1.11 (d, J = 5.5 Hz, 3H).

M_n = 157 kg/mol, M_w/M_n = 1.9, M_n^{theo} = 109 kg/mol.

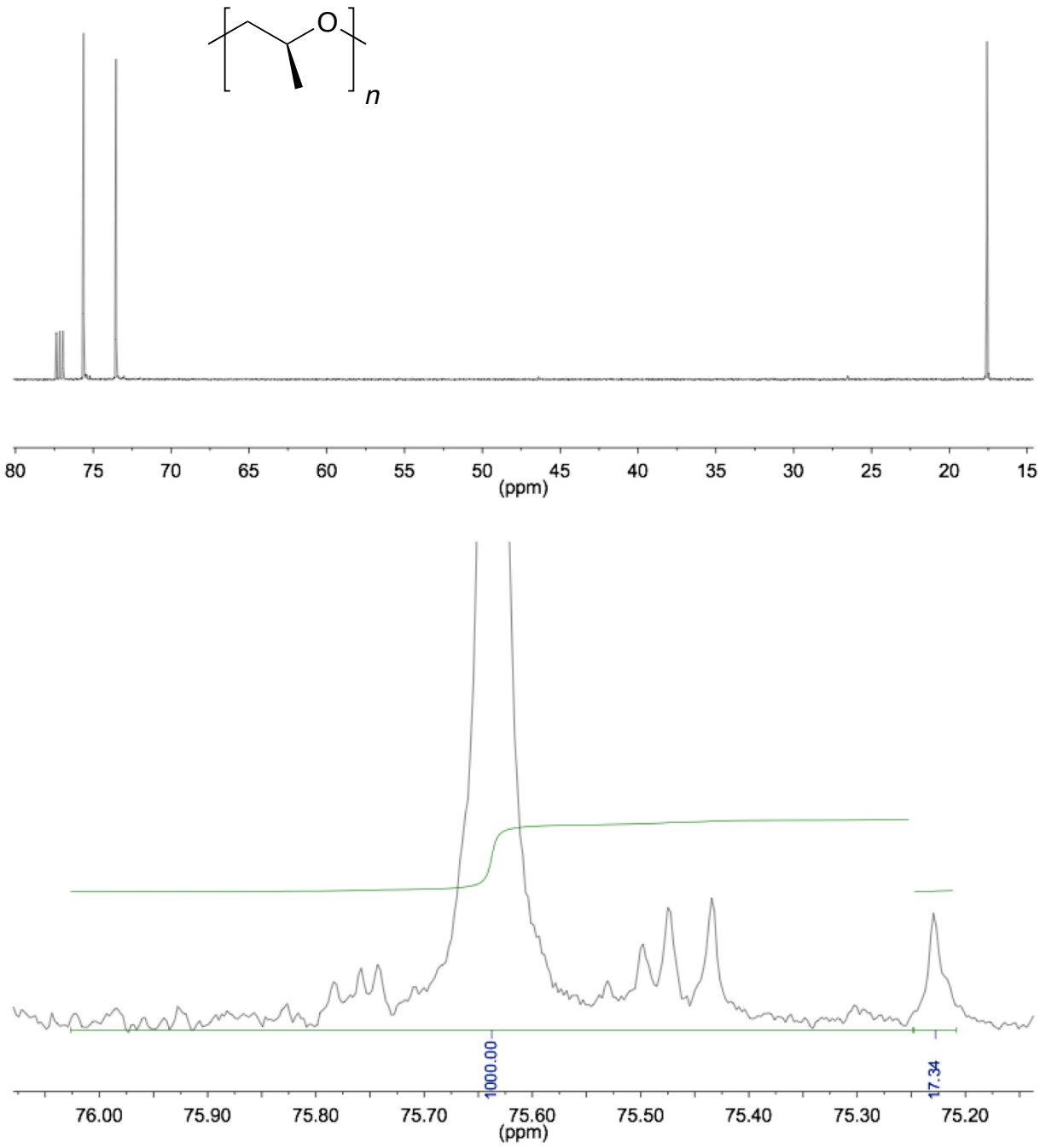

Figure 3.12. ^{13}C NMR spectra of poly(propylene oxide). Top: Full spectrum. Bottom: Methine region.

Polymerization of Racemic 1-Butene Oxide (Table 3.3, entry 1).

The polymerization procedure was the same as that for propylene oxide except that butene oxide was used. Butene oxide (0.981 g, 13.6 mmol) was polymerized with **3.1a** (4.0 mg, 3.5 μmol) and **3.3e** (4.0 mg, 3.5 μmol) in anhydrous DME (6 mL) at 0 °C. After 1 minute all volatiles were rapidly removed under vacuum. Conversion was determined by polymer mass (0.482 g, 49.1%). Polymer tacticity[3] (Figure 3.13): [*mm*]:[*mr* + *rm*]:[*rr*] = [0.989]:[0.0073]:[0.0037]. $ee_{(p)}$ = 99.2%. *s*-factor >300.

$^{13}C\{^{1}H\}$ NMR ($CDCl_3$, 150 MHz): δ 81.07, 72.62, 25.04, 10.06.

^{1}H NMR ($CDCl_3$, 600 MHz): δ 3.63 (m, 1H), 3.53 (m, 1H), 3.41 (m, 1H), 1.62 - 1.48 (m, 2H), 0.95 (3H, t, J = 7.4 Hz).

M_n = 140 kg/mol, M_w/M_n = 2.1, M_n^{theo} = 140 kg/mol.

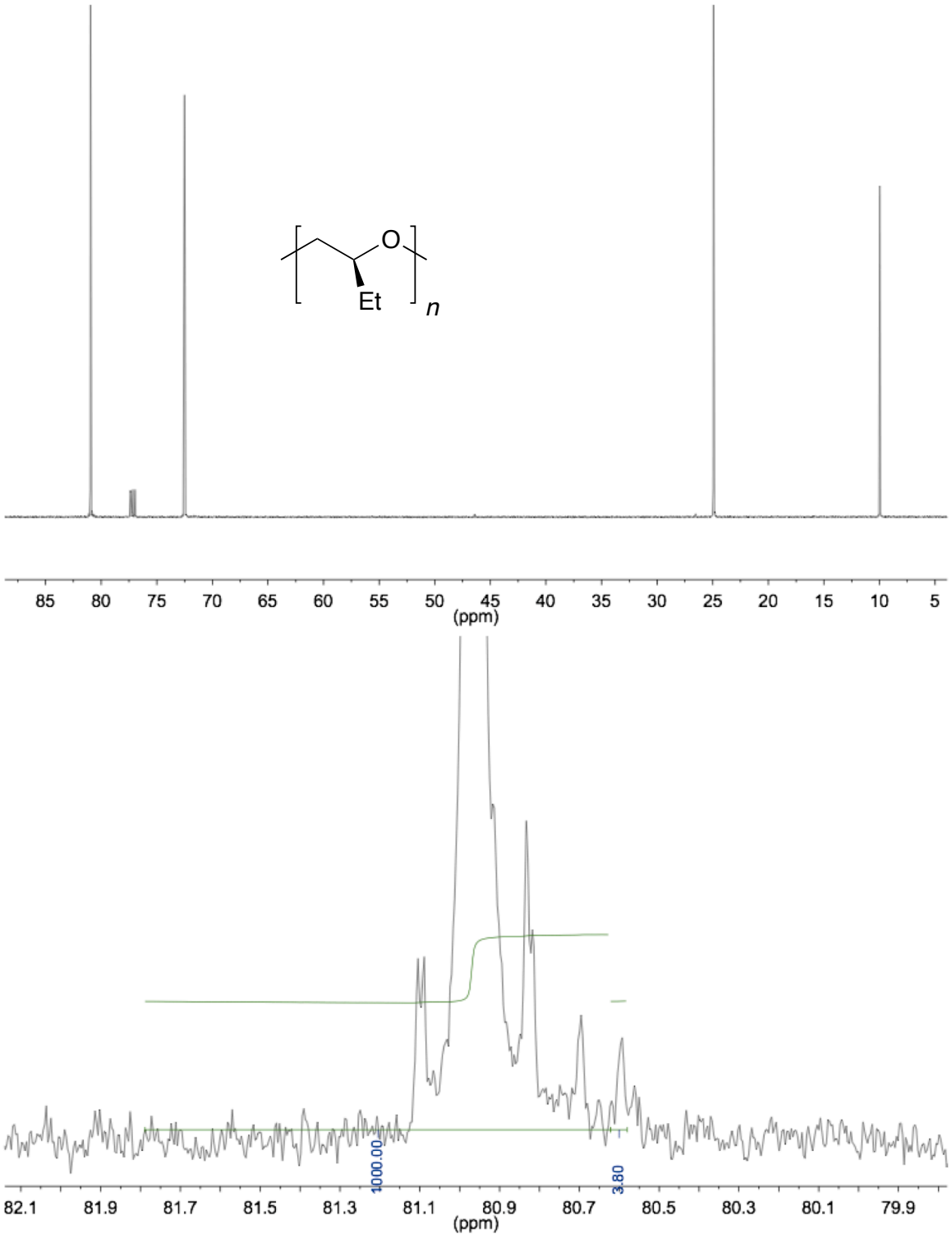

Figure 3.13. ^{13}C NMR spectra of poly(butene oxide). Top: Full spectrum. Bottom: Methine region.

Polymerization of Racemic Phenyl Glycidyl Ether (Table 3.3, entry 2).

The polymerization procedure was the same as that for propylene oxide except phenyl glycidyl ether was used. Phenyl glycidyl ether (2.16 g, 14.3 mmol) was polymerized with **3.1a** (4.0 mg, 3.5 μmol) and **3.3e** (4.0 mg, 3.5 μmol) in anhydrous DME (24 mL) at 0 °C. After 15 seconds, 12 mL acetone was added to the tube to stop the reaction. The polymer was isolated as a white solid by filtration and washed with acetone. Conversion was determined by mass (1.063 g, 49.2%). Polymer tacticity[19] (Figure 3.14): [*mm*]:[*mr* + *rm*]:[*rr*] = [0.969]:[0.021]:[0.010]. $ee_{(p)}$ = 97.9%. *s*-factor >300.

$^{13}C\{^{1}H\}$ NMR (150 MHz, 1,1,2,2-tetrachloroethane-d_2, 135 °C) δ 158.91, 129.13, 120.76, 115.01, 78.47, 70.06, 68.64.

^{1}H NMR (1,1,2,2-tetrachloroethane-d_2, 600 MHz, 135 °C): δ 7.25 – 7.21 (m, 2H), 6.96 – 6.89 (m, 3H), 4.13 (m, 1H), 4.08 (m, 1H), 3.89 – 3.78 (m, 3H).

M_n = 100 kg/mol, M_w/M_n = 2.2, M_n^{theo} = 300 kg/mol.

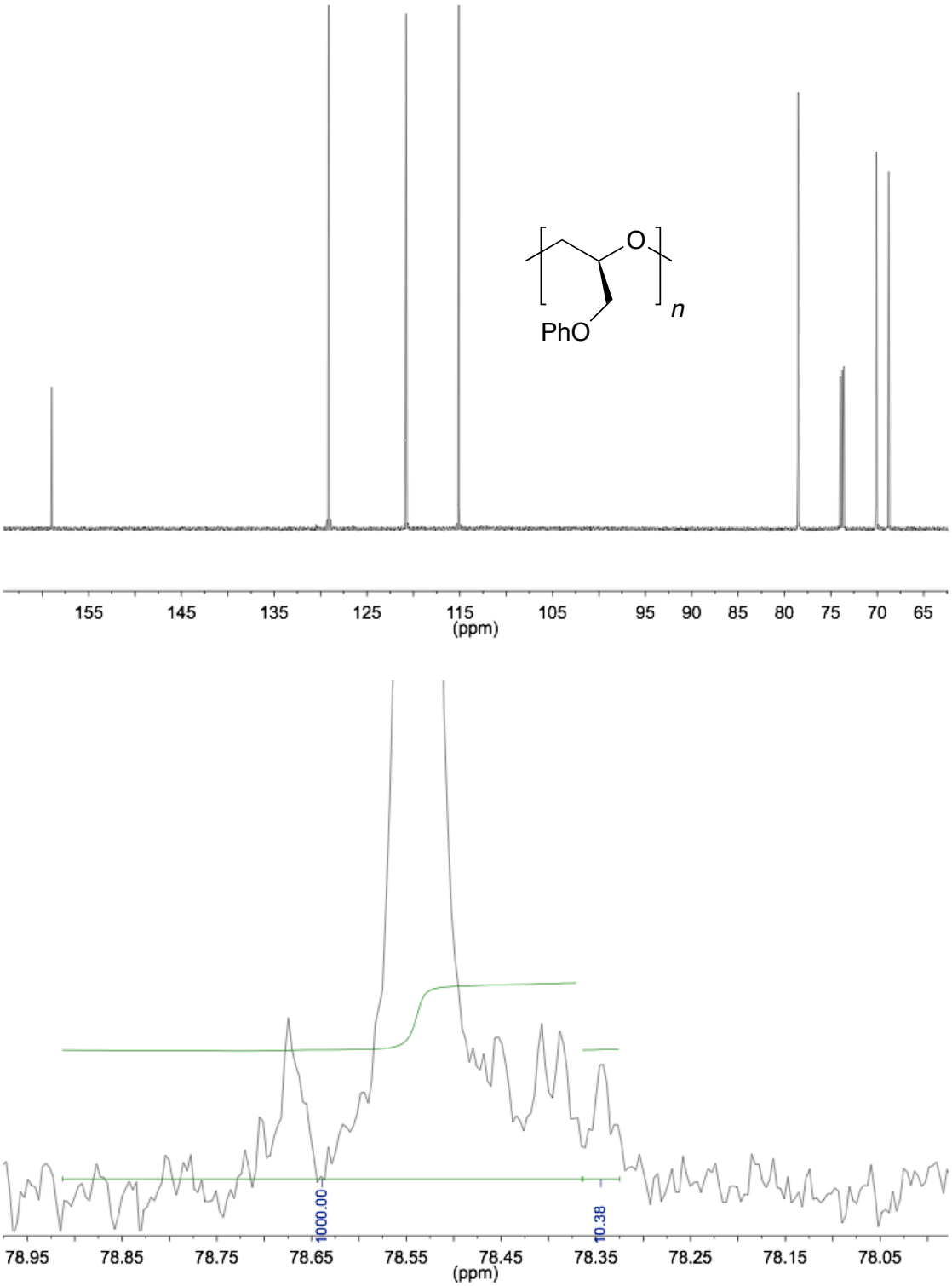

Figure 3.14. ^{13}C NMR spectra of poly(phenyl glycidyl ether). Top: Full spectrum. Bottom: Methine region.

Polymerization of Racemic 3,4-Epoxy-1-Butene (Table 3.3, entry 3).

The polymerization procedure was the same as that for propylene oxide except 3,4-epoxy-1-butene was used. 3,4-Epoxy-1-butene (1.04 g, 14.8 mmol) was polymerized with **3.1a** (4.0 mg, 3.5 μmol) and **3.3e** (4.0 mg, 3.5 μmol) in anhydrous DME (6 mL) at 0 °C. After 15 seconds, all volatiles were rapidly removed under vacuum. Conversion was determined by mass (0.516 g, 49.8%). The polymer displays tetrad resolution of the methylene carbon. Polymer tacticity was confirmed by complete hydrogenation to poly(1-butene oxide)[4] (Figure 3.15): [*mm*]:[*mr* + *rm*]:[*rr*] = [0.876]:[0.083]:[0.041]. $ee_{(p)}$ = 91.4%. *s*-factor 70.

$^{13}C\{^{1}H\}$ NMR ($CDCl_3$, 150 MHz): δ 136.27, 117.64, 80.79, 72.31.

^{1}H NMR ($CDCl_3$, 600 MHz): δ 5.75 (m, 1H), 5.32 (m, 1H), 5.19 (m, 1H), 3.94 (m, 1H), 3.66 (m, 1H), 3.45 (m, 1H).

M_n = 97 kg/mol, M_w/M_n = 2.9, M_n^{theo} = 150 kg/mol.

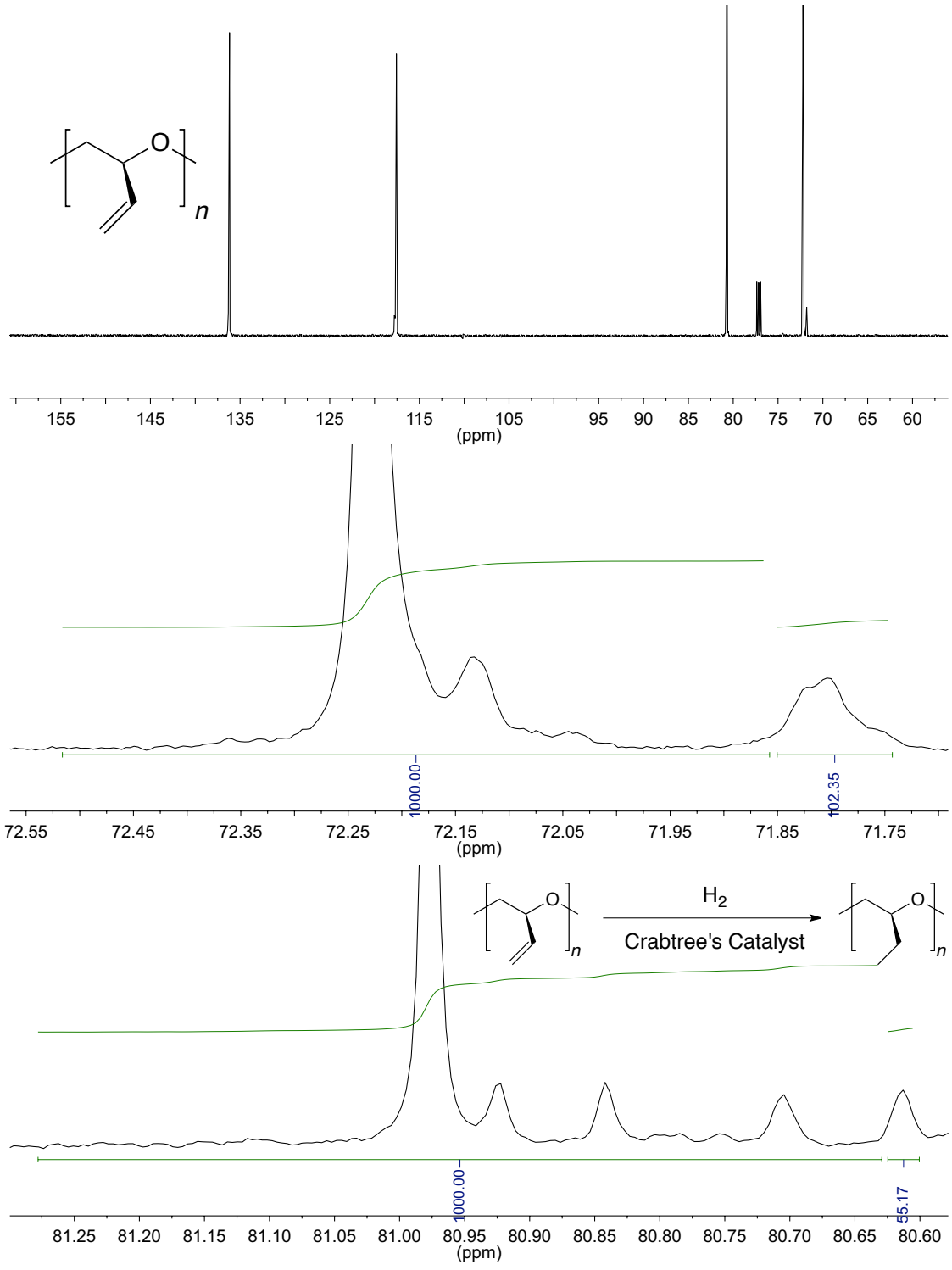

Figure 3.15. ^{13}C NMR spectra of poly(3,4-epoxy-1-butene). Top: Full spectrum. Center: Methylene region. Bottom: Hydrogenated polymer methine region.

Polymerization of Racemic Styrene Oxide (Table 3.3, entry 4).

The polymerization procedure was the same as that for propylene oxide except styrene oxide was used. Styrene oxide (0.845 g, 7.03 mmol) was polymerized with **3.1a** (2.0 mg, 1.7 μmol) and **3.3e** (2.0 mg, 1.7 μmol) in anhydrous DME (2.7 mL) at 0 °C. After 4 minutes, an aliquot was taken, then 12 mL acetone was added to quench and precipitate the polymer as a clear glass. Conversion was determined by ^{1}H NMR to be 47.8%. Polymer tacticity[20] (Figure 3.16): [*mm*]:[*mr* + *rm*]:[*rr*] = [0.985]:[0.010]:[0.005]. $ee_{(p)}$ = 99.0%. *s*-factor >300.

^{13}C NMR{^{1}H} ($CDCl_3$, 150 MHz): δ 139.84, 128.32, 127.67, 127.13, 81.99, 74.40.

^{1}H NMR ($CDCl_3$, 600 MHz): δ 7.41 - 7.32 (m, 5H), 4.57 (m, 1H), 3.69 (m, 1H), 3.55 (m, 1H).

M_n = 77 kg/mol, M_w/M_n = 5.3, M_n^{theo} = 240 kg/mol.

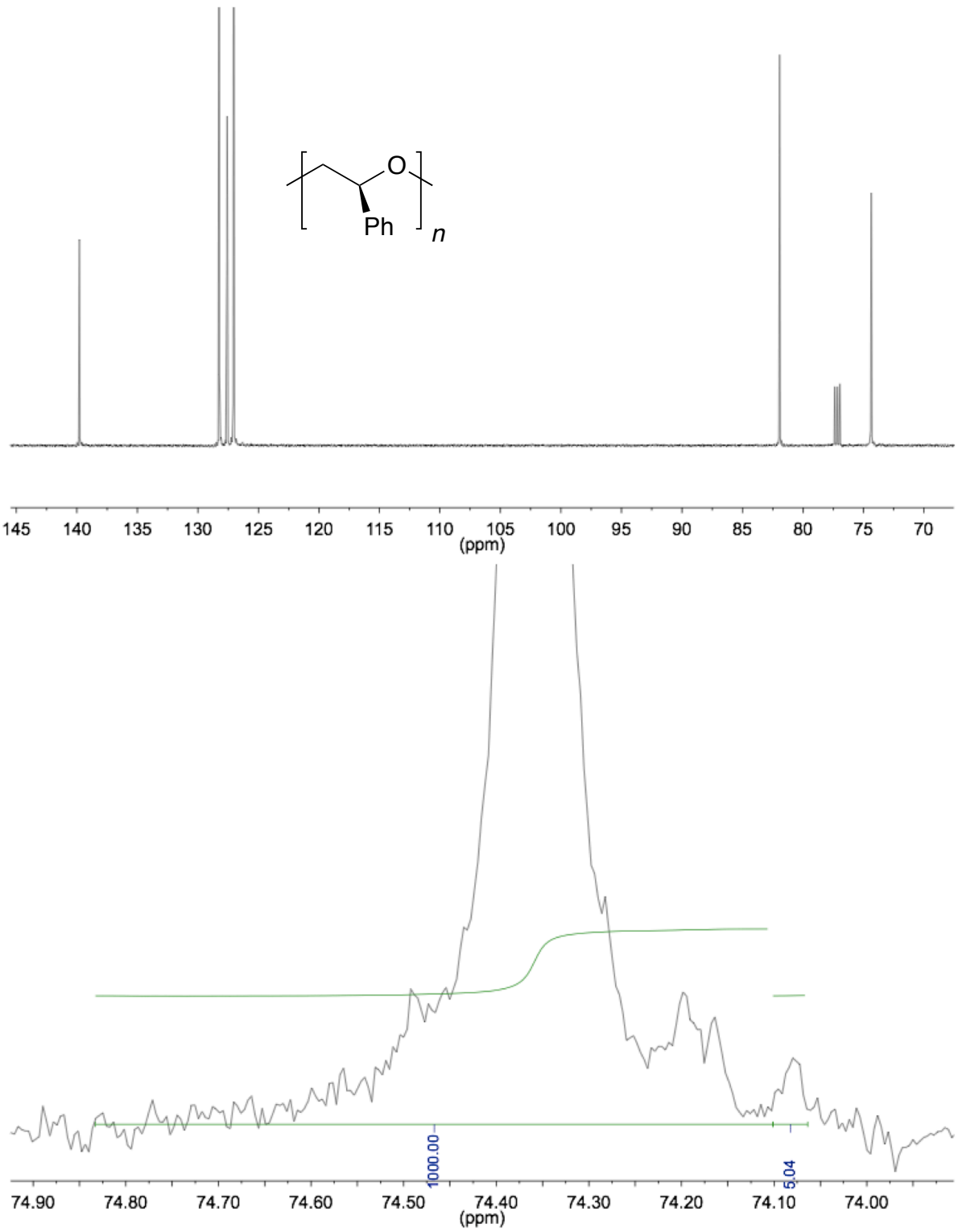

Figure 3.16. ^{13}C NMR spectra of poly(styrene oxide). Top: Full spectrum. Bottom: Methylene region.

Polymerization of Racemic 1,1,1-Trifluoro-2,3-Epoxypropane (Table 3.3, entry 5).

The polymerization procedure was the same as that for propylene oxide except 1,1,1-trifluoro-2,3-epoxypropane was used. 1,1,1-Trifluoro-2,3-epoxypropane (1.63 g, 14.5 mmol) was polymerized with **3.1a** (4.0 mg, 3.5 μmol) and **3.3e** (4.0 mg, 3.5 μmol) in anhydrous DME (6 mL) at 0 °C. After 30 minutes, the volatiles were quickly removed under vacuum. Conversion was determined by polymer mass (0.807 g, 49.3%). Polymer tacticity[21] (Figure 3.17): [*mm*]:[*mr* + *rm*]:[*rr*] = [0.993]:[0.005]:[0.002]. $ee_{(P)}$ = 99.5%. *s*-factor >300.

$^{13}C\{^{1}H\}$ NMR (Acetone-d*6*, 150 MHz): δ 125.0 (quartet, $^{1}J_{CF}$ = 282.2 Hz), 78.84 (quartet, $^{2}J_{CF}$ = 29.8 Hz), 71.45.

^{1}H NMR (Acetone-d*6*, 600 MHz): δ 4.35 (m, 1H), 4.21 (dd, *J* = 10.5, 3 Hz, 1H), 4.05 (dd, *J* = 10.5, 7.5 Hz, 1H).

M_n = 140 kg/mol, M_w/M_n = 1.8, M_n^{theo} = 230 kg/mol.

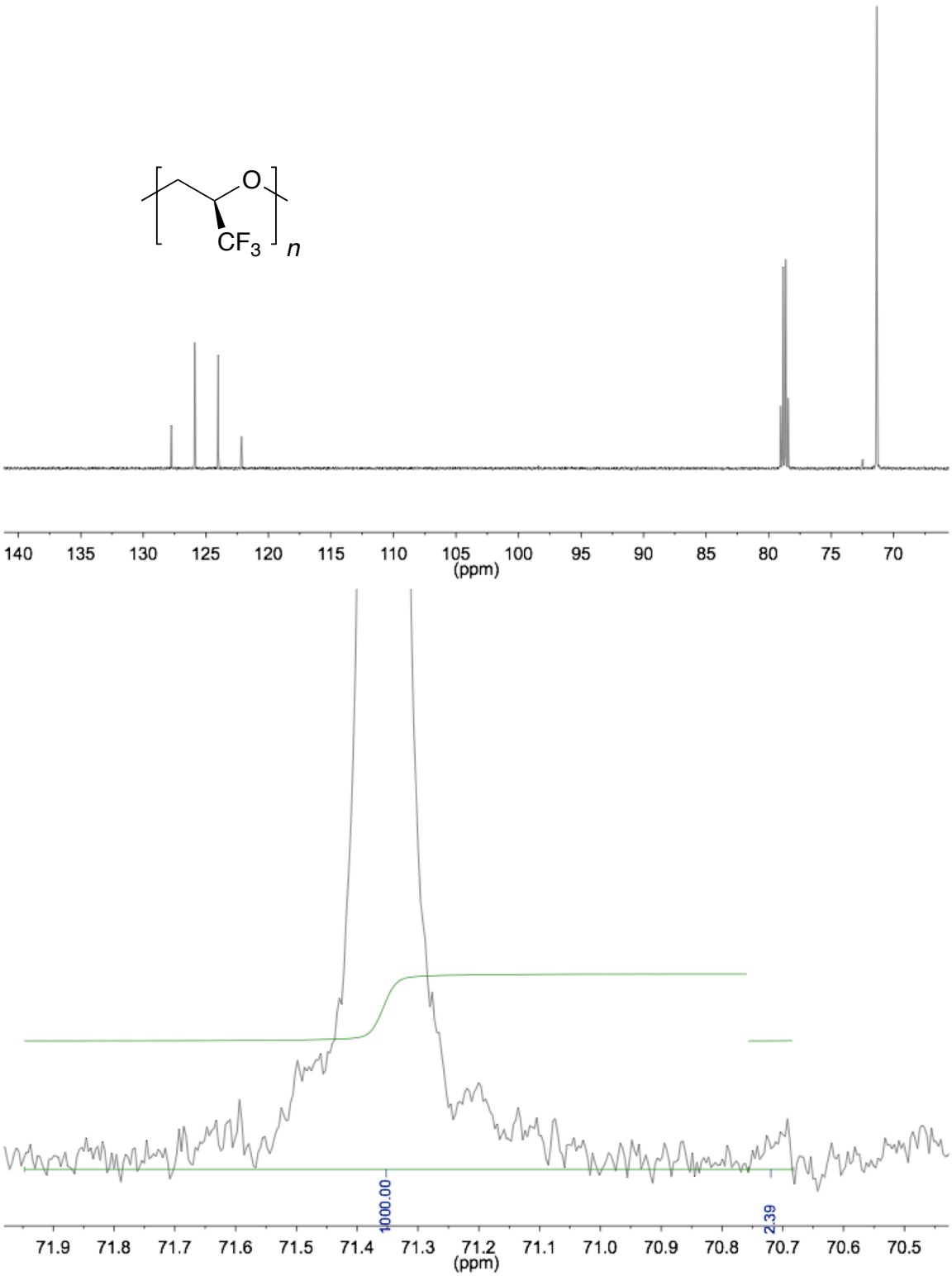

Figure 3.17. ^{13}C NMR spectra of poly(1,1,1-trifluoro-2,3-epoxypropane). Top: Full spectrum. Bottom: Methylene region.

3.5 References and Notes

(1) (a) *Encyclopedia of Chemical Technology*; Kroschwitz, J. I.; Howe-Grant, M., Eds.; Chichester, 1993; Vol. 8, pp 1079-1093. (b) Ajiro, H.; Allen, S. D.; Coates, G. W. Discrete Catalysts for Stereoselective Epoxide Polymerization in *Stereoselective Polymerization with Single Site Catalysts*, Baugh, L. S.; Canich, J. M. Eds. CRC Press, Boca Raton, 2008, Chapter 24, pp 627–644.

(2) (a) Peretti, K. L.; Ajiro, H.; Cohen, C. T.; Lobkovsky, E. B.; Coates, G. W. *J. Am. Chem. Soc.* **2005**, *127*, 11566–11567. (b) Ajiro, H.; Peretti, K. L.; Lobkovsky, E. B.; Coates, G. W. *Dalton Trans.* **2009**, *41*, 8828-8830.

(3) (a) Hirahata, W.; Thomas, R. M.; Lobkovsky, E. B.; Coates, G. W. *J. Am. Chem. Soc.* **2008**, *130*, 17658–17659. (b) Thomas, R. M.; Widger, P. C. B.; Ahmed, S. M.; Jeske, R. C.; Hirahata, W.; Lobkovsky, E. B.; Coates, G. W. *J. Am. Chem. Soc.* **2010**, *132*, 16520-16525.

(4) Widger, P. C. B.; Ahmed, S. M.; Hirahata, W.; Thomas, R. M.; Lobkovsky, E. B.; Coates, G. W. *Chem. Commun.* **2010**, *46*, 2935-2937.

(5) Nielsen, L. P. C.; Stevenson, C. P.; Blackmond, D. G.; Jacobsen, E. N. *J. Am. Chem. Soc.* **2004**, *126*, 1360-1362.

(6) Darensbourg, D. J.; Pala, M.; Rheingold, A. L. *Inorg. Chem*. **1986**, *25*, 125-127.

(7) (a) Darensbourg, D. J.; Mackiewicz, R. M. *J. Am. Chem. Soc.* **2005**, *127*, 14026-14038. (b) Aida, T.; Inoue, S. *J. Am. Chem. Soc.* **1985**, *107*, 1358-1364. (c) Cohen, C. T.; Chu,

T.; Coates, G. W. *J. Am. Chem. Soc.* **2005**, *127*, 10869-10878. (d) Lu, X.; Wang, Y. *Angew. Chem. Int. Ed.* **2004**, *43*, 3574-3577. (e) Aida, T.; Inoue, S. *Acc. Chem. Res.* **1996**, *29*, 39-48. (f) Aida, T.; Ishikawa, M.; Inoue, S. *Macromolecules* **1986**, *19*, 8-13. (g) Darensbourg, D. J.; Billodeaux, D. R. *Inorg. Chem.* **2005**, *44*, 1433-1442. (h) Cohen, C. T.; Coates, G. W. *J. Polym. Sci. A. Polym. Chem.* **2006**, *44*, 5182-5191. (i) Nakano, K.; Hashimoto, S.; Nozaki, K. *Chem. Sci.* **2010**, *1*, 369-373. (j) Sugitomo, H.; Kuroda, K. *Macromolecules* **2008**, *41*, 312-317.

(8) Schwesinger, R.; Link, R.; Wenzl, P.; Kossek, S.; Keller, M. *Chem. Eur. J.* **2006**, *12*, 429-437.

(9) (a) Rexin, O.; Mülhaupt, R. *Macromol. Chem. Phys.* **2003**, *204*, 1102-1109. (b) Rexin, O.; Mülhaupt, R. *J. Polym. Sci. A. Polym. Chem.* **2002**, *40*, 864-873.

(10) Ishio, M.; Katsube, M.; Ouchi, M.; Sawamoto, M.; Inoue, Y. *Macromolecules* **2009**, *42*, 188-193.

(11) Furuyama, R.; Fujita, T.; Fujiyoshi, S.; Funaki, F.; Nobori, T.; Nagata, T.; Fujiwara, K. *Cat. Surv. Asia* **2004**, *8*, 61-71.

(12) We previously reported higher activities and *s*-factors for PO when [**3.1a**]:[**3.2a**]=1:2, this is consistent with the poor solubility of **3.2a** necessitating an excess to form the active species (see reference 3a).

(13) Systems **3.1a**/**3.3g** and **3.1a**/**3.3i** were found to create small (<10% by mass) amounts of acetone-soluble, low tacticity impurities. **3.3g** and **3.3i** showed no activity for polymerization of PO without **3.1a** in DME.

(14) All entries in Table 3.3 display high conversion of the desired enantiomer and high *mm* values. The high activity of system **3.1a**/**3.3e** makes it difficult to stop these reactions at low conversions, thus increasing the errors associated with measuring conversions and subsequent *s*-factors. See: Schaus, S. E.; Brandes, B. D.; Larrow, J. F.; Tokunaga, M.; Hansen, K. B.; Gould, A. E.; Furrow, M. E.; Jacobsen, E. N. *J. Am. Chem. Soc.* **2002**, *124*, 1307–1315.

(15) Fringuelli, F.; Pizzo, F. *Org. Prep. Proced. Int.* **1989**, *21*, 757-761.

(16) Zhang, H. C.; Huang, W. S.; Pu, L. *J. Org. Chem.* **2001**, *66*, 481–487.

(17) Kozitsyna, N. Yu.; Bukharkina, A. A.; Martens, M. V.; Vargaftik, M. N.; Moiseev, I. I. *J. Organomet. Chem.* **2001**, *636*, 69–75.

(18) Shang, R.; Xu, Q.; Jiang, Y.; Wang, Y.; Liu, L. *Org. Lett.* **2010**, *12*, 1000-1003.

(19) Sakakibara, K.; Nakano, K.; Nozaki, K. *Macromolecules* **2008**, *40*, 6136-6142.

(20) Sepulchre, M.; Kassamaly, A.; Moreau, M.; Spassky, N. *Makromol. Chem.* **1988**, *189*, 2485-2501.

(21) Umezawa, J.; Hagiwara, T.; Hamana, H.; Narita, T; Furuhashi, K.; Nohira, H. *Polym. J.* **1994**, *26*, 715-721.

Chapter 4

Synthesis of Telechelic Isotactic Poly(Propylene Oxide) Diols from Racemic Propylene Oxide

4.1. Introduction

End-functionalized polymers with controlled molecular weight (MW) and microstructure are valuable building blocks for materials scientists, but are challenging to synthesize.[1] The reactive terminal groups of end-functionalized polymers allow for their integration into complex materials such as drugs or biomolecule conjugates,[2] modified solid surfaces,[3] or block copolymers.[4] For example, over 4 million tons of end-functionalized poly(propylene oxide) PPO polyols are synthesized annually for use as mid-blocks in polyurethane synthesis.[5] Polyurethanes are an important class of polymers used as adhesives, elastomers, fabrics, foams and insulators, whose properties are largely determined by the structure and properties of the polyols used in their synthesis.[5] Currently, linear di-end-functionalized (telechelic) PPO diols are popular mid-segments due to their low cost and desirable properties.[6]

Telechelic PPO diols are typically synthesized via anionic polymerization of racemic propylene oxide (PO) using glycols as initiators, producing amorphous atactic material.[7] Living catalysts have been developed to control the MW of polyethers,[8] however stereoselective catalysts[9] developed for the synthesis of isotactic PPO diols from racemic PO produce material with moderate tacticity and atactic byproducts.[10] Thus, the properties of highly isotactic PPO diols and their respective polyurethanes remain largely unknown.[11] A facile route to isotactic PPO diols could yield a new class of processable semi-crystalline materials[12] with novel applications.

In 2008, our group reported the bimetallic complex **4.1** for the synthesis of highly isotactic polyethers from racemic epoxides under mild conditions.[13] This complex once activated with an ionic cocatalyst such as bis(triphenylphosphine)iminium ([PPN]) pivalate (**4.2**)[14] is highly active and enantioselective for a variety of terminal epoxides (Figure 4.1).[13] However, this system (**4.1**/**4.2**) displays poor molecular weight control, often producing polyethers with MWs higher than that predicted by one polymer chain per bimetallic complex. The high MWs are attributed to slow or incomplete initiation and rapid propagation,[13] thus MW cannot be controlled by varying the [epoxide]/[**4.1**] ratio.

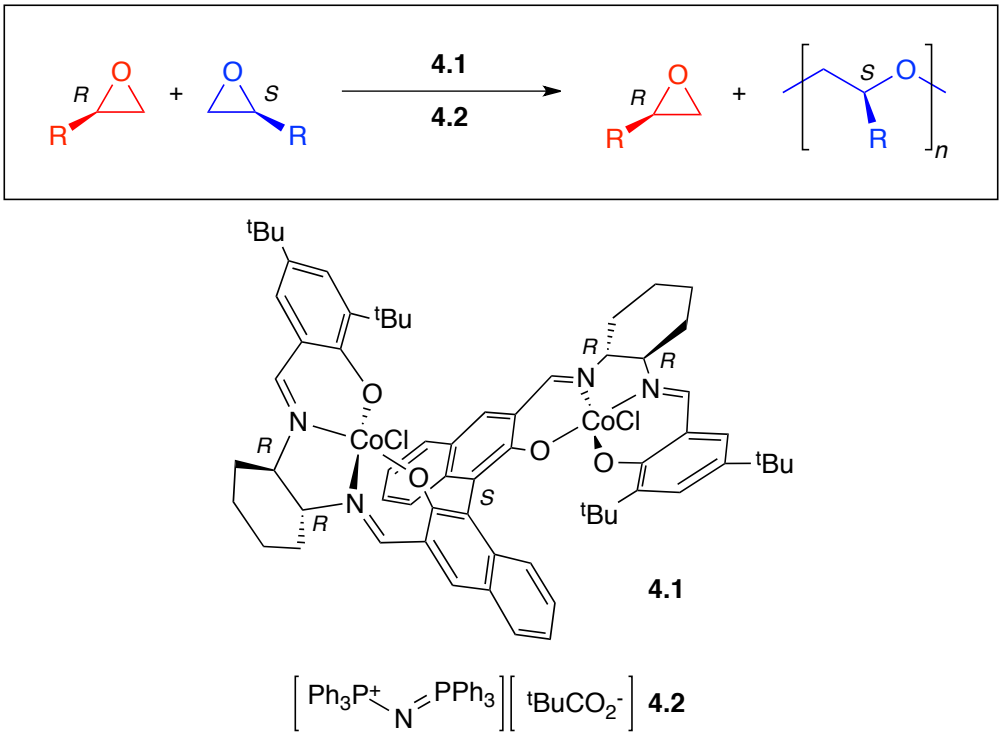

Figure 4.1. Enantioselective polymerization of epoxides using **4.1**/**4.2**.

Chain transfer agents (CTAs) are reagents that can be used in polymerizations to lower and control MW via termination and re-initiation of multiple polymer chains.[1] Inoue demonstrated that addition of alcohols to the living PO polymerization catalyst ((tetraphenylporphinato)-aluminum chloride) did not terminate polymerization. Instead, lower MW atactic PPO was formed.[15] The resulting "immortal" polymerization system produced polymers with MWs determined by the [PO]/[alcohol] ratio and narrow MW distributions (M_w/M_n) due to the rate of propagation being much slower than chain transfer. Industrially, CTAs are used with double metal cyanide (DMC) catalysts, a class of highly active epoxide polymerization catalysts.[16] The addition of low MW polyols, such as 1,2-propylene glycol or glycerine, deactivate DMC catalysts whereas higher MW polyol CTAs allow the synthesis of atactic PPO with high diol content.[16]

Considering previous successes in controlling MW of polymers with CTAs, we hypothesized that Co(III)salen based system **4.1**/**4.2** would be tolerant to protic additives such as alcohols or water.[17] In this paper, we explore the use of alcohols as CTAs with **4.1**/**4.2** to synthesize isotactic PPO with controlled MW and end-groups from racemic PO (Scheme 4.1). We also describe new routes to highly isotactic telechelic PPO diols for potential use in polyurethanes.

Scheme 4.1. Enantioselective Epoxide Polymerization Using Catalyst System **4.1**/**4.2**. A) Without Added Alcohols B) With Added Alcohols as Chain Transfer Agents

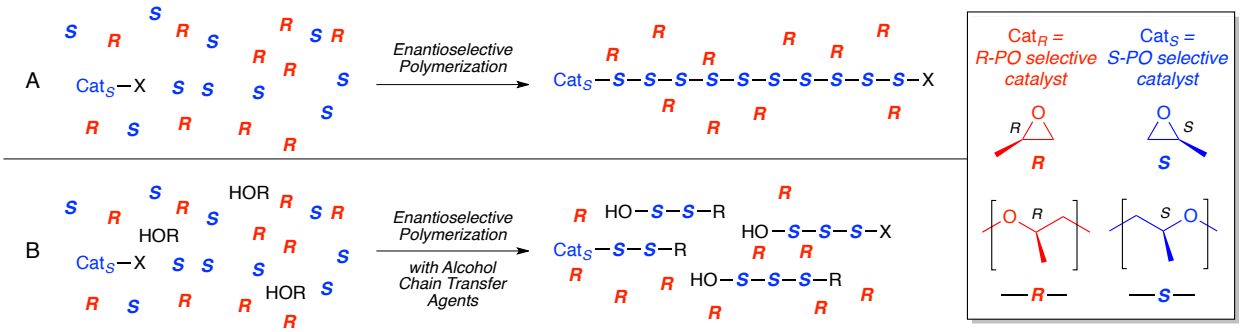

4.2. Results and Discussion

4.2.1. Initial Polymerization Studies with 4.1/4.2 and Alcohols as Chain Transfer Agents

We began our investigation using the catalyst system **4.1**/**4.2** to polymerize PO in the presence of 5 - 40 eq, of ^{i}PrOH CTA (Table 4.1). Regardless of iPrOH loading, the system displays high activity and enantioselectivity, producing PPO with high melting points (T_m), *mm* values, and *s*-factors (k_S/k_R). Analysis of polymer tacticity by ^{13}C NMR spectroscopy showed a ratio of stereoerrors of *mr* = *rm* = *rr*, consistent with an enantiomorphic site control mechanism.[13,18] The M_n values determined by $CHCl_3$ gel-permeation chromatography (GPC), as well as by ^{1}H NMR spectroscopy[19] decreased with additional ^{i}PrOH. The M_n calculated from ^{1}H NMR spectroscopy matched well with the theoretical M_n calculated from 1 chain per ^{i}PrOH at higher alcohol loadings. By ^{13}C NMR spectroscopy, terminal diastereotopic isopropyl methyl resonances were observed.[20] Isopropyl end-groups were also observed by MALDI-MS in entry 5,[18,21] demonstrating that ^{i}PrOH acts as a CTA, controlling MW and end-group identity and prompted us to further explore the behavior of **4.1**/**4.2** with CTAs.

Table 4.1. Polymerization of *rac*-PO Using ^{i}PrOH as CTA and Catalyst System **4.1**/**4.2**[a]

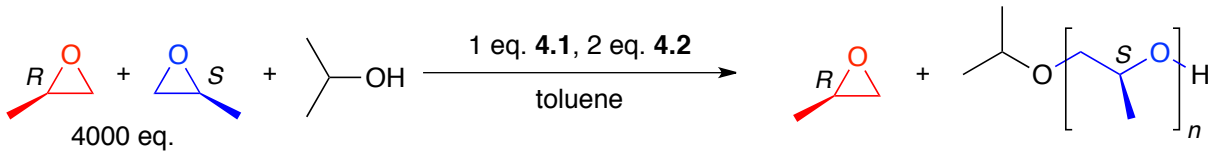

entry	NB	CTA eq.	time (min)	conv. (%)	M_n^{Theo} (kg/mol)	M_n^{NMR} (kg/mol)[b]	M_n^{GPC} (kg/mol)[c]	M_w/M_n[c]	[*mm*] (%)[d]	*s*-factor[d]	T_m (°C)[e]
1	10-277	0	1	47.7	113	-	219	3.1	97.9	>300	65.8
2	6-271	5	1.5	49.8	21.7	28.4	37.2	1.6	97.8	>300	69.6
3	6-283	10	3	45.5	10.9	8.9	18.7	1.5	98.7	>300	67.9
4	6-273	20	4	49.9	5.9	4.7	11.1	1.8	96.6	>300	69.0
5	6-281	40	4	49.2	3.0	3.1	6.0	1.8	99.1	>300	68.0

[a] General conditions: [**4.1**]:[**4.2**]:[PO] = 1:2:4000, T_{rxn} = 0 °C, [PO] = 2 M in toluene. [b] Determined by ^{1}H NMR spectroscopy. [c] Determined by gel-permeation chromatography calibrated with polystyrene standards in $CHCl_3$ at 40 °C. [d] Isotactic *mm* triad content determined by ^{13}C NMR spectroscopy. [e] Determined by differential scanning calorimetry.

There are three stereochemical possibilities when racemic PO is polymerized with a racemic enantioselective catalyst in the presence of alcohol CTAs as shown in Scheme 4.2. **A**: Atactic polymers are formed if the rate of propagation (k_P) is slow relative to the rate of chain transfer (k_{CT}) and the catalyst displays no stereoselectivity in propagation from chiral alcohol-chain-ends ($k_{Matched}$~$k_{Mismatched}$, Scheme 4.2 A). **B**: Stereoblock isotactic polymers are formed if propagation is fast relative to chain transfer and the catalyst displays no stereoselectivity in propagation from chiral alcohol-chain-ends ($k_{Matched}$~$k_{Mismatched}$, Scheme 4.2 B). **C**: Isotactic enantiopure polymer chains are formed regardless of chain transfer rates if the catalyst displays high stereoselectivity for propagating from only one enantiomer of chiral alcohol-chain-ends ($k_{Matched}$>$k_{Mismatched}$, Scheme 4.2 C).

Scheme 4.2. Stereochemical Possibilities During Polymerization of *rac*-PO with *rac*-**4.1**/**4.2** in the Presence of CTAs

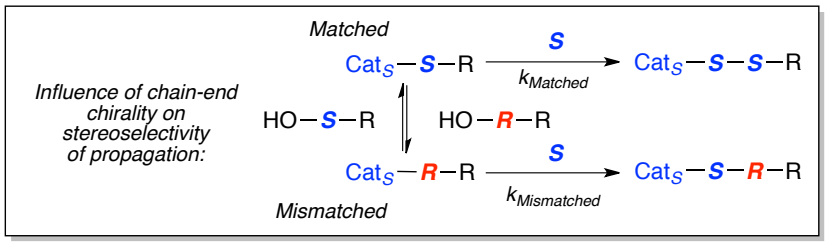

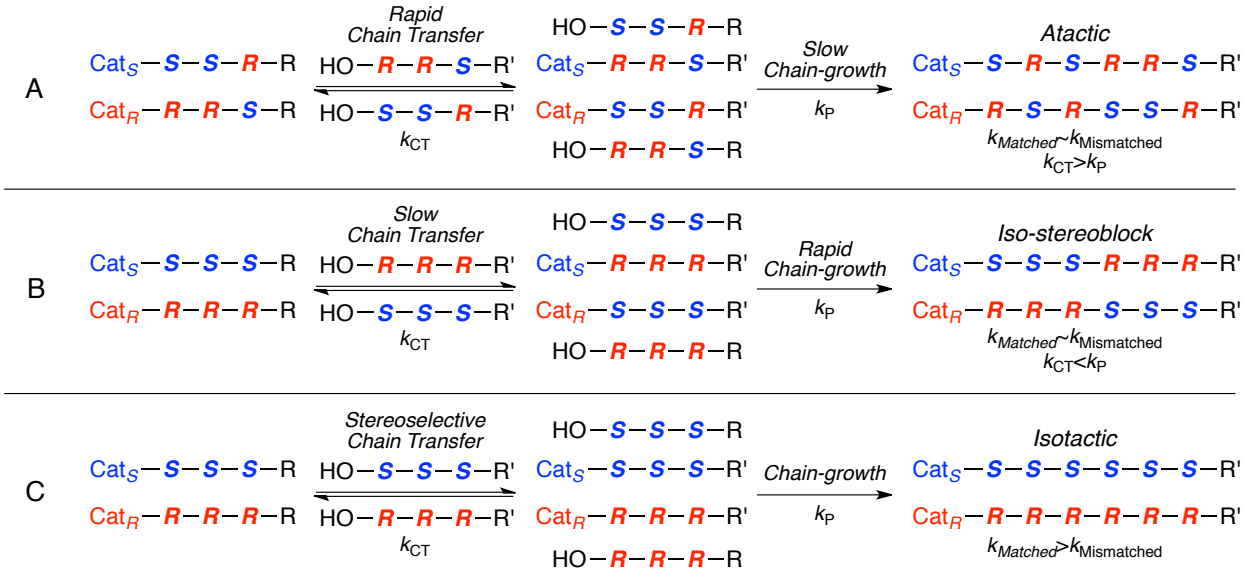

Experiments were performed using chiral alcohols as models of propagating PPO chain-ends to determine the catalyst's rates of propagation from matched and mismatched alcohols (Scheme 4.2). Polymerizations using either enantiomer of enantiopure 1-methoxy-2-propanol as CTA with enantiopure **4.1**/**4.2** gave similar low MW, crystalline, isotactic PPO (Table 4.2). The similar MWs in all entries demonstrate that the catalyst can propagate from both enantiomers of chiral alcohols ($k_{Matched}$~$k_{Mismatched}$, Scheme 4.2). The polymerization of PO with a racemic mixture of **4.1** and its enantiomer (*rac*-**4.1**) using ^{i}PrOH as CTA produced polymers with

isopropoxide end-groups, high T_m and *mm* values, as well as a decrease in MW as the amount of ^{i}PrOH was increased (Table 4.3) Analysis of polymer tacticity by ^{13}C NMR spectroscopy showed a ratio of stereoerrors of *mr* = *rm* > *rr*[18] indicating that stereoerrors are propagated.[22] This is in contrast to polymerizations of PO using *rac*-**4.1** without ^{i}PrOH (entry 1). Use of CTAs with *rac*-**4.1** allows chain transfer of a polymer chain from *R*-PO selective catalyst to its *S*-PO selective enantiomer (or *vice-versa*) followed by further propagation producing isotactic stereoblock PPO.[23] GPC analysis displays a narrowing of MW distribution (M_w/M_n ~ 1.6) compared to polymerizations without added CTA (M_w/M_n > 2), which is indicative of reversible chain transfer.[24] These results are consistent with fast propagation and slow reversible chain transfer between dormant alcohol and propagating polymer alkoxide with low stereoselectivity for propagation from chiral alcohols as in Scheme 4.2 B.

Table 4.2. Polymerization of *rac*-PO Using 1-Methoxy-2-propanol and Catalyst System **4.1**/**4.2**[a]

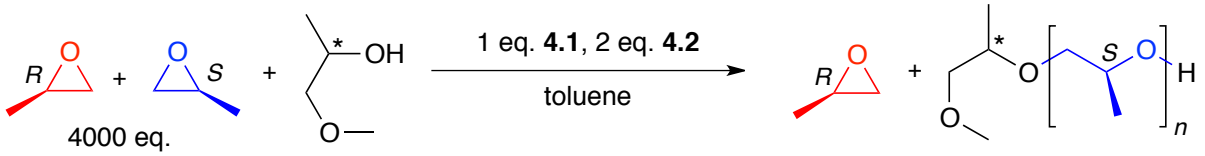

entry	stereochemistry **4.1**	CTA	conv. (%)	M_n^{Theo} (kg/mol)	M_n^{NMR} (kg/mol)[b]	M_n^{GPC} (kg/mol)[c]	M_w/M_n[c]	[*mm*] (%)[d]	T_m (°C)[e]
1	$(R,R)_2S$	*S*	51.8	3.1	1.5	3.3	1.2	97.5	62.6
2	$(S,S)_2R$	*S*	53.5	3.2	1.5	3.2	1.8	96.6	61.1
3	$(R,R)_2S$	*R*	50.8	3.0	1.7	3.7	1.6	98.1	61.5
4	$(S,S)_2R$	*R*	50.9	3.0	1.6	4.0	1.4	98.2	62.8

[a] General conditions: [**4.1**]:[**4.2**]:[1-methoxy-2-propanol]:[PO] = 1:2:40:4000, t = 1 h, T_{rxn} = 20 °C, [PO] = 2 M in toluene. [b] Determined by ^{1}H NMR spectroscopy. [c] Determined by gel-permeation chromatography calibrated with polystyrene standards in $CHCl_3$ at 40 °C. [d] Isotactic *mm* triad content determined by ^{13}C NMR spectroscopy. [e] Determined by differential scanning calorimetry. All entries from NB 10-253.

Table 4.3. Polymerization of *rac*-PO Using ^{i}PrOH and Catalyst System *rac*-**4.1**/**4.2**[a]

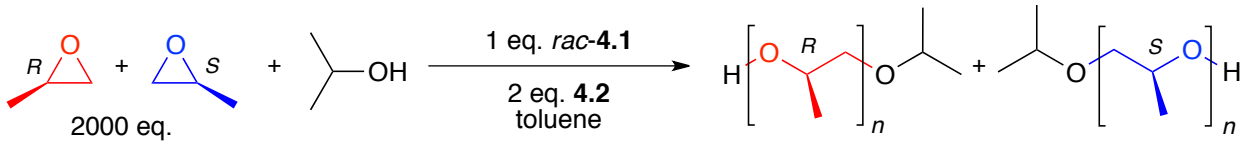

entry	NB	CTA eq.	conv. (%)	M_n^{Theo} (kg/mol)	M_n^{NMR} (kg/mol)[b]	M_n^{GPC} (kg/mol)[c]	M_w/M_n[c]	[*mm*] (%)[d]	T_m (°C)[e]
1	10-279	0	76.4	92.5	-	204	2.3	98.6	65.8
2	10-223	10	67.8	8.0	6.6	23.0	1.5	97.9	67.9
3	10-223	20	74.1	4.4	4.8	13.8	1.5	97.5	67.5
4	10-223	40	67.5	2.0	3.1	6.5	1.4	95.8	63.8

[a] General conditions: [**4.1**]:[**4.2**]:[PO] = 1:2:2000, t = 15 min, T_{rxn} = 20 °C, [PO] = 2 M in toluene. [b] Determined by ^{1}H NMR spectroscopy. [c] Determined by gel-permeation chromatography calibrated with polystyrene standards in $CHCl_3$ at 40 °C. [d] Isotactic *mm* triad content determined by ^{13}C NMR spectroscopy. [e] Determined by differential scanning calorimetry.

4.2.2. Screening of Chain Transfer Agents

To synthesize telechelic PPO diols, we explored the use of water as a diprotic CTA. Unfortunately, the addition of 10 eq. of water relative to **4.1** resulted in a complete loss of polymerization activity for PO. We hypothesized that water or the glycol product from addition of water to PO chelated inside the catalyst cleft[13b] and blocked coordination of monomer. Instead, the polymerization of mono-alcohols was explored with the goal of using a post-polymerization modification to synthesize the desired PPO diols. Addition of the sterically bulky alcohol trimethylsilanol did not lower polymer MW presumably due to its inability to enter the catalyst cleft.

We then screened 4-methoxybenzyl alcohol (PMB) as a CTA with the goal of oxidatively cleaving the ether to yield an alcohol via post-polymerization modification. As shown in Table

4.4 MWs decreased with additional PMB and the samples were highly isotactic. PMB initiation was confirmed by the 1:1 stoichiometry of the PMB initiator and alcohol methine terminus resonances in ^{1}H NMR spectroscopy.[18,25] The samples were oxidatively deprotected using 2,3-dichloro-5,6-dicyanobenzoquinone (DDQ) to give the desired PPO diols. Despite the oxidative instability of polyethers,[26] the conditions were mild enough that MW values were consistent before and after deprotections showing that the oxidation selectively cleaved only the PMB group. ^{1}H and ^{13}C NMR spectroscopy as well as MALDI-MS confirmed the removal of PMB groups to give telechelic isotactic PPO diols.[18] After purification with acetone all samples were isolated as white powders, displayed high *mm* values and were crystalline with high melting points consistent with pure isotactic PPO.

Table 4.4. Polymerization of *rac*-PO Using Catalyst System **4.1**/**4.2** and PMB, Followed by Deprotection with DDQ[a]

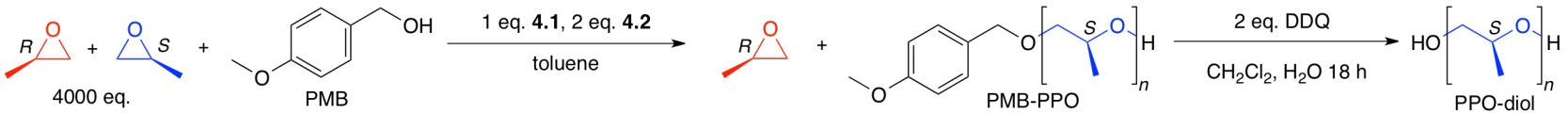

	Synthesis of PMB-PPO							Synthesis of PPO-diol					
entry	CTA eq.	conv. (%)	M_n^{Theo} (kg/mol)	M_n^{NMR} (kg/mol)[b]	M_n^{GPC} (kg/mol)[c]	M_w/M_n[c]	[*mm*] (%)[d]	yield (%)	M_n^{NMR} (kg/mol)[b]	M_n^{GPC} (kg/mol)[c]	M_w/M_n[c]	[*mm*] (%)[d]	T_m (°C)[e]
1	10	51.9	12.3	22.8	31.7	2.1	96.4	68.2	13.3	36.6	2.1	97.0	68.5
2	20	52.5	6.2	7.8	17.9	2.0	95.9	84.0	9.8	17.4	1.9	97.0	67.5
3	40	52.9	3.1	3.6	9.1	1.9	96.3	75.7	3.1	10.8	1.8	97.3	67.1
4	80	54.9	1.6	1.9	5.4	1.7	96.4	80.8	1.9	5.9	2.0	97.8	65.6

[a] General conditions: [**4.1**]:[**4.2**]:[PO] = 1:2:4000, t = 1 h, T_{rxn} = 20 °C, [PO] = 2 M in toluene. [b] Determined by ^{1}H NMR spectroscopy. [c] Determined by gel-permeation chromatography calibrated with polystyrene standards in $CHCl_3$ at 40 °C. [d] Isotactic *mm* triad content determined by ^{13}C NMR spectroscopy. [e] Determined by differential scanning calorimetry. All entries from NB 10-231+232

4.2.3. Diols as Chain Transfer Agents

A more direct synthetic route to PPO diols was sought to avoid post-polymerization modifications. To minimize chelation, we explored the use of polymeric diols as CTAs to synthesize telechelic isotactic PPO. The addition of poly(1-butene) diol[27] as a CTA (Table 4.5) lowered MWs and did not drastically reduce conversion to polymer All products were highly isotactic and crystalline. As shown in Figure 4.2 addition of PO shifted the original poly(1-butene) diol trace to higher MW suggesting the addition of highly isotactic PPO end blocks. NMR spectroscopy verified the disappearance of poly(1-butene) end-groups and appearance of new PPO terminal methine alcohol end-groups consistent with the formation of block copolymers.[18]

Table 4.5. Polymerization of *rac*-PO Using Catalyst System **4.1**/**4.2** and Poly(1-butene) Diol[a]

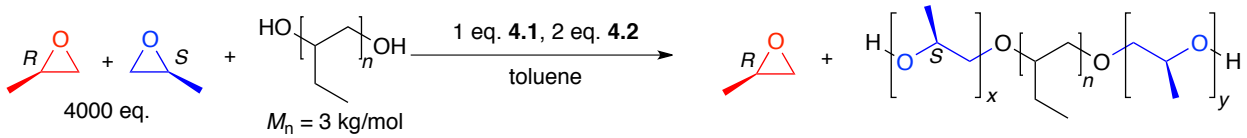

entry	CTA eq.	conv. (%)	M_n^{GPC} (kg/mol)[b]	M_w/M_n[b]	[*mm*] (%)[c]	T_m (°C)[d]	ΔH_f (J/g)[d]
1	0	49.5	231	2.9	96.4	66.2	-43.8
2	10	50.4	28.3	1.7	94.8	67.2	-42.9
3	20	49.9	14.4	1.7	95.8	65.8	-41.9
4	40	32.4	7.1	1.5	99.2	64.3	-23.4

[a] General conditions: [**4.1**]:[**4.2**]:[PO] = 1:2:4000, t = 1 h, T_{rxn} = 20 °C, [PO] = 2 M in toluene. [b] Determined by gel-permeation chromatography calibrated with polystyrene standards in $CHCl_3$ at 40 °C. [c] Isotactic *mm* triad content determined by ^{13}C NMR spectroscopy. [d] Determined by differential scanning calorimetry. All entries from NB 10-219.

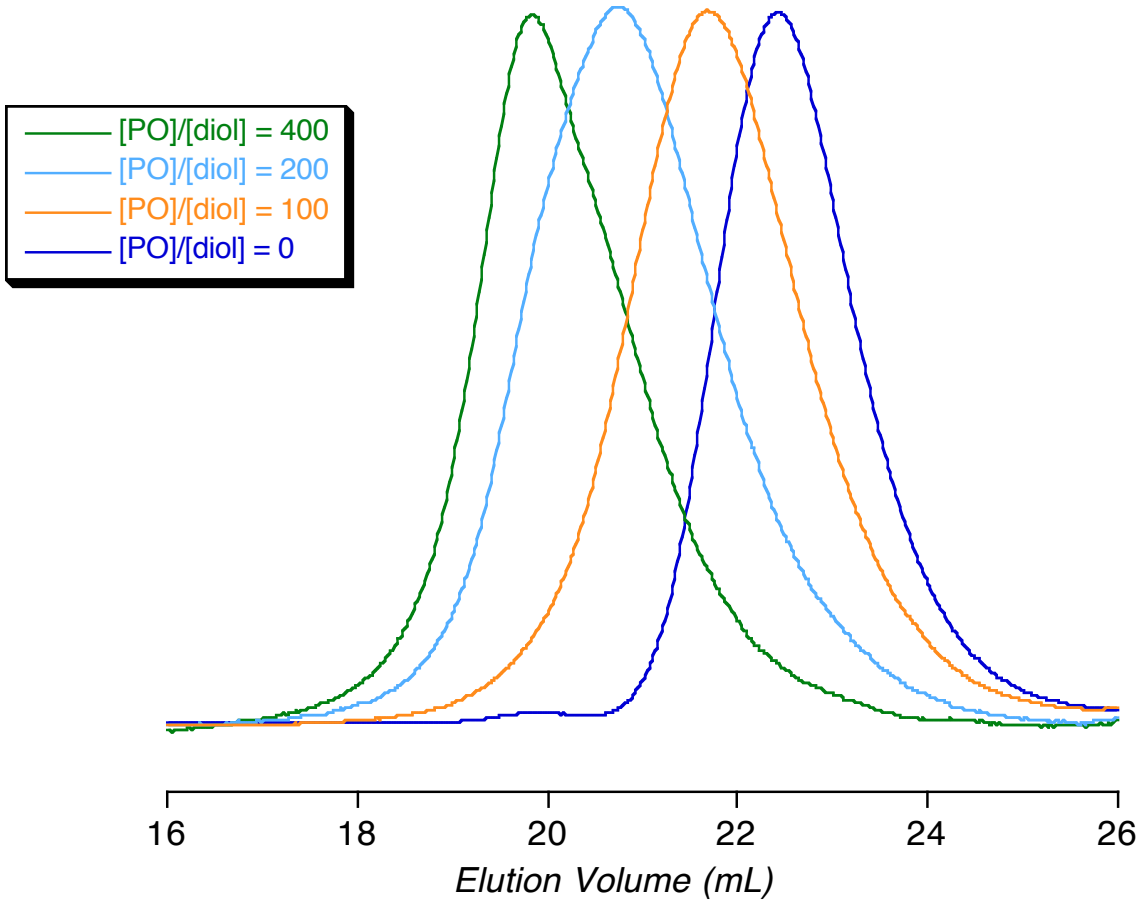

Figure 4.2. GPC chromatographs of poly(1-butene) diolate initiated PPO (Table 4.5).

To maximize the PPO content of our polymeric diols, small molecule diols with alkyl spacers were explored as CTAs. Addition of 1,8-octanediol,[18] or 1,6-hexanediol lowered MWs and did not impact conversion as shown in Table 4.6. All samples were highly isotactic with high *mm* values and melting points. PPO alcohol methine end groups could be seen by ^{1}H (δ = 3.91 ppm) and ^{13}C (δ = 65.60 ppm) NMR spectroscopy and integrated cleanly with the alkyl midsections, showing that aliphatic diols can be used with **4.1**/**4.2** to directly synthesize isotactic telechelic PPO diols from racemic PO.[18]

Table 4.6. Polymerization of *rac*-PO Using Catalyst System **4.1**/**4.2** and 1,6-Hexanediol[a]

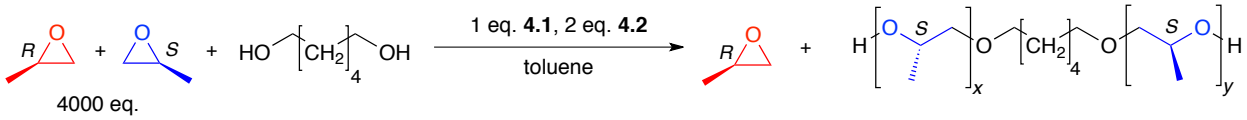

entry	CTA eq.	conv. (%)	M_n^{Theo} (kg/mol)	M_n^{NMR} (kg/mol)[b]	M_n^{GPC} (kg/mol)[c]	M_w/M_n[c]	[*mm*] (%)[d]	T_m (°C)[e]
1	0	49.5	120	-	231	2.9	96.4	66.2
2	10	52.4	12.4	17.6	39.0	1.9	95.8	67.6
3	20	54.3	6.4	9.5	22.5	1.9	95.8	66.3
4	40	50.3	3.0	3.7	11.9	2.0	96.7	64.6
5	80	45.6	1.4	2.2	6.1	1.8	97.6	60.6

[a] General conditions: [**4.1**]:[**4.2**]:[PO] = 1:2:4000, t = 1 h, T_{rxn} = 20 °C, [PO] = 2 M in toluene. [b] Determined by ^{1}H NMR spectroscopy. [c] Determined by gel-permeation chromatography calibrated with polystyrene standards in $CHCl_3$ at 40 °C. [d] Isotactic *mm* triad content determined by ^{13}C NMR spectroscopy. [e] Determined by differential scanning calorimetry. All entries from NB 10-233

4.3. Conclusions

The addition of alcohols to *rac*-PO polymerizations using system **4.1**/**4.2** allows the synthesis of isotactic PPO with controlled MWs and alcohol end groups. Studies with *rac*-**4.1**/**4.2** demonstrate that the catalyst can propagate from both enantiomers of chiral alcohols and the rate of propagation is higher than chain transfer allowing for the synthesis of iso-stereoblock PPO. All PPO samples synthesized were highly tactic and crystalline. PPO diols were synthesized via the deprotection of PMB terminated PPO and through the use of alkyl diols. We are currently exploring the use of isotactic PPO diols in polyurethane syntheses and other applications.

4.4. Experimental

4.4.1. General Considerations

All manipulations of air or water sensitive compounds were carried out under dry nitrogen using a Braun Labmaster drybox or standard Schlenk line techniques. NMR spectra were recorded on Varian INOVA 400 (^{1}H, 400 MHz), or Varian INOVA 600 (^{1}H, 600 MHz) spectrometers. ^{1}H NMR spectra were referenced with residual solvent shifts ($CHCl_3$ = 7.26 ppm). ^{13}C NMR spectra were referenced by solvent shifts ($CDCl_3$ = 77.16 ppm).

4.4.2. Materials

HPLC grade methylene chloride and toluene were purchased from Fisher Scientific and purified over solvent columns. Propylene oxide (PO) was purchased from Aldrich and dried over calcium hydride, degassed through several freeze-pump-thaw cycles, vacuum transferred and stored under nitrogen in a glovebox. Dimethoxyethane (DME) was distilled off of sodium metal after freeze-pump-thawing. (1*R*,2*R*)- and (1*S*,2*S*)- Diaminocyclohexane (99% *ee*) were purchased from Aldrich, and (*S*)- and (*R*)-1,1'-bi-2-naphthol was purchased from TCI. Complex **4.1**,[13] (*S*)- and (*R*)-3,3'-Diformyl-1,1'-bi-2-naphthol [28] and bis(triphenylphosphine)iminium pivalate ([PPN]OPiv, **4.2**)[14] were prepared according to literature procedures. Alcohols were purchased from Aldrich and dried over activated 3 Å molecular sieves. Poly(1-butene) diol (M_n = 3 kg/mol) was purchased from Nisso and dried under vacuum overnight. All other reagents were purchased from commercial sources and used as received.

4.4.3. Polymer Characterization and NMR Quantification of Polymer Tacticity, Enantiomeric Excess and *s*-factor

Number average molecular weights (M_n^{GPC}) and molecular weight distributions (M_w/M_n) were measured by gel-permeation chromatography (GPC) at 40 °C in chloroform using a Waters instrument, (M515 pump, 717+ Autosampler) equipped with a Waters UV486 and Waters 2410 differential refractive index detectors, and three 5 μm PSS SDV columns (Polymer Standards Service; 50 Å, 500 Å, and Linear M porosities) in series. The GPC columns were eluted with chloroform at 1 mL/min and were calibrated with monodisperse polystyrene standards. Number average molecular weights (M_n^{NMR}) were determined by ^{1}H NMR spectroscopy with a relaxation delay of 60 seconds using the relative integrations of the terminal methine (δ = 3.89) ppm compared to the polymeric methine (δ = 3.39 ppm). Polymer melting points (T_m) were measured by differential scanning calorimetry (DSC) using a Mettler Toledo Polymer DSC calorimeter equipped with an automated sampler. Analyses were performed in crimped aluminum pans under nitrogen and data were collected from the second heating run at a heating rate of 10 °C/min from -70 to 200 °C, and processed with StarE system software. Polymer tacticity[29] was characterized by ^{13}C NMR as previously reported.[13] End groups were previously reported or assigned by reference compounds.[15,29] Polymer enantiomeric excess was calculated using: $ee_{(p)} = (2[mm]+[mr]+[rm]-1)^{1/2}$, selectivity (*s*-factor) was calculated using: s = *s*-factor = $k_S/k_R = ln[1-c(1+ee_{(P)})]/ln[1-c(1-ee_{(P)})]$ where c is conversion.[13] Polymer masses and subsequent conversions were corrected by removing the mass of catalyst and CTA.

4.4.4. MALDI-TOF-MS Analysis

MALDI-MS analysis was performed on a MALDI micro MX. The polymer samples were dissolved in THF at a concentration 1 mg/mL. The cationization agent used was potassium trifluoroacetate (Aldrich, >99%) dissolved in THF at a concentration of 1 mg/mL. The matrix used was dithranol (1,8-Dihydroxy-9(10H)-anthracenone, Aldrich 98.5%) dissolved in THF at a concentration of 25 mg/mL. Solutions of matrix, salt and polymer were mixed in a volume ratio of 5:1:1, respectively. The mixed solution was hand spotted on a stainless steel MALDI target and left to dry. The spectra were recorded in positive ion reflectron mode.

4.4.5. Polymerization Procedures and Additional Tables

Representative Polymerization: Synthesis of iPrO-PPO. In a drybox under nitrogen atmosphere, **4.1** (4.0 mg, 3.5 μmol), cocatalyst and [PPN]OPiv (**4.2**, 4.5 mg, 7.0 μmol) were added to a reactor vial containing a stir bar and 6 mL toluene. The vial was sealed and removed from the glove box. Using Schlenck line techniques 140 μL of 1 M isopropanol in toluene was added. PO (0.846 g, 14.3 mmol) was then added via syringe with rapid stirring. After 1 hour all volatiles were quickly removed under vacuum. The product was dried overnight. Conversion was determined gravimetrically (0.417 g, 49.2%). A concentrated sample of polymer (50 mg in 0.7 mL of $CDCl_3$) was analyzed using ^{13}C NMR spectroscopy to determine polymer tacticity. ^{1}H NMR ($CDCl_3$, 600 MHz): δ 3.91 (m, 1H), 3.56-3.49 (m, 106H), 3.39 (m, 53H), 1.11 (d, J = 5.5 Hz, 159H). $^{13}C\{^{1}H\}$ NMR ($CDCl_3$, 150 MHz): δ 75.64, 73.61, 65.60, 22.25, 22.10, 17.64. M_n^{GPC} = 6.0 kg/mol, M_w/M_n = 1.8.

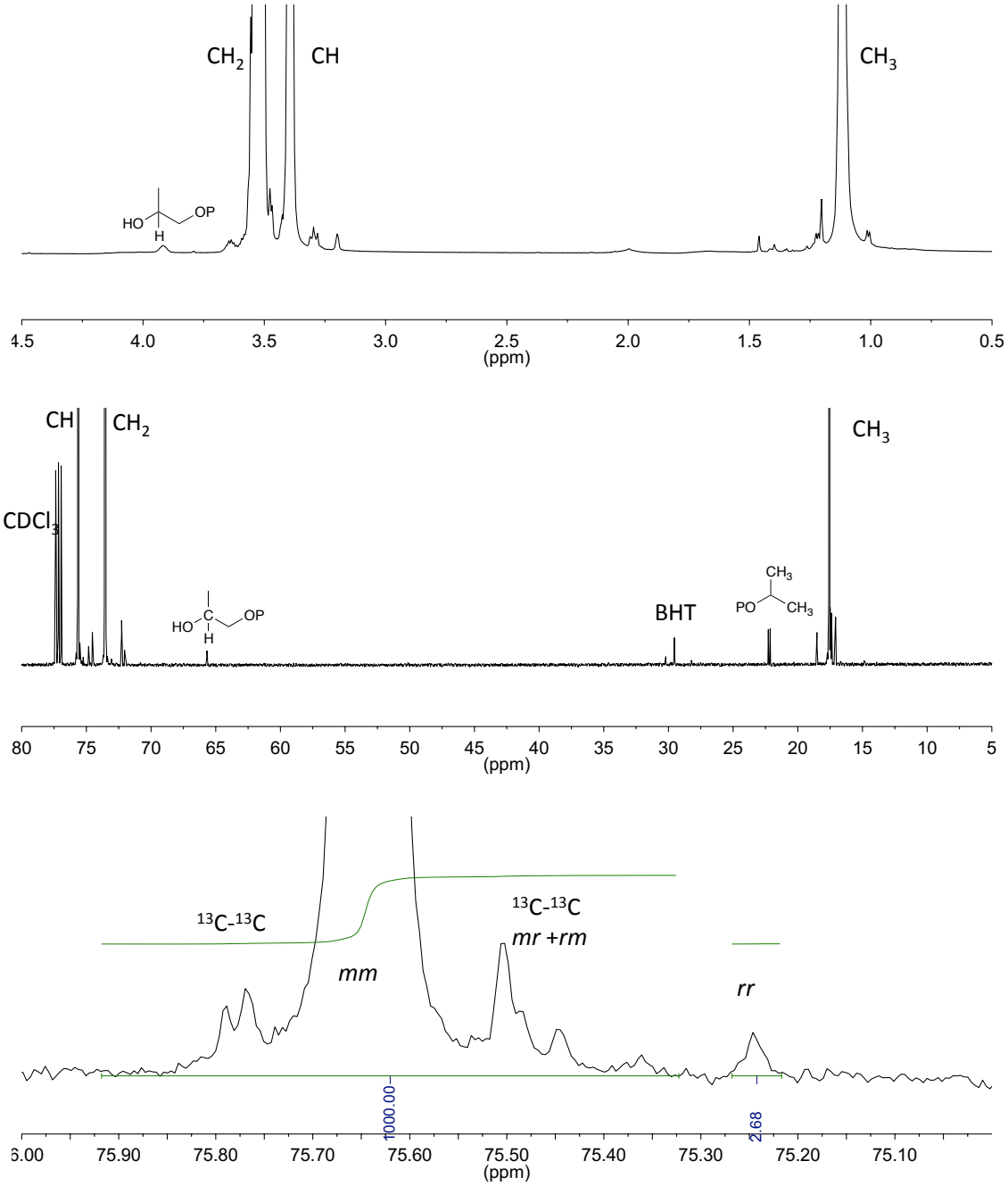

Figure 4.3. Isopropoxide initiated PPO (Table 4.1, entry 5) Top: ^{1}H NMR spectrum in $CDCl_3$. Center: ^{13}C NMR spectrum in $CDCl_3$. Bottom: Expansion of methine region showing predominantly site-control errors.

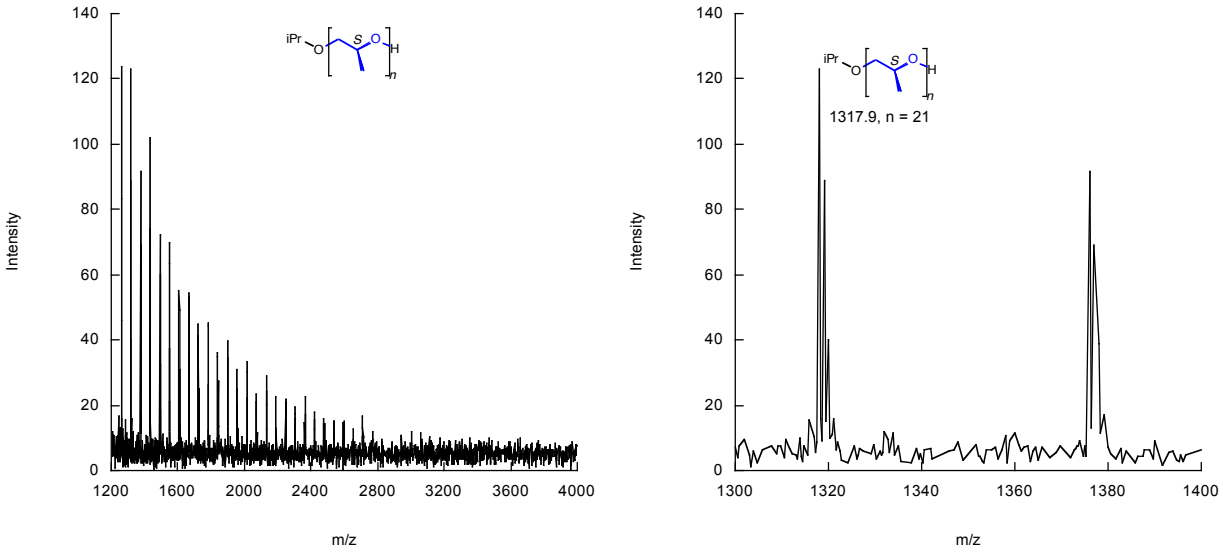

Figure 4.4. MALDI-MS of isopropoxide initiated PPO (Table 4.1, entry 5).

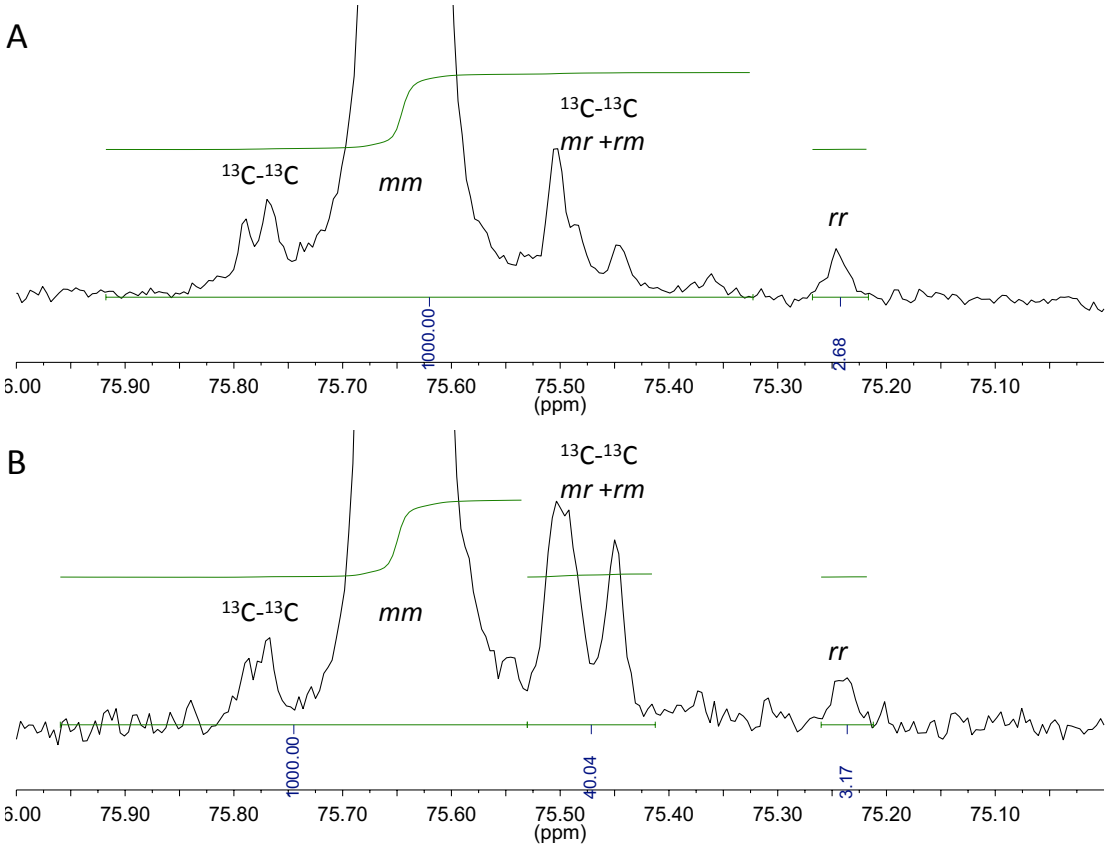

Figure 4.5. NMR spectra of isopropoxide initiated PPO in $CDCl_3$. A: Expansion of methine region showing predominantly site-control errors (Table 4.1, entry 5). B: Expansion of methine region showing predominantly chain-end errors (Table 4.3, entry 4).

Synthesis of 1-methoxy-2-propanol-PPO. The standard procedure was followed, but added 280 μL of 1 M (*S*)-1-methoxy-2-propanol in DME as CTA. Volatiles were quickly removed after 1 hour, and conversion was determined gravimetrically (0.435 g, 51.8%). ^{1}H NMR ($CDCl_3$, 600 MHz): δ 3.91 (m, 1H), 3.56-3.49 (m, 50H), 3.39 (m, 25H), 3.34 (s, 3H), 1.11 (d, J = 5.5 Hz, 75H). ^{13}C{^{1}H} NMR ($CDCl_3$, 150 MHz): δ 75.64, 75.11, 67.40, 65.60, 59.27, 17.64. M_n^{GPC} = 3.3 kg/mol, M_w/M_n = 1.2.

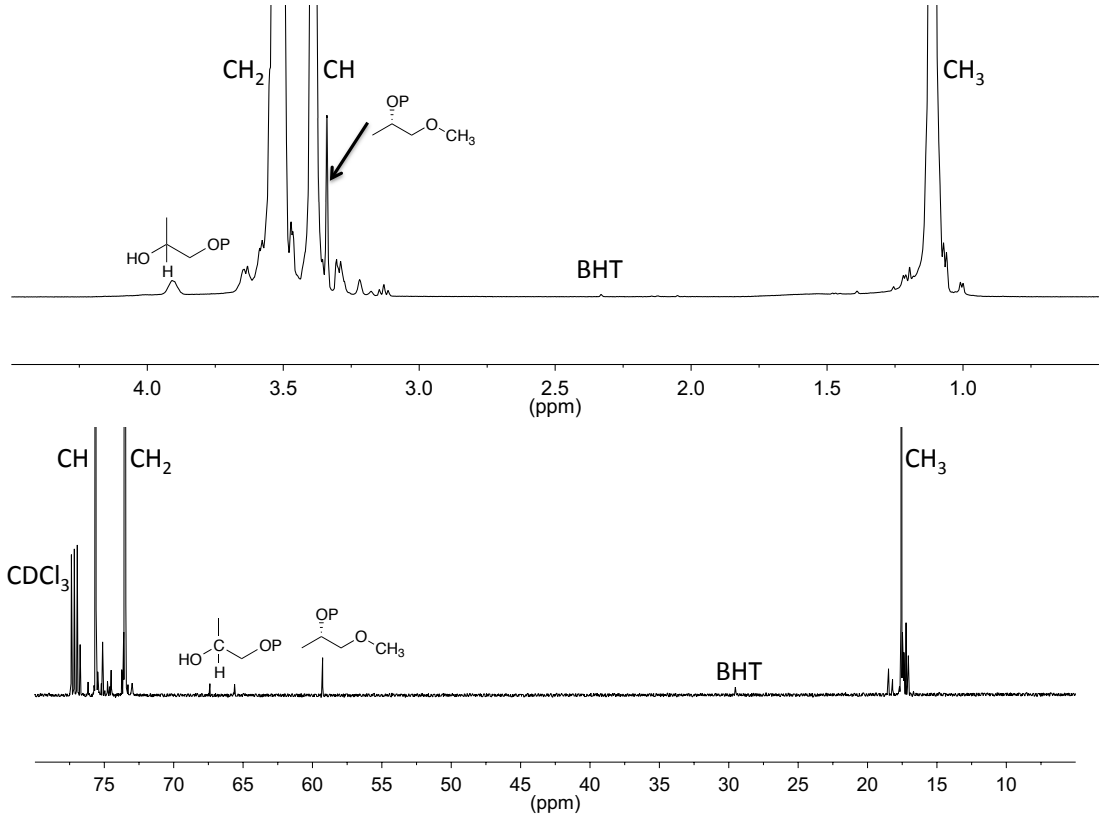

Figure 4.6. NMR spectra of (*S*)-1-methoxy-2-propoxide initiated PPO (Table 4.2, entry 1) in $CDCl_3$. Top: ^{1}H NMR spectrum. Bottom: ^{13}C NMR spectrum.

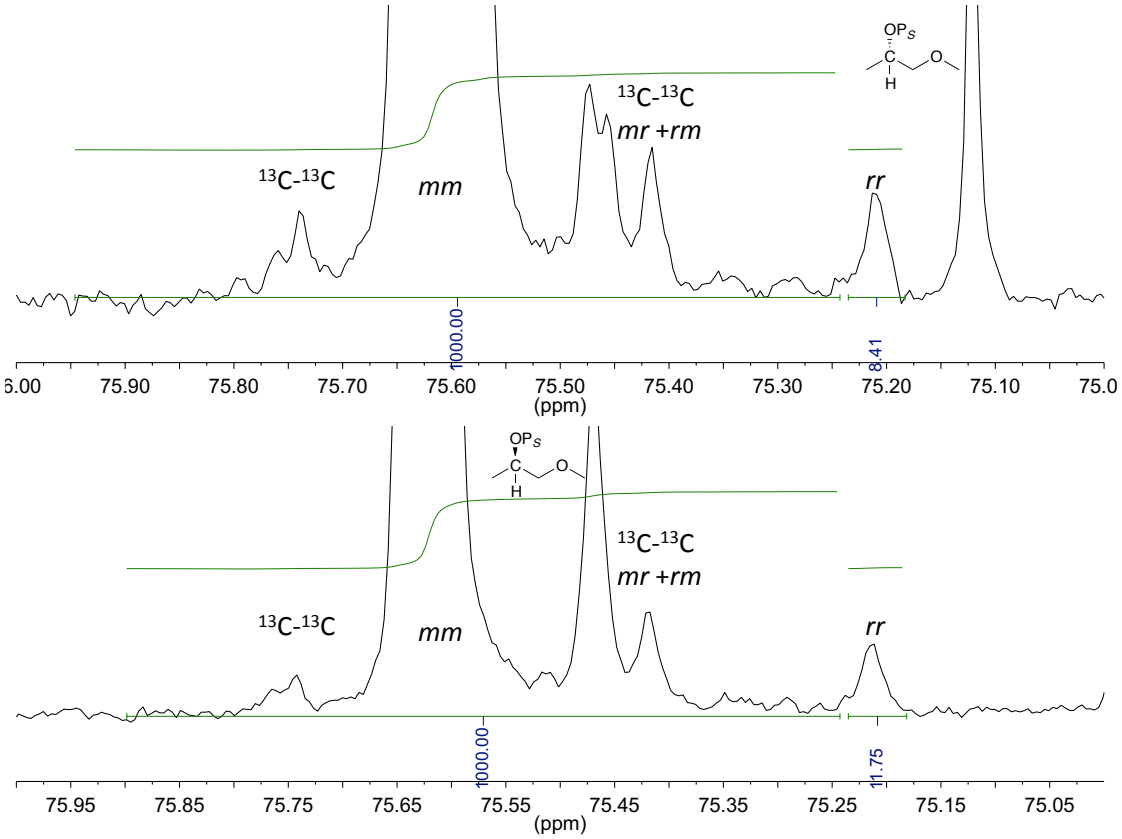

Figure 4.7. ^{13}C NMR spectra of 1-methoxy-2-propoxide initiated PPO in $CDCl_3$ Top: Expansion of methine region (Table 4.2, entry 1). Bottom: Expansion of methine region (Table 4.2, entry 2).

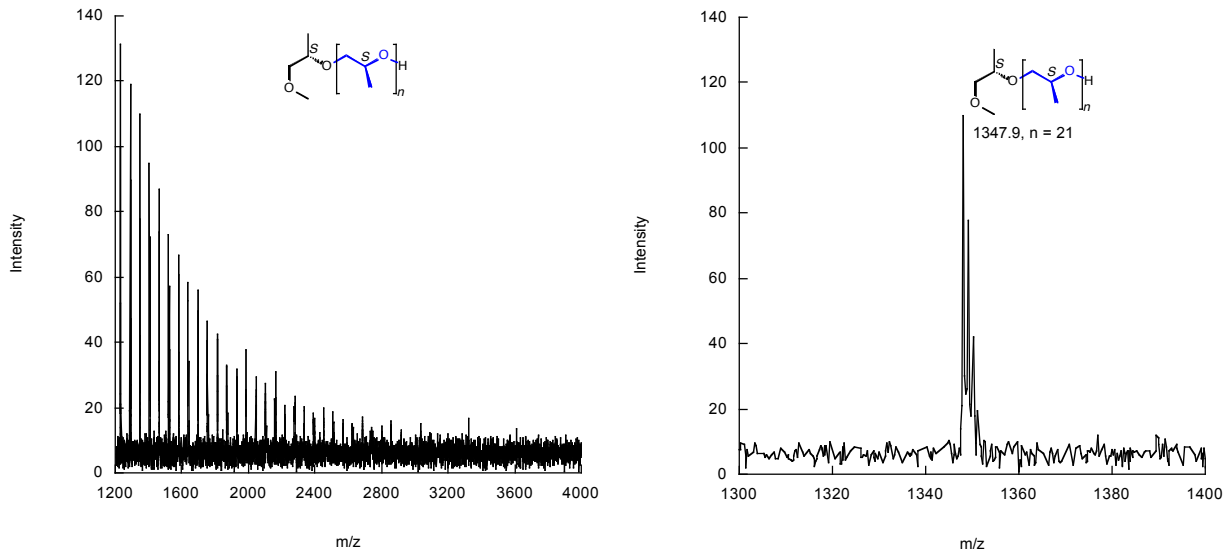

Figure 4.8. MALDI-MS of (*S*)-1-methoxy-2-propoxide initiated PPO (Table 4.2, entry 1).

Synthesis of PMB-PPO. The standard procedure was followed, but used 280 μL of 1 M 4-methoxybenzyl alcohol in dimethoxyethane (DME) as CTA. After 1 hour all volatiles were quickly removed under vacuum. Conversion was determined gravimetrically (0.465 g, 54.9%). ^{1}H NMR ($CDCl_3$, 600 MHz): δ 7.24 (d, J = 8.2 Hz, 2H), 6.85 (d, J = 8.2 Hz, 2H), 4.49 - 4.43 (m, 2H), 3.91 (m, 1H), 3.78 (s, 3H), 3.56-3.49 (m, 66H), 3.39 (m, 33H), 1.11 (d, J = 5.5 Hz, 99H). ^{13}C{^{1}H} NMR ($CDCl_3$, 150 MHz): δ 159.21, 130.59, 129.28, 113.81, 75.64, 73.61, 67.40, 65.60, 55.36, 17.64. M_n^{GPC} = 5.4 kg/mol, M_w/M_n = 1.7.

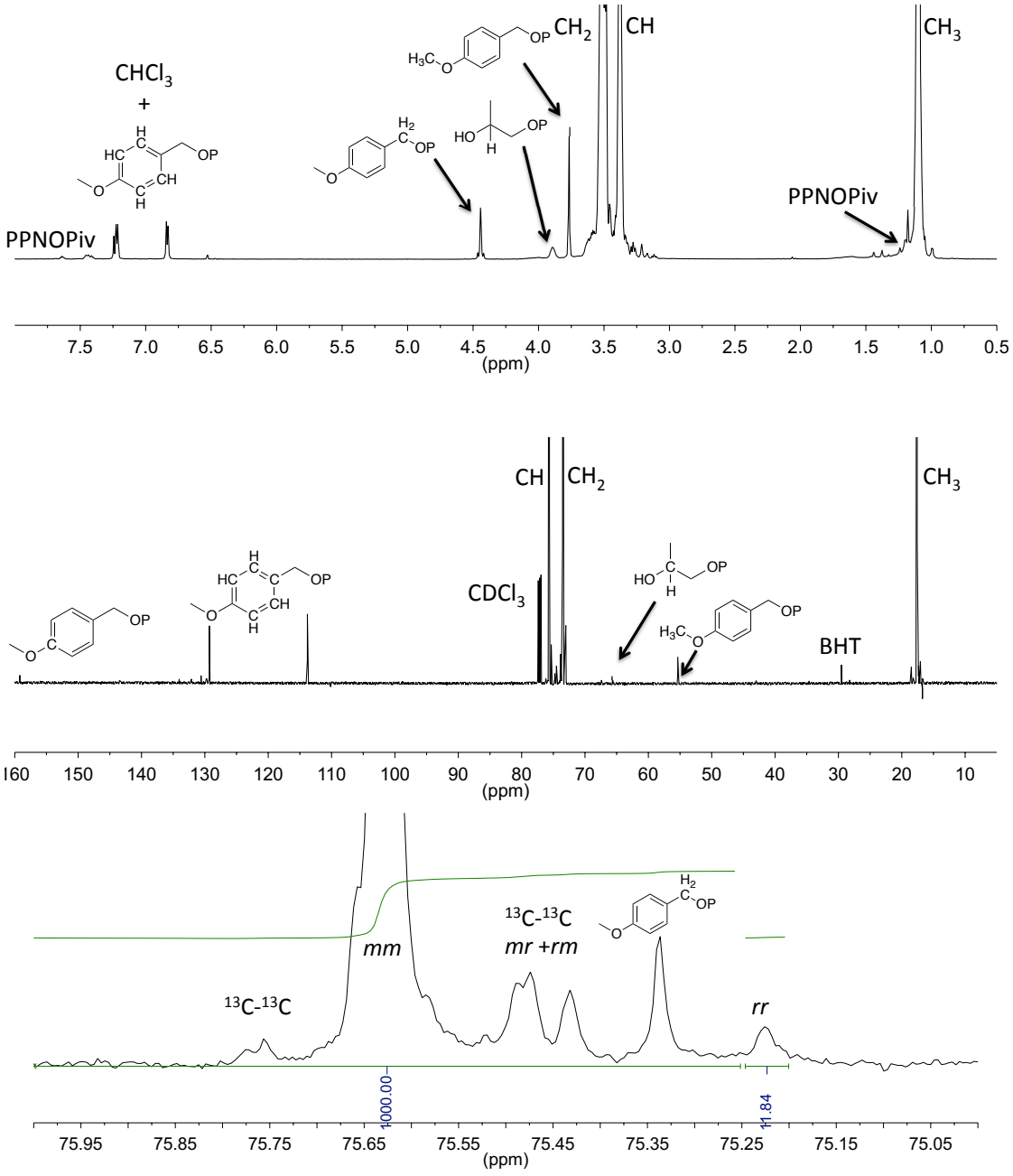

Figure 4.9. NMR spectra of PMB initiated PPO (Table 4.4, entry 4 before deprotection) in $CDCl_3$. Top: ^{1}H NMR spectrum. Center: ^{13}C NMR spectrum. Bottom: Expansion of methine region.

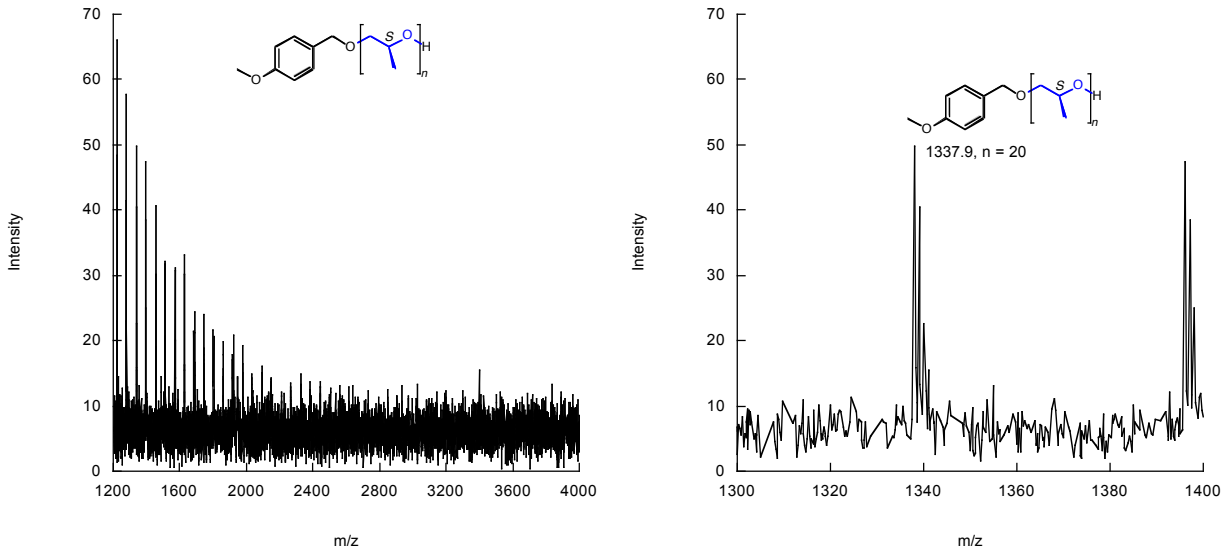

Figure 4.10. MALDI-MS of PMB initiated PPO (Table 4.4, entry 4).

PPO-b-poly(1-butene)-b-PPO. The standard procedure was followed, but 416 mg poly(1-butene) diol (M_n = 3 kg/mol) was dissolved in 6 mL toluene and used as solvent. After 1 hour all volatiles were quickly removed under vacuum, and conversion was determined gravimetrically (269 mg, 32.4%). ^{1}H NMR ($CDCl_3$, 600 MHz): δ 3.91 (m, 2H), 3.56 - 3.49 (m, 66H), 3.39 (m, 33H), 1.43-0.91 (m, 185H), 1.11 (d, J = 5.5 Hz, 99H), 0.88-0.77 (m, 111H). ^{13}C{^{1}H} NMR ($CDCl_3$, 150 MHz): δ 75.70, 73.61, 65.60, 39.41-38.40, 36.19, 33.97-33.29, 30.81-29.58, 27.00-25.78, 10.99-10.10, 17.64. M_n^{GPC} = 7.1 kg/mol, M_w/M_n = 1.5.

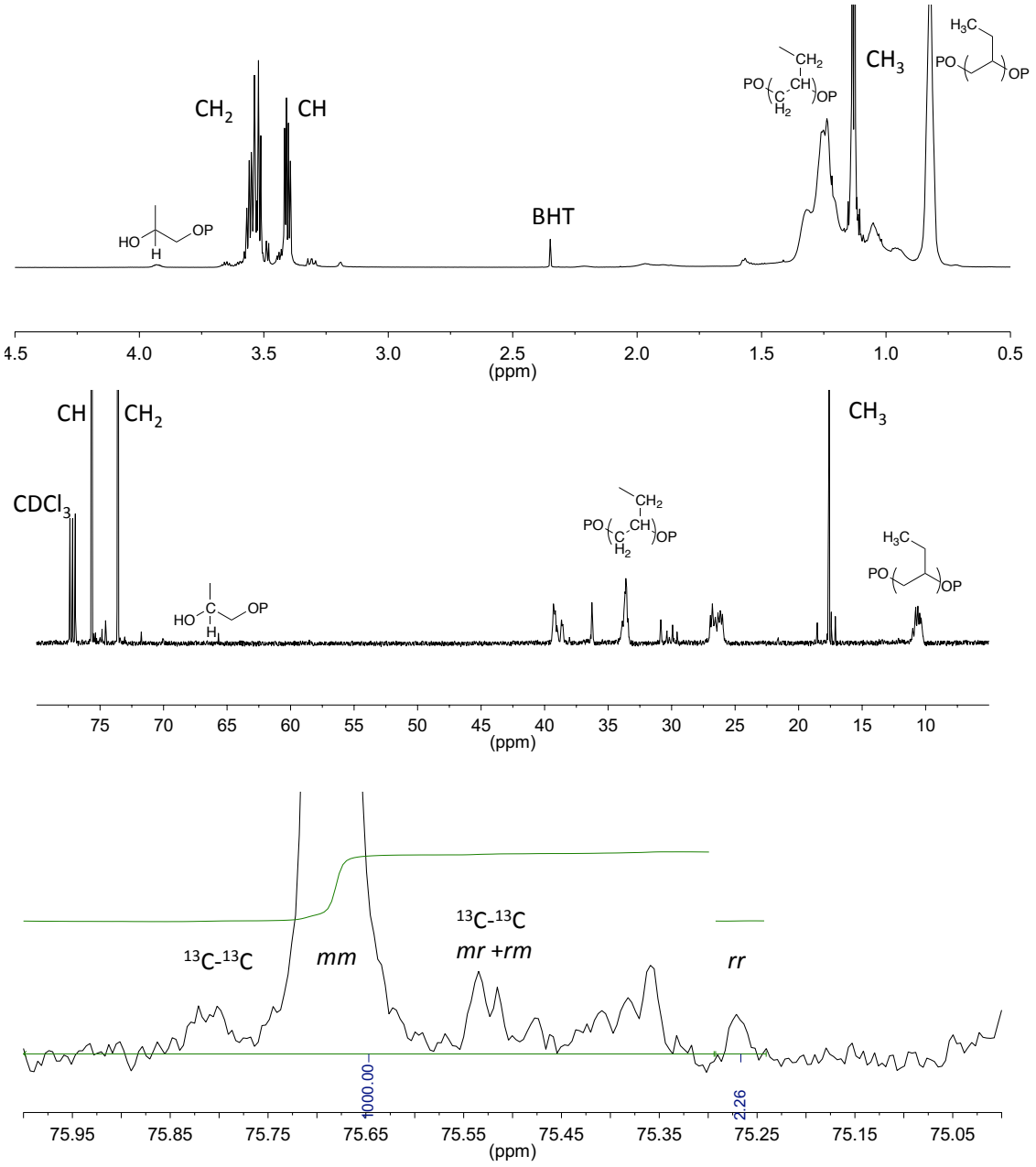

Figure 4.11. Poly(1-butene) diolate initiated PPO. (Table 4.5, entry 4) in $CDCl_3$. Top: ^{1}H NMR spectrum. Center: ^{13}C NMR spectrum. Bottom: Expansion of methine region.

PPO-1,8-octane diol-PPO. The standard procedure was followed, but added 560 μL of 0.5 M 1,8-octane diol in DME as CTA. After 1 hour all volatiles were quickly removed under vacuum,

conversion was determined gravimetrically (426 mg, 50.2%). ^{1}H NMR ($CDCl_3$, 600 MHz): δ 3.91 (m, 1H), 3.56-3.49 (m, 30H), 3.39 (m, 15H), 1.57-1.50 (m, 2H), 1.32-1.25 (m, 4H), 1.11 (d, J = 5.5 Hz, 45H). ^{13}C{^{1}H} NMR ($CDCl_3$, 150 MHz): δ 75.64, 75.30, 73.61, 67.40, 65.60, 29.56, 26.20, 17.64. M_n^{GPC} = 3.6 kg/mol, M_w/M_n = 1.5.

Table 4.7. Polymerization of *rac*-PO Using Catalyst System **4.1**/**4.2** and 1,8-Octanediol[a]

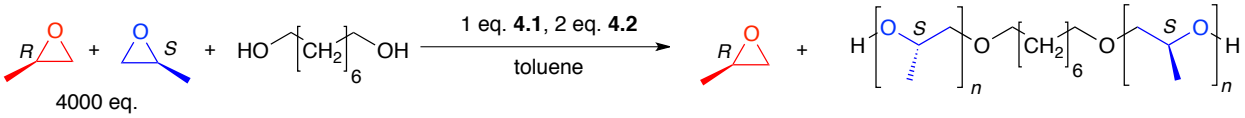

entry	CTA eq.	conv. (%)	M_n^{Theo} (kg/mol)	M_n^{NMR} (kg/mol)[b]	M_n^{GPC} (kg/mol)[c]	M_w/M_n[c]	[*mm*] (%)[d]	T_m (°C)[e]
1	0	49.5	120	-	231	2.9	96.4	66.2
2	10	54.3	12.9	12.2	33.2	2.0	95.2	70.0
3	20	55.9	6.6	8.1	15.5	2.3	95.7	70.7
4	40	55.4	3.3	4.0	8.5	2.1	96.6	68.2
5	80	50.2	1.5	1.8	3.6	1.5	97.5	58.4

[a] General conditions: [**4.1**]:[**4.2**]:[PO] = 1:2:4000, t = 1 h, T_{rxn} = 20 °C, [PO] = 2 M in toluene. [b] Determined by ^{1}H NMR spectroscopy. [c] Determined by gel-permeation chromatography calibrated with polystyrene standards in $CHCl_3$ at 40 °C. [d] Isotactic *mm* triad content determined by ^{13}C NMR spectroscopy. [e] Determined by differential scanning calorimetry. All entries from NB 10-235

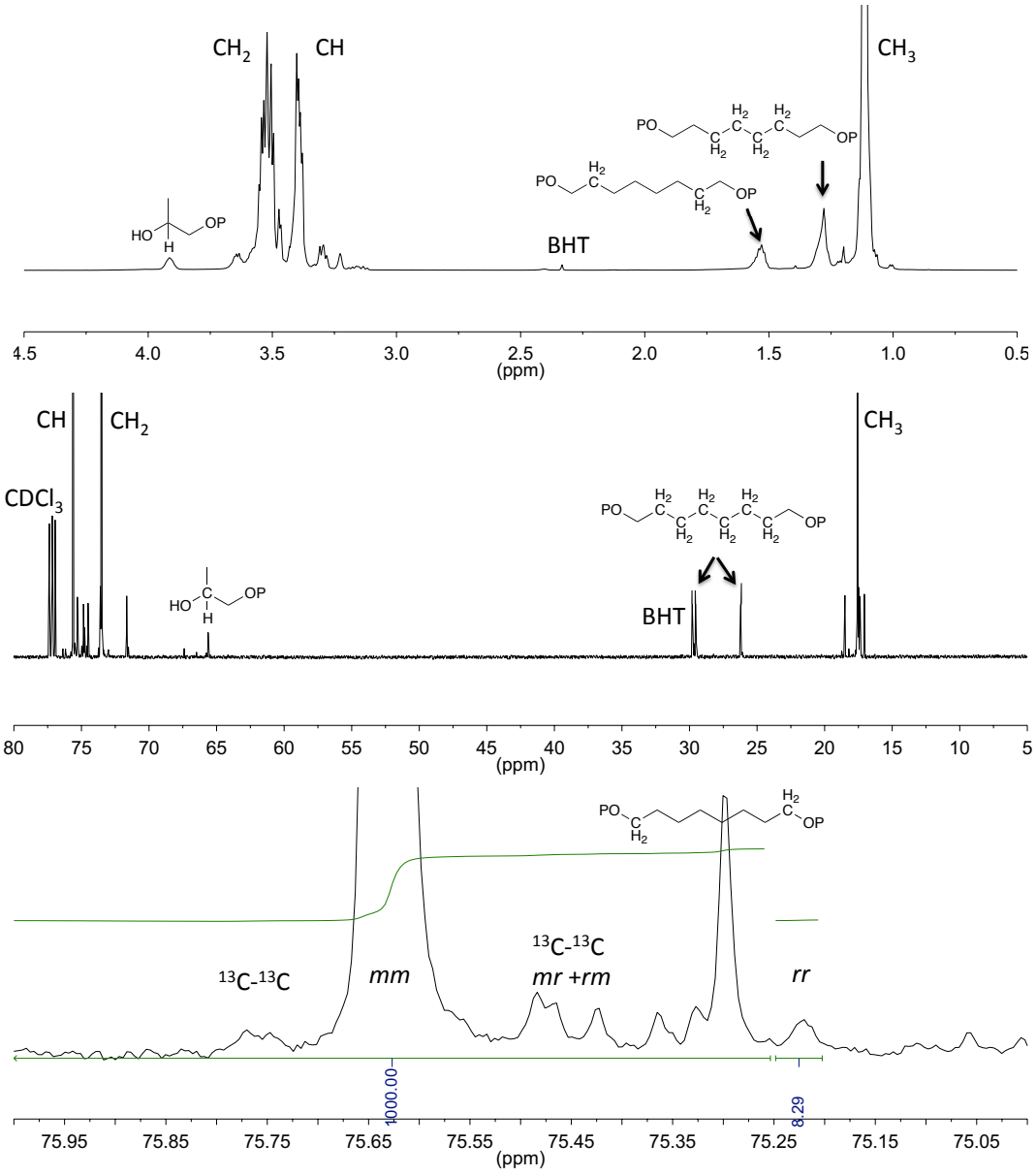

Figure 4.12. NMR spectra of 1,8-octanediolate initiated PPO (Table 4.7, entry 5) in $CDCl_3$. Top: ^{1}H NMR spectrum. Center: ^{13}C NMR spectrum. Bottom: Expansion of methine region.

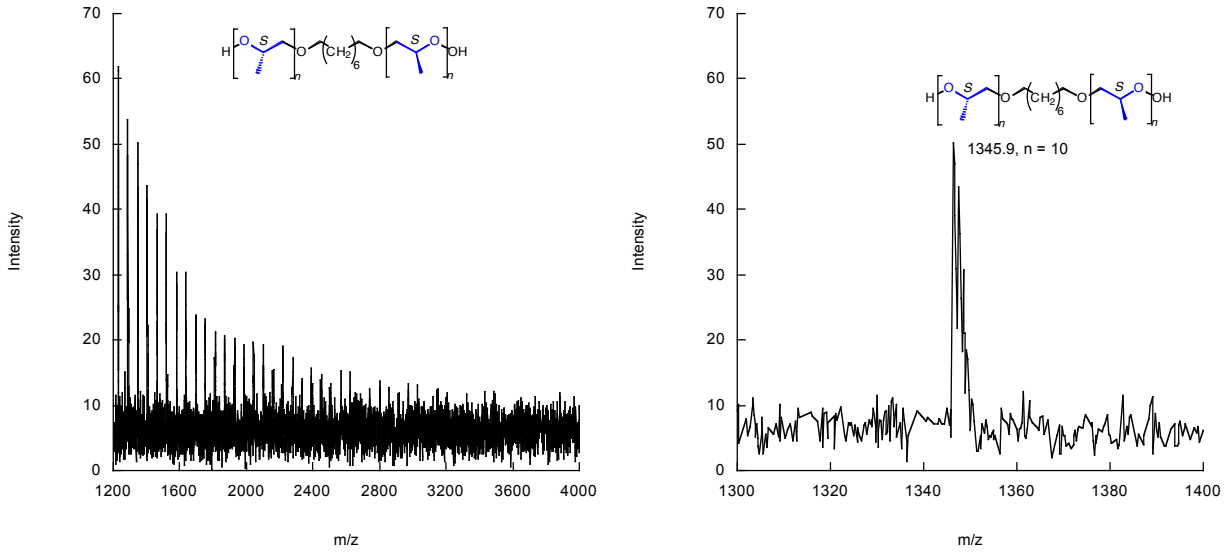

Figure 4.13. MALDI-MS of 1,8-octanediolate initiated PPO (Table 4.7, entry 5).

PPO-1,6-hexane diol-PPO. The standard procedure was followed, but 280 μL of 1 M 1,6-hexane diol in DME was added as CTA. After 1 hour all volatiles were quickly removed under vacuum, and conversion was determined gravimetrically (383 mg, 45.6%). ^{1}H NMR ($CDCl_3$, 600 MHz): δ 3.91 (m, 1H), 3.56-3.49 (m, 38H), 3.39 (m, 19H), 1.60-1.50 (m, 2H), 1.37-1.30 (m, 2H), 1.11 (d, J = 5.5 Hz, 57H). ^{13}C{^{1}H} NMR ($CDCl_3$, 150 MHz): δ 75.64, 75.29, 73.61, 67.40, 65.60, 29.50, 26.09, 17.64. M_n^{GPC} = 6.1 kg/mol, M_w/M_n = 1.8.

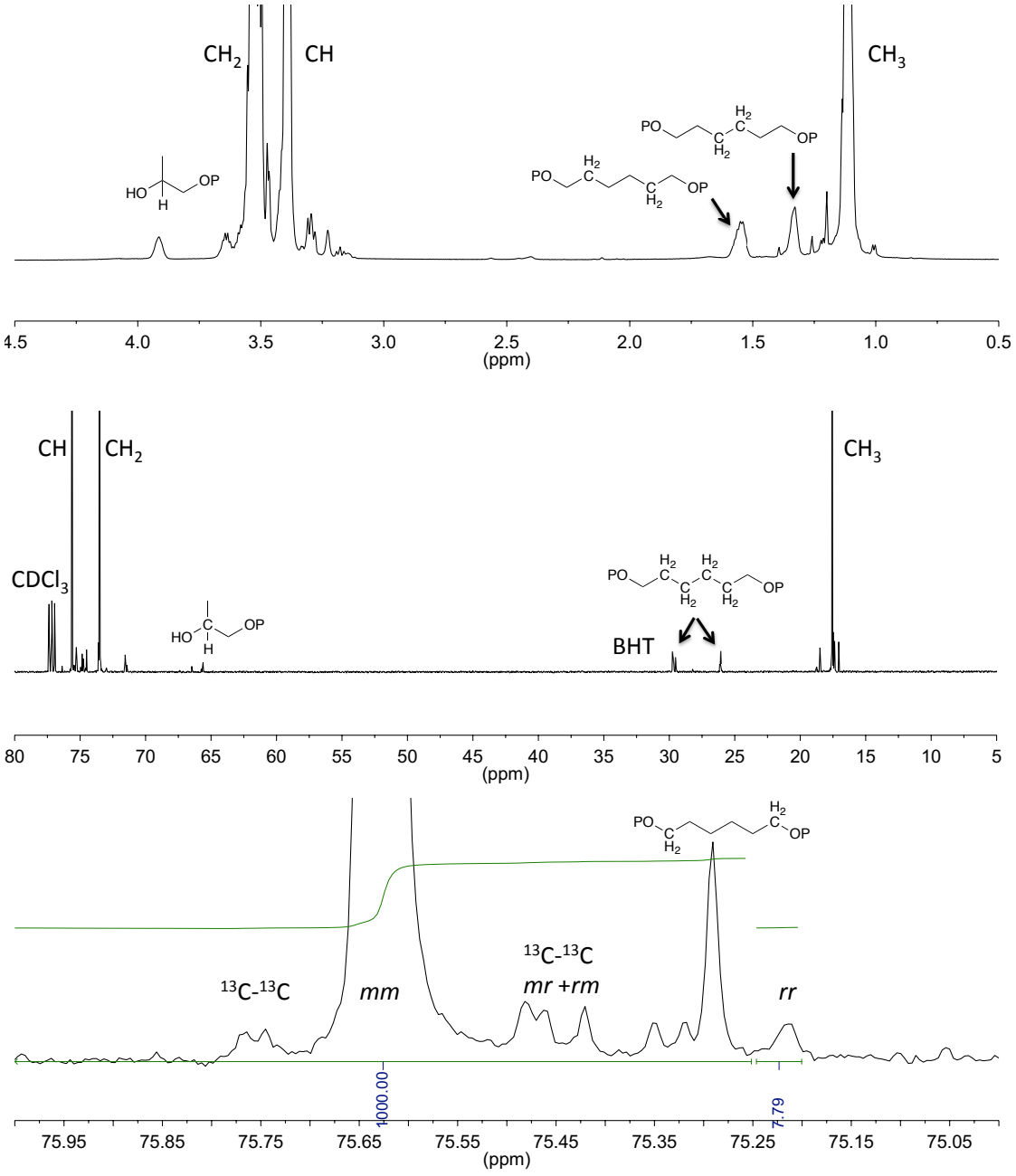

Figure 4.14. NMR spectra of 1,6-hexanediolate initiated PPO (Table 4.6, entry 5) in $CDCl_3$. Top: ^{1}H NMR spectrum. Center: ^{13}C NMR spectrum. Bottom: Expansion of methine region.

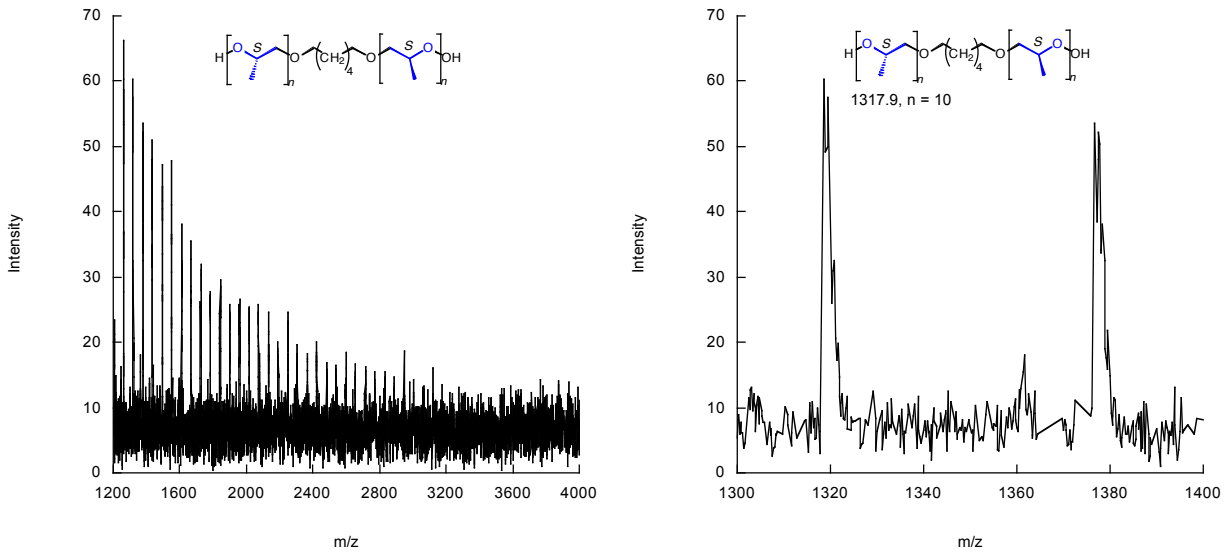

Figure 4.15. MALDI-MS of 1,6-hexanediolate initiated PPO (Table 4.6, entry 5).

Oxidative Synthesis of PPO Diol. PMB-PPO (415 mg) was dissolved in methylene chloride (10 mL). To this solution was added 1 mL water and 126 mg DDQ. Vial was sealed and stirred rapidly at 20 °C for 16 hours then extracted with 2x10 mL water and concentrated on vacuum line. The crude solid was crystallized from 5 mL hot acetone with cooling at -78 °C, and rinsed with 2x5 mL -78 °C acetone. Product isolated by filtration as white solid. Yield: 376 mg, 80.8%. ^{1}H NMR ($CDCl_3$, 600 MHz): δ 3.91 (m, 1H), 3.56-3.49 (m, 66H), 3.39 (m, 33H), 1.11 (d, J = 5.5 Hz, 99H). $^{13}C\{^{1}H\}$ NMR ($CDCl_3$, 150 MHz): δ 75.64, 73.61, 67.40, 65.60, 17.64. M_n^{GPC} = 5.9 kg/mol, M_w/M_n = 2.0.

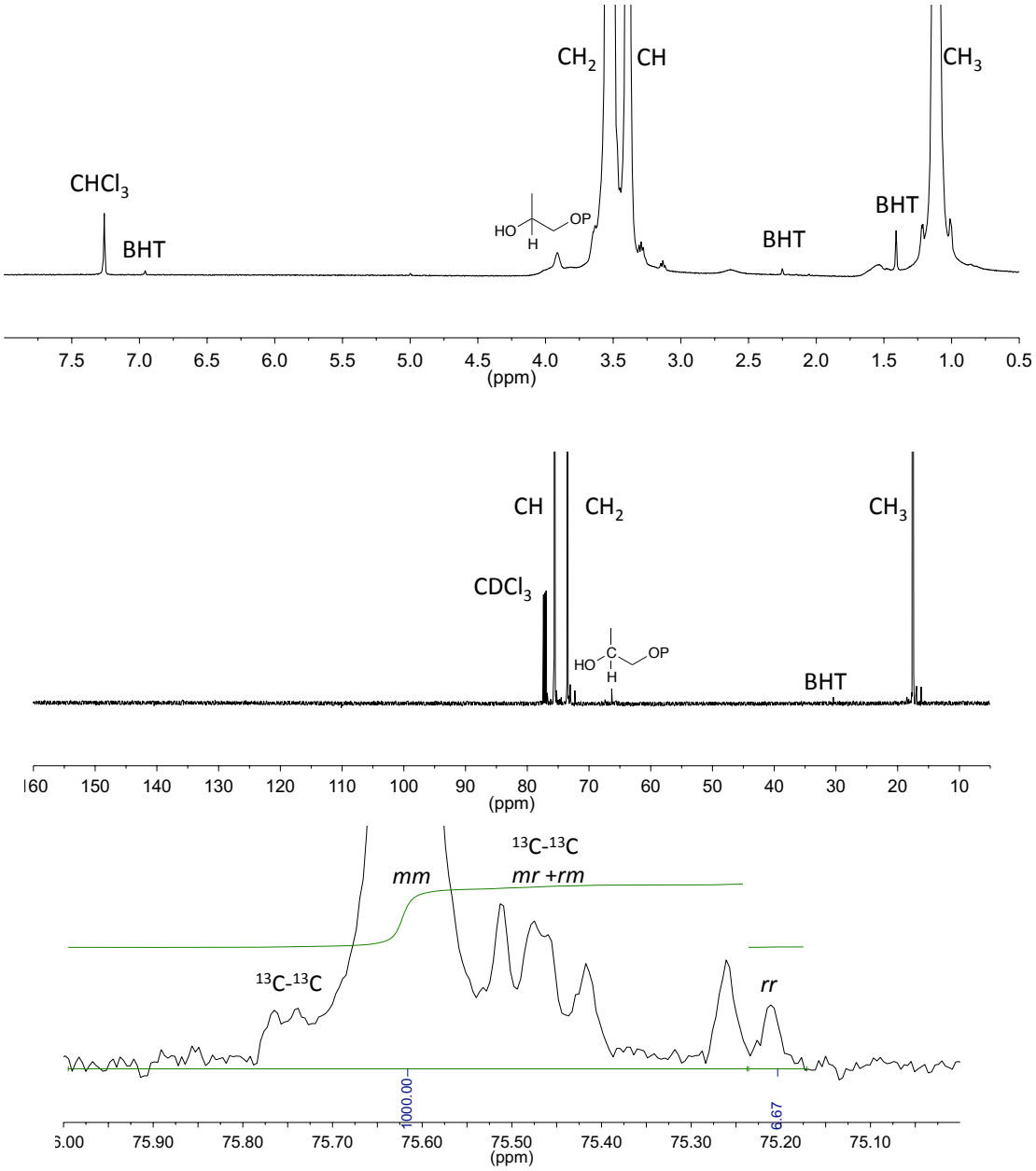

Figure 4.16. NMR spectra of PPO diol (Table 4.4, entry 4 after deprotection) in $CDCl_3$. Top: ^{1}H NMR spectrum. Center: ^{13}C NMR spectrum. Bottom: Expansion of methine region.

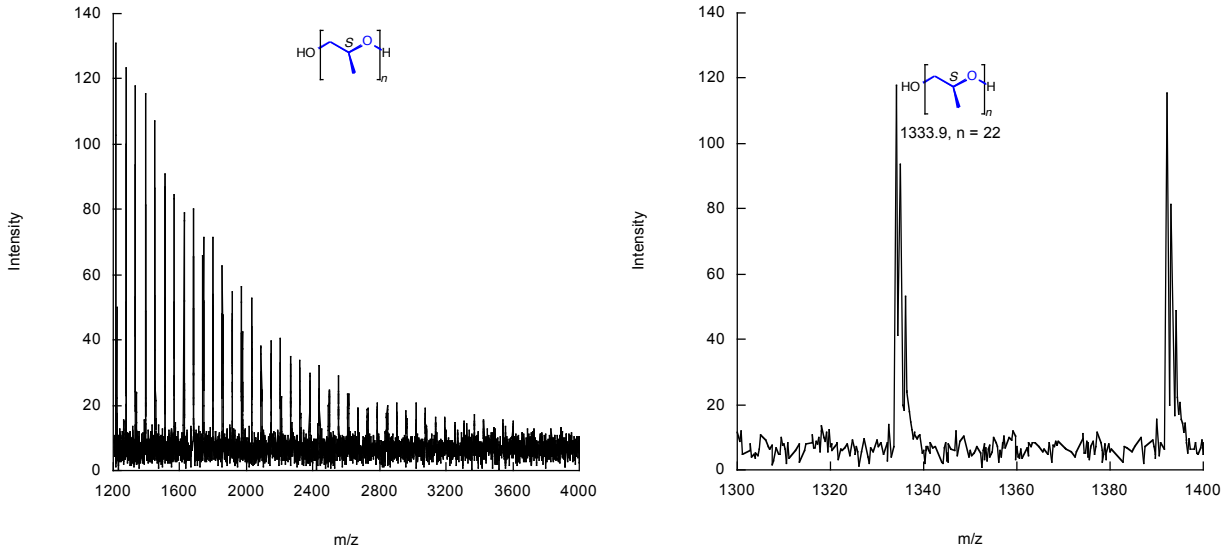

Figure 4.17. MALDI-MS of PPO diol (Table 4.4, entry 4 after deprotection).

4.5. Notes and References

(1) Amin, S. B.; Marks, T. J. *Angew. Chem., Int. Ed.* **2008**, *47,* 2006-2025.

(2) a) Tong, R.; Cheng, J. *Angew. Chem., Int. Ed.* **2008**, *47*, 4830-4834. b) Tong, R.; Cheng, J. *J. Am. Chem. Soc.* **2009**, *141*, 4744-4754.

(3) Nie, Z.; Kumacheva, E. *Nat. Mater.* **2008**, *7*, 277-290.

(4) Yang, S. K.; Ambade, A. V.; Weck, M. *J. Am. Chem. Soc.* **2010**, *132*, 1637-1645.

(5) *The Polyurethanes Book*; Randall, D.; Lee, S., Eds.; Wiley, 2002.

(6) Szycher, M. *Szycher's Handbook of Polyurethanes* CRC Press: Boca Raton, 1999; Chapter 2.

(7) Rexin, O.; Mülhaupt, R. *J. Polym. Sci., Part A: Polym. Chem.* **2002**, *40*, 864-873.

(8) (a) Raynaud, J.; Absalon, C.; Gnanou, Y.; Taton, D. *J. Am. Chem. Soc.* **2009**, *131*, 3201-3209. (b) Gervais,M.; Labbé, A.; Carlotti, S.; Deffieux, A. *Macromolecules* **2009**, *42*, 2395-2400. (c) Labbé, A.; Carlotti, S.; Billouard, C.; Desbois, P.; Deffieux, A. *Macromolecules* **2007**, *40*, 7842-7847. (d) Allgaier, J.; Willbold, S.; Chang, T. *Macromolecules* **2007**, *40*, 518-525. (e) Braune, W.; Okuda, J. *Angew. Chem., Int. Ed.* **2003**, *42*, 64-68. (f) Chakraborty, D.; Rodriguez, A.; Chen, E. Y.-X. *Macromolecules* **2003**, *36*, 470-5481.

(9) Ajiro, H.; Allen, S. D.; Coates, G. W. Discrete Catalysts for Stereoselective Epoxide Polymerization in *Stereoselective Polymerization with Single Site Catalysts*, Baugh, L. S.; Canich, J. M. Eds. CRC Press, Boca Raton, 2008, Chapter 24, pp 627–644.

(10) (a) Schütz, C.; Dwars, T.; Schnorpfeil, C.; Radnik, J.; Menzel, M.; Kragl, U. *J. Polym. Sci., Part A: Polym. Chem.* **2007**, *45*, 3032-3041. (b) Laycock, D. E.; Newman, R.A. *Stud. Surf. Sci. Catal.* **1992**, *73*, 269-277.

(11) Polyurethanes synthesized from partially isotactic PPO can display superior adhesive properties compared to their atactic analogues, see: Reegan, S. L. *J. Appl. Polym. Sci.* **1966**, *10*, 1247-1259.

(12) Król, P. *Prog. Mater. Sci.* **2007**, *52*. 915-1015.

(13) (a) Hirahata, W.; Thomas, R. M.; Lobkovsky, E. B.; Coates, G. W. *J. Am. Chem. Soc.* **2008**, *130*, 17658. (b) Thomas, R. M.; Widger, P. C. B.; Ahmed, S. M.; Jeske, R. C.; Hirahata, W.; Lobkovsky, E. B.; Coates, G. W. *J. Am. Chem. Soc.* **2010**, *132*, 16520.

(14) Widger, P. C. B.; Ahmed, S. M.; Hirahata, W.; Thomas, R. M.; Lobkovsky, E. B.; Coates, G. W. *Chem. Commun.* **2010**, *46*, 2935-2937.

(15) (a) Asano, S.; Aida, T.; Inoue, S. *J. Chem. Soc., Chem. Commun.* **1985**, 1148-1149. (b) Aida, T.; Maekawa, Y.; Asano, S.; Inoue, S. *Macromolecules* **1988**, 2*1*, 1195-1202. (c) Akatsuka, M.; Aida, T.; Inoue, S. *Macromolecules* **1994**, *27*, 2820-2825.

(16) (a) Wegener, G.; Brandt, M.; Duda, L.; Hofmann, J.; Klesczewski, B.; Koch, D.; Kumpf, R.; Orzesek, H.; Pirkl, H.; Six, C.; Steinlein, C.; Weisbeck, M. *Appl. Catal. A: Gen.* **2001**, *221*, 303-335. (b) Kim, I.; Ahn, J.-T.; Ha, C. S.; Yang, C. S.; Park, I. *Polymer* **2003**, *44*, 3417-3428.

(17) (a) Jacobsen, E. N. *Acc. Chem. Res.* **2000**, *33*, 421–431. (b) Cyriac, A.; Lee, S. H.; Varghese, J. K.; Park, E. S.; Park, J. H.; Lee, B. Y. *Macromolecules* **2010**, *43*, 7398–7401. (c) Allen, S. D.; Coates, G. W.; Cherian, A. E.; Simoneau, C. A.; Gridnev, A. A.; Farmer, J. J. PCT Int. Appl. WO 2010028362 (2010) to Novomer Inc.

(18) See Experimental section for details.

(19) Number average MWs (M_n^{NMR})s were determined by ^{1}H NMR spectroscopy using the relative integrations of the terminal methine (δ = 3.89 ppm) compared to the polymeric methine (δ = 3.39 ppm).

(20) No terminal chlorides were detected by 13C NMR spectroscopy (47.3 ppm), see: ref 15C.

(21) The relatively broad M_w/M_ns of these samples and the low MW bias of MALDI-MS makes attaining signal for higher MW polymers difficult. The mass distributions of

polymers that were detected by MALDI-MS did correspond to potassium adducts of our desired polymers. See: Van Rooij, G. J.; Duursma, M. C.; Heeren, R. M. A.; Boon, J. J.; Koster, C. G. *Am. Soc. Mass Spectrom.* **1996**, *7*, 449-457.

(22) Coates, G. W. *Chem. Rev.* **2000**, *100*, 1223-1252.

(23) Ovitt, T. M.; Coates, G. W. *J. Polym. Sci., Part A: Polym. Chem.* **2000**, *38*, 4686-4692.

(24) Hustad, P. D.; Kuhlman, R. L.; Carnahan, E. M.; Wenzel, T. T.; Arriola, D. J. *Macromolecules* **2008**, *41*, 4081-4089.

(25) As conversions exceed 50% in these enantioselective polymerization, a second terminal methine resonance appears by 13C NMR spectroscopy consistent with a terminal chain-end stereoerror.

(26) Hähner, U.; Habicher, W. D; Schwetlick, K. *Polym. Degrad. Stab.* **1991**, *34*, 111-118.

(27) Poly(1-butene) diol: M_n = 4.7 kg/mol, PDI = 1.2 by $CHCl_3$ GPC with PS reference.

(28) Zhang, H. C.; Huang, W. S.; Pu, L. *J. Org. Chem.* **2001**, *66*, 481–487.

(29) Schilling, F. C.; Tonelli, A. E. *Macromolecules*, **1986**, *19*, 1337-1343.